Reevaluating Maniraptoran Pelvic Musculature: Cursoriality, Convergence, and Caudal Decoupling

by

Matthew Michael Rhodes

A thesis submitted in partial fulfillment of the requirements for the degree of

Master of Science

in

Systematics and Evolution

Department of Biological Sciences
University of Alberta

Abstract

Maniraptora is a clade of non-avian theropod dinosaurs comprising avians and several "bird-like" groups with semilunate wrist bones. Maniraptorans tend to exhibit anterior migration in centre of mass, enlargement of the pectoral region, and progressive decrease in tail length and bulk. This culminates in birds with a habitually crouched posture, development of wings, and radical reorganization of leg and tail musculature that caused profound changes in locomotion. However, the evolution of these archetypal "avian" features is not entirely understood. Thus, a desire exists to characterize how and when these adaptations were acquired, and the resultant palaeobiological effects. Did these changes affect running ability (cursoriality)? Were similar adaptations gained independently (convergence)? Did disentanglement of tail from hip musculature (caudal decoupling) also proceed in a stepwise fashion, mirroring reduction of the tail as a whole? Previous studies addressing these questions have tended to focus strictly on osteology. However, soft tissue reconstruction affords a new perspective not possible using only skeletal. Furthermore, does soft tissue evidence corroborate adaptations inferred from osteology?

Relatively recent fossil discoveries of caenagnathids, dromaeosaurids, therizinosaurians, and troodontids permit reconstruction of maniraptoran locomotory musculature to infer adaptations and compare to skeletal evidence. Major locomotory muscles moor to the pelvis, which is also a junction between the leg and the tail. Direct observation of fossil pelvic material for osteological correlates of muscle attachments was done with reference to the closest living relatives to infer the presence or absence of major locomotory muscles. Extant conditions were determined by dissection and supplemented by literature review on soft tissue morphology and homology. Relative sizes of muscles and muscle groups allowed qualitative comparison within and between theropod taxa.

Skeletal and myological inferences are variably consistent. In the therizinosaurian *Falcarius*, muscular reconstruction reveals reduction in major leg extensors. This is consistent with therizinosaurian evolution but suggests that basal maniraptorans had a punctuated onset of caudal decoupling. In Caenagnathidae, moderate reduction of major leg extensors contradicts alleged high cursoriality inferred from limb proportions and metatarsus structure, but corroborates gradual, progressive caudal decoupling preceding the evolution of birds. Troodontid muscular reconstruction instead upholds postulated high cursoriality in derived members, an adaptation gained secondarily and predominantly owing to intrinsic hip muscles. In Dromaeosauridae, the microraptorine lateral pubic tubercle is considered homologous with other osteological correlates of the pubogastralial ligament. The relationship between the tubercle and the pubic apron, to which locomotory muscles attach, may explain why a pronounced tubercle or process is unique to Microraptorinae. Reconstruction of maniraptoran pelvic musculature reveals a complex relationship with skeletal data. However, this facilitates a reevaluation of locomotory adaptations such as cursoriality, convergence, and caudal decoupling in non-avian maniraptorans.

Preface

Some of the research conducted for this thesis forms part of collaborative research, led by Matthew Rhodes and including colleagues at the University of Alberta. G. F. Funston provided a caenagnathid silhouette for modified use in Figures 1.1, 2.1, 3.1, 4.1, 5.1, and 6.2. All measurements and general descriptions of pelvic morphology presented in this thesis were respectively taken and written by the author. P. J. Currie was the supervisory author and was involved with concept formation and manuscript edits for all chapters.

At the time of thesis submission, all four data chapters had been submitted for consideration of publication. Chapter 2 was submitted as Rhodes, M. M. and Currie, P. J., "Pelvic myology of the basal therizinosaurian *Falcarius* and evolution of locomotion in Therizinosauria and Maniraptora" to *The Anatomical Record*. I conducted data collection, analysis, and manuscript writing, and P. J. Currie provided manuscript edits. Chapter 3 was submitted as Rhodes, M. M., Funston, G. F., and Currie, P. J., "New material reveals the pelvic myology of Caenagnathidae (Theropoda, Oviraptorosauria)" to *Cretaceous Research*. G. F. Funston and I performed data collection and analysis, morphological interpretation, and manuscript writing. P. J. Currie contributed to manuscript edits. Chapter 4 was submitted as Rhodes, M. M. and Currie, P. J., "Troodontid pelvic myology offers insight into the convergence of cursoriality in Theropoda" to *Palaeontology*. I did data collection, analysis, and manuscript writing. P. J. Currie added to data collection, manuscript edits, and provided specimen photographs and data of some troodontid pelvic material that was also used in Figure 5.13. Chapter 5 was submitted as Rhodes, M. M. and Currie, P. J. "The homology, form, and function of the microraptorine lateral pubic tubercle" to *Journal of Vertebrate Paleontology*. I conducted data collection, analysis, and manuscript writing. P. J. Currie offered manuscript edits.

Selected Quote

"Any one of the larger carnivorous dinosaurs would meet the case. Among them are to be found all the most terrible types of animal life that have ever cursed the Earth or blessed a museum."

~ Doyle 1912, p. 100, "The Lost World" (Professor Challenger simultaneously describing the ferocity, public appeal, and enigmatic essence of non-avian theropod dinosaurs)

Acknowledgements

I firstly thank my supervisor P. J. Currie for his contributions both integral and peripheral to this thesis. This includes guiding research, mentorship, and leading field crews that have prepared me for lab and field work alike. I thank M. W. Caldwell for guidance and support despite my clear affliction with "dinosaur syndrome". On more than a few occasions, my ability to critically analyze and assess various concepts was tested, but simultaneously improved. I also thank E. B. Koppelhus for assistance and encouragement throughout my program, especially for reminding me about the wonderful world of fossil plants. I am grateful for the advice and patience of my committee as it kept my program on track and developed my abilities as a researcher. Funding that enabled research for this thesis was generously provided by the Department of Biological Sciences, Dinosaur Research Institute, Government of Alberta, Graduate Students' Association, Natural Sciences and Engineering Research Council of Canada, and University of Alberta Faculty of Graduate Studies and Research.

For access to collections, I thank R. Esplin and R. Scheetz (BYUVP); K. Corneli and K. Carpenter (CEUM); J. Mallon, K. Shepherd, and M. Currie (CMN); A. Atwater and J. Scannella (MOR); A. Howell (RM); B. Iwama and K. Seymour (ROM); B. Strilisky and D. Brinkman (TMP); C. Coy and H. Gibbins (UALVP); B. Barr (UAMZ); and C. Levitt-Bussain and R. Irmis (UMNH). The hospitality and assistance provided made for enjoyable collections visits and helped me to find some fantastic specimens that I may have otherwise overlooked.

I owe appreciation to the many folks of my cohort that contributed in major and minor ways. I thank T. Miyashita for counsel and meaningful, thought-provoking questions that provided timely motivation to refocus on the bigger picture. I thank G. Funston, whose wit kept me on my toes to try and match his many quips, but whose intellect also helped to adjust my

approach to various research problems. I thank M. Powers for discussions and banter that balanced work and fun in the field, in the lab, and on our many research trips. I also thank my other former and current lab mates and cohorts (A. Dyer, A. LeBlanc, A. van der Reest, A. McIntosh, B. Stettner, F. Garberoglio, I. Paparella, K. Bramble, M. Campbell-Mekarski, M. Dueck, O. Vernygora, P. Jiménez Huidobro, R. Vice, S. Hamilton, S. Mohr, S. Persons, S. Sinha, T. Simões, and Y. Wang) for discussion, positivity, and fun at social gatherings over the years.

To others that helped in academic ways or alleviating conversations during my graduate studies, I thank A. Murray, A. Richard Palmer, A. Rhodes, A. Torices, B. Barr, C. Hatley, C. Sullivan, D. Evans, D. Henderson, D. Brinkman, G. Bradley, J. Theodor, J. Voris, M. Pruden, R. Brown, R. Dievert, R. Holmes, R. Nottrodt, R. Sissons, and V. Arbour. Regarding fossil preparation, I thank A. Lindoe for technical advice and countless puns, and Evening Dino Lab volunteers for company and conversation during weekly sessions. Additionally, I thank T. Trump for being a great roommate while we tackled our theses. I am also grateful for other friends, family, and colleagues not explicitly mentioned that made their impact along the way.

A great deal of gratitude goes to Mom, Dad, Kathryn, Grandma, and Grandpa for their unwavering love and support that encouraged me to chase my dreams and bestowed me with the skills to do so. I deeply appreciate their tolerance for obscure anatomical and veterinary questions, patience during excited but lengthy explanations of my research, and homemade food that gave me the energy needed to write. I am also indebted to S. Wong for her endless care and support throughout this endeavor. I am incredibly grateful for your encouragement and for being my rock the whole way through.

Table of Contents

List of Tables

List of Figures

List of Institutional Abbreviations

AMNH, American Museum of Natural History, New York City, New York, USA.

BYUVP, Brigham Young University Museum of Paleontology, Provo, Utah, USA.

CEUM, College of Eastern Utah Museum, Price, Utah, USA.

CM, Carnegie Museum of Natural History, Pittsburgh, Pennsylvania, USA.

CMN, Canadian Museum of Nature, Ottawa, Ontario, Canada.

DLXH, Dalian Xinghai Museum, Dalian, Liaoning, China.

IVPP, Institute for Vertebrate Paleontology and Paleoanthropology, Beijing, China.

RM, Redpath Museum, Montréal, Québec, Canada.

ROM, Royal Ontario Museum, Toronto, Ontario, Canada.

TMP, Royal Tyrrell Museum of Palaeontology, Drumheller, Alberta, Canada.

UALVP, University of Alberta Laboratory for Vertebrate Palaeontology, Edmonton, Alberta, Canada.

UAMZ, University of Alberta Museum of Zoology, Edmonton, Alberta, Canada.

UMNH VP, Utah Museum of Natural History, Salt Lake City, Utah, USA.

List of Anatomical Abbreviations

M, muscle

Mm, muscles

Chapter 1. Introduction

1.1 General overview

The palaeobiology of theropod dinosaurs remains fascinating to researchers and public audiences, partly due to their phylogenetic position and consequential bearing on the origin of birds (Fig. 1.1) (Xu et al. 2014). Non-avian theropods attained global distribution by the Early Jurassic and developed a wide range of forms and high species diversity (Hendrickx et al. 2015). Some theropod lineages gave rise to dominant, large, terrestrial predators, including a recently described specimen of *Tyrannosaurus* with an estimated mass greater than any other member of its species (Persons et al. 2019). Other theropod lineages led to small, four-winged forms such as *Microraptor* with debated aerial abilities (Chatterjee and Templin 2007, Alexander et al. 2010, Evangelista et al. 2014b, 2014a, Palmer 2014, Sullivan et al. 2017, Segre and Banet 2018). Traditional wisdom holds that feathers are an avian characteristic, but *Microraptor* and several other non-avian theropods show that feathers evolved long before the divergence of birds (Foth et al. 2014, Brusatte 2017, Sullivan et al. 2017). Research continues to illuminate whether or not classically avian structures are in fact unique to this group. A backwards-pointing (retroverted) pubis is one such structure (Barsbold 1979), which may be more strongly correlated with ventilation than with diet in dinosaurs (Macaluso and Tschopp 2018). This study also highlighted the variable nature of maniraptoran hips in that opisthopuby evolved convergently multiple times within this clade, meaning that pubic retroversion is not exclusive to birds. Beyond the evolution of "avian" features prior to the appearance of birds, features like pubic retroversion are tied to, and thus have implications for, vital functions such as locomotion.

1.2 Locomotor modules

Like the evolution of feathers and opisthopuby, the acquisition of "bird-like" locomotion seems to be a gradual, stepwise process that long preceded the evolution of birds (Hutchinson and Allen 2009, Brusatte et al. 2014). Basal theropods were bipedal (Carrano 2000, Xu et al. 2014, Hendrickx et al. 2015), a condition inherited from their basal dinosaurian ancestors and inherited by their avian descendants. Early theropods achieved terrestrial locomotion by pelvic and caudal musculature that rotated the hind limb around the hip joint as a single module (Gatesy and Dial 1996). Compared to maniraptorans, many of these more basal theropods have long tails with large spaces available for leg extensor musculature (Gatesy 1990, Persons and Currie 2011). Birds represent the opposite end of an evolutionary continuum, typified by a habitually crouched posture and highly reduced tail (Gatesy 1995, Carrano and Biewener 1999, Hutchinson and Gatesy 2000, Allen et al. 2013, Grossi et al. 2014, Xu et al. 2014). For terrestrial locomotion with a sub-horizontal femur, birds rely only on intrinsic pelvic muscles that primarily rotate the leg around the knee joint. Tail muscles are reduced and functionally detached from the leg, being instead assimilated into the flight apparatus for tail control (Gatesy and Dial 1996, Dececchi and Larsson 2013). Caudal decoupling describes the gradual process of functional separation between caudofemoral muscles and the hind limb over the evolutionary history of theropods. Although tail reduction was previously considered the main factor affecting posture, recent studies suggest that development of the pectoral girdle was a stronger force (Allen et al. 2013). Patterns in the arms, legs, and centre of mass suggest that all three are highly integrated in this evolutionary transition, which resulted in steady, anterior migration in whole-body centre of mass across much of Theropoda. This trend is more pronounced in Maniraptora and appears linked to the evolution of flight. Nonetheless, adaptations of the leg and tail remained important.

1.3 Cursoriality

Discussion about cursoriality is a running theme throughout this thesis. Broadly defined, cursoriality is the condition of being adapted for running, which can be recognized by a suite of morphological features (Carrano 1999). In theropods, these features typically include reduced arms, long distal leg and foot elements relative to femoral lengths, hinge-like joints, tightly appressed or fused metatarsi, symmetrical feet, lateral pedal digit reduction or loss, and elongate third toes (Lull 1904, Coombs 1978, de Bakker et al. 2013, Lovegrove and Mowoe 2014). Without the ability to observe behaviour or directly measure other aspects of locomotor performance (e.g. physiology) in non-avian theropods, recognizing cursoriality in these taxa relies entirely on morphological features preserved in the fossil record. Because of this caveat, this thesis is unable to differentiate types of cursors that share many of these features—such as sprinters and endurance runners—and therefore collectively refers to them as well adapted for running or "highly cursorial". As noted by previous authors (Carrano 1999, Lovegrove and Mowoe 2014), the complex relationship of variables that influence locomotion make it difficult to explicitly define cursoriality but demonstrate that it is better represented as a spectrum than as categories of locomotor performance. This thesis adopts these perspectives and uses muscle reconstruction as an additional means to evaluate how well various groups were adapted for cursoriality. High cursoriality is treated as interchangeable with strong running ability, although elucidating specific cursorial styles (e.g. sprinting vs. endurance running) is beyond the scope of this work.

Bipedalism tends to be associated with exacerbation of cursorial features (Coombs 1978), which evolved alongside parasagittal hind limb posture prior to the evolution of dinosaurs

(Carrano 2000). Bipedalism in dinosaurs may in fact be functionally tied to cursoriality based on advantages imparted by retention of the caudofemoral muscle complex (Persons and Currie 2017). Basal dinosaurs additionally gained other features that restricted mediolateral rotation and abduction of the femur associated with bipedalism, erect postures, and parasagittal gaits (Hutchinson and Gatesy 2000). The preacetabular and postacetabular portions of the ilium gradually expanded in basal theropods, which also increased available area for musculature that protracted (flexed) and retracted (extended) the hind limb (Carrano 2000). These adaptations in turn may have enhanced the effectiveness of other cursorial adaptations already present. At least in predatory theropods, there is a similar evolutionary trend of increasing cursoriality from more basal to more derived members (Persons and Currie 2016). Locomotion was driven by both pelvic and caudal musculature that rotated the hind limb primarily around the hip joint (Gatesy and Dial 1996, Hutchinson 2006).

1.4 Locomotory adaptations

This section is arranged phylogenetically from basal to derived within Theropoda (Fig. 1.1) (Hendrickx et al. 2015). Theropods that attained large adult body sizes, such as tyrannosaurids, may have consequently reduced their running abilities with age (Hutchinson and Garcia 2002, Hutchinson 2004). However, accounting for allometric changes in limb proportions maintains that tyrannosaurids were adapted for cursoriality (Paul 1998, Persons and Currie 2016). Allometry also relates to tyrannosaurid maneuverability as it minimizes increases in rotational inertia with body size, simultaneously maximizing relative agility (Henderson and Snively 2004). Additionally, the tyrannosaurid foot is modified into an arctometatarsus, a structure in which the third metatarsal is proximally pinched and tightly interlocked between

adjacent metatarsals (Holtz 1994, Snively and Russell 2001, 2003). Acquisition of this feature is generally associated with high cursoriality (Persons and Currie 2016), which may be due to its increased efficiency at handling torsional forces and prevention of toe splaying (Snively et al. 2004). Although controversy surrounds adult tyrannosaurid running abilities (Farlow et al. 2000), these adaptations in proportionately long limbed, lightly built juveniles reinforces inferences of high cursoriality in young tyrannosaurids (Currie 1998, Hutchinson 2004).

The arctometatarsalian condition evolved convergently in alvarezsaurids, caenagnathids, ornithomimids, and troodontids (Snively et al. 2004). A subarctometatarsalian condition may have enhanced agility in some other theropods (White 2009). Continuing in phylogenetic fashion, ornithomimids are widely recognized as impressively cursorial creatures. This is partly because of their arctometatarsalian feet, but also due to overall gracile build and slender, elongate hind limbs (Russell 1972, Paul 1998). The extent of caudofemoral musculature in ornithomimids is intermediate between more basal theropods and maniraptorans (Gatesy 1990, Gatesy and Dial 1996). A reduced, albeit raised, fourth trochanter on the femur indicates the insertion site, complimented by a wide, deep brevis fossa and modest tail space as the origin sites indicative of a moderately large muscle complex. The divergence of Maniraptora leads to a strong reduction in caudofemoral musculature (Gatesy 1990). Convergent pubic retroversion (Macaluso and Tschopp 2018) and resulting functional shifts in pelvic musculature followed (Hutchinson and Gatesy 2000). Furthermore, concomitant changes in pectoral girdle and hind limb development accelerated (Allen et al. 2013) as maniraptorans deviated from the typical theropod bauplan. Although more basal theropods were morphologically restricted by bipedalism and primarily terrestrial locomotion (Gatesy and Middleton 1997), maniraptorans began occupying more diverse ecomorphospaces. Dromaeosaurids seem to secondarily lose several

cursorial adaptations in limb proportions, metatarsus structure, and caudofemoral musculature (Carrano 1999, Persons and Currie 2012, 2016). In contrast, closely related troodontids retain some of these adaptations (Holtz 1994, Carrano 1999, Snively et al. 2004, Persons and Currie 2016). Anterior migration in centre of mass throughout theropod evolution required postural changes that imparted different loading regimes on leg elements (Carrano 1998, Bishop et al. 2018b). Living birds occupy a variety of ecomorphospaces that are reflected in hind limb morphology (Gatesy and Middleton 1997, Zeffer et al. 2003). Changes in locomotor modules and the evolution of flight made aerial locomotion viable (Gatesy and Dial 1996). However, much research interest remains for grounded birds restricted to terrestrial locomotion. Ostriches and emus are particularly well known as strong cursors, which is intriguing from musculoskeletal and biomechanical perspectives, but also has implications for non-avian theropod locomotion (Alexander 1985, Fowler 1991, Fuss 1996, Patak and Baldwin 1998, Smith et al. 2006, 2007, Jindrich et al. 2007, Schaller et al. 2009, Rubenson et al. 2011, Chadwick et al. 2014, Lamas et al. 2014, Hutchinson et al. 2015, Rankin et al. 2016, Daley et al. 2016).

1.5 Identifying muscle attachment sites

Romer (1923a, 1923b, 1923c, 1927) established foundational studies of muscle reconstruction in dinosaurs in the early twentieth century by examining extant crocodylians and avians. He noted similar bony landmarks could be identified in extinct taxa, and the musculature reconstructed. Muscles connect to bone either directly, by fleshy attachment, or indirectly, by a tendon or aponeurosis that bridges the gap via fibrous connective tissue (Romer 1962). Tendinous or aponeurotic sites of attachment typically have scars or reasonably clear borders, whereas fleshy attachments are usually smooth (Bryant and Seymour 1990). Due to the

locomotory importance of pelvic and hind limb muscles for bipedalism, a handful of studies attempted to reconstruct archosaur pelvic and hind limb muscles during the twentieth century (Russell 1972, Walker 1977, Tarsitano 1983, Perle 1985). Some studies note the low proportion of former muscle attachment sites that can be positively identified based on surficial osteological features alone, which even then does not often record specific muscle sizes or orientations (McGowan 1979). Furthermore, the relationships between the sizes and strengths of muscles are complex, even during *in vivo* experiments (Bamman et al. 2000, Jones et al. 2008). This limits the inferences that can be made with any confidence about certain muscle properties and forces. However, more recent studies emphasize the importance of phylogenetic context and ways of categorizing confidence levels for inferring soft tissue in extinct taxa (Bryant and Russell 1992, Witmer 1995). Surface microscopy has recently shown some promise in identifying both fleshy and tendinous muscle attachment sites in extant and extinct specimens (Rothschild et al. 2015).

Shortly after the establishment of more rigorous and consistent methods, a thorough study incorporating palaeontological and neontological data reconstructed the evolution of the archosauromorph pelvis (Hutchinson 2001a) and femur (Hutchinson 2001b). Ascertaining the evolution of the osteological correlates to which muscles attached was done with a homology based approach and led to a subsequent summary of archosaur muscle evolution (Hutchinson 2002). Ever since, this revised framework, combined with more conservative means to constrain and categorize speculation, has been a major reference for many dinosaur muscle reconstructions in ornithischians (Maidment and Barrett 2011, 2012, Maidment et al. 2014a, 2014b), sauropodomorphs (Langer 2003), and theropods (Carrano and Hutchinson 2002, Hutchinson et al. 2005, 2008, Grillo and Azevedo 2011, Bates et al. 2012, Bates and Schachner 2012, Bishop et

al. 2018a). These types of studies can establish baselines for musculoskeletal changes in larger clades and provide quantitative, dynamic models to infer aspects of stance, speed, and gait.

1.6 Gaps in knowledge

Despite this extensive knowledge base, the condition of locomotory musculature in many dinosaur taxa is unknown. Many previous studies focus on a single species, sometimes on a single well preserved specimen, to limit variables and speculation. Other broad studies often encompass large clades to assess macroevolutionary trends. This framework not only establishes a protocol to identify former soft tissue attachment sites in dinosaurs, but also provides an opportunity to continue closing existing gaps in unexamined groups. In the wake of soft tissue reconstruction, these new data can be placed in proper evolutionary context. It is then possible to assess how well or poorly it aligns with previous interpretations based on other data, or add to discussion on controversial issues. Tyrannosaurid cursoriality is one such example. Based on skeletal features and morphological adaptations, adult tyrannosaurids should be expected to be well adapted for cursoriality (Holtz 1994, Paul 1998, Snively and Russell 2001, 2003, Henderson and Snively 2004, Snively et al. 2004, Persons and Currie 2016). However, accounting for musculoskeletal and biomechanical demands, this may not have been biologically feasible (Hutchinson and Garcia 2002, Hutchinson et al. 2005). At the same time, studies like this open up discussion beyond speculation about the potential for highly cursorial abilities in ontogenetically younger members of this family (Currie 1998, Paul 1998, Hutchinson 2004, Persons and Currie 2016).

In some cases, muscular reconstruction was not possible until recently because of a lack of well preserved fossils of certain taxa. Recent fossil discoveries provide material that can be

analyzed and amalgamated into the existing body of research. Understanding the conditions present in more taxa, especially on the evolutionary continuum to birds, will increase resolution and contribute to a richer discussion on the evolution of various locomotory adaptations.

1.7 Research design and hypotheses

The main goal of this thesis is to reevaluate inferences about locomotory adaptations in select non-avian theropod dinosaurs based on pelvic musculature reconstruction. In other words, how well do inferences garnered from muscle reconstruction reflect those based on skeletal data? Given the controversies about locomotion in some theropods, myological and osteological data may conflict. Maniraptoran theropods are of notable interest due to the rate and variety of morphological changes that occur in this clade (Allen et al. 2013). The purported pattern of the stepwise accumulation of "avian" features poses another point of interest (Hutchinson and Allen 2009, Brusatte et al. 2014). Locomotory muscle reconstruction—although dependent on osteological data—offers a second perspective on skeletal adaptations. It also has the potential to reveal whether or not the evolution of maniraptoran pelvic musculature also follows a stepwise trend. Therefore, the null hypothesis is that locomotory inferences from myological reconstruction are consistent with those gathered from osteology. Conversely, the alternative is that myological and osteological data clash, meaning that one data set alone cannot be used to explain locomotory adaptations in the focal taxon.

1.7.1 Pelvic musculature

Locomotory inferences are primarily gained from qualitative, comparative analysis of muscles and muscle groups. Reconstruction is limited to the pelvis to focus on the effect of

flexors (protractors) and extensors (retractors) that move the entire hind limb. Proximal limb muscles originating on the hip are primary to locomotory functions and adaptations (e.g. degree of cursoriality), whereas lower limb muscles are secondary and predominantly control more distal limb elements. The pelvis is also a junction between hind limb and tail locomotor modules, which offers information on their level of interaction in the context of caudal decoupling. Lower limb musculature is therefore not considered here. Soft tissue inferences depend on osteological correlates, or morphological features of the bones. This effectively makes soft tissue inferences second degree inferences in the ecological hierarchy as they rely on osteological data, which itself must also be interpreted. This is summarized nicely by Witmer (1995: fig. 2.1) and underscores the intimate association between bones and soft tissues. In the context of the Extant Phylogenetic Bracket, dissection was performed on a savannah monitor (*Varanus exanthematicus*), a spectacled caiman (*Caiman crocodilus*), and a common raven (*Corvus corax*) to examine pelvic musculature. This was done to compliment literature review for pelvic musculature in squamates (Russell and Bauer 2008, Dick and Clemente 2016), crocodylians (Otero et al. 2010, Allen et al. 2015), and birds (Shufeldt 1890, Hudson et al. 1959, Halvorson 1972, Gheţie 1976, Jacobson and Hollyday 1982, Baumel et al. 1990, 1993, Mellett 1994, Patak and Baldwin 1998, Verstappen et al. 1998, Gangl et al. 2004, Paxton et al. 2010).

1.7.2 A note on homology

Homology is a fundamental, underlying notion of muscle reconstruction in extinct taxa. Essentially, homology is a conceptual framework that allows evaluation of similar comparative anatomical features. Homologous features are therefore characters considered as “equivalent” in different taxa that were acquired by shared ancestry (Patterson 1982, de Pinna 1991). Muscle

reconstruction not only relies on homologies of osteological elements among taxa, but also between muscles and muscle groups (Witmer 1995). Homologies of muscles in the deep dorsal group were historically perplexing, but more recent evidence suggests that archosaur muscles are largely conserved (Rowe 1986, Hutchinson 2002). Considerable changes in the arrangement and number of muscles among archosaurs have led some to treat such changes as essentially multistate characters (Hutchinson 2001a). Similarly, this thesis follows an approach that emphasizes transformational homology. Structures may be recognized as homologous if they pass the three classic "tests" of homology (Patterson 1982), with congruence an important test of the agreement between characters (Rieppel 1994). In this way, muscles and other soft tissues must directly correspond to a feature on the skeleton (osteological correlate) and distinguish a monophyletic group (Witmer 1995). However, changes in the arrangement and number of muscles in a muscle group may simply be the result of muscles splitting into multiple heads (i.e. crocodilian M. iliofemoralis into the avian M. iliotrochantericus caudalis and M. iliofemoralis externus), or merging into one another (i.e. crocodilian Mm. iliotibiales 2–3 into the avian M. iliotibialis lateralis) (Hutchinson 2002). In this way, a transformational approach (de Pinna 1991) recognizes these modifications as character state changes rather than character gain or loss. The latter perspective may erroneously lead to absence coding, non-additive binary coding, or other problematic types of character creation (Simões et al. 2017). Myological changes inferred in extinct taxa are only used here to map onto preexisting phylogenies to glean comparative and evolutionary changes. As muscle reconstruction ultimately relies on the osteology, this creates potential for overweighting skeletal characters that are also a correlate for muscle attachment.

1.7.3 Phylogenetic scope

Based on available maniraptoran pelvic material, caenagnathids, dromaeosaurids, therizinosaurians, and troodontids were chosen to examine musculoskeletal data. Although these essentially represent point samples rather than a broad collection of data, information gained can be added to existing literature. Therizinosauria is an early branching clade within Maniraptora with features suggesting a departure from the typical morphology of maniraptoran theropods (Fig. 1.1) (Zanno 2006, 2010a, Hendrickx et al. 2015). Caenagnathidae diverged slightly later and occupies an intermediate position within Maniraptora, and a basal position within Pennaraptora (Fig. 1.1) (Foth et al. 2014). Anatomical features of the metatarsus and hind limb are suggestive of cursoriality, but a reduced tail may have implications for caudal locomotory input and overall running ability. Troodontidae is closely related to birds (Fig. 1.1) (Hendrickx et al. 2015) and its members typically possess features associated with high cursoriality. However, tail space was limited, and early troodontids have marked differences in pelvic morphology. The microraptorine dromaeosaurid *Hesperonychus elizabethae* (Longrich and Currie 2009) possesses a pair of wing-like lateral pubic processes. It shares this feature with other microraptorines, but the identity and potential functional implications of this structure are unclear. Exploration of these problems in the context of locomotory muscle reconstruction will address these questions about the degree of cursoriality, convergence, and caudal decoupling.

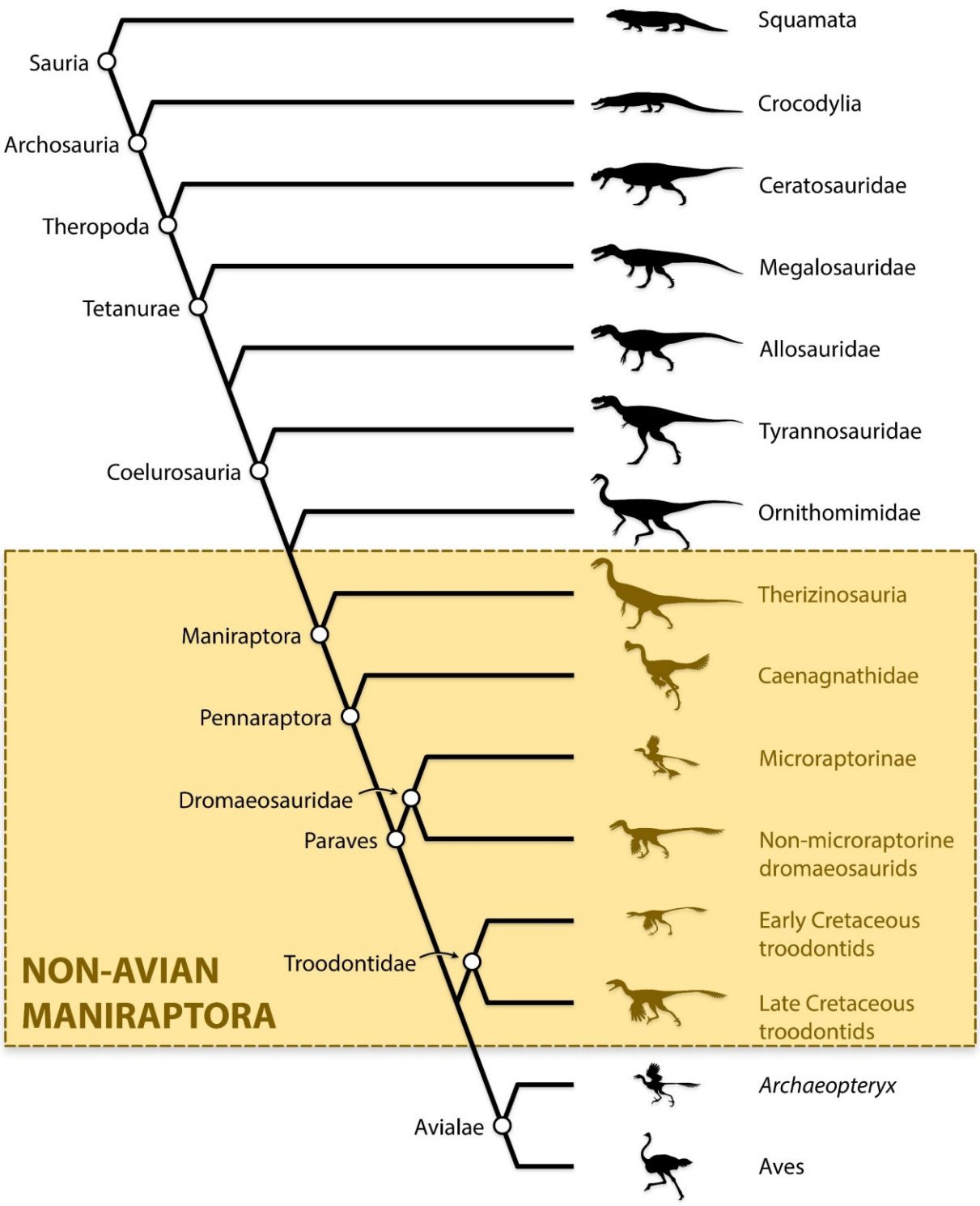

Figure 1.1. Simplified phylogeny of non-avian Maniraptora within Sauria. Focal clade highlighted among Theropoda and closest living kin. Topology based on Hendrickx et al. (2015).

Chapter 2. Pelvic myology of the basal therizinosaurian *Falcarius* and evolution of locomotion in Therizinosauria and Maniraptora

2.1 Introduction

Therizinosauria is a clade of theropod dinosaurs with a convoluted taxonomic history (Paul 1984, Xu et al. 1999a, Clark and Xu 2009, Zanno 2010b), originally thought to have affinities with turtles based on rib and hand fragments (Maleev 1954). Derived therizinosaurians evolved a tetradactyl foot with a weight-bearing first digit evident in the skeleton (Barsbold and Perle 1980, Clark and Xu 2009, Zanno et al. 2009) and trackways (Fiorillo and Adams 2012, Gierlinski and Lockley 2013). Other features including an edentulous beak, lanceolate teeth lacking wear facets, tooth occlusion, limited bite force, broad hips enabling enlarged gut capacity, and a long neck with increased mobility at the expense of craniocervical musculature indicate herbivory with some reliance on oral processing of food (Zanno and Makovicky 2011, Smith et al. 2011, Lautenschlager 2013). Variability in jaws and claws also suggests some dietary plasticity and related changes in food gathering (Lautenschlager 2014, 2017). The combination of these features is atypical of most theropods, which led some to appropriately describe Therizinosauria as "aberrant" (Barsbold and Perle 1980, Zanno 2010a). It also made classification difficult until discovery of more basal members such as *Beipiaosaurus* (Xu et al. 1999a) and *Falcarius* (Kirkland et al. 2005). Therizinosauria is now recognized as an early diverging clade within Maniraptora (Fig. 2.1) (Zanno et al. 2009, Turner et al. 2012, Hendrickx et al. 2015).

The most basal therizinosaurian, *Falcarius*, retains a three-toed foot, distally positioned first toe, and relatively high bite force (Clark and Xu 2009, Botelho et al. 2017, Lautenschlager

2017). However, it also exhibits leaf-shaped teeth, broad hips with a laterally flared preacetabular hook, tall ilia with long preacetabular and short postacetabular portions, a relatively low tibia:femur length, a more robust shoulder with modified range of motion, and dietary shift from hypercarnivory more similar to derived therizinosaurians (Barsbold 1979, Barsbold and Perle 1980, Kirkland et al. 2005, Zanno 2006, 2010a, Zanno and Makovicky 2011). *Beipiaosaurus* is relatively basal and retains a tridactyl foot, but developed a longer and deeper preacetabular portion of the ilium and a robust first toe (Xu et al. 1999a). More derived species tend to further exaggerate these features (Li et al. 2008a, Zanno et al. 2009, Pu et al. 2013, Yao et al. 2019). Despite knowledge of dietary trends and morphological development, locomotory adaptations remain unclear. This is underscored in *Falcarius* by its mix of features and phylogenetic position among theropods with varying cursorial abilities (Carrano 1999, Persons and Currie 2016) and caudofemoral musculature input (Gatesy 1990, Gatesy and Dial 1996).

Falcarius presents an intriguing opportunity to evaluate two aspects of theropod evolution with one study. As the most basal therizinosaurian, its anatomy offers insight into the early evolution of the group. Because this clade diverges early within Maniraptora (or earliest sensu Zanno et al. 2009), it also closely approximates the common ancestor of maniraptorans. Near this taxonomic intersection, *Falcarius* can reveal functional trends and conditions at early stages of both Therizinosauria and Maniraptora, the latter of which has an accelerated rate of body shape evolution (Allen et al. 2013). However, therizinosaurians are conspicuously absent from this study, and functional studies of basal members are lacking (Zanno 2010a).

Inspection of *Falcarius* pelvic elements for former soft tissue attachment sites allows reconstruction of locomotory musculature. This provides another perspective on locomotion and therizinosaurian evolution aside from observations of skeletal data. It also fits into an existing

framework of theropod locomotion for comparison to other taxa. Besides providing a reference for reconstruction in other therizinosaurians, it also creates a reference for early maniraptorans. The locomotory musculature of *Falcarius* allows us to create and assess functional inferences that have implications for theropod locomotion and palaeobiology alike.

2.2 Materials and Methods

Pelvic material of *Falcarius* (Table 2.1) was examined for gross morphology and to identify former soft tissue attachment sites. Reconstruction is limited to the pelvis to concentrate on the effect of proximal limb muscles with a primary relationship to locomotion. Although distal limb muscles also control leg movements, their actions are secondary and mainly to manipulate the foot and toes. The pelvis also connects the tail and leg. This allows examination of some tail muscles in the context of caudal decoupling during theropod evolution (Gatesy and Dial 1996) and as a proxy for caudofemoral extensor musculature (Gatesy 1990). The latter may contribute a substantial portion of leg extensor musculature, which could be important for locomotory and other functional inferences (Persons and Currie 2011, 2012, Persons et al. 2014). Origin or insertion area does not necessarily reflect muscle size or strength (Bryant and Seymour 1990, Barrett and Maidment 2017), but allows estimates to make general comparisons.

A detailed osteological description of *Falcarius utahensis* was previously done (Zanno 2010a) and applies readily to the material observed here. Nonetheless, a summary is provided to emphasize osteological correlates of locomotory musculature and offer minor corrections to a few features associated with muscle attachment sites. Additionally, CEUM material was recovered from a different locality than UMNH material and may represent a different species of *Falcarius* (Zanno 2010a, 2010b). However, the overall similarity of all observed material

suggests limited interspecific variation, if any, which justifies reconstruction at the generic level. Therefore, gross morphology and muscle attachment sites herein represent *Falcarius*. Although all observed material is disarticulated, a reconstructed pelvis was created by scaling pelvic elements to match based on contact surfaces, a CEUM cast, and published literature (Zanno 2010a).

Identification of former soft tissues relies on the Extant Phylogenetic Bracket to infer the likelihood of presence or absence in the focal taxon based on osteological correlates and conditions in the closest living relatives (Fig. 2.1) (Bryant and Russell 1992, Witmer 1995). This study follows comparative methods of previous dinosaur locomotion studies to identify pelvic muscle attachment sites (Hutchinson 2001a, Carrano and Hutchinson 2002, Hutchinson et al. 2005, 2008, Maidment et al. 2014a, 2014b). A savannah monitor (*Varanus exanthematicus*), a spectacled caiman (*Caiman crocodilus*), and a common raven (*Corvus corax*) were dissected to understand the relationship of tissues in members of the Extant Phylogenetic Bracket. Comparative skeletal material of various squamates, crocodylians, and birds provided additional data on osteological correlates in extant taxa (Table 2.1). Pelvic muscle homologies were also reviewed (Romer 1923a, Gheţie 1976, Rowe 1986, Proctor and Lynch 1993, Hutchinson 2001a, Carrano and Hutchinson 2002, Gangl et al. 2004, Hutchinson et al. 2005, 2008, Smith et al. 2006, 2007, Lamas et al. 2014) and summarized in Table 2.2. Inferences on muscle presence were categorized following Witmer (1995) and restricted to those that met criteria for Level I, I', II, or II' to limit speculation (Table 2.3). Photographs were taken with a digital camera and illustrations were generated using Adobe Photoshop CS6 and a Wacom drawing tablet.

2.3 Morphology of the pelvic girdle

The ilia of *Falcarius* deviate from the typical dolichoiliac form of most theropods, being instead characterized as altiliac based on their dorsoventrally tall and anteroposteriorly long preacetabular portions (Fig. 2.2) (Zanno 2010a). In contrast, the postacetabular portions are comparatively short in both anteroposterior length and dorsoventral height (Fig. 2.2). Although the preacetabular portion is displaced dorsally relative to the acetabulum of other theropods (Zanno 2010a), it is not quite as extreme in dorsoventral height as in derived therizinosaurians. The preacetabular hook is flared laterally and ends in a blunt, ventrally directed point, best seen in CEUM 77189 (Fig. 2.2A). Its medial side has a shallow concavity that is covered in subtle striae. Contra Zanno (2010a), the cuppedicus fossa is interpreted as present in this space. It occupies the medial side of the preacetabular hook (Figs. 2.2–2.3) and is delineated dorsally by a low, arcuate ridge confluent with a narrow, medially projecting shelf (Fig. 2.3). The difference in interpretation between here and Zanno (2010a) may stem from the shallowness of the cuppedicus fossa and lack of a bony medial edge like that present in ornithomimids or tyrannosaurids. The anterior iliac margin is gently convex, whereas its dorsal margin is approximately straight and anterodorsal-posteroventrally inclined in lateral view (Fig. 2.2). Subtle, radiating striations are present on the lateral sides of the anterior and dorsal edges of the iliac blade. The posterior iliac margin is roughly squared off so that the postacetabular process appears subrectangular in lateral view. Along the ventral margin of the postacetabular portion, the posterior half is straight and sub-horizontal, whereas the anterior half is concave and curves ventrally into the ischiadic peduncle. Most of the lateral surface of the ilium is smooth except for a triangular patch of roughened texture on the postacetabular portion, its apices connecting the transition between straight and concave ventral margin, posterodorsal corner, and posteroventral corner of the ilium.

The brevis fossa is narrow and shallow, bound dorsally by the brevis shelf (Fig. 2.2). The ischiadic peduncle is anteroposteriorly short and mediolaterally wide, whereas the opposite is the case with the pubic peduncle (Fig. 2.2). The anterolateral surface of the pubic peduncle may have a slight depression, but this feature is shallow when present.

Falcarius has a pubic shaft that appears sigmoid in both anterior and in lateral views (Fig. 2.4) (Zanno 2010a). On the proximal end of the pubis, the preacetabular tubercle forms a low, proximodistally oriented ridge on the anterolateral edge of the shaft (Figs. 2.4–2.5). This tubercle is best seen in CEUM 52424 and UMNH VP 14540 distal to the iliac contact and anterior to the ischiadic contact (Fig. 2.4). A small, oval patch of rugose texture is preserved adjacent to the preacetabular tubercle on its lateral side. The pubic apron (Fig. 2.4) is a transversely broad sheet of bone that tends to curve posteriorly toward its medial edge. Striations are preserved on both its anterior and posterior surfaces. Toward the proximal end of the apron, a broken medial edge indicates where it was formerly attached to the contralateral pubis. However, distally, a smooth medial edge that is concave in anterior view repersents part of the margin of the slit-like pubic fenestra (Fig. 2.4). The pubic boot is often incompletely preserved, although seems to be intact in CEUM 77195 with a short, rounded anterior projection and long posterior projection that tapers to a rounded point (Fig. 2.4E–F).

The ischium of *Falcarius* is blade-like and boomerang-shaped in lateral view (Fig. 2.6). The iliac and pubic peduncles at the proximal end surround about a quarter of the acetabulum. A small, triangular obturator process is situated about midshaft, and merges proximally with the ischial shaft and distally with the ischial apron (Fig. 2.6). Striations carpet the lateral side of the obturator process, but do not encroach on the ischial shaft (Fig. 2.7C–D). Because of the pointed obturator process and curvature of the ischium, the anterior and posterodorsal margins are both

concave in lateral view. The ischial apron is convex ventrally, which makes the ventral margin of the ischium sigmoid in the same view. The shaft tapers to a point at its distal end. A pair of small tuberosities are preserved along the posterodorsal edge of the shaft, one at the proximal end and the other at the distal end (Fig. 2.6). Accompanied by light scarring, the proximal ischial tuberosity is slightly raised into a low, triangular eminence partially preserved here, but better preserved in a previously described specimen (Zanno 2010a). The distal ischial tuberosity is less conspicuous. Between these tuberosities, but closer to the proximal one, is a longitudinal groove on the posterodorsal edge of the ischial shaft (Fig. 2.7A–B).

2.4 Myology of the pelvic girdle

2.4.1 Triceps femoris

Pelvic musculature belonging to the triceps femoris consists of the Mm. iliotibiales 1–3 (IT1–3) and M. ambiens (AMB). Light scarring with a radial pattern (striae perpendicular to the edge of the bone) along the anterior margin of the preacetabular portion of the ilium indicates the origin of IT1 (Fig. 2.8A). This scarring is continuous along the dorsal margin for the origins of IT2 and IT3. Exact distinctions between the three heads of this muscle are unclear and divisions are estimated based on other theropod pelvic muscle reconstructions (Carrano and Hutchinson 2002, Hutchinson et al. 2005, 2008, Bates et al. 2012) and the condition in extant birds and crocodylians. The extent of these origins can be determined based on the extent of scarring, which terminates around the anteroventral corner of the preacetabular hook for the IT1, and at the posterodorsal corner of the ilium for the IT3. The narrow area for attachment along the lateral side of the ilium is consistent with other theropods and suggests that the IT1–3 were similarly broad, sheet-like muscles in *Falcarius*.

Joining the IT1–3, the AMB originated on the pubis near the preacetabular tubercle from a roughly oval patch of rugose texture (Fig. 2.8A). This contrasts with the findings of Zanno (2010a), who did not find a defined origin for this muscle. Although faint, the patch of textured bone surface near the preacetabular tubercle is identified here as the osteological correlate for the AMB (Hutchinson 2001a). This interpretation is also consistent with other theropods (Hutchinson et al. 2005, 2008, Bates et al. 2012).

2.4.2 M. iliofibularis (ILFB)

The origin of M. iliofibularis (ILFB) is on the lateral surface of the ilium (Fig. 2.8A). The postacetabular portion of the ilium serves as the ILFB attachment site (Hutchinson 2002), but its smooth texture hinders exact identification of its extent. Consideration of the Extant Phylogenetic Bracket indicates that the ILFB does not extend anteriorly beyond the acetabulum and is surrounded by other muscles. Therefore, the ILFB was likely restricted to a roughly triangular area posterior to the centre of the acetabulum and ventral to IT2–3.

2.4.3 Deep dorsal group

Muscles of the deep dorsal group chiefly produce leg flexion and include the M. iliofemoralis externus (IFE), M. iliotrochantericus caudalis (ITC), and Mm. puboischiofemorales interni 1–2 (PIFI1–2). The origin of IFE is dorsal to the acetabulum on the lateral side of the ilium (Fig. 2.8A). Like other muscles originating on the iliac blade, this muscle had a fleshy attachment not clearly defined on the surface of the bone. Evidence from the insertion site at least clarifies that the IFE and ITC became divided in basal dinosauromorphs such as *Lagerpeton*, *Lagosuchus*, and *Lewisuchus*, and basal dinosaurs like *Eoraptor* and herrerasaurids

(Hutchinson 2001b, 2002). This division is indicated by development of a prominent trochanteric shelf on the proximal end of the femur. However, this does not help to elucidate the relative size of the IFE. Its origin is tenuously reconstructed as being small compared to the ITC based on inferred reduction in basal tetanuran theropods (Hutchinson 2001a, 2002) and observed small size in extant birds.

Anterior to the IFE, the origin of ITC encompasses much of the preacetabular portion of the ilium (Fig. 2.8A). This origin is restricted by surrounding muscles including the IT1 anteriorly, IT2 dorsally, and IFE and ILFB posteriorly. The ventral edge of the ilium constrains the remaining border of the origin of ITC. Because of both anterior and dorsal expansion of the preacetabular portion of the ilium, the origin of ITC was also enlarged relative to those of other muscles. Faint scarring on the lateral side of the preacetabular hook dorsal to a small portion of smooth bone toward its tip suggests that a small area was not covered by muscle.

The origin of PIFI1 is on the anterolateral edge of the pubic peduncle between the preacetabular hook and acetabulum (Fig. 2.8A). Its general size can be approximated by the shallow depression preserved in some specimens. The origin of PIFI1 is not inferred to extend onto the base of the preacetabular hook or cuppedicus shelf, nor is there evidence for to suggest that part of it occupied the medial side of the blade.

Inside the cuppedicus fossa, the origin of PIFI2 apparently covers the entire medial side of the preacetabular hook based on muscle scarring (Fig. 2.8B–C). This texture, and the origin by extension, is dorsally constrained by the cuppedicus ridge and shelf. The anterior and ventral range is only limited by the edges of the bone. Surface texture is continuous across the origin, indicative of a single, undivided head. This is more similar to the state in crocodylians, and opposed to the divided and separated pair of homologous avian muscles (ITCR+ITM, Table 2.2),

like that reconstructed in other theropods. However, the origin of PIFI2 in a crocodilian is on the posterior dorsal vertebrae rather than the ilium.

2.4.4 Flexor cruris group

The tibial flexor group is comprised of the M. flexor tibialis internus 1 and 3 (FTI1, 3) and M. flexor tibialis externus (FTE). The correlate for the FTI1 is the distal ischial tuberosity (Fig. 2.8A). At the distal end of the ischium along its dorsal edge, the origin is offset to the lateral side. Much like the tuberosity from which the FTI1 originates, the muscle was likely highly reduced.

The origin of FTI3 is on the proximal ischial tuberosity (Fig. 2.8A). This eminence is more pronounced than its distal counterpart, but not as prominent or rugose as in more plesiomorphic theropods such as tyrannosaurids (Carrano and Hutchinson 2002, Hutchinson et al. 2005). Muscle scarring indicative of former FTI3 attachment is more distinct on the lateral side of this process as opposed to the medial side.

On the ilium, the triangular patch of textured bone near the posteroventral corner of the blade on its lateral side marks the origin of FTE (Fig. 2.8A). The muscle likely occupied about the same area as indicated by scarring, which helps to constrain nearby muscles like the ILFB and IT3. The origin of FTE occupies the remaining space on the lateral side of the ilium between these other muscles and the edges of the iliac blade.

2.4.5 Mm. adductores femorum (ADD)

The Mm. adductores femorum 1–2 (ADD1–2) are a pair of pelvic muscles that originate from the ischium. The origin of ADD1 can be identified by striae coating the lateral surface of

the obturator process (Fig. 2.8A). The ischial shaft forms one boundary of this origin, which is otherwise restricted by the extent of the obturator process. Distally, the exact limit of the origin of ADD1 is unclear as striae are continuous onto the ischial apron, from which another pelvic muscle takes its origin. This division is estimated roughly at the junction between the obturator process and ischial apron.

On the posterodorsal edge of the ischial shaft, the origin of ADD2 is demarcated by a longitudinal groove (Fig. 2.8A,C). The origin of ADD2 is proximodistally elongate and adjacent to the origin of FTI3. Based on the extent of the longitudinal groove, it seems to terminate about halfway between the proximal and distal ischial tuberosities.

2.4.6 Mm. puboischiofemorales externi (PIFE)

The Mm. puboischiofemorales externi 1–3 (PIFE1–3) share similar functions and insertion points. Striations on the anterior surface of the pubic apron show the origin of PIFE1 (Fig. 2.8C–D). The anterior surface of the pubic shaft is largely devoid of this texture, which indicates that the origin was restricted to only the pubic apron, typical of non-avian theropods (Hutchinson 2001a). The origin of PIFE1 reaches the proximal end of the pubic apron and around the distal end of the pubic fenestra. It is unknown whether the pubic fenestra was hollow, filled with cartilage, covered by a membrane, or overlaid by another type of unpreserved soft tissue underneath the skin, so it is also unknown if the origin of PIFE1 covered this area too.

On the posterior side of the pubic apron, the origin of PIFE2 is similarly marked by striae (Fig. 2.8). Muscle scars may cover posteromedial parts of the pubic shafts, but the origin is more or less limited to the apron itself. Much like the first head of this muscle group, the second head had a proximal extent that matches the proximal edge of the pubic apron, and a distal extent

around the distal end of the pubic fenestra and base of the pubic boot. This condition is also exhibited by most non-avian theropods.

The origin of PIFE3 occupies the lateral surface of the ischial apron (Fig. 2.8A). Neighbouring the ADD1 to its anterior, the PIFE3 would have been restricted by this other muscle. Striations on the apron are continuous with those on the obturator process, making exact boundaries unclear. The origin of PIFE3 does not appear to cover the ischial shaft and is otherwise limited by the extent of the bone itself.

2.4.7 M. ischiotrochantericus (ISTR) and M. caudofemoralis brevis (CFB)

On the medial side of the ischium, the origin of M. ischiotrochantericus (ISTR) is at the proximal end toward the posterior side (Fig. 2.8C). Fleshy attachment and resultant lack of clear borders in extant relatives and non-avian theropods make it somewhat difficult to precisely reconstruct this muscle. However, CEUM 74717 has a subtle rugose texture in this area that may coincide with the origin of ISTR. Despite the inconsistency of the presence of this texture across other *Falcarius* material, it is of appropriate location and size compared to the origin of ISTR other theropods (Hutchinson 2001a, 2002, Carrano and Hutchinson 2002).

The shallow, narrow brevis fossa is the origin of CFB (Fig. 2.8B–C). Relative to more plesiomorphic theropods, the area of attachment and available volume for musculature is considerably reduced. However, the size of the brevis fossa is similar in some more derived theropods, especially caenagnathids. The CFB likely filled the entire brevis fossa, but did not encompass the lateral side of the ilium nor the posterior edge of the ischiadic peduncle.

2.5 Discussion

2.5.1 General remarks

Future directions could include a more detailed assessment of pelvic musculature within Therizinosauria. Identification and description of pelvic muscle attachment sites in the most basal member establishes a template for more derived members, or for expansion within *Falcarius* to include the entire hind limb for a more comprehensive study of locomotory adaptations. This study is qualitative by nature and would also be complemented by quantitative biomechanical analysis. Regardless, the data here create a framework for future research on musculature reconstruction and locomotion. Some aspects of this study are phylogenetically dependent and may change pending future discoveries. However, the inferences here are justified as reasonable given the general stability of Therizinosauria at or near the base of Maniraptora (Zanno 2010b, Pu et al. 2013, Xu et al. 2014, Hendrickx et al. 2015, Yao et al. 2019).

The pelvic musculature of *Falcarius* mimics its pelvic osteology, which deviates from the typical maniraptoran theropod bauplan, but generally maintains a similar layout. This also falls in line with other aspects of its anatomy, such as changes in the pectoral girdle (Zanno 2006), skull (Lautenschlager 2017), and diet (Zanno and Makovicky 2011). Iliac muscle origins track osteological changes in enlargement of the preacetabular portion and reduction in the postacetabular region. In turn, muscle origins of the deep dorsal group and others responsible for hip flexion and knee control are expanded, whereas those of extensors that drove locomotion (e.g. ILFB, posterior portion of IT2, IT3) are shrunken. A similar pattern probably occurs in caenagnathids with similarly proportioned ilia, but not in oviraptorids or ornithomimids with different pelvic anatomy (Zanno 2010a). Emphasis on leg flexors and knee control, especially in the face of extensor reduction, may indicate a change in posture and/or locomotory mode that

focused on stability over speed. Furthermore, the narrow and shallow brevis fossa drastically limits space available for the origin of the short head of the caudofemoral complex (CFB), which indicates tail muscles that functioned as extensors were similarly reduced. The origins of PIFI1 and PIFI2 appear to be distinctly separate, which differs from closely related, more plesiomorphic theropods. In ornithomimids, the cuppedicus fossa and PIFI2 origin are adjacent to the origin of PIFI1. Additionally, both the fossa and its associated muscle origin are posterior to—and separate from—the preacetabular hook. In contrast, the cuppedicus fossa of *Falcarius* appears less distinct because it lacks a medial wall. Thus, only about one quarter of the fossa is circumscribed by bone, which appears more like a concavity delineated by a low ridge rather than a proper fossa with a distinct medial shelf or wall (Fig. 2.3). The origin of PIFI2 also migrated anteriorly onto the medial side of the preacetabular hook and became further separated from the origin of PIFI1. Perhaps this reorganization of the deep dorsal group is linked to gradual changes in posture during theropod evolution and development of "knee-driven" locomotion (Hutchinson and Gatesy 2000, Allen et al. 2013, Bishop et al. 2018a). Muscles originating from the pubis are clarified with identification of the preacetabular tubercle and origin of AMB. The transversely broad pubic apron inherently provided more space for the first and second heads of the external puboischiofemoral muscle group. These muscles were primarily involved in femoral flexion with some capacity for lateral rotation, although the latter is likely limited given the propubic nature of *Falcarius* (Hutchinson and Gatesy 2000). On the ischium, crural flexor origins seem to be reduced, but other muscle attachment sites are unremarkable. These locomotory adaptations are not unexpected and in fact matches previously hypothesized changes in locomotory adaptations tied to dietary and postural changes (Zanno 2010a). However, some

aspects of locomotory musculature offer insight on the development of these changes both in Therizinosauria and more broadly in Maniraptora.

2.5.2 Evolutionary trends in Therizinosauria

Pelvic musculature reveals another perspective on locomotory adaptations in *Falcarius* along with other morphological features of therizinosaurians (Table 2.4). The clade exhibits a steady decrease in the proportion of distal limb segments (Zanno 2010a). This pattern is generally seen as an indicator of decreased running ability, which is emphasized when compared to highly cursorial theropods such as tyrannosaurids and troodontids (Persons and Currie 2016). Here, cursoriality is defined generally as running ability. High cursoriality can be identified by anatomical features such as elongate distal limb elements (tibiae and metatarsi), tight interlocking or fusion of metatarsal bones, and reduction of weight-bearing toes, among others (Lull 1904, Coombs 1978, Carrano 1999, de Bakker et al. 2013, Lovegrove and Mowoe 2014). This definition cannot discern running style as cursors that engage in either long-range running or sprinting share many of these adaptations, although examination of these features still provides insight on general running ability. *Falcarius* retains a tibia that is longer than the femur and an elongate metatarsus relative to the tibia (Table 2.4). Despite a distally positioned first toe, *Falcarius* also retains a tridactyl foot (Clark and Xu 2009, Botelho et al. 2017) as opposed to the tetradactyl nature of therizinosaurids. The addition of a functional pedal digit and relative shortening of distal limb segments in therizinosaurids both counter the expectation of adaptations for high cursoriality (Coombs 1978). The ratio of metatarsal to femoral length may be more closely related to home range (Carrano 1999), but a relatively long metatarsal still contributes to distal limb length and higher cursoriality (Lovegrove and Mowoe 2014) and reduction in this

ratio reflects a reduction in therizinosaurid cursoriality nonetheless. Two other features that remain fairly consistent throughout Therizinosauria, however, are moderate development of the fourth trochanter on the femur and lack of an arctometatarsus (Table 2.4) (Xu et al. 1999a, Zanno et al. 2009, Zanno 2010a, Pu et al. 2013, Yao et al. 2019). The fourth trochanter is the insertion site for the M. caudofemoralis longus, the counterpart to the CFB, which together formed the caudofemoral muscle complex that functioned in leg extension (Gatesy 1990, Hutchinson 2001b). More plesiomorphic theropods tend to rely on these extensors for a considerable portion of propulsion (Persons and Currie 2011). The estimated total number of caudal vertebrae and the number of those with transverse processes in *Falcarius* are in line with ornithomimids and dromaeosaurids (Gatesy 1990, Kirkland et al. 2005), but their morphologies vary considerably. Contrasting the dorsally elevated and angled transverse processes in ornithomimid anterior caudal vertebrae that provided more space for M. caudofemoralis longus attachment (Persons and Currie 2011), the transverse processes of the squat anterior caudals of *Falcarius* extend horizontally and are not dorsally elevated (Kirkland et al. 2005, Zanno 2010a). Therefore, the origin of M. caudofemoralis longus was reduced in *Falcarius* compared to ornithomimids. Modest development of caudofemoral musculature in therizinosaurians suggests it maintained a role in locomotion, albeit reduced compared to more plesiomorphic theropods. This is emphasized by reduction in the origin of CFB, represented by a narrow and shallow brevis fossa (Figs. 2.2, 2.8), which reveals that both parts of the caudofemoral complex were reduced in basal therizinosaurians. The arctometatarsus is considered an adaptation in animals well adapted for cursoriality (Holtz 1994, Snively et al. 2004). Therizinosaurians lack this structure (Table 2.4), which suggests they were not suited for fast running or high agility. A broad cnemial crest in *Falcarius* is reasonably comparable to typical theropods and acts to increase the leverage of the

triceps femoris group muscles that passed over it (Hutchinson 2002). Reduction of this feature throughout Therizinosauria (Zanno et al. 2009, Zanno 2010a) likely also reduced the extensor moment arm of such muscles and, consequently, running ability. This, combined with decreasing distal limb proportions through evolutionary time, may also be related to postural changes becoming more upright (Zanno 2010a). The distal displacement of the cranial tubercle of the fibula—the insertion site of the ILFB—may be related to these changes as well. The ILFB functioned to extend the leg and flex the knee (Hutchinson 2002). Reduction of its origin qualitatively suggests decreased strength, but distal displacement of the insertion site presumably also affected its moment arm. Perhaps this had a similar effect as the distal displacement of the fourth trochanter in hadrosaurs relative to tyrannosaurids, which gave the caudofemoral muscles more leverage for more efficient running in the former, but increased strength in the latter (Persons and Currie 2014). The distally displaced ILFB insertion in *Falcarius* relative to other theropods may have likewise increased its leverage at some expense of strength, although this requires testing and likely has more implications for knee rotation than hip rotation given that the ILFB inserted on the fibula. Combined with reduction of the CFB, ILFB, IT3, and other muscles involved in leg extension, *Falcarius* does not seem well adapted for cursoriality. This ability is progressively reduced even further throughout the evolutionary history of Therizinosauria.

A diminished cursorial ability leads to a discussion on predator avoidance strategies. If escape by means of running was not a feasible option, alternative measures were likely employed. Previous studies on inner ear length in therizinosaurians notes an increase in cochlear length (Smith et al. 2011, 2018). In reptiles and birds, this is a proxy for hearing ability whereby a longer cochlea is associated with more complex vocalizations and a higher degree of sociality (Walsh et al. 2009). Extrapolating from this suggests an increased likelihood of larger social

aggregations in therizinosaurians, which complements, but does not confirm, inferred sociality based on the paucispecific *Falcarius* bonebed (Kirkland et al. 2005, Smith et al. 2018). Although inferred gregarious behaviour in *Falcarius* is by no means unique among theropods (Currie 1998, Lockley and Matsukawa 1999, Roach and Brinkman 2007, Currie and Eberth 2010, Funston et al. 2016), the lessened cursorial capacity and inferred herbivory of *Falcarius*, and Therizinosauria by extension, may preclude pack hunting as the purpose of aggregation. Rather than gathering to find food, therizinosaurians may have done so to avoid becoming food. A putatively increased degree of vocal complexity and sociality would probably have been useful to communicate among larger groups to find safety in numbers. This proposition is admittedly tenuous, but would be consistent with reduced cursoriality.

2.5.3 Caudal decoupling and tail functional anatomy

Reduction in caudofemoral musculature also signals an intermediate stage in caudal decoupling, a process by which the caudofemoral muscles became functionally separated from extensive control of the hind limb during theropod evolution (Gatesy and Dial 1996). More plesiomorphic theropods have integrated pelvic and caudal muscles that operated the hind limb, whereas birds assimilate tail muscles into the flight apparatus (Gatesy and Dial 1996). Maniraptoran theropods occupy a grade between these two ends in which the tail and its musculature are intermediate, but still linked to the hind limb (Gatesy 1990). Changes in body and locomotor modules also experienced radical changes during the evolution of non-avian maniraptorans (Allen et al. 2013). Among these changes are an anterior shift in centre of mass and concurrent reduction in caudofemoral musculature. The tail of therizinosaurids convergently becomes reduced in the number and the anteroposterior length of caudal vertebrae (Zanno et al.

2009, Zanno 2010a), thereby reducing available space for caudofemoral musculature. Although transverse process length is not a good proxy for the size of the M. caudofemoralis longus, haemal spine length may offer insight (Persons and Currie 2011). The haemal spines of *Falcarius* (Kirkland et al. 2005, Zanno 2010a) appear reduced in relative length compared to those of ornithomimids and more plesiomorphic theropods (Gatesy 1990), which also suggests reduced space available for the M. caudofemoralis longus. Additionally, substantial reduction of the brevis fossa and CFB apparent in *Falcarius* shows that this trend was already well underway in basal therizinosaurians, and in both parts of this muscle group to boot. *Falcarius* also "approximates" the conditions of basal maniraptorans due to its phylogenetic position; although it does not represent the common ancestor of maniraptorans, it offers a reasonable interpretation of the conditions near the base of Maniraptora. This is admittedly phylogenetically dependent and warrants investigation of other closely related members, like alvarezsaurs, that were not examined in this study. Substantial reduction of the caudofemoral musculature corroborates a locomotor transition within Maniraptora, but reveals that it began well before Eumaniraptora as conservatively reported previously (Allen et al. 2013). These morphological features are rather similar to closely related caenagnathids but are in stark contrast to the condition of ornithomimids and tyrannosaurids. Instead of a smooth, gradual transition, the state in *Falcarius* suggests a more punctuated step in tail reduction and caudal decoupling near the base of Maniraptora than previously reported. That being said, the conditions in *Falcarius* are still largely consistent with the general model of caudal decoupling and the stepwise acquisition of avian-like features (Hutchinson and Allen 2009).

Besides evidence of partial caudal decoupling, another aspect of therizinosaurian tail functionality may be better elucidated by exceptional fossil preservation. To date, the closest

relatives of *Falcarius* are the therizinosaurian *Jianchangosaurus* and the most basal therizinosauroid *Beipiaosaurus* (Zanno 2010b, Pu et al. 2013, Yao et al. 2019). The latter two are known from fossils that preserved impressions of elongate broad filamentous feathers (Xu et al. 2009, Pu et al. 2013). Due to their morphology and distribution, feathers of this type are inferred to primarily function in display (Xu et al. 2009). Further to this, a pygostyle-like structure is present in *Beipiaosaurus* (Xu et al. 2003a). Rectrices are not apparent and in this case lack of fossilization may in fact represent true absence given the preservation of other, densely packed integument on the tail. Curiously, the opposite condition—preserved rectrices but no pygostyle—is present in the oviraptorosaurian *Caudipteryx* (Xu et al. 2003a). The inferred function of this tail feather fan is also display, supported by adequate tail musculature to manipulate such a structure (Persons et al. 2014). However, *Falcarius* lacks both a pygostyle-like structure and direct evidence of feathers, so similarities in tail structure may be convergent between therizinosaurians and oviraptorosaurians (Persons et al. 2014, Persons and Currie 2019). Regardless, therizinosaurians and oviraptorosaurians exhibit similarities in potential tail function that cannot currently be determined as either convergent or shared. Although modifications at the distal end of the tail differ between these groups, reduction at the proximal end inferred from reduction of the CFB offers some insight. Caudal muscles that were tightly integrated with locomotion in earlier theropod groups are somewhat freed up for other functions—such as display—in therizinosaurians and oviraptorosaurians. In this way, partial caudal decoupling may have permitted other caudal adaptations in each clade. This does not necessarily mean that partial caudal decoupling itself should be treated as evidence for tail functions such as display. Instead, it simply suggests that the possibility was reasonable, and perhaps plausible if in tandem with other structures more closely linked to a given function. In this case, the potential for tail use

other than locomotion is also congruent with the presence of feathers likely used for display (Xu et al. 2009). However, differences in Oviraptorosauria, such as the presence of a tail feather fan in some taxa, require another explanation. Oviraptorosaurians are the most basal theropods with evidence of pennaceous feathers, which united them and Paraves into the clade Pennaraptora (Xu et al. 2010b, Foth et al. 2014). Therizinosaurians diverge prior to this group and remain without evidence of pennaceous feathers even with good preservation in some specimens (Xu et al. 2003a, 2009). The presumed primary function is display for both elongate broad filamentous feathers in therizinosaurians immediately prior to the divergence of Pennaraptora, and in oviraptorosaurians immediately following (Xu et al. 2009, Foth et al. 2014). Persons and Currie (2019) suggested that sexual selection drove the elaboration of feathers in coelurosaurians, which is congruent with a primary function for display. Hence, therizinosaurians and oviraptorosaurians may have exhibited similarities not only in tail display functions, but also in pelvic osteology, partial caudal decoupling, and tail structure.

2.6 Summary of *Falcarius* pelvic myology

The pelvic myology of *Falcarius* is reconstructed with reference to other theropods and the closest living relatives. Pelvic musculature of *Falcarius* represents expected conditions given its phylogenetic position as a basal therizinosaurian and maniraptoran. For this reason, this reconstruction also approximates the conditions of the common ancestor of Therizinosauria and, to some extent, Maniraptora. Locomotory musculature tracks changes in pelvic proportions, hind limb ratios, and other anatomical changes suggestive of decreased cursoriality. Derived therizinosaurians experienced further reduction in cursorial ability, accompanied by exaggerated features of the pelvis, hind limb, and other parts of the skeleton already divergent from the

typical theropod bauplan in *Falcarius*. This is supported by simultaneous reduction in caudal musculature, which also indicates that basal maniraptorans may have experienced a punctuated onset of caudal decoupling that continued during their evolutionary history. This functional study corroborates previously hypothesized changes in posture and locomotion of early therizinosaurians and shows that locomotory musculature is not independent of other palaeobiological changes. Modifications to locomotory adaptations are consistent with, but do not themselves corroborate, the possibility that therizinosaurians may have employed anti-predator strategies that relied more on social behaviours than on running ability.

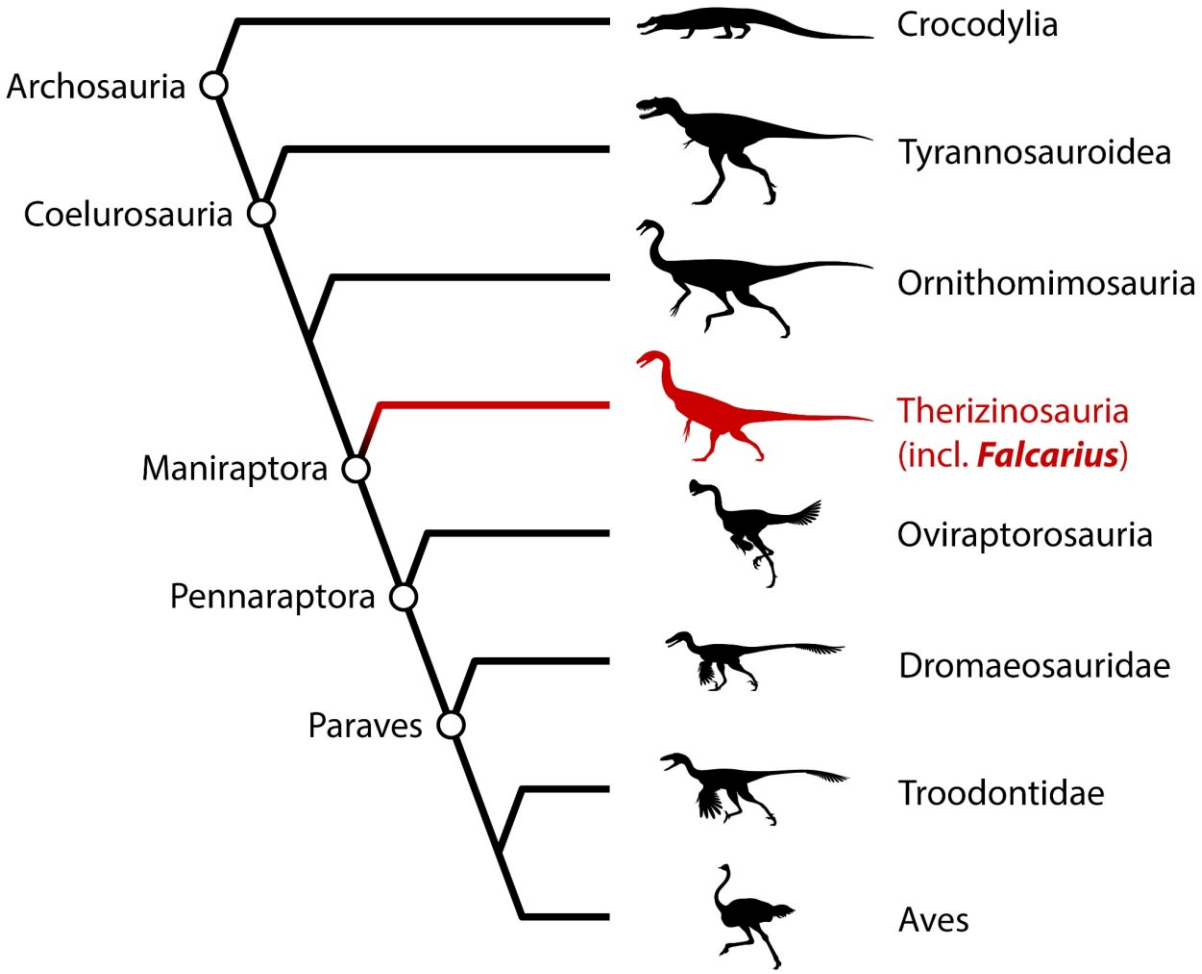

Figure 2.1. Simplified phylogeny of *Falcarius* among Archosauria. Phylogeny includes other contemporaneous, extinct theropods and representatives of its Extant Phylogenetic Bracket (Crocodylia and Aves).

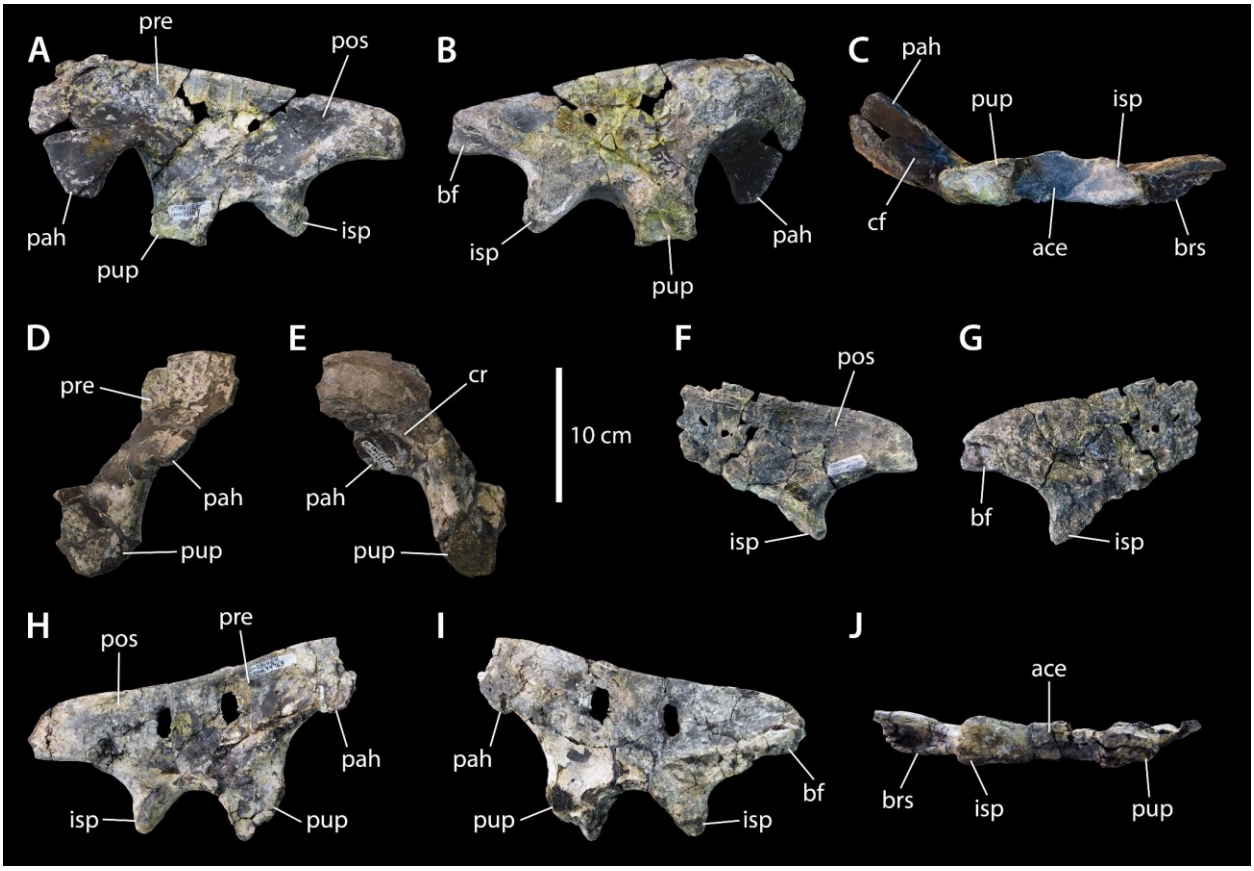

Figure 2.2. *Falcarius* ilia examined for muscle attachment sites. Limited to well preserved material (see Table 2.1 for observed material). Left ilium of *Falcarius* sp. (CEUM 77189) in lateral (A), medial (B), and ventral (C) views. Right ilium of *Falcarius* sp. (CEUM 53312) in lateral (D) and medial (E) views. Left ilium of *Falcarius* sp. (CEUM 78223) in lateral (F) and medial (G) views. Right ilium of *Falcarius* sp. (CEUM 74763) in lateral (H), medial (I), and ventral (J) views. Scale bar is 10 cm and applies to all images. **Abbreviations: ace,** acetabulum; **bf,** brevis fossa; **brs,** brevis shelf; **cf,** cuppedicus fossa; **cr,** cuppedicus ridge; **isp,** ischiadic peduncle; **pah,** preacetabular hook; **pos,** postacetabulum; **pre,** preacetabulum; **pup,** pubic peduncle.

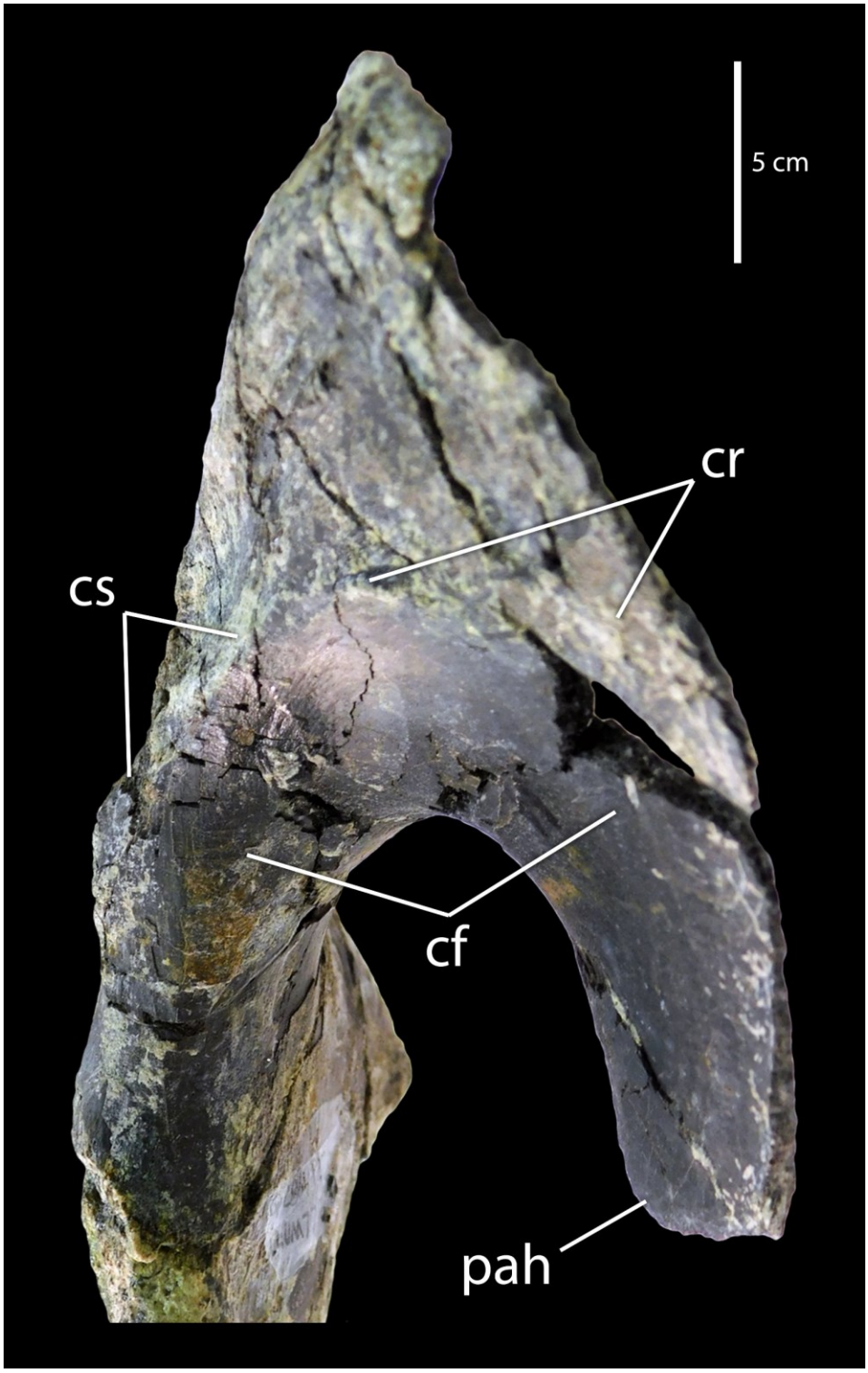

Figure 2.3. Cuppedicus fossa of *Falcarius*. Left ilium of *Falcarius* sp. (CEUM 77189) in anterior view. Scale bar is 5 cm. **Abbreviations: cf,** cuppedicus fossa; **cr,** cuppedicus ridge; **cs,** cuppedicus shelf; **pah,** preacetabular hook.

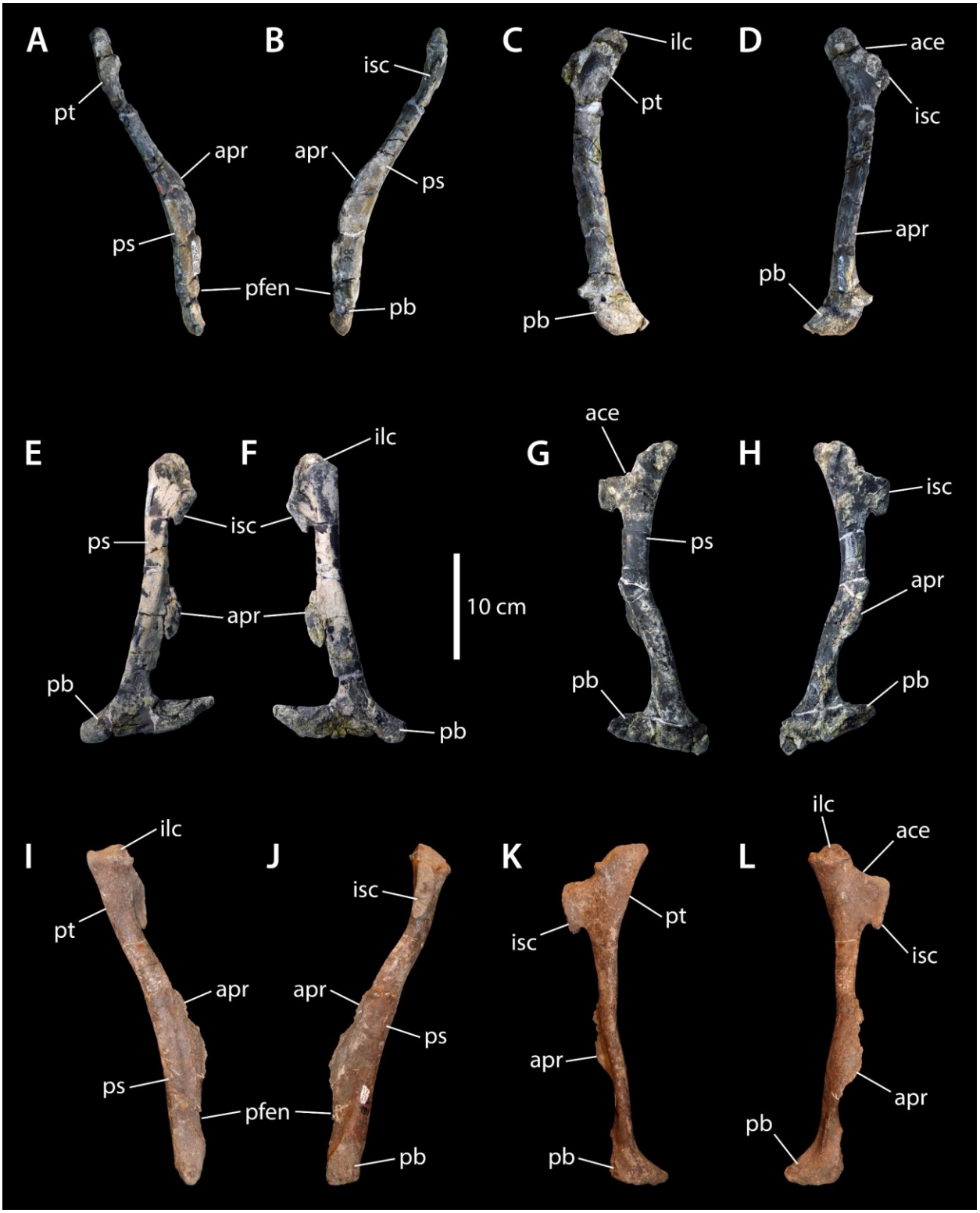

Figure 2.4. *Falcarius* pubes examined for muscle attachment sites. Limited to well preserved material (see Table 2.1 for observed material). Right pubis of *Falcarius* sp. (CEUM 52424) in

anterior (A), posterior (B), lateral (C), and medial (D) views. Slightly taphonomically distorted left pubis of *Falcarius* sp. (CEUM 77195) in lateral (E) and medial (F) views. Right pubis of *Falcarius* sp. (CEUM 77233) in lateral (G) and medial (H) views. Right pubis of *Falcarius utahensis* (Courtesy of Natural History Museum of Utah, UMNH VP 14540) in anterior (I), posterior (J), lateral (K), and medial (L) views. Scale bar is 10 cm and applies to all images. **Abbreviations: ace,** acetabulum; **apr,** pubic apron; **ilc,** iliac contact; **isc,** ischiadic contact; **pb,** pubic boot; **pfen,** pubic fenestra; **ps,** pubic shaft; **pt,** preacetabular tubercle.

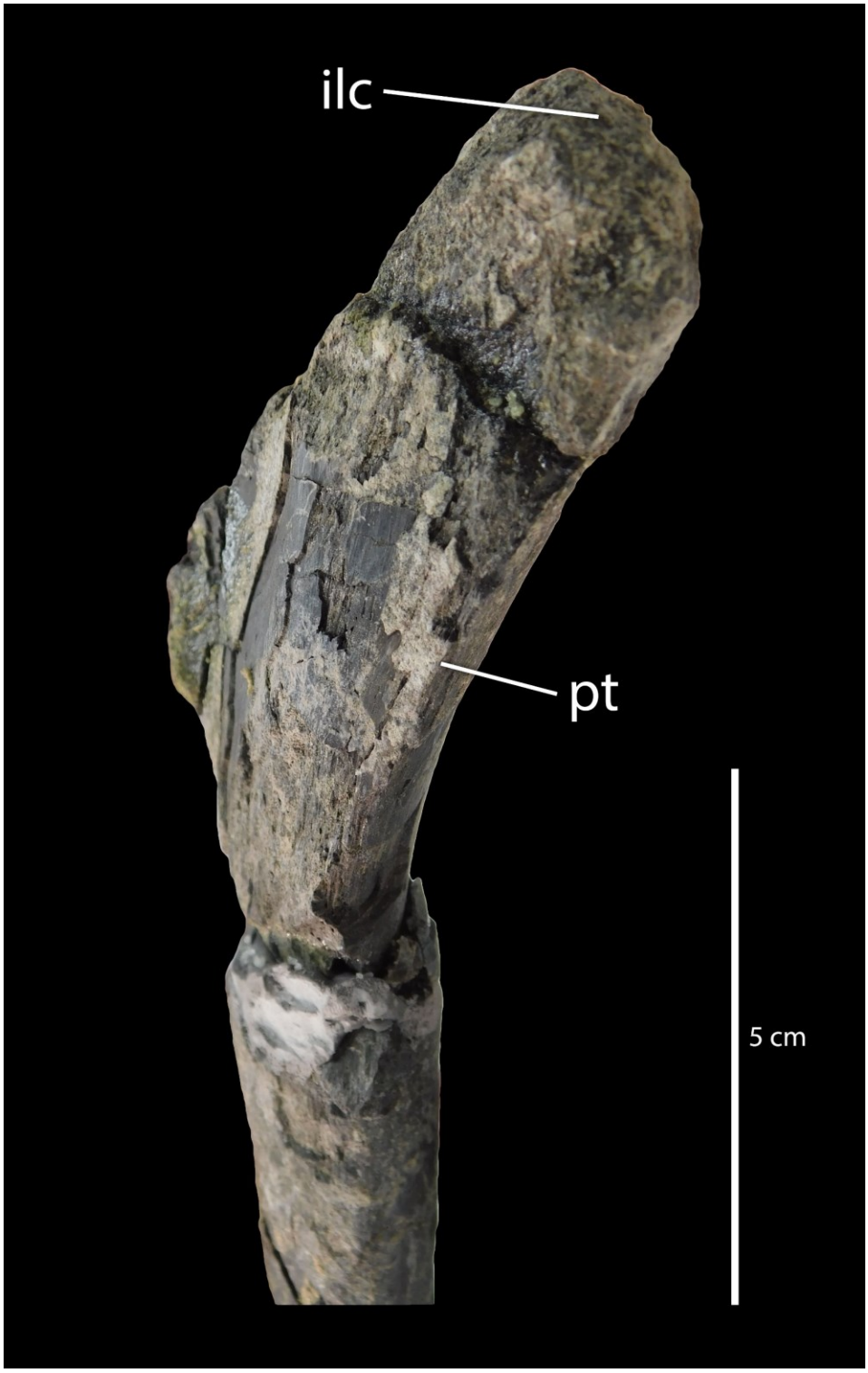

Figure 2.5. Proximal portion of the pubis of *Falcarius*. Right pubis of *Falcarius* sp. (CEUM 52424) in anterolateral view. Scale bar is 5 cm. **Abbreviations: ilc,** iliac contact; **pt,** preacetabular tubercle.

Figure 2.6. *Falcarius* ischia examined for muscle attachment sites. Limited to well preserved material (see Table 2.1 for observed material). Right ischium of *Falcarius* sp. (CEUM 52482) in lateral (A) and medial (B) views. Right ischium of *Falcarius* sp. (CEUM 74717) in lateral (C) and medial (D) views. Left ischium of *Falcarius utahensis* (Courtesy of Natural History Museum of Utah, UMNH VP 12374) in lateral (E), medial (F), posterodorsal (G), and anteroventral (H) views. Scale bar is 10 cm and applies to all images. **Abbreviations: dist,** distal ischial tuberosity; **ilc,** iliac contact; **isa,** ischial apron; **iss,** ischial shaft; **op,** obturator process; **pist,** proximal ischial tuberosity; **puc,** pubic contact.

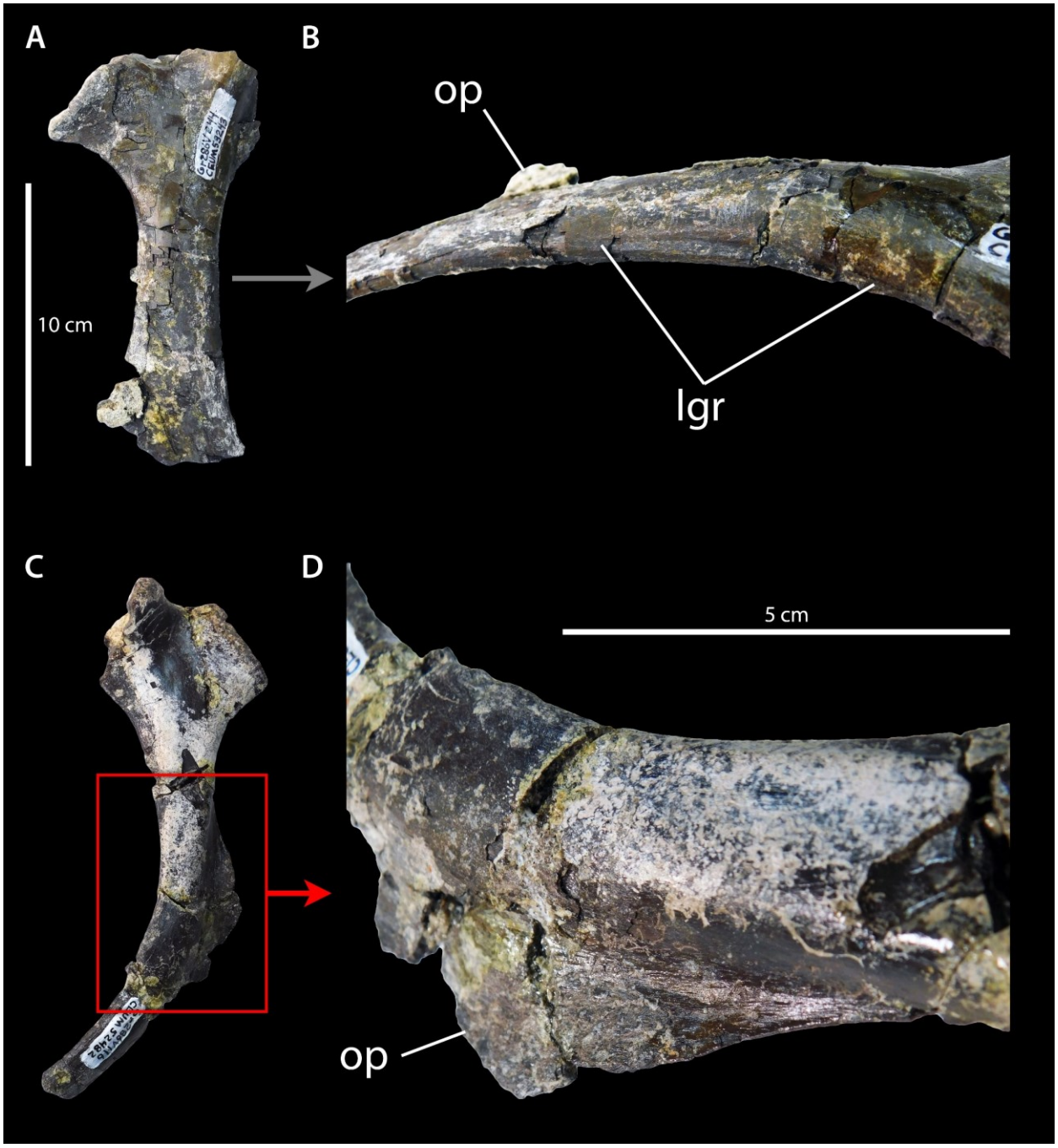

Figure 2.7. Osteological correlates on *Falcarius* ischia. Left ischium of *Falcarius* sp. (CEUM 53243) in lateral view (A) with close-up of posterodorsal edge of ischial shaft (B) showing shallow, longitudinal groove. Right ischium of *Falcarius* sp. (CEUM 52482) in lateral view (C) with close-up of obturator process (D) showing striae. Scale bar is 10 cm for A–C, and 5 cm for D. **Abbreviations: lgr,** longitudinal groove; **op,** obturator process.

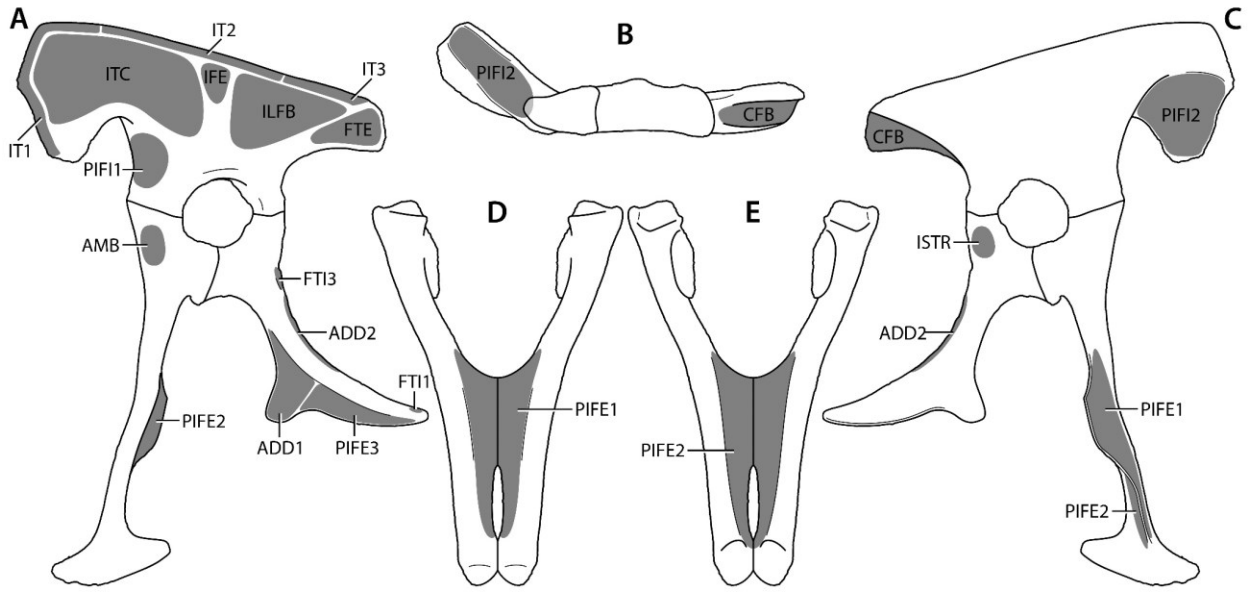

Figure 2.8. Pelvic myology of *Falcarius*. Pelvis in lateral view (A), ilium in ventral view (B), pelvis in medial view (C), and pubes in anterior (D) and posterior (E) views. The reconstructed pelvis is a composite based on *Falcarius* sp. (CEUM 77189, ilium; CEUM 74717, ischium) and *Falcarius utahensis* (Courtesy of Natural History Museum of Utah, UMNH VP 14540, pubis). Pelvic bones were scaled to match based on contact surfaces with reference to previous reconstructions (Zanno 2010a) and a CEUM pelvis cast. **Abbreviations: ADD1,** M. adductor femoris 1; **ADD2,** M. adductor femoris 2; **AMB,** M. ambiens; **CFB,** M. caudofemoralis brevis; **FTE,** M. flexor tibialis externus; **FTI1,** M. flexor tibialis internus 1; **FTI3,** M. flexor tibialis internus 3; **IFE,** M. iliofemoralis externus; **ILFB,** M. iliofibularis; **ISTR,** M. ischiotrochantericus; **IT1,** M. iliotibialis 1; **IT2,** M. iliotibialis 2; **IT3,** M. iliotibialis 3; **ITC,** M. iliotrochantericus caudalis; **PIFE1,** M. puboischiofemoralis externus 1; **PIFE2,** M. puboischiofemoralis externus 2; **PIFE3,** M. puboischiofemoralis externus 3; **PIFI1,** M. puboischiofemoralis internus 1; **PIFI2,** M. puboischiofemoralis internus 2.

Table 2.1. Pelvic material examined for muscle attachment sites. Note: CEUM, College of Eastern Utah Museum; RM, Redpath Museum; ROM, Royal Ontario Museum; UAMZ, University of Alberta Museum of Zoology; UMNH VP, Utah Museum of Natural History.

Taxon	Specimen number	Status and element(s)
Therizinosauria		
Falcarius utahensis	UMNH VP 12370, 12371, 12374, 14540, 14659, no # (juvenile pubis), UMNH VPC 639	Fossil (cast for UMNH VPC 639); disarticulated pubes and ischia
Falcarius sp.	CEUM 52424, 52482, 52520, 53243, 53252, 53305, 53312, 53349, 53361, 73681, 73709, 73963, 73964, 74706, 74717, 74727, 74739, 74763, 74794, 74842, 77035, 77037, 77045, 77051, 77053, 77081, 77114, 77173, 77189, 77194, 77195, 77233, 77241, 77290, 78223	Fossil; disarticulated ilia, pubes, and ischia
Nothronychus graffami	UMNH VP 16420	Fossil; disarticulated pelvis (ilia not seen)
Aves		
Apteryx haastii	RM 8369	Articulated skeleton mount
Corvus corax	UAMZ (uncatalogued)	Dissected
Dromaius novaehollandiae	ROM R6843, ROM R7654, UAMZ B-FIC2014.260	Disarticulated, associated skeletons (ROM); articulated skeleton mount (UAMZ)
Gallus gallus	RM 8355	Articulated skeleton mount
Rhea americana	RM 8499	Disarticulated, associated skeleton
Struthio camelus	ROM 1080, ROM 1162, ROM 1933, ROM 2136, ROM 2305, UAMZ 7159	Disarticulated, associated skeletons
Crocodylia		
Alligator mississippiensis	ROM R343	Postcranial skeleton
Alligator sp.	UAMZ HER-R654	Articulated skeleton mount
Caiman crocodilus	RM 5242; UAMZ (uncatalogued)	Disarticulated, associated skeleton (RM), dissected (UAMZ)
Osteolaemus tetraspis	RM 5216	Articulated skeleton mount

Squamata		
Tupinambis teguixin	ROM R436	Semi-prepared skeleton
Varanus albigularis	RM 5220	Disarticulated, associated skeleton
Varanus exanthematicus	UAMZ (uncatalogued)	Dissected
Varanus jobiensis	RM 5219	Disarticulated, associated skeleton
Varanus komodoensis	ROM R7565	Disarticulated, associated skeleton
Varanus niloticus	RM 5221	Disarticulated, associated skeleton
Varanus rudicollis	ROM R7318	Articulated skeleton mount
Varanus salvator	RM 5222, RM 5223, RM 5224	Disarticulated, associated skeleton

Table 2.2. Pelvic muscle homologies in crocodylians and avians. Modified from Carrano and Hutchinson (2002) and Hutchinson et al. (2005).

Crocodylia	Aves
Triceps femoris	
M. iliotibialis 1 (IT1)	M. iliotibialis cranialis (IC)
M. iliotibialis 2, 3 (IT2, IT3)	M. iliotibialis lateralis (IL)
M. ambiens (AMB)	M. ambiens (AMB)
M. iliofibularis (ILFB)	M. iliofibularis (ILFB)
Deep dorsal group	
M. iliofemoralis (IF)	M. iliofemoralis externus (IFE) + M. iliotrochantericus caudalis (ITC)
M. puboischiofemoralis internus 1 (PIFI1)	M. iliofemoralis internus (IFI)
M. puboischiofemoralis internus 2 (PIFI2)	M. iliotrochantericus cranialis (ITCR) + M. iliotrochantericus medius (ITM)
Flexor cruris group	
M. puboischiotibialis (PIT)	(absent)
M. flexor tibialis internus 1 (FTI1)	(absent)
M. flexor tibialis internus 2 (FTI2)	(absent)
M. flexor tibialis internus 3 (FTI3)	M. flexor cruris medialis (FCM)
M. flexor tibialis internus 4 (FTI4)	(absent)
M. flexor tibialis externus (FTE)	M. flexor cruris lateralis pars pelvica (FCLP)
Mm. adductores femorum	
M. adductor femoris 1 (ADD1)	M. puboischiofemoralis pars medialis (PIFM)
M. adductor femoris 2 (ADD2)	M. puboischiofemoralis pars lateralis (PIFL)
Mm. puboischiofemorales externi	
M. puboischiofemoralis externus 1 (PIFE1)	M. obturatorius lateralis (OL)
M. puboischiofemoralis externus 2 (PIFE2)	M. obturatorius medialis (OM)
M. puboischiofemoralis externus 3 (PIFE3)	(absent)
M. ischiotrochantericus (ISTR)	M. ischiofemoralis (ISF)
Mm. caudofemorales	
M. caudofemoralis brevis (CFB)	M. caudofemoralis pars pelvica (CFP)
M. caudofemoralis longus (CFL)	M. caudofemoralis pars caudalis (CFC)

Table 2.3. Pelvic muscles inferred as present in *Falcarius*. Muscles originating from the pelvis are listed by functional/anatomical group. Modified from Carrano and Hutchinson (2002) using levels of inference based on Witmer (1995).

Muscle	Origin	Level of inference
Triceps femoris		
IT1	Lateral surface of anterodorsal margin of ilium	(I)
IT2	Dorsolateral surface of dorsal margin of ilium	(I)
IT3	Dorsolateral surface of postacetabular margin of ilium	(I)
AMB	Near preacetabular tubercle	(I)
M. iliofibularis		
ILFB	Lateral surface of postacetabular portion of ilium between IFE and FTE	(I')
Deep dorsal group		
IFE	Lateral surface of ilium between ITC and ILFB	(I)
ITC	Lateral surface of preacetabular portion of ilium	(I)
PIFI1	Shallow depression on anterolateral surface of pubic peduncle of ilium	(II)
PIFI2	Cuppedicus fossa of ilium including medial side of preacetabular hook	(II)
Flexor cruris group		
FTI1	Tubercle on dorsal edge of ischial shaft at distal end	(II')
FTI3	Faint scar distal to ISTR on dorsal edge of ischial shaft	(II)
FTE	Posterolateral corner of ilium, posterior to ILFB	(I)
Mm. adductores femorum		
ADD1	Anteroventral portion of lateral surface of obturator process	(I')
ADD2	Faint scar distal to FTI3 on dorsal edge of ischial shaft	(II)
Mm. puboischiofemorales externi		
PIFE1	Anterior surface of pubic apron	(II)
PIFE2	Posterior edges of pubic shafts	(II)
PIFE3	Ischial apron and posterior portion of obturator process, distal to ADD1	(II)
M. ischiotrochantericus		
ISTR	Medial side of ischium at proximal end, near iliac contact	(II)
Mm. caudofemorales		
CFB	Brevis fossa of ilium	(II)

Table 2.4. Morphological features associated with locomotion. Features are provided for *Falcarius* representing basal Therizinosauria, *Beipiaosaurus* for basal Therizinosauroidea, and generally for derived therizinosaurians. *Some data summarized from a previous description (Zanno 2010a).

Feature	**State in *Falcarius* (Therizinosauria)**	**State in *Beipiaosaurus* (Therizinosauroidea)**	**State in Therizinosauridae**
*Relative femoral length to tibial length	Femur < tibia	Subequal	Femur > tibia
*Proportion of metatarsus length to tibial length	45%	39%	32–37%
Functional pedal digits	3	3	4
Fourth trochanter	Moderately developed	Moderately developed	Moderately developed
Arctometatarsus	Absent	Absent	Absent
*Cnemial crest	Broad, prominent	?	Reduced, laterally deflected
*Cranial tubercle of fibula (insertion of M. iliofibularis)	?distally positioned sensu Zanno (2010a)	?	Distally positioned

Chapter 3. Pelvic myology and locomotion of Caenagnathidae

3.1 Introduction

Caenagnathids were strikingly bird-like, oviraptorosaurian theropods that occupy a basal position within Pennaraptora (Fig. 3.1) (Osmólska 1976, Hendrickx et al. 2015). Members of Caenagnathidae are predominantly found in North America and characterized by an edentulous beak with fused mandibles, a short tail, and elongate fingers and hind limbs. Caenagnathid material is often fragmentary or isolated, but recent discoveries such as *Anzu wyliei* (Lamanna et al. 2014) provide associated material that exemplifies these characters. In typical caenagnathids the pelvis, an attachment site for many locomotory muscles and structural support for the entire body, possesses ilia with longer preacetabular blades than postacetabular blades (Osmólska et al. 2004), nearly straight-shafted pubes, and plate-like ischia each with a triangular obturator process.

Previous studies on caenagnathid locomotion have focused on relative limb proportions or metatarsus anatomy (Holtz 1994, Carrano 1999, Snively et al. 2004). Muscles play a vital role in locomotion, so reconstructing soft tissue can reveal adaptations otherwise unseen by strictly observing osteology. Muscles anchor to bone directly or through tendons (Romer 1962), which often leaves osteological correlates that indicate former attachment sites (Nicholls and Russell 1985, Rothschild et al. 2015). These correlates have been used to recreate theropod pelvic musculature, with mixed success, for allosauroids (Bates et al. 2012, Bates and Schachner 2012), dromaeosaurids (Perle 1985, Hutchinson et al. 2008), ornithomimids (Russell 1972, Bates and Schachner 2012), troodontids (Bishop et al. 2018a), and tyrannosaurids (Romer 1923a, 1923b, 1923c, Tarsitano 1983, Perle 1985, Carrano and Hutchinson 2002, Hutchinson et al. 2005).

Similar studies on archosaur pelvic and hind limb soft tissues are aimed toward macro-scale evolutionary trends and include non-caenagnathid oviraptorosaurs (Hutchinson 2001a, 2001b, 2002). Additionally, caenagnathids occupy an intriguing taxonomic position with respect to theropod locomotor module evolution and decoupling of pelvic and caudal musculature (Gatesy and Dial 1996). However, caenagnathids cannot be placed in this context without locomotory muscle reconstruction.

The long hind limbs and large feet of *Chirostenotes pergracilis* were suggested as suitable for wading (Currie and Russell 1988). This proposition was supported with sedimentological evidence for a preference toward wetter environments in caenagnathids based on burial in sediments associated with mesic habitats (Lamanna et al. 2014). Conversely, Osmólska et al. (2004) interpreted the slender hind limbs of oviraptorosaurs as a cursorial adaptation. Caenagnathids were also interpreted as highly cursorial due to metatarsus structure (Holtz 1994, Snively et al. 2004) and limb proportions (Carrano 1999). Although wading and cursoriality are not mutually exclusive, the locomotion and lifestyle of this enigmatic clade remains controversial.

To address these shortcomings, caenagnathid pelvic material is described to identify general anatomical features and myological correlates. Pelvic morphology can give useful insight into locomotor behaviour and lifestyle in living (Ibáñez and Tambussi 2012) and recently extinct (Degrange 2017) theropods, and may provide a better understanding of their Mesozoic ancestors. The first reconstruction of caenagnathid pelvic musculature is used to make functional inferences on locomotion and forms a foundation for future biomechanical studies.

3.2 Materials and Methods

Caenagnathid pelvic material (Table 3.1) was inspected for morphology and osteological correlates of soft tissue attachment. Osteological descriptions summarize previous works on caenagnathid pelvic anatomy (Currie and Russell 1988, Lamanna et al. 2014, Currie et al. 2015, Funston et al. 2015, Funston and Currie 2016). Because caenagnathid species are poorly known and there is minor variation in pelvic morphology across the family, the aim of this study is to uncover general muscle arrangement and functional trends at the familial level. Although an articulated caenagnathid pelvis has not yet been discovered, the reconstruction here is derived from observation of well preserved, disarticulated elements and their contact surfaces with reference to literature (Currie and Russell 1988, Sues 1997, Barsbold et al. 2000, Clark et al. 2001, Lü 2002, Lü et al. 2004, 2013, 2017, Sullivan et al. 2011, Xu et al. 2013, Lamanna et al. 2014, Funston et al. 2018).

Soft tissue inferences employ the Extant Phylogenetic Bracket, using the closest living relatives of the focal taxon to offer the best evidence for the presence or absence of muscles (Bryant and Russell 1992, Witmer 1995). Comparative techniques similar to those of previous dinosaur pelvic muscle reconstruction studies are used to infer soft tissue attachment based on osteological correlates (Hutchinson 2001a, Carrano and Hutchinson 2002, Hutchinson et al. 2005, 2008, Maidment et al. 2014a). Dissections of a savannah monitor (*Varanus exanthematicus*), a spectacled caiman (*Caiman crocodilus*), and a common raven (*Corvus corax*) were undertaken to observe soft tissue arrangement in extant relatives. Comparative crocodylian and avian material was examined to identify osteological correlates in extant archosaurs, additionally observing squamate material as an outgroup (Table 3.1). This was supplemented with review of homology and reconstructions of archosaur pelvic musculature (Table 3.2)

(Romer 1923a, Hutchinson 2001a, Carrano and Hutchinson 2002, Gangl et al. 2004, Hutchinson et al. 2005, 2008, Smith et al. 2006, 2007). Inferences on soft tissue were categorized according to Witmer (1995) and limited to include only those that meet a Level I, I', II, or II' inference to reconstruct soft tissue in Caenagnathidae (Table 3.3). Level III and III' inferences were omitted to avoid excessive speculation.

Soft tissue reconstruction is limited to the pelvis as the main objective is to understand the effect of hind limb flexors (protractors) and extensors (retractors) on locomotion. These proximal limb muscles have a primary relationship to locomotory function and adaptations as they control the entire limb, whereas lower limb muscles serve mainly to manipulate more distal elements within the limb. Although the area of muscle origin or insertion is variably reliable at predicting muscle size or strength (Bryant and Seymour 1990, Barrett and Maidment 2017), it provides a rough estimate that is useful to make comparative inferences between taxa.

Measurements of pelvic elements (Fig. 3.8) were recorded using a ruler or measuring tape (Table 3.4). Photographs were taken with a digital camera and illustrations were generated using Adobe Photoshop CS6 and a Wacom drawing tablet.

3.3 Morphology of the pelvic girdle

Examination of pelvic material of *Chirostenotes pergracilis* (Currie and Russell 1988, Sues 1997), *Epichirostenotes curriei* (Sues 1997, Sullivan et al. 2011), and several indeterminate caenagnathids (Table 3.1) reveals evidence of former muscle attachments. Observed material is broadly similar to other caenagnathids such as *Anzu wyliei* (Lamanna et al. 2014) and *Gigantoraptor erlianensis* (Xu et al. 2007). This material is also readily comparable to some non-caenagnathid oviraptorosaurs like *Nomingia gobiensis* (Barsbold et al. 2000). Typical pelvic

morphology is described by each pelvic bone to identify major features and osteological correlates following those of other oviraptorosaurs (Barsbold et al. 2000, Lamanna et al. 2014).

Caenagnathid ilia are dolichoiliac in that each has a relatively long preacetabular process (Fig. 3.2). The preacetabular process tends to be slightly anteroposteriorly longer and dorsoventrally taller than the postacetabulum. Despite their incomplete nature, the ilia of *Chirostenotes pergracilis* (Fig. 3.2A–C) and TMP 1992.036.0674 (Fig. 3.2J–L) each have an intact postacetabulum that is either equal to, or shorter than, the anteroposterior length of what is preserved of the preacetabulum (Table 3.4). Therefore, if the rest of the preacetabular portions of these ilia were preserved, each would be longer than the corresponding postacetabulum. In UALVP 59791, the preacetabulum is mostly intact and preserves a rounded preacetabular hook (Fig. 3.2S). This hook forms the lateral boundary of the cuppedicus fossa (Fig. 3.2). Much of the cuppedicus fossa is smooth, although a small concavity and shallow ridge are present on the medial side of the preacetabular hook. The iliac margin is gently convex along the anterior and dorsal edges of the preacetabulum in lateral view. The dorsal margin of the postacetabulum is relatively straight and oriented anterodorsal-posteroventral, and the postacetabular ala tapers moderately toward the posterior edge when viewed laterally. Along the iliac margin are striae or rugosities, which terminate just anterior to the posterior edge of the blade. In lateral view, the posterior end of the blade may be triangular, as in *Chirostenotes pergracilis* (Fig. 3.2A) and TMP 1998.093.0013 (Fig. 3.2M), rounded as in TMP 1992.036.0674 (Fig. 3.2J), or square as in other Caenagnathidae indet. (Fig. 3.2D,G,P). The lateral surface of the blade is generally smooth. Only at the posterolateral corner is a triangular to rectangular patch of slightly rugose texture. This patch extends no further anteriorly than about halfway between the ischiadic peduncle and posterior end of the ilium. The ischiadic peduncle (Fig. 3.2) is mediolaterally wide and

anteroposteriorly short. It is typically triangular in medial or lateral view, and its contact surface is semicircular in ventral view. Conversely, the pubic peduncle (Fig. 3.2) is mediolaterally narrow and anteroposteriorly long. On its anterolateral surface is a shallow depression. Opposite the acetabulum, the brevis shelf forms a concave dorsal boundary of the brevis fossa (Fig. 3.2). Caenagnathids typically have a modestly sized brevis fossa compared to other non-avian theropods. It is not as spacious as in more plesiomorphic theropods such as tyrannosaurids (Hutchinson et al. 2005), but comparable to that of the basal therizinosaurian *Falcarius utahensis* (Zanno 2010a). The caenagnathid brevis fossa is larger than in more derived theropods such as dromaeosaurids (Hutchinson et al. 2008). Oddly, the brevis fossa of TMP 1992.036.0674 is highly reduced, even compared to other caenagnathids. However, this is probably a pathological artefact resulting from swelling of its brevis shelf (Fig. 3.2K).

The caenagnathid pubis is characterized by a fossa on the medial side of the proximal end of the bone (Sullivan et al. 2011) (Fig. 3.3). In anterior view, the shaft is somewhat sinuous with the proximal end bowed laterally, although TMP 1982.016.0275 (Fig. 3.3E–H) is nearly straight-shafted. Viewed laterally, the proximal portion of the pubis is anteriorly concave, but straight along its distal portion. The iliac contact is separated from the ischiadic contact by about one-quarter of the acetabulum (Fig. 3.3). In UALVP 55638 (Fig. 3.3O–Q), there is a low, rounded eminence on the lateral side of the proximal end of the shaft. This preacetabular tubercle is not clearly expressed in other specimens, possibly due to taphonomic damage in *Epichirostenotes curriei* and to smaller size in the other specimens. It is sometimes associated with a nearby oval patch of lightly rugose texture, which is also variably clear, anterior and ventral to the centre of the acetabulum. The pubic apron is composed of a pair of shelves (Fig. 3.3) that together form a transverse sheet of bone that spans the gap between the right and left pubes. In articulated pubes,

the apron has a concave proximal margin and extends approximately one-third the total proximodistal length of the shaft (Fig. 3.3I,K,P,Q). The apron is offset toward the anterior surface of the shaft. This results in the anterior surfaces of the apron and shafts being nearly flat, whereas the posterior surface of the apron forms an embayment. The anterior surface of the apron is also covered with striations, but the posterior surface is smooth and untextured. Instead, the posterior edges of the shafts are covered in similar striae and small rugosities.

As exemplified by the ischium of *Anzu wyliei* (Lamanna et al. 2014), caenagnathid ischia are generally boomerang-shaped bones that are only about half the lengths of the pubes (Fig. 3.4). A triangular obturator process projects ventromedially from the shaft roughly halfway along its proximodistal length. The apex of the obturator process is pointed anteroventrally in lateral view (Fig. 3.4A,G), which gives the anterior margin of the ischium a concave outline. Posteriorly, the obturator process is confluent with the ischial apron, a thin plate of bone that extends to the distal tip of the ischium (Fig. 3.4). Striations and scarring are evident along parts of the anterolateral margins of the ischia and the lateral surfaces of both the obturator processes and ischial aprons in *Chirostenotes pergracilis* and *Epichirostenotes curriei* (Fig. 3.4F,I). The ischial shaft is curved posterodistally and is mediolaterally compressed (Fig. 3.4). A reduced pair of tuberosities on the posterodorsal edge of the ischium are accompanied by light scarring. The proximal ischial tuberosity is a low, proximodistally elongate crest near the iliac peduncle. The distal ischial tuberosity is a small tubercle near the distal end of the ischium. It protrudes slightly from the ischial shaft which, if articulated with its counterpart, orients the distal ischial tuberosity dorsolaterally. Between this pair of tuberosities, the posterodorsal edge of the ischial shaft has another proximodistally elongate patch of light scarring.

3.4 Myology of the pelvic girdle

Pelvic and hind limb muscles inferred as present in caenagnathids are described according to anatomical/functional muscle group. This is summarized in Table 3.3 and mapped onto a reconstructed articulated caenagnathid pelvis (Fig. 3.5). The organization of pelvic muscles in caenagnathids is largely consistent with other theropods, but the M. puboischiofemoralis externus 2 is a notable exception. Moreover, relative changes in muscle origin size to more plesiomorphic and derived theropod taxa are recorded in the osteology that allows for comparison to make functional inferences.

3.4.1 Triceps femoris

Concerning the pelvis, muscles of the triceps femoris group include the Mm. iliotibiales 1–3 (IT1–3) and M. ambiens (AMB). The origins of IT1–3 together occupy the lateral side of the anterior and dorsal margins of the ilium (Fig. 3.5A). The origin of each part is indicated by striae or rugose texturing, which reveals a narrow band available for attachment. Similar to birds (Gangl et al. 2004), all parts of this muscle group were likely broad sheets of muscle based on these narrow origins. Separation between the origin of each part along the iliac margin is less clear. Although a small gap is visible dividing the origin of IT2 from that of IT3, the division between the origin of IT1 and that of IT2 is estimated based on other non-avian theropod reconstructions (Hutchinson et al. 2005, 2008). Striae or slight scarring along the anterior margin of the iliac blade marks the origin of IT1. The IT2 attached along the dorsal rim of the blade along a striated or rugose bone surface, most clearly seen in *Chirostenotes pergracilis* or UALVP 59791. It probably terminated anteriorly near the anterodorsal corner of the ilium, and posteriorly dorsal to the ischiadic peduncle. The origin of IT3 is a scarred region or small, rugose

ridge along the dorsal edge of the postacetabular blade of the ilium. It is posterior to the IT2 origin and best visible in either *Chirostenotes pergracilis* or TMP 1998.093.0013. Its posterior boundary is located immediately before the posterior tip of the ilium tapers to a rounded point.

A roughening or rugosity on the anterolateral surface of the pubis marks the origin of AMB (Fig. 3.5A). This origin is associated with the preacetabular tubercle but does not necessarily encompass it. The outline of the origin of AMB is oval and longer proximodistally than anteroposteriorly. Whereas some crocodylians possess a double-headed AMB (Romer 1923a, Hutchinson 2002), it is usually single-headed in birds and non-avian theropods (Romer 1923a, 1927, Carrano and Hutchinson 2002, Hutchinson et al. 2005, 2008). This is also the case in caenagnathids as only one origin is evident in any specimen.

3.4.2 M. iliofibularis (ILFB)

The origin of ILFB occupies most of the lateral surface of the postacetabular iliac blade posterodorsal to the acetabulum (Fig. 3.5A). The postacetabulum is a general correlate for this origin (Hutchinson 2002), although its borders are not entirely clear in many specimens due to the smooth, untextured lateral surface of the iliac blade. However, it is constrained by surrounding origins of other muscles—anteriorly by the ITC and IFE, posteriorly by the FTE, and dorsally by the IT3. The ridge on the lateral surface of TMP 1981.023.0035 (Fig. 3.2G) may indicate the approximate posterodorsal extent of the origin of ILFB, but other specimens lack this feature. The ILFB origin extends anteriorly to a point no further than the centre of the acetabulum, and posteriorly to around the midpoint of the brevis shelf. Dorsally, it extends to the origins of IT2–3, and ventrally to the margin of the acetabulum and the postacetabular portion of the ilium.

3.4.3 Deep dorsal group

Mainly in control of flexing, or protracting, the femur, the deep dorsal group includes the M. iliofemoralis externus (IFE), M. iliotrochantericus caudalis (ITC), and Mm. puboischiofemorales interni 1–2 (PIFI1–2). The IFE attached to the lateral surface of the iliac blade, dorsal and slightly anterior to the centre of the acetabulum (Fig. 3.5A). In crocodylians, this muscle is not separated from the ITC, in contrast with the divided condition in avians (Table 3.2). The smooth lateral surface of the iliac blade and lack of clear origins makes the condition in caenagnathids equivocal if only relying on the origin site and comparison with the closest living relatives. Using the insertion site on the femur as a proxy, the ITC and IFE are inferred as separate in basal dinosaurs, and the IFE reduced in size compared to the ITC in basal tetanuran theropods (Hutchinson 2001b, 2002). Both of these states were achieved well before the divergence of Caenagnathidae. Therefore, the origin of IFE is inferred as separate from the ITC in caenagnathids. The origin is relatively small compared to surrounding muscle origins that constrain it, namely, the IT2 dorsally, the ILFB posteriorly, and the ITC anteroventrally. Iliac subdivision of preacetabular and postacetabular muscle groups is unclear, making it difficult to precisely identify the posterior boundary of the IFE. The reconstruction here is based on those of other theropods that bracket Caenagnathidae (Hutchinson et al. 2005, 2008).

Most of the lateral aspect of the preacetabular iliac blade was occupied by the ITC (Fig. 3.5A). The origin is bordered by the IT1 anteriorly, and the IFE and ILFB posteriorly. Dorsally, the IT2 marks the edge of the origin, whereas the pubic peduncle and margin of the preacetabular hook bound it ventrally. As the osteological correlate for the ITC, the preacetabulum, which is

anteroposteriorly longer and dorsoventrally taller than the postacetabulum, provides a large area for attachment of this muscle.

Indicated by slight scarring, the PIFI1 attached to the anterolateral surface of the pubic peduncle of the ilium (Fig. 3.5A). Its origin is dorsal to the ilium-pubis contact. A shallow depression on the anterolateral surface of the pubic peduncle generally marks the origin of PIFI1, but does not precisely outline its extent.

The origin of PIFI2 occupies most of the cuppedicus fossa, including part of the medial side of the preacetabular hook (Fig. 3.5B–C). Whereas a bird has a divided pair of muscle heads (Table 3.2), the texture in the cuppedicus fossa lacks evidence of division, suggesting the muscle had a single head. The ilio-pubic ligament attachment on the tip of the preacetabular hook delimits the ventral edge of the PIFI2 origin. A medial shelf and subtle ridge that separates the rest of the medial surface of the ilium from the excavated concavity forming the cuppedicus fossa marks the dorsal boundary in medial view.

3.4.4 Flexor cruris group

Muscles of the tibial flexor group are typically found on the posterolateral surface of the ilium and on the ischium. The M. flexor tibialis internus 1 and 3 (FTI1, 3) and M. flexor tibialis externus (FTE) comprise muscles of the flexor cruris group originating from the pelvis. A small, scarred tubercle at the distal end of the ischial shaft marks the origin of FTI (Fig. 3.5A). This distal ischial tuberosity is oval in dorsal view, its proximodistal axis longer than its mediolateral axis. The tubercle, and thus the origin of FTI1, is displaced slightly to the lateral side, and is largely obscured in medial view. The distal ischial tuberosity is reduced, suggesting that FTI1 was similarly relatively small.

Along the posterodorsal margin of the ischial shaft is the origin of FTI3 (Fig. 3.5A). The proximal ischial tuberosity, a low, proximodistally elongate ridge, indicates the site of attachment. Unlike the pronounced ischial tuberosity of tyrannosaurids indicating the origin of FTI3 (Carrano and Hutchinson 2002, Hutchinson et al. 2005), this osteological correlate (and by extension, the FTI3) was drastically reduced in size. The belly of this muscle was restricted proximally by that of the ISTR passing around the ischial shaft and distally by the ADD2.

A small, approximately rectangular or triangular origin on the posterolateral corner of the ilium provided attachment for the FTE (Fig. 3.5A). The origin is not consistently clearly demarcated as some other muscles of the ilium, but in a few specimens, there is a rough patch of textured bone on the posterior end of the postacetabulum that approximately outlines its shape. It was constrained dorsally by the IT3, anteriorly by the ILFB, and both ventrally and posteriorly by the edge of the ilium.

3.4.5 Mm. adductores femorum (ADD)

The ischium provides attachment space for a pair of hind limb adductors found on the pelvis, namely, the Mm. adductores femorum 1–2 (ADD1–2). Muscle scars reveal the origin of ADD1 on the anterolateral side of the ischial obturator process (Fig. 3.5A). This sub-triangular origin extends to the anterior and ventral margins of the obturator process and the ischial shaft. The distal boundary is less clear as the entire surface of the adjacent ischial apron is similarly blanketed in striae, a texture that is continuous with that found on the obturator process.

A proximodistally elongate scar on the dorsal edge of the ischial shaft indicates the ADD2 origin (Fig. 3.5A,C). It is confined by the origin of FTI3 at its proximal end. The origin of

FTI1 limits its distal extent; however, a gap in the scarred texture on *Chirostenotes pergracilis* (TMP 1979.020.0001) suggests that it did not completely fill this space.

3.4.6 Mm. puboischiofemorales externi (PIFE)

Three muscles comprise the Mm. puboischiofemorales externi 1–3 (PIFE1–3). Subtle roughening of the entire anterior surface of the pubic apron and anteromedial edges of the pubic shafts demarcate the origin of PIFE1 (Figs. 3.4C–D, 3.6). The proximal boundary of the origin mirrors the proximal extent of the pubic apron, limited to the point at which the apron tapers into the shaft. The origin did not extend further laterally than the most anterior edges of the pubic shafts. The distal boundary is near the proximal end of the pubic boot around the pubic fenestra.

Striations restricted to the posterior edges of the pubic shafts indicate the origin of PIFE2 (Figs. 3.4A,C,E, 3.7). These striations generally form a pair of proximodistally elongate oval attachment sites. Proximally, the origin terminates about halfway between the ischiadic process and proximal edge of the pubic apron. Distally, the origin boundary is approximately equal to the distal end of the pubic apron and pubic fenestra. The posterior surface of the pubic apron is smooth and lacks evidence of muscle attachment.

The origin of PIFE3 covers the posterolateral portion of the obturator process and the lateral surface of the ischial apron (Fig. 3.5A). It is posterior to, and constrained by, the origin of ADD1. Like the ADD1, this muscle attachment extended ventrally to the margin of the obturator process and ischial apron and dorsally to the ischial shaft. Posteriorly, the origin of PIFE3 tapers with the ischial apron toward the distal end of the ischium.

3.4.7 M. ischiotrochantericus (ISTR) and M. caudofemoralis brevis (CFB)

The origin of ISTR is at the proximal end of the ischial shaft on its medial side (Fig. 3.5C). Small rugosities may indicate former muscle attachment. Its origin is largely estimated from a shallow concavity on the iliac process.

The brevis fossa on the ventral side of the postacetabular portion of the iliac blade provided attachment for the CFB (Fig. 3.5B,C). Slight scarring indicates that the CFB filled this fossa but did not extend onto the lateral surface of the ilium. The CFB extended anteriorly as much as the brevis shelf, but likely no further.

3.5 Discussion

3.5.1 General remarks

The extent of interpretations made here are limited by a few caveats and aspects outside the scope of this study. An articulated caenagnathid pelvis has not yet been discovered, leaving the exact angles and synarthroses between pelvic bones unknown. This reconstruction is based mainly on contact surfaces between bones based on specimens, or parts thereof, not strongly affected by taphonomy. Additionally, well preserved specimens of closely related, non-caenagnathid oviraptorosaurians (Barsbold et al. 2000, Clark et al. 2001, Lü 2002, Lü et al. 2004, 2013, 2017, Xu et al. 2013, Funston et al. 2018) offer a reasonable idea of the morphology of an articulated pelvis. Functional implications based on muscle action assume the same function in other theropods. Biomechanical tests could be used to analyze the functions of these muscles at different joint angles, or to assess the microstructure of cancellous bone within hind limb elements with respect to posture (Bishop et al. 2018a). Lifestyle inferences are based on

qualitative assessments; however, these data could be incorporated into an analysis using quantitative comparison, such as morphometrics.

Pelvic musculature reconstruction reveals, for the most part, an expected intermediate arrangement compared to theropods that bracket Caenagnathidae, such as tyrannosaurids (Hutchinson et al. 2005) and dromaeosaurids (Hutchinson et al. 2008). However, the origin of PIFE2 in Caenagnathidae does not match the condition in other theropods, nor does it occupy any state previously scored for other archosaurs (Hutchinson 2001a, 2002). Theropods with a pubic apron typically possess striae or roughening on the posterior surface of the apron that indicate former attachment of this muscle. The avian homolog (M. obturatorius medialis) originates from the medial surface of the puboischiadic membrane as the pubic apron is absent. Both of these surfaces can be rejected as correlates for the PIFE2 in caenagnathids. Foremost, the presence of muscle scars on the posterior edges of the pubic shafts indicate former muscle attachments on the bone instead of a membrane. Secondly, the absence of scarring on the posterior surface of the pubic apron is unusual and inconsistent with other theropods, which suggests that muscle was not attached to this surface. Lastly, the morphology of the puboischiadic membrane makes it unlikely to have anchored this muscle from the medial side. Following Hutchinson (2001a), the puboischiadic membrane of non-avian theropods had paired, lateral parts and a single, median part. The osteological correlate of the lateral membrane is a proximodistal ridge on the medial side of the pubis that is continuous with the proximal margin of the pubic apron. The median membrane attached along the pubic symphysis, extending from the proximal end of the pubic apron to the distal end of the pubic boot along its posterior side and midsagittal plane. Both of these correlates are present in caenagnathids (Fig. 3.3), and also both medial to the origin of PIFE2 and pubic apron. Hence, attachment of the PIFE2 to the

medial side of the puboischiadic membrane was rather unlikely given the lateral position of this muscle with respect to the membrane. Although the pubic apron still serves as an osteological correlate for the PIFE1, it cannot be used as a landmark for the PIFE2 in caenagnathids.

3.5.2 Comparisons with other theropods

The morphology of the pelvis and its associated musculature display additional features that suggest increased reliance on hip flexors and knee control. The preacetabular portion of the ilium is proportionally longer than the postacetabular portion, which contrasts with the typical condition of more plesiomorphic theropods. Muscles originating from the preacetabular region are largely involved in hind limb flexion (protraction) and have a relatively larger area to anchor themselves than postacetabular muscles involved in hind limb extension (retraction). Notably, the ITC occupied a large region of the pelvis compared to other muscles and also performed a role in medial rotation of the femur. In extant birds, the ITC is likewise proportionally large and counters the ground reaction force, which stabilizes the hip (Hutchinson and Gatesy 2000). The PIFE2 (OM of birds, Table 3.2) is the antagonistic partner to the ITC and functions to extend (retract) and laterally rotate the femur. Partial pubic retroversion (mesopuby) in caenagnathids probably had a similar effect on the PIFE2 as in dromaeosaurids, in which this condition appears to decrease the capacity for extension of the femur, but without restricting lateral rotation (Hutchinson and Gatesy 2000, Hutchinson et al. 2008). The development of this antagonistic pair of muscles in caenagnathids suggests that they required an increased degree of control for mediolateral femoral rotation compared to earlier diverging theropod lineages. Additionally, pennaraptorans have a reduced supraacetabular rim, as opposed to the laterally expanded supraacetabular crest possessed by earlier diverging theropod lineages that resisted femoral

abduction and axial rotation (Tsai et al. 2018). This could mean that a reduced supraacetabular rim allows for greater femoral axial rotation. This adaptation is important for stability and distal hind limb control in birds because of their crouched posture (Gatesy 1995, Carrano and Biewener 1999, Hutchinson and Gatesy 2000, Allen et al. 2013, Grossi et al. 2014, Xu et al. 2014). Consequently, birds have a sub-horizontal femur and walk largely by rotation of the leg around the knee joint. Furthermore, an increased capacity for axial rotation is congruent with the co-development of the ITC and PIFE2 as paired, antagonistic, mediolateral rotators of the femur. Altogether, reduction of the supraacetabular crest to a rim in conjunction with enlargement of the ITC and PIFE2 may signal a change in posture from the more upright stance of more plesiomorphic theropods to the more crouched stance of birds.

The brevis fossa housed the CFB, which was a hind limb extensor (Gatesy 1990). The caenagnathid brevis fossa is reduced in size relative to that of more plesiomorphic theropods, such as *Ornitholestes*, ornithomimids, and tyrannosaurids, that relied on caudal musculature for a substantial portion of locomotive propulsion (Osborn 1903, Gatesy 1990, Carpenter et al. 2005, Persons and Currie 2011). However, it is larger than the brevis fossa of dromaeosaurids (Persons and Currie 2012), and the CFB probably maintained an important role in locomotion, as in other oviraptorosaurs (Persons et al. 2014). In this context, an intermediate condition in caenagnathids is unsurprising, but does corroborate the model of theropod locomotor module evolution put forth by Gatesy and Dial (1996). Preceding the evolution of birds, a reduction in the brevis fossa and, by extension, a reduction in caudal musculature, suggests that decoupling of pelvic and caudal muscles began as early as the divergence of Pennaraptora. Basal oviraptorosaurians *Caudipteryx* and *Similicaudipteryx* possess ilia with similarly reduced postacetabular regions (Qiang et al. 1998, He et al. 2008) that limit the space available for hind limb extensors.

Additionally, a reduced brevis fossa in caenagnathids corroborates the inferred reduction in caudofemoral musculature in *Caudipteryx* based on the lack of a raised fourth trochanter (Jones et al. 2000). Not only does this study show that the origin of CFB was reduced in Caenagnathidae and likely also close relatives such as *Caudipteryx*, but that the insertion of caudofemoral muscles (CFB included) was also reduced. Furthermore, this reduction is not new to caenagnathids, but instead was inherited from more basal oviraptorosaurians that indicate caudal musculature reduction was already well underway. A reduction in space available for caudofemoral muscles at both the origin and insertion sites is shared among other pennaraptorans such as dromaeosaurids, exacerbated even further in *Archaeopteryx* and avialans (Gatesy 1990, Allen et al. 2013). The intermediate condition in caenagnathids among non-avian theropods highlights the gradual nature of the loss of caudal musculature in locomotion as it became decoupled from the pelvic module.

3.5.3 Considerations for inferred lifestyle

The muscular reconstructions presented here allow more detailed discussion of caenagnathid lifestyle. Although wading and highly cursorial lifestyles are not mutually exclusive, pelvic myological evidence argues more in favour of the former. The reduced postacetabular portion of the caenagnathid ilium is a feature shared with modern wading birds, whereas an elongate postacetabulum is a trait amongst cursorial and diving birds (Ibáñez and Tambussi 2012, Stoessel et al. 2013, Degrange 2017). Although some morphological features of the tail and pelvis vary substantially between caenagnathids and birds, the origins of many major hind limb extensors are on the posterior portion of the hip. Because the postacetabulum provides attachment for hind limb extensors that provide locomotory torque to propel the body forward

(Picasso 2010), a reduced postacetabulum suggests that caenagnathids were less adapted for cursoriality. Such a condition is reflected in the reconstruction of caenagnathid pelvic musculature presented here (Fig. 3.5). This is supported by the high reduction in—or absence of—a raised fourth trochanter on the femur in other caenagnathids (Currie and Russell 1988, Funston et al. 2015) and oviraptorosaurs (Jones et al. 2000) as it is the insertion site for caudofemoral musculature (Gatesy 1990). Discussion on cursoriality here is limited to inferring general running ability because these results cannot elucidate finer aspects of locomotion. Reduction in hind limb extensors presumably also diminished rapid acceleration and sprinting ability, but could also relate to lessened endurance for sustained running over long distances. Additionally, femoral orientation affects limb proportions, which complicates using this method to infer cursoriality, at least in birds (Gatesy 1991). Wading birds were noted for having low femur:tibiotarsus ratios, which more strongly reflects avian body plan constraints than it does cursorial ability. Therefore, theropods approaching an avian-like posture that are categorized as cursorial based on limb proportions may be an artefact of the relationship between femoral orientation and constraint on femoral length (Gatesy 1991). Furthermore, wading birds have characteristically long limbs (Zeffer et al. 2003) as a result of relatively elongate tibiotarsi and tarsometatarsi (Barbosa and Moreno 1999a, 1999b). These long distal limb segments are accompanied by small pelves, an apparent tradeoff reversed in most swimming birds (Stoessel et al. 2013). Despite their elongate limbs, waders have relatively limited top speed compared to ground dwelling birds of similar leg length, suggesting that the underlying selection pressure was foraging, not cursoriality (van Coppenolle and Aerts 2004). Because of this, an inferred shift toward a more bird-like body plan in the caenagnathid hind limb with increased reliance on hip flexors and knee control raises skepticism about running ability determined on limb proportions

alone. The morphology of the caenagnathid foot (Sternberg 1932, Currie and Russell 1988) may also support wading over cursoriality. Whereas highly cursorial animals tend to reduce the number of digits (Lull 1904, Coombs 1978, de Bakker et al. 2013), caenagnathids retain a relatively large first toe. Their relatively flexible toes with curved unguals could be adaptations for increased grip (Varricchio 2001, Longrich et al. 2010, 2013), which may have helped on soft substrates, or at least improved stability. Despite limb proportions, metatarsus adaptations, and potentially tail musculature consistent with enhanced running ability (Holtz 1994, Carrano 1999, Snively et al. 2004, Pittman et al. 2013, Persons et al. 2014), pelvic muscle reconstruction challenges these claims and suggests that caenagnathids were less cursorial than previously thought.

3.6 Summary of caenagnathid pelvic myology

The description of muscle attachment sites in new pelvic material allows a reasonable hypothetical reconstruction of caenagnathid pelvic musculature that provides insights into locomotory adaptations. Pelvic myology is consistent with other theropods except for the PIFE2, which occupies a previously unidentified state among Archosauria. Simultaneous expansion of the preacetabular blade of the ilium and its musculature relative to the reduction of the postacetabulum and caudal muscles suggests increased reliance on hip flexors and knee control. Caudal musculature retained some locomotive importance but is reduced and indicates that caudal decoupling was well underway as early as the divergence of Pennaraptora. Reduced hip extensors, increased hip flexors, increased ability for femoral long axis rotation, and an enlarged foot with a relatively large first digit offer evidence more consistent with wading than a highly cursorial lifestyle.

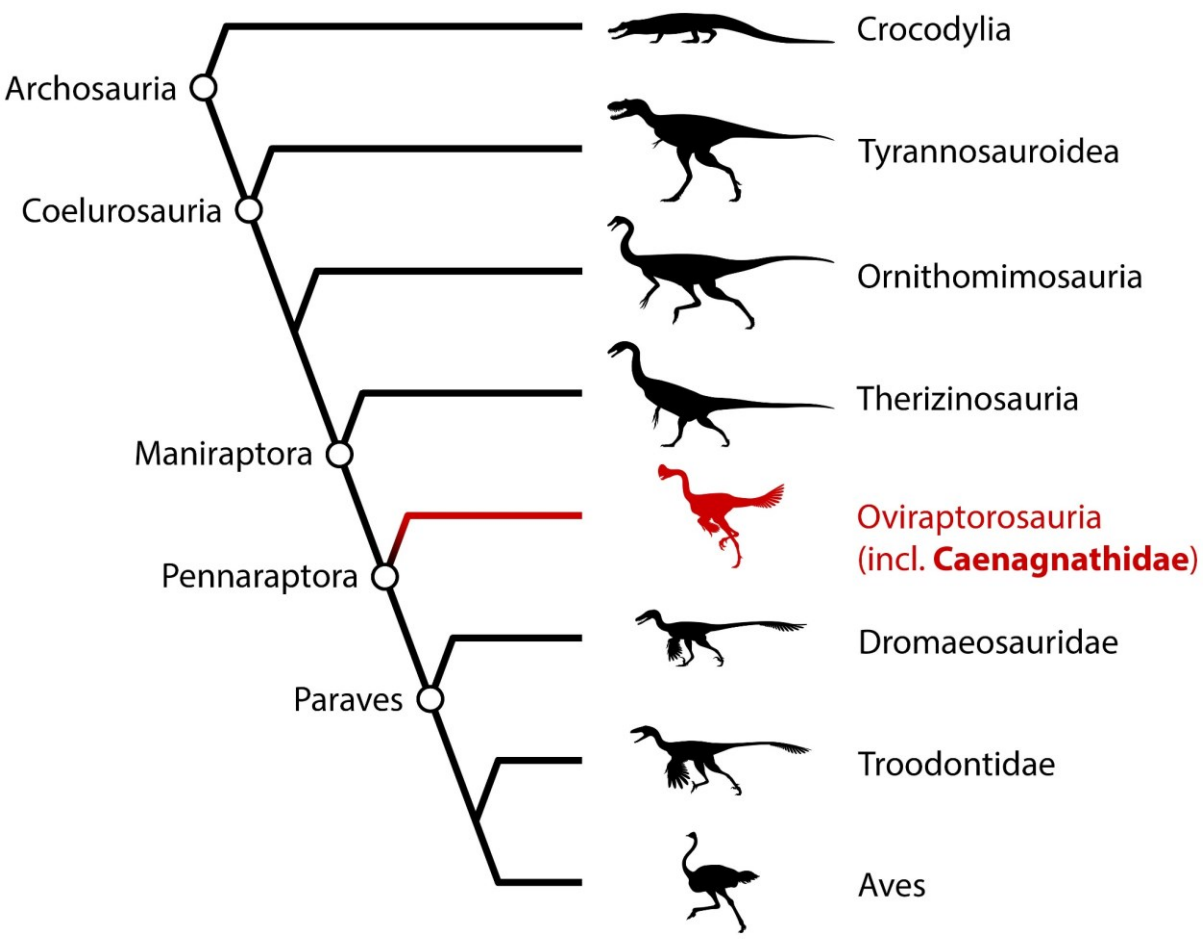

Figure 3.1. Simplified phylogeny of Caenagnathidae among Archosauria. Phylogeny includes other contemporaneous, extinct theropods and representatives of its Extant Phylogenetic Bracket (Crocodylia and Aves).

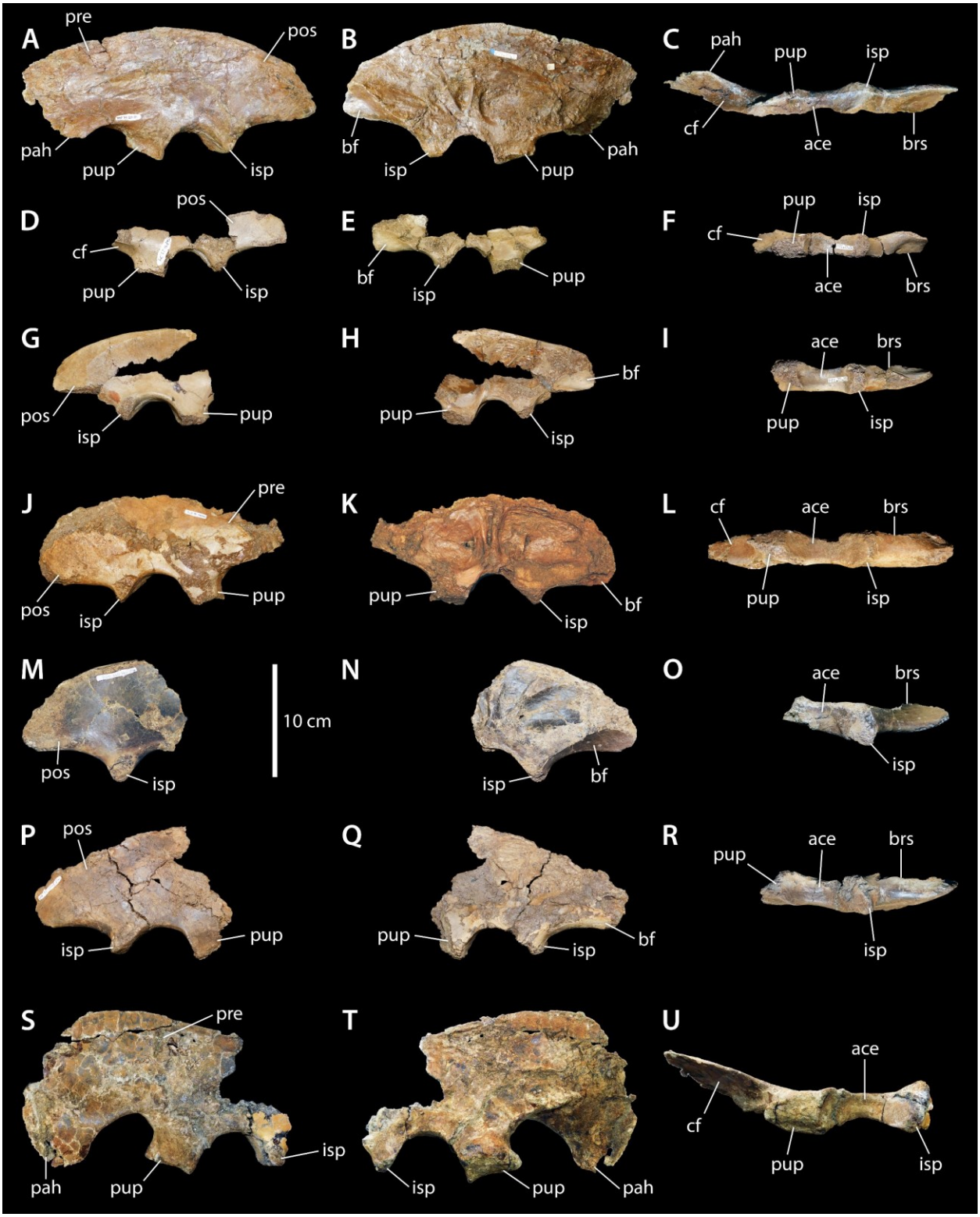

Figure 3.2. Caenagnathid ilia examined for muscle attachment sites. Left ilium of *Chirostenotes pergracilis* (TMP 1979.020.0001) in lateral (A), medial (B), and ventral (C)

views. Left ilium of Caenagnathidae indet. (TMP 1981.023.0034) in lateral (D), medial (E), and ventral (F) views. Right ilium of Caenagnathidae indet. (TMP 1981.023.0035) in lateral (G), medial (H), and ventral (I) views. Right ilium of Caenagnathidae indet. (TMP 1992.036.0674) in lateral (J), medial (K), and ventral (L) views. Right ilium of Caenagnathidae indet. (TMP 1998.093.0013) in lateral (M), medial (N), and ventral (O) views. Right ilium of Caenagnathidae indet. (TMP 2002.012.0103) in lateral (P), medial (Q), and ventral (R) views. Left ilium of Caenagnathidae indet. (UALVP 59791) in lateral (S), medial (T), and ventral (U) views. Scale bar is 10 cm and applies to all images. **Abbreviations: ace,** acetabulum; **bf,** brevis fossa; **brs,** brevis shelf; **cf,** cuppedicus fossa; **isp,** ischiadic peduncle; **pah,** preacetabular hook; **pos,** postacetabulum; **pre,** preacetabulum; **pup,** pubic peduncle.

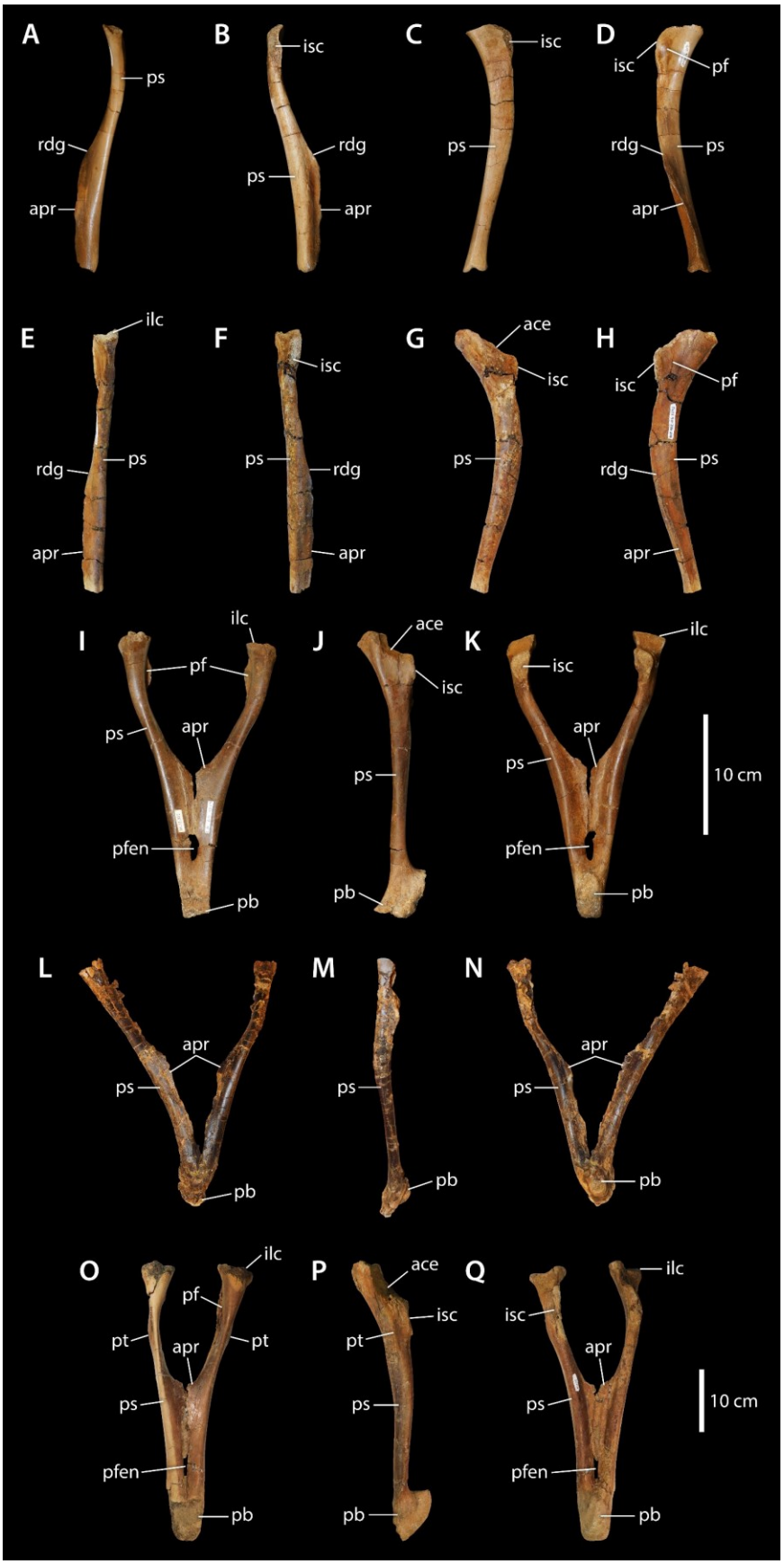
A
ps
rdg
apr
B
isc
rdg
ps
apr
C
isc
ps
D
isc
pf
rdg
ps
apr
E
ilc
rdg
ps
apr
F
isc
ps
rdg
apr
G
ace
isc
ps
H
isc
pf
rdg
ps
apr
I
ilc
pf
ps
apr
pfen
pb
J
ace
isc
ps
pb
K
ilc
isc
apr
ps
pfen
pb
10 cm
L
apr
ps
pb
M
ps
pb
N
apr
ps
pb
O
ilc
pf
pt
apr
pt
ps
pfen
pb
P
ace
isc
pt
ps
pb
Q
ilc
isc
apr
ps
pfen
pb
10 cm

Figure 3.3. Caenagnathid pubes examined for muscle attachment sites. Left pubis of Caenagnathidae indet. (TMP 1980.016.2095) in anterior (A), posterior (B), lateral (C), and medial (D) views. Left pubis of Caenagnathidae indet. (TMP 1982.016.0275) in anterior (E), posterior (F), lateral (G), and medial (H) views. Pubes of Caenagnathidae indet. (TMP 1994.012.0603) in anterior (I), left lateral (J), and posterior (K) views. Pubes of *Epichirostenotes curriei* (ROM 43250) in anterior (L), left lateral (M), and posterior (N) views. Pubes of Caenagnathidae indet. (UALVP 55638) in anterior (O), left lateral (P), and posterior (Q) views. Scale bars are both 10 cm; upper scale applies to A–K, lower scale applies to L–Q. **Abbreviations: ace,** acetabulum; **apr,** pubic apron; **ilc,** iliac contact; **isc,** ischiadic contact; **pb,** pubic boot; **pf,** pubic fossa; **pfen,** pubic fenestra; **ps,** pubic shaft; **pt,** preacetabular tubercle; **rdg,** ridge.

Figure 3.4. Caenagnathid ischia examined for muscle attachment sites. Right ischium of *Chirostenotes pergracilis* (TMP 1979.020.0001) in lateral (A), medial (B), dorsal (C), and ventral (D) views, plus close-up dorsal view of the distal end of the ischium (E) and lateral view of the obturator process (F). Right ischium of *Epichirostenotes curriei* (ROM 43250) in lateral (G) and medial (H) views, plus close-up lateral view of obturator process (I). Scale bar is 10 cm and applies to A–D and G–H. **Abbreviations: dist,** distal ischial tuberosity; **ilc,** iliac contact; **isa,** ischial apron; **iss,** ischial shaft; **op,** obturator process; **pist,** proximal ischial tuberosity; **puc,** pubic contact.

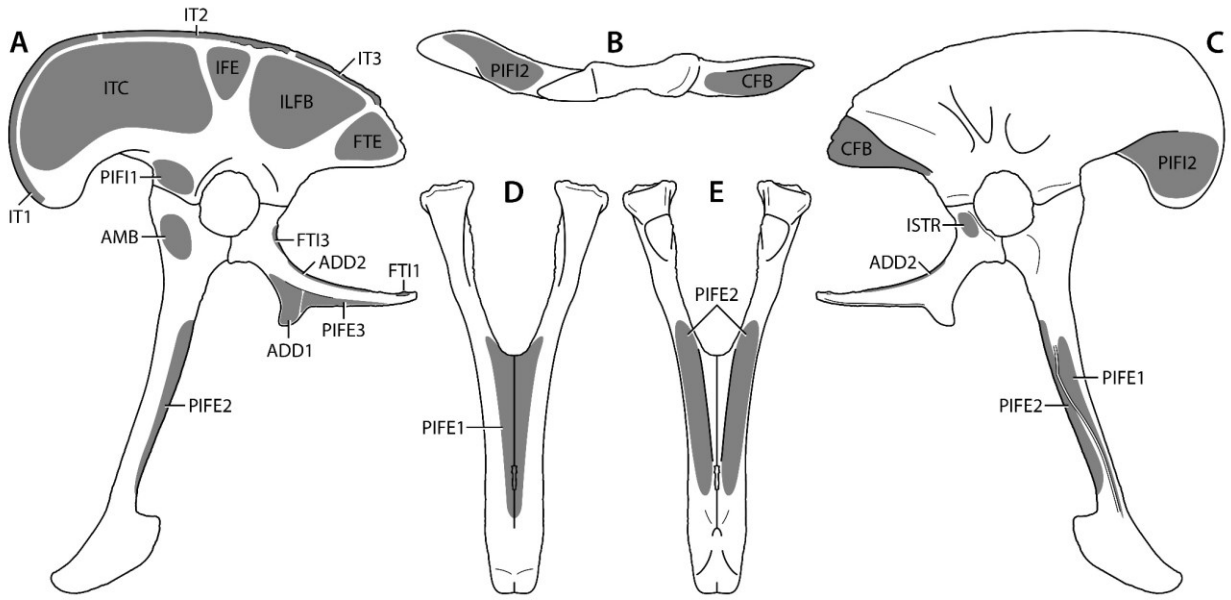

Figure 3.5. Pelvic myology of Caenagnathidae. Pelvis in lateral view (A), ilium in ventral view (B), pelvis in medial view (C), and pubes in anterior (D) and posterior (E) views. The reconstructed pelvis is a composite based on *Chirostenotes pergracilis* (TMP1979.020.0001, ilium and ischium) and indeterminate caenagnathids (UALVP 56638, pubis; UALVP 59791, preacetabular portion of ilium), the pubis scaled to match the ilium and ischium based on the contacts between these bones. **Abbreviations: ADD1,** M. adductor femoris 1; **ADD2,** M. adductor femoris 2; **AMB,** M. ambiens; **CFB,** M. caudofemoralis brevis; **FTE,** M. flexor tibialis externus; **FTI1,** M. flexor tibialis internus 1; **FTI3,** M. flexor tibialis internus 3; **IFE,** M. iliofemoralis externus; **ILFB,** M. iliofibularis; **ISTR,** M. ischiotrochantericus; **IT1,** M. iliotibialis 1; **IT2,** M. iliotibialis 2; **IT3,** M. iliotibialis 3; **ITC,** M. iliotrochantericus caudalis; **PIFE1,** M. puboischiofemoralis externus 1; **PIFE2,** M. puboischiofemoralis externus 2; **PIFE3,** M. puboischiofemoralis externus 3; **PIFI1,** M. puboischiofemoralis internus 1; **PIFI2,** M. puboischiofemoralis internus 2.

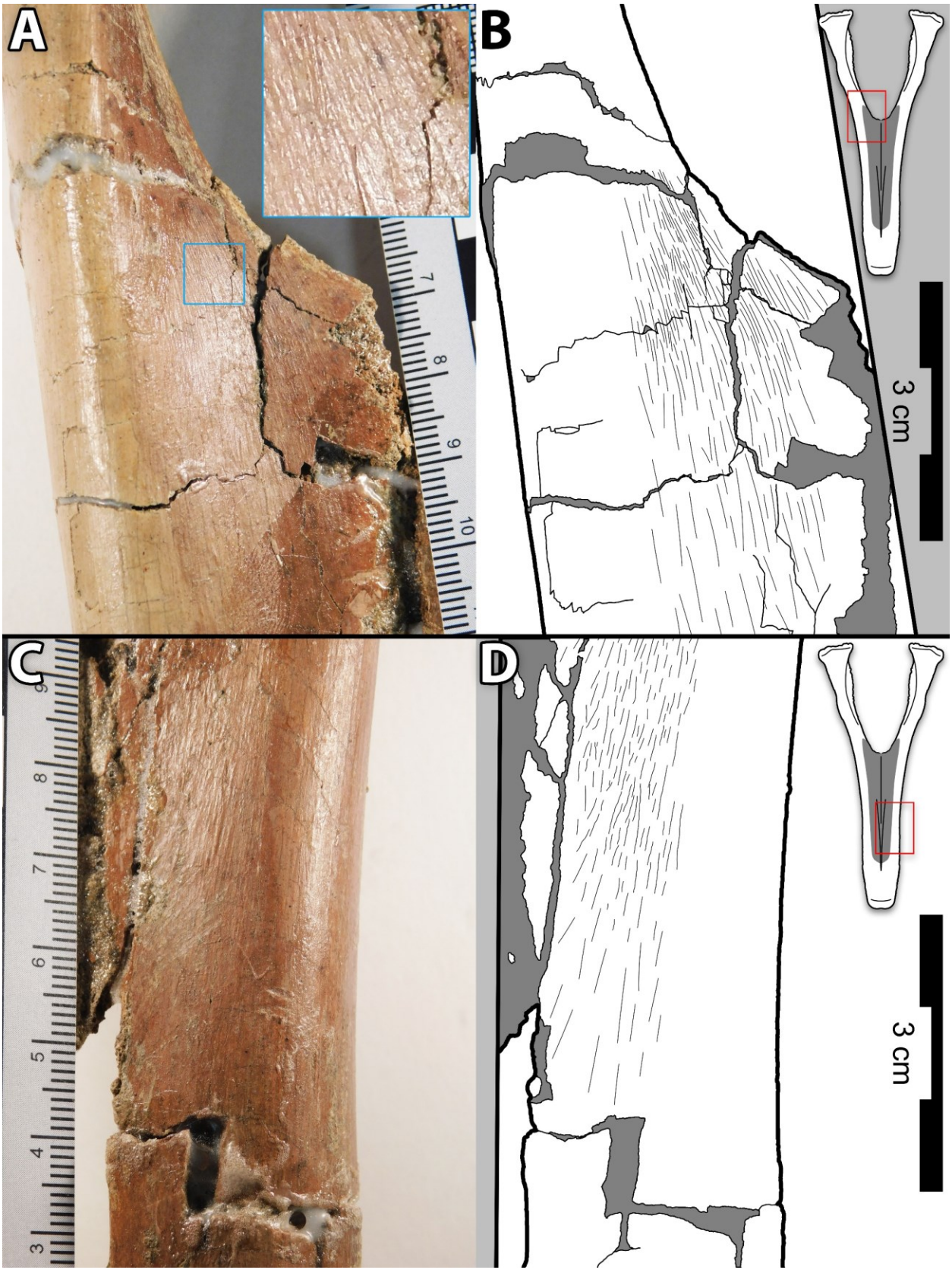
A
B
3 cm
C
D
3 cm

Figure 3.6. Osteological correlate for M. puboischiofemoralis externus 1 (PIFE1). Pubes of an indeterminate caenagnathid (UALVP 56638) in anterior view at proximal (A–B) and distal (C–D) ends of the pubic apron. Striae are visible across the anterior surface of the pubic apron (A including popout with detail, C), illustrated in line drawing of the same areas (B, D).

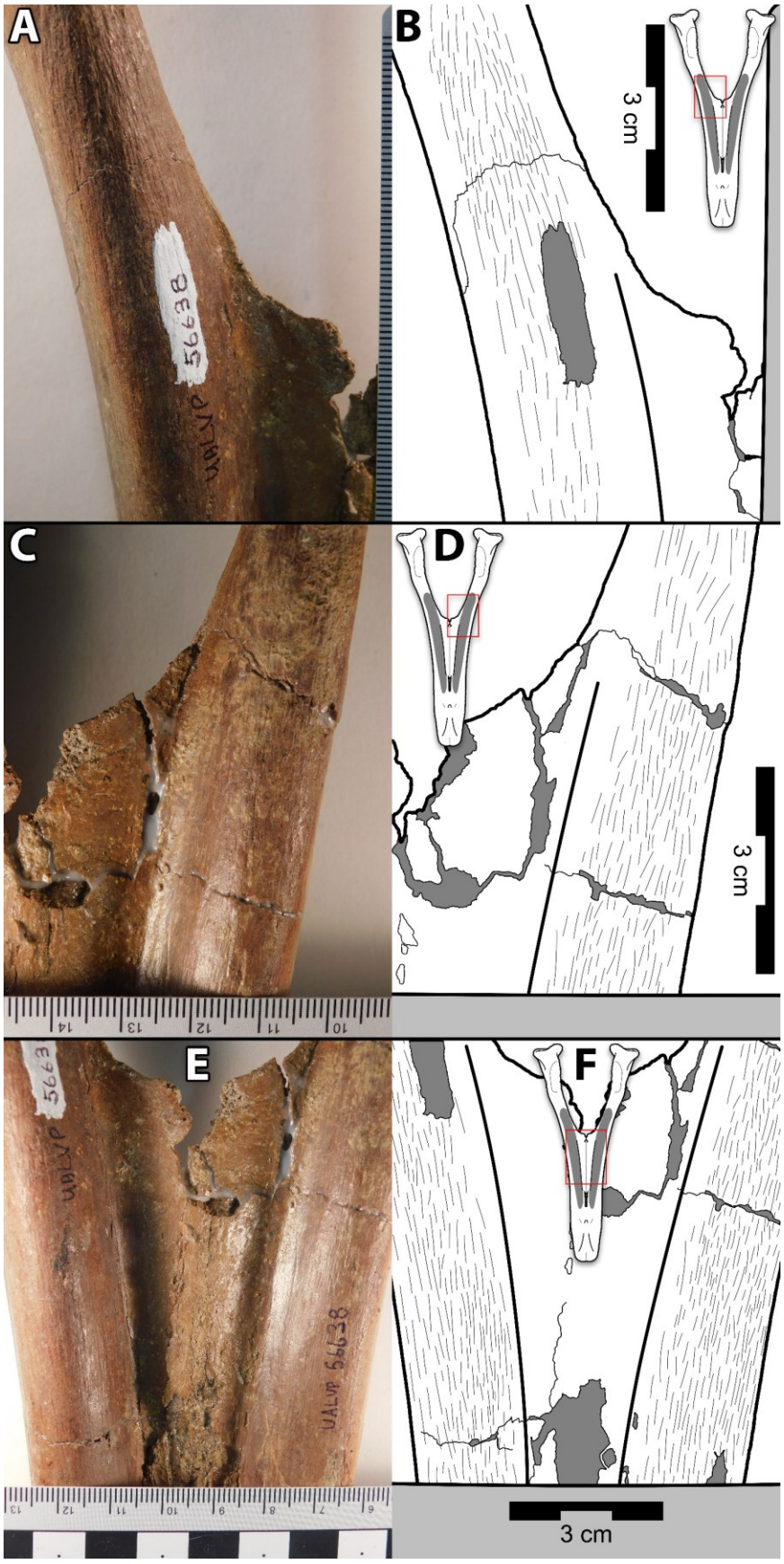
A
B
3 cm
C
D
3 cm
E
F
3 cm

Figure 3.7. Osteological correlate for M. puboischiofemoralis externus 2 (PIFE2). Pubes of an indeterminate caenagnathid (UALVP 56638) in posterior view toward proximal (A–D) and middle (E–F) portions of the pubic shaft. Striae are visible along the posterior edges of the pubic shafts, but not the apron (A, C, E), illustrated in line drawing of the same areas (B, D, F).

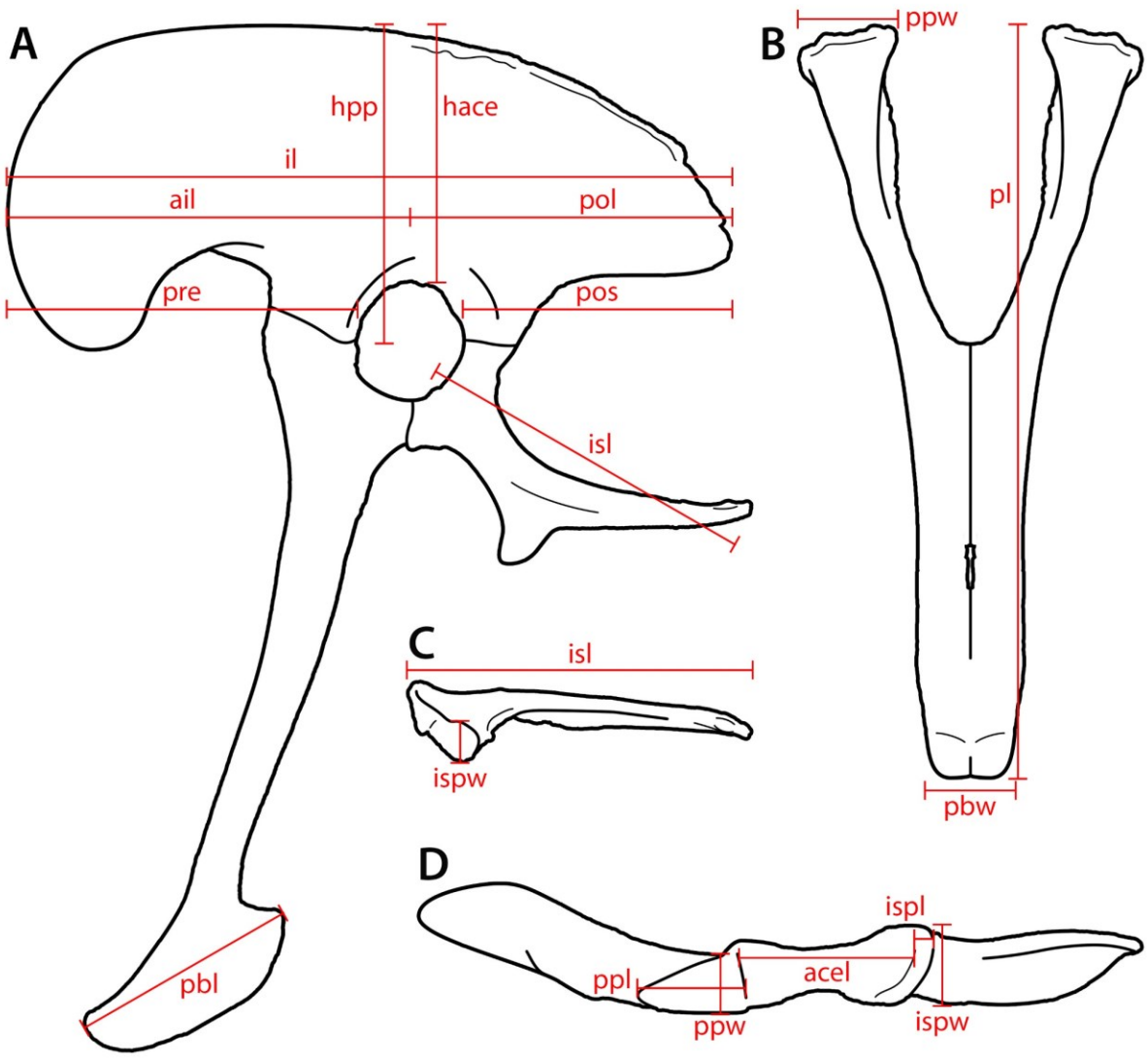

Figure 3.8. Measurement protocol. Reconstructed caenagnathid pelvis in left lateral view (A), pubes in anterior view (B), ischium in dorsal view (C, anterior to left), and ilium in ventral view (D, anterior to left). Ilium and ischium based on *Chirostenotes pergracilis* (TMP 1979.020.0001) and an indeterminate caenagnathid (UALVP 59791), and pubes based on an indeterminate caenagnathid (UALVP 56638). **Abbreviations: acel,** acetabulum length; **ail,** antilium length; **hace,** height above acetabulum; **hpp,** height above pubic peduncle; **il,** ilium length; **isl,** ischium length; **ispl,** ischiadic peduncle length; **ispw,** ischiadic peduncle width; **pbl,** pubic boot length;

pbw, pubic boot width; **pl,** pubis length; **pol,** postilium length; **pos,** postacetabulum length; **ppl,** pubic peduncle length; **ppw,** pubic peduncle width; **pre,** preacetabulum length.

Table 3.1. Pelvic material examined or referenced for muscle attachment sites. Note: CM, Carnegie Museum of Natural History; RM, Redpath Museum; ROM, Royal Ontario Museum; TMP, Royal Tyrrell Museum of Palaeontology; UALVP, University of Alberta Laboratory for Vertebrate Palaeontology; UAMZ, University of Alberta Museum of Zoology.

Taxon	Specimen number	Status and element(s)
Caenagnathidae		
Anzu wyliei	CM 78000	Fossil; left ilium, pubes, ischia
Epichirostenotes curriei	ROM 43250	Fossil; ilia, right ischium, pubes
Chirostenotes pergracilis	TMP 1979.020.0001	Fossil; left ilium, right ischium
Caenagnathidae indet.	TMP 1980.016.2095	Fossil; partial left pubis
Caenagnathidae indet.	TMP 1981.023.0034	Fossil; partial left ilium
Caenagnathidae indet.	TMP 1981.023.0035	Fossil; partial right ilium
Caenagnathidae indet.	TMP 1982.016.0275	Fossil; partial left pubis
Caenagnathidae indet.	TMP 1992.036.0674	Fossil; partial right ilium
Caenagnathidae indet.	TMP 1994.012.0603	Fossil; nearly complete pubes
Caenagnathidae indet.	TMP 1998.093.0013	Fossil; partial right ilium
Caenagnathidae indet.	TMP 2002.012.0103	Fossil; partial right ilium
Caenagnathidae indet.	UALVP 56638	Fossil; nearly complete pubes
Caenagnathidae indet.	UALVP 59791	Fossil; partial left ilium
Aves		
Apteryx haastii	RM 8369	Articulated skeleton mount
Corvus corax	UAMZ (uncatalogued)	Dissected
Dromaius novaehollandiae	ROM R6843, ROM R7654, UAMZ B-FIC2014.260	Disarticulated, associated skeletons (ROM); articulated skeleton mount (UAMZ)
Gallus gallus	RM 8355	Articulated skeleton mount
Rhea americana	RM 8499	Disarticulated, associated skeleton
Struthio camelus	ROM 1080, ROM 1162, ROM 1933, ROM 2136, ROM 2305, UAMZ 7159	Disarticulated, associated skeletons
Crocodylia		
Alligator mississippiensis	ROM R343	Postcranial skeleton
Alligator sp.	UAMZ HER-R654	Articulated skeleton mount
Caiman crocodilus	RM 5242; UAMZ (uncatalogued)	Disarticulated, associated skeleton (RM), dissected

		(UAMZ)
Osteolaemus tetraspis	RM 5216	Articulated skeleton mount
Squamata		
Tupinambis teguixin	ROM R436	Semi-prepared skeleton
Varanus albigularis	RM 5220	Disarticulated, associated skeleton
Varanus exanthematicus	UAMZ (uncatalogued)	Dissected
Varanus jobiensis	RM 5219	Disarticulated, associated skeleton
Varanus komodoensis	ROM R7565	Disarticulated, associated skeleton
Varanus niloticus	RM 5221	Disarticulated, associated skeleton
Varanus rudicollis	ROM R7318	Articulated skeleton mount
Varanus salvator	RM 5222, RM 5223, RM 5224	Disarticulated, associated skeleton

Table 3.2. Pelvic muscle homologies in crocodylians and avians. Modified from Carrano and Hutchinson (2002) and Hutchinson et al. (2005).

Crocodylia	Aves
Triceps femoris	
M. iliotibialis 1 (IT1)	M. iliotibialis cranialis (IC)
M. iliotibialis 2, 3 (IT2, IT3)	M. iliotibialis lateralis (IL)
M. ambiens (AMB)	M. ambiens (AMB)
M. iliofibularis (ILFB)	M. iliofibularis (ILFB)
Deep dorsal group	
M. iliofemoralis (IF)	M. iliofemoralis externus (IFE) + M. iliotrochantericus caudalis (ITC)
M. puboischiofemoralis internus 1 (PIFI1)	M. iliofemoralis internus (IFI)
M. puboischiofemoralis internus 2 (PIFI2)	M. iliotrochantericus cranialis (ITCR) + M. iliotrochantericus medius (ITM)
Flexor cruris group	
M. puboischiotibialis (PIT)	(absent)
M. flexor tibialis internus 1 (FTI1)	(absent)
M. flexor tibialis internus 2 (FTI2)	(absent)
M. flexor tibialis internus 3 (FTI3)	M. flexor cruris medialis (FCM)
M. flexor tibialis internus 4 (FTI4)	(absent)
M. flexor tibialis externus (FTE)	M. flexor cruris lateralis pars pelvica (FCLP)
Mm. adductores femorum	
M. adductor femoris 1 (ADD1)	M. puboischiofemoralis pars medialis (PIFM)
M. adductor femoris 2 (ADD2)	M. puboischiofemoralis pars lateralis (PIFL)
Mm. puboischiofemorales externi	
M. puboischiofemoralis externus 1 (PIFE1)	M. obturatorius lateralis (OL)
M. puboischiofemoralis externus 2 (PIFE2)	M. obturatorius medialis (OM)
M. puboischiofemoralis externus 3 (PIFE3)	(absent)
M. ischiotrochantericus (ISTR)	M. ischiofemoralis (ISF)
Mm. caudofemorales	
M. caudofemoralis brevis (CFB)	M. caudofemoralis pars pelvica (CFP)
M. caudofemoralis longus (CFL)	M. caudofemoralis pars caudalis (CFC)

Table 3.3. Pelvic muscles inferred as present in Caenagnathidae. Muscles originating from the pelvis are listed by functional/anatomical group. Modified from Carrano and Hutchinson (2002) and using levels of inference based on Witmer (1995).

Muscle	Origin	Level of inference
Triceps femoris		
IT1	Lateral surface of anterodorsal margin of ilium	(I)
IT2	Dorsolateral surface of dorsal margin of ilium	(I)
IT3	Dorsolateral surface of postacetabular margin of ilium	(I)
AMB	Near preacetabular tubercle	(I)
M. iliofibularis		
ILFB	Lateral surface of postacetabular portion of ilium between IFE and FTE	(I')
Deep dorsal group		
IFE	Lateral surface of ilium between ITC and ILFB	(I)
ITC	Lateral surface of preacetabular portion of ilium	(I)
PIFI1	Shallow depression on anterolateral surface of pubic peduncle of ilium	(II)
PIFI2	Cuppedicus fossa of ilium including medial side of preacetabular hook	(II)
Flexor cruris group		
FTI1	Tubercle on dorsal edge of ischial shaft at distal end	(II')
FTI3	Faint scar distal to ISTR on dorsal edge of ischial shaft	(II)
FTE	Posterolateral corner of ilium, posterior to ILFB	(I)
Mm. adductores femorum		
ADD1	Anteroventral portion of lateral surface of obturator process	(I')
ADD2	Faint scar distal to FTI3 on dorsal edge of ischial shaft	(II)
Mm. puboischiofemorales externi		
PIFE1	Anterior surface of pubic apron	(II)
PIFE2	Posterior edges of pubic shafts	(II)
PIFE3	Ischial apron and posterior portion of obturator process, distal to ADD1	(II)
M. ischiotrochantericus		
ISTR	Medial side of ischium at proximal end, near iliac contact	(II)
Mm. caudofemorales		
CFB	Brevis fossa of ilium	(II)

Table 3.4. Measurements of caenagnathid pelvic elements. All measurements in millimetres (mm) following system depicted in Fig. 3.8. Note: ROM, Royal Ontario Museum; TMP, Royal Tyrrell Museum of Palaeontology; UALVP, University of Alberta Laboratory for Vertebrate Palaeontology; ?, unknown/not measurable; *, preserved fragment; n/a, not applicable; $^{L/R}$, paired elements; a-p, anteroposterior; d-v, dorsoventral; m-l, mediolateral; p-d, proximodistal.

Measurement	Axis	ROM 43250	TMP 1979.020.0001	TMP 1980.016.2095	TMP 1981.023.0034	TMP 1981.023.0035	TMP 1982.016.0275	TMP 1992.036.0674	TMP 1994.012.0603	TMP 1998.093.0013	TMP 2002.012.0103	UALVP 56638	UALVP 59791
ILIUM													
Length (il)	a-p	n/a	255*	n/a	158*	138*	n/a	212*	n/a	145*	171*	n/a	227*
Antilium (ail)	a-p	n/a	145*	n/a	?	?	n/a	104*	n/a	?	?	n/a	179
Postilium (pol)	a-p	n/a	110	n/a	85*	90*	n/a	104	n/a	120	125	n/a	?
Preacetabulum (pre)	a-p	n/a	125*	n/a	?	?	n/a	72*	n/a	?	?	n/a	145
Postacetabulum (pos)	a-p	n/a	75	n/a	63*	62	n/a	73	n/a	92	78	n/a	?
Acetabulum length (acel)	a-p	n/a	55	n/a	45	46	n/a	60	n/a	?	70	n/a	66
Height over pubic peduncle (hpp)	d-v	n/a	120*	n/a	?	82*	n/a	90*	n/a	?	?	n/a	130
Height over acetabulum (hace)	d-v	n/a	91	n/a	?	62	n/a	70	n/a	?	84	n/a	81
Pubic peduncle length (ppl)	a-p	n/a	34	n/a	28	25	n/a	30	n/a	?	?	n/a	44
Pubic peduncle width (ppw)	m-l	n/a	18	n/a	19	21*	n/a	23	n/a	?	23	n/a	35
Ischiadic peduncle length (ispl)	a-p	n/a	8	n/a	10*	8	n/a	6	n/a	9	8	n/a	8
Ischiadic peduncle width (ispw)	m-l	n/a	24	n/a	20*	23	n/a	20	n/a	29	32	n/a	35
PUBIS													
Length (pl)	p-d	418^{L}/ 418^{R}	n/a	195*	n/a	n/a	224*	n/a	219*	n/a	n/a	416*	n/a
Pubic boot length (pbl)	a-p	55*	n/a	?	n/a	n/a	?	n/a	50^{*L}/ 45^{*R}	n/a	n/a	92	n/a
Pubic boot width (pbw)	m-l	?	n/a	?	n/a	n/a	?	n/a	18*	n/a	n/a	30	n/a
ISCHIUM													
Length (isl)	p-d	190	138	n/a	n/a	n/a	n/a	n/a	n/a	n/a	n/a	n/a	n/a

Chapter 4. Troodontid pelvic myology offers insight on the evolution of cursoriality in Theropoda

4.1 Introduction

Theropod dinosaurs evolved a variety of locomotory adaptations to survive in their environments. Birds as living theropods exhibit bipedalism and are usually restricted to terrestrial movement using only the hind limbs, an adaptation inherited from their non-avian ancestors. Despite this limitation, various bird groups became adapted to a range of environments, reflected in leg morphology (Zeffer et al. 2003). Non-avian theropods also display a range in hind limb morphology, albeit less than modern birds (Gatesy and Middleton 1997). Musculature may provide insight into locomotory adaptations in extinct taxa, which can be done by comparison using the Extant Phylogenetic Bracket (Witmer 1995), comprising crocodylians and birds in the case of theropods. Troodontidae, a non-avialan paravian family closely related to birds (Hendrickx et al. 2015), is an interesting candidate for locomotory muscle reconstruction. This family is believed to be adapted for cursoriality and their close avian affiliation can provide information about the condition in basal birds.

Variation in theropod body form seems to increase within Maniraptora (Allen et al. 2013). Theropods more basal to this clade tend to have ilia with longer postacetabula than preacetabula, mirroring a reliance on hind limb extensors and tail muscles for locomotory power (Gatesy and Dial 1996, Persons and Currie 2011). Some maniraptorans deviate strongly from this trend (Zanno 2010a, 2010b) and exhibit reduction of the postacetabular ala and tail (Gatesy and Dial 1996, Allen et al. 2013). Troodontids have longer postacetabula compared to the preacetabula (Russell and Dong 1993, Currie and Dong 2001, Tsuihiji et al. 2014, van der Reest

and Currie 2017, Pei et al. 2017), but are phylogenetically nested well within Maniraptora (Hendrickx et al. 2015), which posits an interesting question as to their degree of cursoriality and dependence on tail or hip muscles.

Troodontids are believed to be well adapted for cursoriality based on leg proportions (Russell 1969, Wilson and Currie 1985, Carrano 1999, Persons and Currie 2016). Although they resemble typical theropods in having three pedal digits, only two were probably functional (Li et al. 2008b). Digit reduction is also associated with increased cursoriality (Coombs 1978). Derived troodontids additionally possesses an arctometatarsus, an adaptation for agility whereby the third metatarsal is proximally pinched between its neighbours to enhance stability and resistance to shear and torsional forces (Wilson and Currie 1985, Holtz 1994, Snively and Russell 2003, Snively et al. 2004). Pelvic muscles have been reconstructed in some theropods and offer insight about their adaptations (Romer 1923b, Russell 1972, Tarsitano 1983, Perle 1985, Hutchinson 2001a, Carrano and Hutchinson 2002, Hutchinson et al. 2005, 2008, Bates et al. 2012, Bates and Schachner 2012, Degrange 2017). The pelvic myology of a troodontid was recently modeled in a phylogenetically derived taxon (Bishop et al. 2018a), but evolutionary patterns of musculature within the family remain undocumented.

Examination of troodontid pelvic material allows identification of muscle scars. Although derived, Late Cretaceous troodontids differ appreciably in pelvic morphology from their basal, Early Cretaceous precursors, remarkable similarity exists within each of these groups. Muscle reconstruction permits comparison of muscle groups to one another to make inferences about locomotory adaptations and evolution in Troodontidae. Furthermore, these results can be compared to other contemporaneous taxa to gain a better understanding of competition and potential niche partitioning with other theropods. Beyond palaeoecological implications,

troodontid pelvic musculature also offers information on the evolutionary timing of avian-like muscle organization.

4.2 Materials and Methods

General methodology for identification of soft tissue attachment sites in extinct taxa follows the Extant Phylogenetic Bracket methodology (Bryant and Russell 1992, Witmer 1995). Using this method, the closest living relatives of the focal taxon are compared to provide evidence for the likelihood of muscle presence or absence (Fig. 4.1). Comparative techniques similar to previous dinosaur muscle reconstructions are followed to infer soft tissue attachment based on osteological correlates, which are landmarks on the bone that anchor muscles or tendons (Hutchinson 2001a, Carrano and Hutchinson 2002, Hutchinson et al. 2005, 2008, Maidment et al. 2014b). Inferences of muscle presence or absence were categorized following Witmer (1995), avoiding those that fulfill Level III and III' criteria leading to unwarranted speculation. Besides literature review to understand associations between pelvic tissues in living relatives, dissections of a lizard (savannah monitor, *Varanus exanthematicus*), a crocodylian (spectacled caiman, *Caiman crocodilus*), and a bird (common raven, *Corvus corax*) were completed. Relevant muscle studies of extant archosaurs (Gangl et al. 2004, Smith et al. 2006, 2007, Otero et al. 2010, Klinkhamer et al. 2017, Bishop et al. 2018a) and comparative skeletal material were also reviewed for osteological correlates (Table 4.1). Archosaur muscle homologies are listed in Table 4.2.

Troodontid pelvic material (Table 4.1) was examined for osteological correlates to identify former muscle attachment sites. Osteological descriptions of troodontids with pelvic material were reviewed (Russell and Dong 1993, Currie and Dong 2001, Norell et al. 2009,

Zanno et al. 2011, Tsuihiji et al. 2014, Xu et al. 2017, van der Reest and Currie 2017, Pei et al. 2017). North American material was examined directly for this project, but unpublished conditions in Asian material were assessed from photographs (Fig. 4.2). A recently published musculoskeletal model of a derived, North American troodontid (Bishop et al. 2018a) was compared to muscle scars observed on available material. Although more basal, Early Cretaceous troodontids differ appreciably in pelvic morphology from derived, Late Cretaceous species, each of these groups show strong resemblances within each time period. Henceforth, 'more basal' is used as approximately synonymous with 'Early Cretaceous' and 'more derived' is more or less equivalent with 'Late Cretaceous'. The conditions in more plesiomorphic members such as *Jianianhualong tengi* (Xu et al. 2017) and *Sinovenator changii* (Xu et al. 2002) were primarily used as representatives of Early Cretaceous forms, whereas derived members including *Latenivenatrix mcmasterae* (van der Reest and Currie 2017), *Saurornithoides mongoliensis* (Norell et al. 2009), and *Talos sampsoni* (Zanno et al. 2011) were used to represent Late Cretaceous species. The main goal of this study is to reconstruct pelvic muscles at both early and late evolutionary stages in the family, which is possible by using a composite pelvis of Early and Late Cretaceous troodontid material as muscle groups vary little within either of these stages. Proximal muscles have a close relationship to hind limb flexors (protractors), extensors (retractors), and locomotory function, whereas distal limb muscles mainly control the lower portions of the limb and the foot. Attachment sites were determined primarily by observation of available fossil material, and secondarily by reference to literature with detailed descriptions and photographs. Descriptions of muscle attachment areas allow reconstructions and comparisons with other theropod taxa. Measurements of pelvic elements (Fig. 4.10, Table 4.4) were recorded

using a ruler or measuring tape. Photographs were taken with a digital camera and illustrations were generated using Adobe Photoshop CS6 and a Wacom drawing tablet.

4.3 Morphology of the pelvic girdle

Troodontid pelvic material (Figs. 4.2–4.3) preserves muscle scars and other osteological correlates indicative of former soft tissue attachment. More basal and more derived members of this family show general morphological consistency within their respective groups. Observed elements of Early Cretaceous troodontids compare well with other more basal forms such as *Sinornithoides youngi* (Russell and Dong 1993, Currie and Dong 2001). Similarly, observed material of Late Cretaceous troodontids mostly resembles the same elements in *Almas ukhaa* (Pei et al. 2017) and are strongly evocative of *Gobivenator mongoliensis* (Tsuihiji et al. 2014). General pelvic morphology is described by each pelvic bone and then divided into more basal and more derived members of Troodontidae. Features are outlined following previous studies (Russell and Dong 1993, Currie and Dong 2001, Xu et al. 2002, 2017, Norell et al. 2009, Zanno et al. 2011, Tsuihiji et al. 2014, van der Reest and Currie 2017, Pei et al. 2017).

The ilia of more basal troodontids tend to be dolichoiliac and small relative to femoral lengths (Currie and Dong 2001, Xu et al. 2002, 2017). However, this bone in *Jianianhualong tengi* is badly crushed, and in *Sinovenator changii* it is missing parts of the preacetabular portion of the blade (Fig. 4.2A,I,K). The iliac margin tends to be straight along its dorsal edge, although is reported as slightly concave in *Jianianhualong tengi* (Xu et al. 2017). The dorsal margin of the postacetabular portion of the ilium slopes anterodorsal-posteroventrally and has a slightly rugose texture around the edge. Posteriorly, the postacetabulum tapers to a rounded point in *Sinovenator changii* and appears to have a slightly textured surface (Fig. 4.2I,K). The ventral margin is

roughly horizontal when the ilia are in life position. In lateral view, the ischiadic peduncle is small and triangular, whereas the pubic peduncle is anteroposteriorly and proximodistally long and squared-off (Fig. 4.2I,K). Ventrally, the ischiadic peduncle is mediolaterally wider than it is anteroposteriorly long, whereas the pubic peduncle has the opposite dimensions (Fig. 4.2J,L). The anterolateral surface of the pubic peduncle has a shallow depression enclosed dorsally by a circular rim confluent with the ventral margin of the preacetabulum. A shallow brevis fossa (Russell and Dong 1993) is limited in both its mediolateral and dorsoventral extent (Fig. 4.2). This is mirrored by the shallow cuppedicus fossa opposite the acetabulum from the brevis fossa and enclosed by a modest preacetabular hook. More derived troodontids such as *Almas ukhaa* (Pei et al. 2017), *Gobivenator mongoliensis* (Tsuihiji et al. 2014), and *Latenivenatrix mcmasterae* (van der Reest and Currie 2017) reverse the trend in more basal species, in that each has a postacetabulum that is longer than the preacetabulum. The preacetabular hook tends to be ventrally rounded when preserved (Fig. 4.3A) (Pei et al. 2017). A shallow notch along the anterior margin of the iliac blade interrupts an otherwise convex profile in *Latenivenatrix mcmasterae*. The dorsal edge of the ilium is gently convex, causing the postacetabulum to taper slightly towards the posterior end (Fig. 4.3A). Along the entire margin of the ilium from the anterior edge of the preacetabular hook to the posterodorsal corner, striae are preserved where muscles formerly attached. Striated regions are narrow at the anterior end, but gradually widen posteriorly. A rugose, anteroposteriorly elongate ridge extends along the dorsal margin of the iliac blade from mid-preacetabulum to mid-postacetabulum in *Latenivenatrix mcmasterae* (Fig. 4.3A). The posterior end of the ilium may be round (Tsuihiji et al. 2014) or square (Fig. 4.3A). Laterally, a triangular patch of textured surface between the posterodorsal and posteroventral corners of the iliac blade extends about halfway to the ischiadic peduncle. The ischiadic and

pubic peduncles in derived troodontids are comparable to those of more basal forms. The pubic peduncles in derived troodontids lack the circular depressions on their lateral sides seen in more basal members, although some striae cover the anterolateral surface. A shallow cuppedicus fossa is partly enclosed by the preacetabular hook. Opposite the acetabulum, a moderately large brevis fossa is mediolaterally wider and dorsoventrally deeper than in any basal troodontid.

More basal troodontids have pubes about twice the length of the ischia (Currie and Dong 2001) with transversely broad pubic aprons (Fig. 4.2) (Currie and Dong 2001, Xu et al. 2017). The proximal portions of the shafts generally appear round in *Jianianhualong tengi* and oval in *Sinovenator changii* (Fig. 4.2) (Currie and Dong 2001). In anterior or posterior view, the lateral margins of the pubes appear weakly sinuous. This is because of a slight lateral bulge about one-third the distance from the proximal to the distal end of the apron. In lateral view, the shaft tends to appear straight to slightly convex anteriorly. The anterior surface of the pubic apron is confluent with the shaft, giving it an overall convex appearance. Posteriorly, the apron forms a broad longitudinal trough (Fig. 4.2). This concavity extends laterally so that the posterior margin of the pubic shaft is mediolaterally compressed into a rounded ridge. Striae are visible in this embayment along virtually the entire posterior surface of the apron. The pubic boot is reduced to a knob-like structure that is not expansive either anteriorly or posteriorly (Fig. 4.2G–H). In more derived troodontids, the pubis appears slightly anteriorly concave to straight-shafted in lateral view (Fig. 4.3A,D,K) (Tsuihiji et al. 2014, Pei et al. 2017). A prominent preacetabular tubercle at the proximal end of the pubis is hypertrophied into an anterolaterally-projecting process (Fig. 4.3A) (Tsuihiji et al. 2014). In *Latenivenatrix mcmasterae*, the concave, anteroventral portion of this process is mediolaterally compressed into a spine-like crest with striae. The proximal ends of the pubic shaft in more derived troodontids is oval in cross section with an anteroposterior long

axis (Fig. 4.3). Some troodontids such as *Almas ukhaa* have a longitudinal groove on the medial side of the shaft proximal to the pubic apron (Pei et al. 2017). However, others including *Latenivenatrix mcmasterae* and *Talos sampsoni* have longitudinal depressions in these regions (Fig. 4.3E,I,L), each partially bordered by a proximodistal ridge that merges distally with the pubic apron. A small portion of the pubic aprons are preserved in *Latenivenatrix mcmasterae* and *Talos sampsoni*, and in each it has a weakly concave proximal edge (Fig. 4.3). In these taxa, texturing on the anterior surface of the pubes is limited to the apron, but striations cover the posterior surfaces of the apron and shaft. The morphology of the pubic boot is well preserved in *Almas ukhaa* and *Gobivenator mongoliensis*, which appear to possess both anterior and posterior expansions, but differ as to which projection is larger (Tsuihiji et al. 2014, Pei et al. 2017).

The ischium of a more basal troodontid is mainly represented here by *Jianianhualong tengi* (Fig. 4.2A–B). The ischia are relatively small, plate-like bones, only about half the length of the pubes (Xu et al. 2002, 2017). A triangular obturator process at the distal end of the ischium contributes to the concave anteroventral margin and straight distal edge of this bone. Striae carpet the lateral surface of the obturator process. Two distinct dorsal tubercles are present and accompanied by a slightly rugose texture (Fig. 4.2B) (Xu et al. 2002, 2017). The posterior corner of the distal end of the ischium is triangular and slightly rounded. More derived troodontids differ notably in the morphology of their ischia (Fig. 4.3F–H,M–O), but share with more basal species short, plate-like ischia only about half the length of the pubes (Tsuihiji et al. 2014). The obturator process is generally triangular (when preserved) and its lateral surface is covered in striae (Fig. 4.3). That being said, *Almas ukhaa* and *Gobivenator mongoliensis* have spike-like projections at the obturator processes (Tsuihiji et al. 2014, Pei et al. 2017). The apex of the obturator process is one-half to one-third the length from the distal end of the ischium

(Norell et al. 2009, Tsuihiji et al. 2014, Pei et al. 2017). A posterolateral ridge demarcates the extent of the obturator process along the edge of the ischial shaft (Fig. 4.3). Along the dorsolateral edge of the ischial shaft, the proximal and distal ischial tuberosities are reduced to low eminences or are simply patches of rugose texture. The proximal dorsal tuberosity is opposite a concave notch formed between the pubic peduncle and anterior edge of the obturator process. The distal dorsal tuberosity is near the distal end of the shaft. Between these tuberosities, a proximodistally elongate region of light scarring occupies the dorsolateral edge of the ischial shaft.

4.4 Myology of the pelvic girdle

Pelvic myology can provide information about locomotory adaptations and capabilities. Pelvic musculature in Troodontidae—described separately for more plesiomorphic and derived taxa—can be interpreted through dissection of extant animals, literature review, and observation of fossil material. In turn, muscle groups (flexors, extensors, abductors, adductors, rotators) can be reconstructed to qualitatively assess variation among taxa and infer the degree of cursoriality in troodontids. This provides information on the condition and arrangement of pelvic muscles as an outgroup to birds. Troodontid pelvic musculature was found to be generally consistent with that of other theropods, but with notable differences regarding muscle group sizes and osteological correlates compared to other maniraptorans (Table 4.3, Figs. 4.4–4.5).

4.4.1 Triceps femoris

The triceps femoris muscles that attached to the pelvis include the Mm. iliotibiales 1–3 (IT1–3) and the M. ambiens (AMB). The origins of IT1–3 occupy the lateral surface of the iliac

margin on its anterior and dorsal edges (Figs. 4.4A, 4.5A). Although the area of attachment for IT1 is not well preserved in more plesiomorphic troodontids, it does not vary much between disparate theropod families and is not expected to vary extensively within Troodontidae. Furthermore, the extents of the origins of IT2 and IT3 do not differ considerably between more basal and more derived troodontids. The origin of IT1 is visible on the anterodorsal corner of the ilium in *Latenivenatrix* (UALVP 55804), best seen in right lateral view. Light striae along the anterior edge are bordered by small rugosities a few millimeters away from the margin, following the gently sinuous curve of the anterior edge of the preacetabular blade. Dorsally, these striae become oriented obliquely, terminating dorsal to the cuppedicus fossa around the anterior edge of the pubic peduncle. This gives the origin of IT1 an overall L-shaped outline. The origin of IT2 is adjacent and posterior to that of IT1 and continues posteriorly along the dorsolateral edge of the ilium. In *Latenivenatrix*, the origin of IT2 becomes dorsoventrally expanded and texturally rougher in the same direction. This morphology is unusual compared to all other non-avian theropods observed in that the origin is embossed on the surface of the blade. Similarities in the origin of IT2 have been noted in the dromaeosaurid *Saurornitholestes* (MOR 660) and troodontid *Latenivenatrix* (van der Reest and Currie 2017). However, this origin in *Latenivenatrix* is embossed on an otherwise vertical iliac blade, whereas in *Saurornitholestes* the entire dorsal edge of the iliac blade is laterally deflected. The posterior edge of this origin is directly dorsal to the most anterior point of the brevis fossa along the horizontal part of the ventral margin of the postacetabular portion of the iliac blade. The origin of IT3—indicated by oblique striations along the dorsolateral edge of the postacetabular portion of the blade—is posterior to that of IT2. This origin ends at the posterodorsal corner of the iliac blade.

The origin of AMB is adjacent to the preacetabular tubercle. Its morphology in more basal troodontids is unremarkable. However, derived forms such as *Latenivenatrix* preserve a spine-like preacetabular tubercle that projects anterolaterally. In this case, the origin of AMB extends along a proximodistally elongate crest at the ventral edge of the preacetabular tubercle (Fig. 4.5A). This crest, and area for AMB attachment, appears anteroventrally concave in lateral view, distal to the iliac contact but proximal to the pubic apron. This appearance is shared with *Saurornithoides* (Norell et al. 2009) and *Gobivenator* (Tsuihiji et al. 2014). Overall morphology of the preacetabular tubercle generally resembles that seen in certain paleognath birds as the tubercle is similarly mediolaterally compressed in both *Apteryx* and *Struthio*. The preacetabular tubercle is a straight finger-like projection in *Apteryx*, and curves dorsally toward its anterior into a hooked process in *Struthio* (Gangl et al. 2004). Some crocodylians and paleognath birds are noted to have, or appear to possess, a double-headed AMB (Hutchinson 2002, Allen et al. 2015, Hutchinson et al. 2015). The AMB is inferred as being present with a single head in Troodontidae as a second origin cannot be identified on either the pubis (like some crocodylians) or the ilium (as in some paleognaths).

4.4.2 M. iliofibularis (ILFB)

Much of the lateral surface of the postacetabular portion of the iliac blade is the origin of M. iliofibularis (ILFB; Figs. 4.4A, 4.5A). The exact boundaries of this muscle origin are not clear, but can be estimated using osteological landmarks and adjacent muscle attachment sites. The anterior edge of the origin of ILFB is approximately mid-acetabulum. Its posterior margin is indicated by a change in bone surface texture about halfway between the ischiadic peduncle and posterior edge of the ilium. The dorsal border of the origin of ILFB is adjacent to the origin of

IT2–3, and its ventral edge follows the contour of the brevis shelf. These boundaries remain the same between more basal and more derived troodontids, but the area available for attachment in later forms appears larger.

4.4.3 Deep dorsal group

The deep dorsal group is primarily responsible for hip flexion and is comprised of the M. iliofemoralis externus (IFE), M. iliotrochantericus caudalis (ITC), and Mm. puboischiofemorales interni 1–2 (PIFI1–2). The origin of IFE is dorsal to the acetabulum (Figs. 4.4A, 4.5A). The site of attachment is marked by a triangular area in which weak striae are oriented anteroventrally-posterodorsally. Similar to other muscles on the lateral surface of the ilium, it would have been constrained by surrounding muscles (ILFB, IT2, and ITC). Derived members each appear to have an anteroposteriorly elongate origin of IFE based on observed muscle scars.

The origin of ITC occupies much of the lateral surface of the preacetabular region of the iliac blade (Figs. 4.4A, 4.5A). Its fleshy attachment in phylogenetically bracketing taxa suggests it would have likewise been anchored directly to the ilium, leaving no clear trace on the bone. However, neighbouring muscle origins delineate the origin of ITC, which is encircled anteriorly by IT1, dorsally by IT2, posteriorly by IFE, and ventrally by PIFI2 and the ventral margin of the iliac blade.

A shallow depression on the anterolateral surface of the pubic peduncle indicates the origin of PIFI1 (Figs. 4.4A–C, 4.5A–C). In more basal troodontids, this depression is circular and distinct on the lateral side of the pubic peduncle. In derived forms, it is relatively small and dorsoventrally elongate, situated on the anterior margin of the pubic peduncle and visible in both

medial and lateral views. The dorsal extent of the origin of PIFI1 approximately matches that of the acetabulum, and its ventral limit lies just dorsal to the ilium-pubis contact.

Within the small cuppedicus fossa, a rough texture denotes the origin of PIFI2 (Figs. 4.4B–C, 4.5B–C). This texture covers the medial surface of the preacetabular hook and appears to extend close to the edges of the iliac blade. In the ventral view of *Latenivenatrix* (UALVP 55804), the posterior perimeter of the patch of rugosity can be seen to occupy the posterior end of the cuppedicus fossa about halfway between the preacetabular hook and pubic peduncle.

4.4.4 Flexor cruris group

The flexor cruris group includes several hamstring muscles such as M. flexor tibialis internus 1 and 3 (FTI1, 3) and M. flexor tibialis externus (FTE). The origin of FTI1 is on the dorsal side of the distal end of the ischium (Figs. 4.4A,F, 4.5A). A distinct distal dorsal tuberosity denotes this site in troodontid specimens that are Early Cretaceous in age such as *Jianianhualong* (DLXH 1218) or *Sinovenator* (IVPP V12615). Late Cretaceous troodontids either have a reduced distal dorsal tuberosity as in *Saurornithoides* (AMNH FR 6516) or lack a distinct one like *Talos* (UMNH VP 19479), but a roughened patch of striations in the same region are at the distal ends of the ischia.

A proximodistally elongate tuberosity situated on the proximal part of the dorsal edge of the ischium indicates the origin of FTI3 (Figs. 4.4A,F, 4.5A). This proximal dorsal tuberosity is pronounced in plesiomorphic troodontids. Although not as prominent in derived members as in other maniraptorans (Novas and Puerta 1997), the proximal dorsal tuberosity is still clear on the ischia of *Saurornithoides* (AMNH FR 6516) and *Talos* (UMNH VP 19479). The edge of this low crest is offset toward the medial side of the ischium, resulting in the origin of FTI3 being visible

only in lateral or dorsal view. In an articulated pelvis, this crest would be more or less dorsally aligned due to the ventromedially angled orientation of the ischia.

Near the posterior end of the ilium, the origin of FTE occupies the lateral surface of the postacetabular process (Figs. 4.4A, 4.5A). Its anterior extent is limited by the origin of ILFB, and dorsally it meets that of IT3. The margin of the ilium itself forms the ventral and posterior boundaries of the origin of FTE. A rugose texture indicating former muscle attachment covers part of the ventral region of the postacetabular portion of the ilium here. The ilia of *Sinovenator* (IVPP V12615) each appear to have a rounded prominence in this area, whereas it is flat but scarred in *Latenivenatrix* (UALVP 55804).

4.4.5 Mm. adductores femorum (ADD)

Two muscles make up the Mm. adductores femorum 1–2 (ADD1–2). On the ischium, the origin of ADD1 covers part of the lateral surface of the obturator process (Figs. 4.4A,F, 4.5A). Striations carpet the lateral side of the ischium and the concave, ventral portion of the posterolateral ridge in *Talos* (UMNH VP 19479) (Zanno et al. 2011). This muscle would have attached to the anterior edge of the obturator process and extended dorsally up the striated surface to the posterolateral ridge. However, the posterior border of its origin is unclear. Neighbouring ADD1 is PIFE3, which occupied the posterior portion of the obturator process and restricted ADD1 coverage of the obturator process (see M. puboischiofemorales externi).

Both ischia of *Talos* (UMNH VP 19479) viewed dorsally show the origins of ADD2 as proximodistally elongate scars immediately distal to the proximal dorsal tuberosities and origin sites of FTI3 (Figs. 4.4A,C, 4.5A,C,F). A rugose texture with proximodistally oriented striae outlines the extent of this origin. The origin of ADD2 is about 3 cm on *Talos* along its long axis,

preserved entirely on both ischia. This origin does not appreciably differ among plesiomorphic or derived troodontids.

4.4.6 Mm. puboischiofemorales externi (PIFE)

The Mm. puboischiofemorales externi 1–3 (PIFE1–3) are on the pubis and ischium, wrapping around to insert on the posterior side of the femoral head in extant reptiles. On the pubis, the origin of PIFE1 covers the anterior surface of the pubic apron (Figs. 4.4C–D, 4.5C–D). The right pubis of *Talos* (UMNH VP 19479) is missing the surface of this portion of bone, but the left pubis of this specimen and both pubes of *Sinovenator* (IVPP V12583) and *Latenivenatrix* (UALVP 55804) are intact enough to discern the attachment sites. Proximodistally oriented striations restricted to the anterior surface of the pubic apron indicate the attachment of PIFE1 in troodontids, as in other non-avian theropods.

The origin of PIFE2 is on the posterior surface of the pubis (Figs. 4.4C,E,G, 4.5A,C,E). Both *Jianianhualong* (DLXH 1218) and *Sinovenator* (IVPP V12583) preserve striae covering the posterior surfaces of the pubic aprons and medial edges of the pubic shafts. The muscle scars of PIFE2 in more basal troodontids cover this embayment on the posterior surfaces of the pubes, but do not encroach on the lateral surface of the bone. In derived troodontids, the morphology is unusual even when compared broadly to other archosaurs. *Latenivenatrix* (UALVP 55804) and *Talos* (UMNH VP 19479) each have clear striations engraved into the posterior surfaces of both the pubic apron and the pubic shafts, the lateral extent of which is visible in lateral view. These striations indicate that the origin of PIFE2 extends proximally to a point about halfway between the ischiadic peduncle of the pubis and proximal edge of the pubic apron, including a small depression on the medial side of the pubis. The PIFE2 in a crocodylian arises from the posterior

surface of the pubic apron only, as is the typical case in non-avian theropods (Hutchinson 2001a, 2002). Its avian homolog, the M. obturatorius medialis, arises from the medial surface of the puboischiadic membrane (Hutchinson 2002, Gangl et al. 2004). Derived troodontids appear to occupy a state in between these two conditions. The morphology is more similar to that of non-avian theropods than to birds, but clearly encompasses the posterior and lateral surfaces of the pubic shaft in addition to the pubic apron as indicated by obliquely oriented muscle scars (van der Reest and Currie 2017). However, it is doubtful that the PIFE2 origin was located on the medial side of the puboischiadic membrane in troodontids. Muscle scars clearly indicate the origin on the bone surface (Fig. 4.3C–E,J–L). Furthermore, the osteological correlate for the lateral parts of the membrane along the proximal edge of the pubic apron is continuous with the correlate for the median portion along the pubic symphysis (Hutchinson 2001a), which are both medial to the scarred areas. A complicated transformation would be required for the origin of PIFE2 to migrate onto the medial side of the puboischiadic membrane given this morphological arrangement.

Posterior to the origin of ADD1 on the ischium, the origin of PIFE3 occupies the remainder of the available area on the lateral surface of the obturator process (Figs. 4.4A, 4.5A,F). Its exact anterior extent is unclear, but ventrally it was limited by the edge of the ischium, and dorsally by the posterolateral ridge representing the edge of the ischial shaft. As the osteological correlate for this origin is the posterior edge of the obturator process, both the process and origin of PIFE3 are distally positioned in more plesiomorphic troodontids and appear closer to the midshaft in derived members.

4.4.7 M. ischiotrochantericus (ISTR) and M. caudofemoralis brevis (CFB)

The origin of the M. ischiotrochantericus (ISTR) can be found on the medial side of the ischium at its proximal end (Figs. 4.4C, 4.5C). Exact boundaries are unclear, but a slight depression toward the dorsal edge of the ischium between the iliac contact and proximal dorsal tuberosity gives an idea as to the size of the origin. The ISTR in troodontids seems typical of other non-avian theropods and is limited to the medial surface of the ischium.

The brevis fossa houses the origin of the M. caudofemoralis brevis (CFB), and is visible in medial and ventral views (Figs. 4.4B–C, 4.5B–C). Whereas more basal species have a mediolaterally narrow brevis fossa, derived members each possess a modestly wide brevis fossa. However, it is still not as mediolaterally extensive as in plesiomorphic theropods such as tyrannosaurids (Fig. 4.6), nor as wide as in ornithomimids (Fig. 4.7). In fact, the brevis fossa in Early Cretaceous troodontids appears similar to, or smaller than, those in caenagnathids (Figs. 4.8–4.9). The CFB filled the brevis fossa and was dorsally constrained by the brevis shelf, consistent with other non-avian theropods (Hutchinson et al. 2005, 2008) and not yet in a lateral position as seen in birds (Lamas et al. 2014, Hutchinson et al. 2015).

4.5 Discussion

4.5.1 General remarks

Certain aspects of this study unavoidably introduced limitations. Although identification and description of pelvic muscle attachment sites are necessary to establish a framework for subsequent research, it is qualitative by nature and should be complemented by a more rigorous test of muscle actions. The hip is a system comprising a dynamic joint with the hind limb and the roles of some pelvic muscles can change drastically under different circumstances (e.g. highly

flexed versus highly extended). The muscles themselves are dynamic as well, and may have multiple roles depending on the axis about which the leg rotates. Another caveat of this study is that reconstruction was performed at the family level. Although this offers general clues about the ecology of the family, it does not fully represent each species, nor does it account for potential changes in ontogeny. Other analyses of particular species or growth stages are restricted primarily by the availability of such fossils and may be difficult or impossible to execute until more troodontid material is discovered. These limitations, however, do not destroy the value of this study. Description and reconstruction of troodontid pelvic musculature provides a scaffold for future studies on locomotion or myology. Additionally, it presents new evidence supporting previous hypotheses and inferred palaeoecology. Lastly, it catalogues the conditions of pelvic muscles in a non-avian family closely related to basal birds that offers a point of comparison to other maniraptorans and avialans alike.

Pelvic muscle reconstruction supports the hypothesis of troodontids as highly adapted for cursoriality, at least in derived members of the family. Troodontid hips have an expanded postacetabular region for hip extensor muscles responsible for locomotory torque. Notably, derived members of this family each possess a large origin of ILFB and a moderately large brevis fossa for the origin of CFB (Fig. 4.9). The caudal muscles of troodontids are linked to the hind limb and operate as a single locomotor module (Gatesy and Dial 1996). However, the contribution of the tail muscles to hind limb extension appears reduced. Pelvic muscles such as the ILFB appear to have taken over more of this role than in more ancestral non-avian theropods, which tend to have wide brevis fossae to accommodate tail musculature and modest origins of ILFB. Altogether, this suggests that troodontids relied more on intrinsic muscles of the pelvis and hind limb for locomotion than muscles of the tail compared to other non-avian theropods.

The proportionately long postacetabular region compared to the preacetabular region of the hip (Fig. 4.9) also increases the moment arm of these extensors. The same principle applies to the IT2 (posterior portion), IT3, and FTE due to the posterior displacement of the origin relative to its position in other maniraptorans such as *Velociraptor* (Hutchinson et al. 2008). Anterior to the acetabulum, the ITC is large compared to other hip flexors and had an additional role in medial rotation of the hind limb. The PIFE2 probably functioned similarly in hip flexion and occupied a larger region on the pubis than if the origin was limited to the posterior surface of the pubic apron. Although the preacetabular tubercle itself is unusually large as in *Gobivenator* (Tsuihiji et al. 2014), the origin of AMB is slightly, but not exceptionally, larger than those in other theropod taxa. This may have slightly increased the capacity for force generation of this muscle, although it remains the smallest muscle of the triceps femoris group that shares a common tendon for insertion. Muscles arising from the ischium follow the same layout as in other non-avian theropods. Interestingly, the arrangement of pelvic muscles in derived troodontids shows incipient resemblances to those of some paleognath birds. In *Struthio*, the fastest extant biped, the AMB, ILFB, and ITC have the largest moment arms of the pelvic muscles (Smith et al. 2007, Hutchinson et al. 2015). The AMB and ITC are the strongest hip flexors, whereas the ILFB is the strongest hip extensor and knee flexor (Smith et al. 2006, 2007). Troodontids also possess large origins of ILFB and ITC, relative to the total available area for muscle attachment on the hip (Fig. 4.4A). The arrangement and relative sizes of the locomotory muscles provide support for troodontids as speedy, cursorial creatures that depended more on extensor muscles originating from the hip than from the tail compared to other non-avian theropods.

4.5.2 Comparisons with other theropods

Comparison of troodontid locomotory muscle arrangement with contemporaneous cursors highlights interesting similarities and differences. Other dinosaurs inferred as cursorial by Carrano (1999) that may have lived alongside troodontids include caenagnathids, dryosaurids, hypsilophodontids, ornithomimids, and tyrannosaurids. All theropod families listed here also had members that each have an arctometatarsus, a structure associated with increased cursoriality (Holtz 1994, Carrano 1999). Ornithischians are of limited relevance to this discussion due to differences in the evolution of their hips and resultant radical changes in associated musculature. Non-avian theropods are overall fairly conservative in pelvic morphology, with similar layouts of locomotory muscles in distantly related members like *Tyrannosaurus* (Hutchinson et al. 2005) and *Velociraptor* (Hutchinson et al. 2008). Of the more cursorial taxa, tyrannosaurids possess relatively wide brevis fossae (Fig. 4.6)—among other features of the hip and tail—indicative of large caudal muscles with substantial roles in hind limb extension (Persons and Currie 2011). Ornithomimids likewise possess wide brevis fossae (Fig. 4.7) and have rather similar pelvic morphologies to those of tyrannosaurids, evocative of the shared cursorial ancestry put forward by Carrano (1999). In each of these families, muscles associated with both the pelvis and tail played a substantial role in locomotion, which is different from the condition in caenagnathids. Although skeletal data suggest a cursorial nature for Caenagnathidae, members of this family have postacetabula that are proportionately shorter than the preacetabula and reduced brevis fossae (Fig. 4.8) that in turn provide only limited space for hind limb extensors and caudal musculature. Caenagnathids relied more on muscles within the pelvis and hind limb for locomotive torque than did plesiomorphic theropods. However, tail muscles were still integrated into a shared locomotor module with the hind limb (Gatesy and Dial 1996) and were useful in

locomotion as in other oviraptorosaurs (Persons et al. 2014). Troodontids are more similar to caenagnathids than to the other two taxa in this respect, reflecting increased reliance on intrinsic pelvic muscles for locomotion. On the other hand, these taxa show stark differences in the preacetabular to postacetabular length ratios of their ilia (Fig. 4.9), indicating a clear disparity in the amount of area available area for hip flexors and extensors originating on the pelvis. Note that incomplete preservation of one *Sinovenator changii* specimen (IVPP V12583) prevents accurate preacetabulum:postacetabulum comparison (Fig. 4.9D). Among cursorial dinosaurs, these patterns suggest that several lineages achieved high cursoriality in different ways. With this in mind, the question of competition amongst cursorial Cretaceous creatures must be addressed. Was the Mesozoic big enough for them all, or did some degree of ecological separation between taxa allow them to coexist?

Besides locomotive adaptations, other aspects of palaeobiology may provide information about competition amongst these dinosaurs. Whereas hypsilophodontids and dryosaurids were herbivorous, highly cursorial theropods varied in dietary preference. Tyrannosaurids exhibit overwhelming evidence for carnivory (Zanno and Makovicky 2011) in their teeth and in tooth marks on herbivores that succumbed to the jaws of *Tyrannosaurus* (Erickson and Olson 1996, Erickson et al. 1996, Carpenter 1998, Barrett and Rayfield 2006, Zanno and Makovicky 2011, DePalma et al. 2013). Ornithomimids tend to ally with herbivores based on the presence of a rhamphotheca and gastroliths (Kobayashi et al. 1999, Norell et al. 2001, Barrett 2005). Caenagnathids have been treated as highly cursorial by some (Carrano 1999) and are tentatively inferred as herbivorous, but may have been suited for omnivory (Zanno and Makovicky 2011, Funston and Currie 2014). In contrast, troodontids appear suited neither for herbivory nor hypercarnivory and probably sought smaller or softer prey items for a diet of omnivory or

carnivory (Ryan et al. 1998, Zanno and Makovicky 2011, Hendrickx et al. 2015, Torices et al. 2018). Thus, competition for food was probably limited between troodontids and contemporaneous cursorial dinosaurs.

However, the carnivorous nature of derived troodontids is shared with tyrannosaurids. Torices et al. (2018) suggest that troodontids were not well suited to handle prey that was large, hard, or otherwise risked tooth damage, clearly differing from direct evidence of such behaviour in tyrannosaurids (Erickson and Olson 1996, Erickson et al. 1996). Despite the capability of adult tyrannosaurids for bone-crushing feeding, some studies suggest that they may not have been well suited for running due innate biomechanical limitations and lack of necessary extensor musculature (Hutchinson and Garcia 2002, Hutchinson 2004). Also, apparent changes in relative limb proportions between juvenile and adult tyrannosaurids may be controlled by allometry (Persons and Currie 2016). However, compared to adults, these proportionately long distal leg segments and lower body masses in juveniles may reflect higher cursoriality (Currie 1998, Paul 1998, Hutchinson 2004). Perhaps this indicates niche partitioning between speedier juveniles and larger-bodied adults. Young tyrannosaurids may have sought smaller prey items that were easier to handle due to limitations of small body size or preference, but gregarious behaviour documented in *Albertosaurus* challenges this position (Currie 1998, Currie and Eberth 2010). Overlap in cursorial ability and potentially diet between troodontids and young tyrannosaurids may have put these two groups in competition with one another for resources, at least during certain times of the year. Other differences in behaviour, such as habitat preference, may have restricted the amount of interaction experienced between these families. Regardless, some overlap between the two families does not exclude them from coexisting. Furthermore, differences in tooth performance between troodontids and other theropods suggests that specific

diets varied among carnivorous dinosaurs, even ones that employed the same feeding mechanisms. Studies of dental biomechanics and the like are better suited to shed light on feeding behaviour and niche partitioning, but this is only part of the challenge of food acquisition; animals must be able to pursue and catch prey, or escape predators, in order to survive. This is where locomotory adaptations offer some insight.

4.5.3 Theropod cursoriality

Of the diverse forms evolved in Maniraptora, those suggesting high cursoriality curiously evolved several times. Additionally, this occurred during an interval of theropod evolution marked by the steady reduction of caudal musculature involved in locomotion (CFB and its counterpart), which seemed only to amplify within Maniraptora (Allen et al. 2013). In spite of wide divergence in dietary adaptations and stepwise exclusion of hind limb extensors originating from the tail, adaptations for agility and fleetness arose repeatedly. Unfortunately, this does not resolve much more about predator-prey relationships discussed in Carrano (1999). Predation on young tyrannosaurids by troodontids is as much a possibility as vice versa. Cursorial adaptations likewise may have evolved to catch prey as well as to avoid becoming prey, and these options are not mutually exclusive. In fact, enhanced running ability imparts benefits to both of these behaviours. Locomotory muscle reconstruction does, however, demonstrate that high cursoriality is not tightly tied to dietary preference or gradual loss of tail musculature. Troodontidae represents a family of maniraptorans that appeared to accommodate this loss of locomotory power from the tail by regaining it from the pelvis. An enlarged ILFB (among other hind limb extensors) provides this strength, but also has a role in knee flexion. Allen et al. (2013) remarked that this may reflect a stage in the gradual transition from a “hip-driven” to “knee-driven” mode

of locomotion in which hamstring muscles acting about the knee progressively replace femoral extensors like the CFB. The cancellous bone anatomy in the proximal and distal ends of theropod hind limb bones (Bishop et al. 2018b) and both musculoskeletal and finite element analysis models (Bishop et al. 2018a) corroborate the transition from hip- to knee-driven locomotion hypothesis. Internal bone microstructure of the troodontid femur is intermediate between that of plesiomorphic theropods and birds (Bishop et al. 2018b). Whereas a tyrannosaurid femur is similarly adapted to a human femur to bending-dominated loading and a bird femur is adapted to torsional loading, a troodontid femur is suited for an intermediate condition with a mixture of these regimes. Additionally, biomechanical models reflect the inferred mid-stance posture of troodontids as intermediate between the more upright stance with a subvertical femur in tyrannosaurids and the more crouched posture with a sub-horizontal femur of birds (Bishop et al. 2018a). Therefore, evidence from bone microstructure, musculoskeletal models, and finite element analysis suggests that troodontids had a mid-stance femoral posture somewhere between subvertical, like plesiomorphic theropods, and sub-horizontal, as in birds. The increased size of the origins of knee flexor muscles may be linked to this transition in femoral posture, but comparison to extant birds suggests otherwise. Relatively large origins of muscles involved in hind limb extension and knee flexion (e.g. ILFB) compared to muscles involved in opposing actions (e.g. ITC) are apparent in emus (Lamas et al. 2014) and ostriches (Smith et al. 2006). On the other hand, less cursorially adapted chickens (Paxton et al. 2010) show the reverse in that the origin of muscles that flex the hind limb are larger. With this in mind, an enlarged ILFB and moderately sized CFB in troodontids is consistent with an intermediate position in the transition from hip- to knee-driven locomotion, simultaneously supportive of increased reliance on muscles acting about the knee with respect to plesiomorphic theropods and enhanced cursoriality.

4.5.4 Evolution of locomotory adaptations within Troodontidae

Reconstructions of locomotory muscles at both early and late stages in troodontid history offer a glimpse at evolutionary patterns in their family history (Figs. 4.4–4.5). The triceps femoris group changed slightly in that the origins of AMB and IT2 became more pronounced in later members, but overall retained a comparable arrangement. In a similar manner, the CFB and ILFB did not change dramatically, but enlarged as the postacetabular ilium expanded and brevis fossa widened. This increase in area available for attachment of hind limb extensors may indicate increasing cursoriality through evolutionary time, suggesting that high cursoriality was secondarily developed in Troodontidae. The trajectory of increasing cursoriality through evolutionary time based on pelvic musculature corroborates similar patterns in foot morphology and development of a subarctometatarsus into a full-fledged arctometatarsus (Fowler et al. 2011). Selection pressure(s) for secondarily increased cursoriality remain enigmatic, but secondarily lost volancy may be a major factor. Although the closely related paravian *Anchiornis* probably had some capacity for flight, basal troodontids such as *Jinfengopteryx* have relatively small arms unsuitable for volancy (Evangelista et al. 2014a, Sullivan et al. 2017). Causal mechanisms for secondarily lost flight adds another degree of separation from the evolution of pelvic musculature, but if a major factor, may be attributable to another means of niche partitioning with dromaeosaurids (Fowler et al. 2011). Without aerial locomotion as a means of transport, troodontids may have reinvested in terrestrial locomotion and secondarily enlarged leg extensor musculature. Deep dorsal group muscles stayed much the same throughout the Cretaceous, as did those of the flexor cruris group, Mm. adductores femorum, and the ISTR. The osteological correlates of the FTI1 and FTI3, respectively the distal and proximal dorsal tuberosities, were

reduced over evolutionary time. Two likely explanations for this trend are that it is an artefact of body size, or a signal of reduction in flexor cruris muscles and associated pelvic ligaments. The troodontids examined here include more plesiomorphic species with smaller body sizes and pronounced ischial tuberosities compared to derived members that tend towards larger body sizes and reduced ischial tuberosities, which might support the argument for an inverse relationship to body size. However, *Talos* is a more derived, Late Cretaceous taxon with reduced ischial tuberosities and histological evidence for smaller adult body size than other troodontids of the time (Zanno et al. 2011). This might be interpreted as support for gradual reduction in these muscles and ligaments, maybe functionally replaced by other muscles performing similar roles. However, it is unclear whether *Talos* represents a trend or an anomaly, making it difficult to rule out either explanation. Alternatively, the increased length of the ischial shaft over troodontid evolution probably increased the moment arm of the FTI1 that arose from the distal end of the bone. It is possible that an increase in moment arm—and consequently, an increase in leverage—compensated for a reduction in muscle size or strength, similar to the tradeoff between leverage and strength for caudofemoral muscles in hadrosaurids and tyrannosaurids (Persons and Currie 2014). Within the Mm. puboischiofemorales externi, the origin of PIFE2 changed radically in that it expanded both proximally and laterally to encompass a large area of the pubic bones. Early in troodontid evolution, the origin of PIFE2 expanded laterally, reflected in the embayment of the posterior side of the pubes. This resulted in concomitant mediolateral compression of the posterior edges of the pubic shafts that border the pubic apron. Late Cretaceous troodontids show subsequent proximal and further lateral expansion of the PIFE2, which may suggest an increase in the importance of hip flexion and lateral hip rotation, its main actions. Beyond non-avian theropods, the arrangement of pelvic musculature in Troodontidae sets a baseline for the

condition of basal avialans. Despite controversy around fine scale paravian relationships, troodontids consistently express a close relationship to early birds and are often recovered as the sister taxon to Avialae (e.g. Hendrickx et al. 2015). While new discoveries continue to adjust and refine our understanding of the exact relationships between basal avialans, troodontids stand as a closely related avian outgroup that helps to characterize their early evolution. Evolutionary changes between non-avian theropods and birds in the context of locomotion are well documented (Hutchinson and Allen 2009). The reconstruction of troodontid pelvic muscles here further validates the gradual, stepwise evolution of muscles in theropod dinosaurs. Non-avian theropods, up to and including their most derived members, were remarkably conservative in numbers of pelvic muscles and their arrangements. The condition of troodontid locomotory musculature shows some reorganization of hip extensors, and that the caudal and pelvic locomotor modules were not yet fully separated. Conservative muscle arrangement and reorganization in non-avian theropods is consistent with previous studies that note relatively rapid changes in early bird evolution (Pittman et al. 2013). Additionally, the muscle attachment sites identified here are nearly identical to those proposed by Bishop et al. (2018b) despite using different specimens, corroborating the identification and layout of troodontid pelvic musculature. That being said, a few muscle origins exhibit unusual morphology. The PIFE2 of a derived troodontid extends laterally beyond the pubic apron to cover the posterior and lateral sides of the pubic shafts. In other taxa including more basal troodontids, the PIFE2 is restricted to the posterior surface of the pubic apron and lacks extensive coverage of the pubic shafts. Its avian homolog migrated laterally and originates farther from the midline on the puboischiadic membranes in birds, additionally shifting primary function from hip flexor to lateral rotator as the pelvis became opisthopubic (Hutchinson and Gatesy 2000). Consideration of this membrane

in Troodontidae further complicates this scenario. The proximal edge of the troodontid PIFE2 origin is bordered by a proximodistally elongate ridge on the medial side of the pubis. This ridge is considered an osteological correlate for part of the puboischiadic membrane, specifically for paired, lateral membranes (Hutchinson 2001a). Because this ridge, and thus the puboischiadic membrane, is medial to the origin of PIFE2, a somewhat complex migration of the PIFE2 is required to end up on the medial surface of this membrane. Due to the condition in early troodontids and relative position of other soft tissues, it seems that the lateral migration of the PIFE2 in Troodontidae and Aves is the result of convergent evolution. The same can be said for reduction of the FTI1, which had a prominent osteological correlate in early troodontids, but was reduced convergently in derived troodontids and reduced to the point of loss in birds. Dorsoventral expansion of the postacetabular portion of the ilium and concomitant enlargement of the ILFB is yet another independently gained feature between these two groups. An unusual origin for IT2 is also identified in *Latenivenatrix*, but has limited bearing on the broader evolutionary transition from non-avian theropods to birds. These features underscore that the condition of early troodontids better represents an outgroup to birds than that of derived troodontids. Additionally, it shows that troodontids, as an outgroup to basal avialans, had a single-headed PIFI2 and that both the FTI1 and PIFE3 were present, unlike in modern birds.

4.6 Summary of troodontid pelvic myology

Description and reconstruction of more basal and more derived troodontid pelvic muscles fill a gap in the knowledge of theropod locomotory muscle evolution. An unusual origin of IT2 and unique PIFE2 morphology highlight peculiar or previously unrecognized aspects of troodontid pelvic myology. The arrangements and relative sizes of locomotory muscles

qualitatively support derived troodontids as adapted for high cursoriality, an adaptation they gained secondarily. This permits their placement in ecological context with other Cretaceous cursors. Predator-prey interactions remain complex and unclear, but troodontid locomotory muscles underscore the convergence of cursoriality among theropods with widely varied diets and differences in the degree of interconnection between caudal and pelvic muscles. Pelvic muscles account for reduced caudal input to hind limb extension during a gradual evolutionary shift towards a locomotory mode driven by intrinsic muscles of the hip and hind limb. Further to this, our understanding of the condition of pelvic musculature in early avialans is improved by reconstruction in troodontids as a closely related outgroup. Several aspects of pelvic musculature were convergently evolved between derived troodontids and birds including lateral migration of the PIFE2, reduction or loss of the FTI1, and dorsoventral expansion of the postacetabular portion of the ilium. This reconstruction stands as a framework that permits more rigorous and quantitative hypothesis testing in future studies.

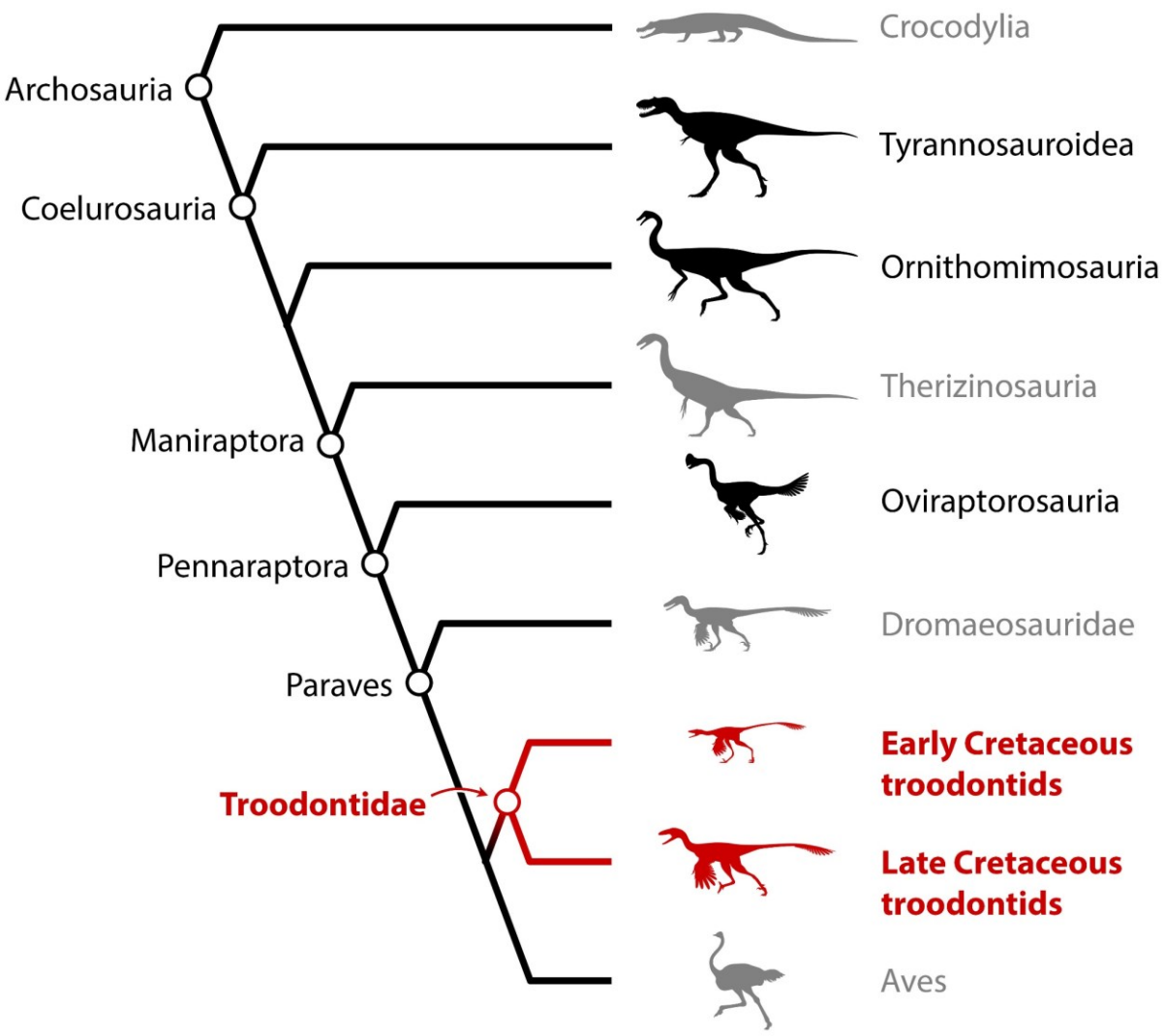

Figure 4.1. Simplified phylogeny of Troodontidae among Archosauria and contemporaneous cursorial theropods of North America during the Late Cretaceous. Phylogeny includes other contemporaneous, extinct theropods and representatives of its Extant Phylogenetic Bracket (Crocodylia and Aves). Coeval taxa shaded based on whether they are inferred as highly cursorial based on osteological correlates (black) or not (grey).


A
ris
lis
rp
lp
B
pdt
ddt
op
C
isc
pa
D
isc
pa
E
pa
F
pa
pb
G
pa
H
pa
pb
I
dep
pp
ace
isp
J
pp
ace
isp
bf
K
isp
ace
dep
pp
L
bf
isp
ace
pp
cf

Figure 4.2. Basal troodontid material examined for muscle attachment sites. Pelvis of *Jianianhualong tengi* (DLXH 1218) in block (A), left ischium in lateral view (B), and pubes in posterior view (C). Elements of *Sinovenator changii* (IVPP V12583, V12615) including pubes of V12615 in posterior view (D), right pubis of V12583 in anterior (E), posterior (F), lateral (G), and medial (H) views, left ilium of V12583 in lateral (I) and ventral (J) views, and right ilium of V12615 in lateral (K) and ventral (L) views. All scale bars are 5 cm. **Abbreviations: ace,** acetabulum; **bf,** brevis fossa; **cf,** cuppedicus fossa; **ddt,** distal dorsal tuberosity; **dep,** depression; **ic,** iliac contact; **isc,** ischiadic contact; **isp,** ischiadic peduncle; **lis,** left ischium; **lp,** left pubis; **op,** obturator process; **pa,** pubic apron; **pah,** preacetabular hook; **pb,** pubic boot; **pc,** pubic contact; **pdt,** proximal dorsal tuberosity; **plr,** posterolateral ridge; **pp,** pubic peduncle; **pt,** preacetabular tubercle; **ris,** right ischium; **rp,** right pubis.

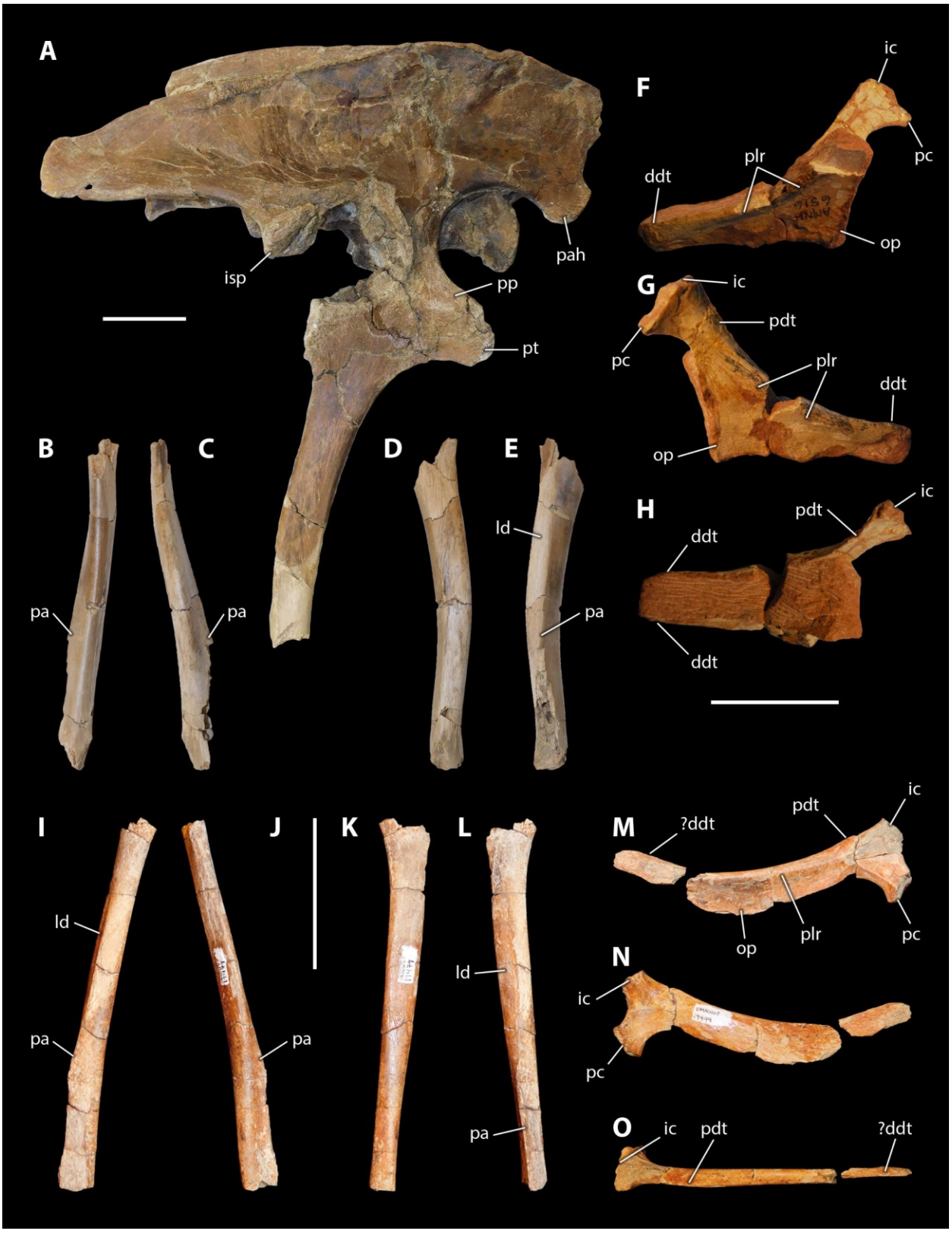
A
isp
pah
pp
pt
B
pa
C
pa
D
E
ld
pa
F
ic
pc
plr
ddt
op
G
ic
pdt
pc
plr
ddt
op
H
pdt
ic
ddt
ddt
I
ld
pa
J
pa
K
L
ld
pa
M
?ddt
pdt
ic
op
plr
pc
N
ic
pc
O
ic
pdt
?ddt

Figure 4.3. Derived troodontid material examined for muscle attachment sites. Pelvis of *Latenivenatrix mcmasterae* (UALVP 55804) including right ilium and pubis in lateral view (A), and left pubis in anterior (B), posterior (C), lateral (D), and medial (E) views. Ischia of *Saurornithoides mongoliensis* (AMNH FR 6516) in right lateral (F), left lateral (G), and dorsal (H) views. Elements of *Talos sampsoni* (Courtesy of Natural History Museum of Utah, UMNH VP 19479) including pubis in anterior (I), posterior (J), lateral (K), and medial (L) views, and right ischium in lateral (M), medial (N), and dorsal (O) views. All scale bars are 5 cm. **Abbreviations: ace,** acetabulum; **bf,** brevis fossa; **cf,** cuppedicus fossa; **ddt,** distal dorsal tuberosity; **dep,** depression; **ic,** iliac contact; **isc,** ischiadic contact; **isp,** ischiadic peduncle; **ld,** longitudinal depression; **lis,** left ischium; **lp,** left pubis; **op,** obturator process; **pa,** pubic apron; **pah,** preacetabular hook; **pb,** pubic boot; **pc,** pubic contact; **pdt,** proximal dorsal tuberosity; **plr,** posterolateral ridge; **pp,** pubic peduncle; **pt,** preacetabular tubercle; **ris,** right ischium; **rp,** right pubis.

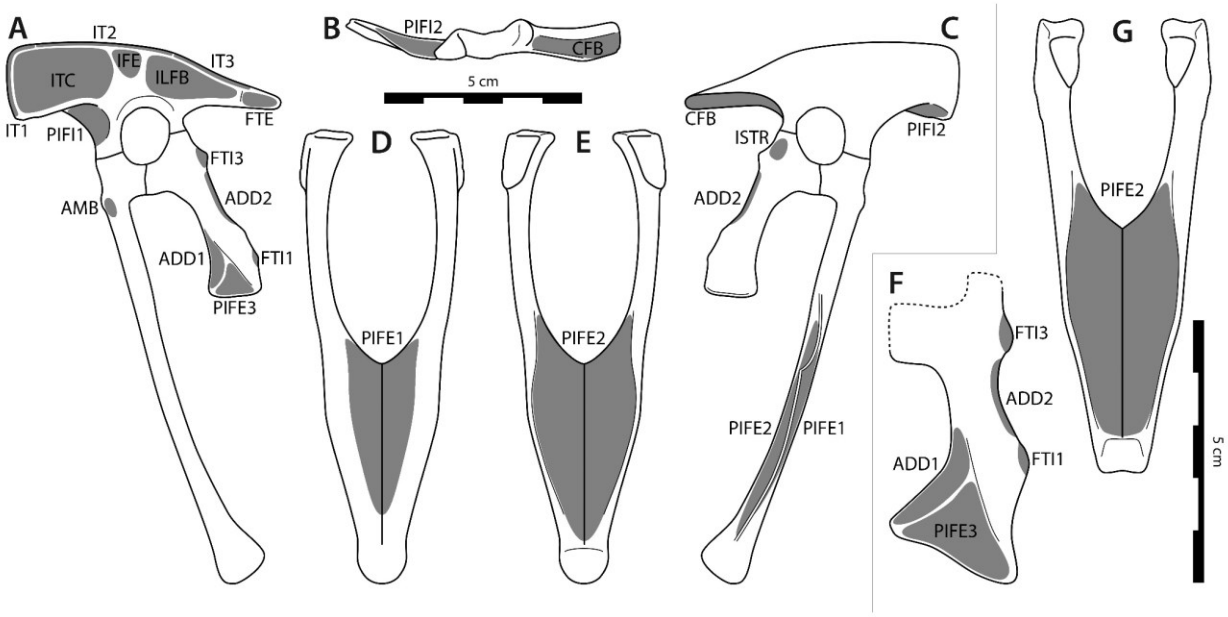

Figure 4.4. Basal troodontid pelvic myology. Pelvis of *Sinovenator changii* modified from Xu et al. (2002) in lateral view (A), ilium (IVPP V12615) in ventral view (B), pelvis in medial view (C), pubes (IVPP V12583) in anterior (D) and posterior (E) views, and pelvic elements of *Jianianhualong tengi* (DLXH 1218) including left ischium in lateral view (F) and pubes in posterior view (G). Dashed outline in F indicates estimated reconstruction of poorly preserved fossil in the specimen. Both scale bars are 5 cm, each one representing either *Sinovenator changii* (A–E) or *Jianianhualong tengi* (F–G). **Abbreviations: ADD1,** M. adductor femoris 1; **ADD2,** M. adductor femoris 2; **AMB,** M. ambiens; **CFB,** M. caudofemoralis brevis; **FTE,** M. flexor tibialis externus; **FTI1,** M. flexor tibialis internus 1; **FTI3,** M. flexor tibialis internus 3; **IFE,** M. iliofemoralis externus; **ILFB,** M. iliofibularis; **ISTR,** M. ischiotrochantericus; **IT1,** M. iliotibialis 1; **IT2,** M. iliotibialis 2; **IT3,** M. iliotibialis 3; **ITC,** M. iliotrochantericus caudalis; **PIFE1,** M. puboischiofemoralis externus 1; **PIFE2,** M. puboischiofemoralis externus 2; **PIFE3,** M. puboischiofemoralis externus 3; **PIFI1,** M. puboischiofemoralis internus 1; **PIFI2,** M. puboischiofemoralis internus 2.

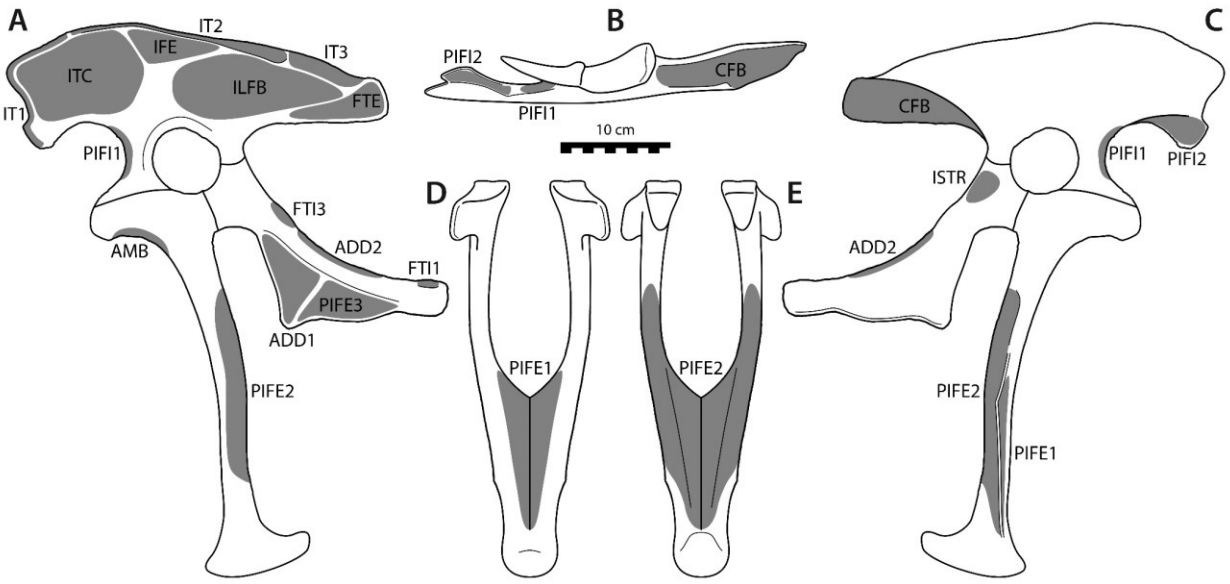

Figure 4.5. Derived troodontid pelvic myology. Composite pelvis created from ilia and pubes of *Latenivenatrix mcmasterae* (UALVP 55804), pubic boot of *Gobivenator mongoliensis* modified from Tsuihiji et al. (2014), and ischium of *Saurornithoides mongoliensis* (AMNH FR 6516) scaled to fit according to contact surfaces with other pelvic bones. Pelvis in lateral view (A), ilium in ventral view (B), pelvis in medial view (C), and pubes in anterior (D) and posterior (E) views. Scale bar is 10 cm. **Abbreviations: ADD1,** M. adductor femoris 1; **ADD2,** M. adductor femoris 2; **AMB,** M. ambiens; **CFB,** M. caudofemoralis brevis; **FTE,** M. flexor tibialis externus; **FTI1,** M. flexor tibialis internus 1; **FTI3,** M. flexor tibialis internus 3; **IFE,** M. iliofemoralis externus; **ILFB,** M. iliofibularis; **ISTR,** M. ischiotrochantericus; **IT1,** M. iliotibialis 1; **IT2,** M. iliotibialis 2; **IT3,** M. iliotibialis 3; **ITC,** M. iliotrochantericus caudalis; **PIFE1,** M. puboischiofemoralis externus 1; **PIFE2,** M. puboischiofemoralis externus 2; **PIFE3,** M. puboischiofemoralis externus 3; **PIFI1,** M. puboischiofemoralis internus 1; **PIFI2,** M. puboischiofemoralis internus 2.

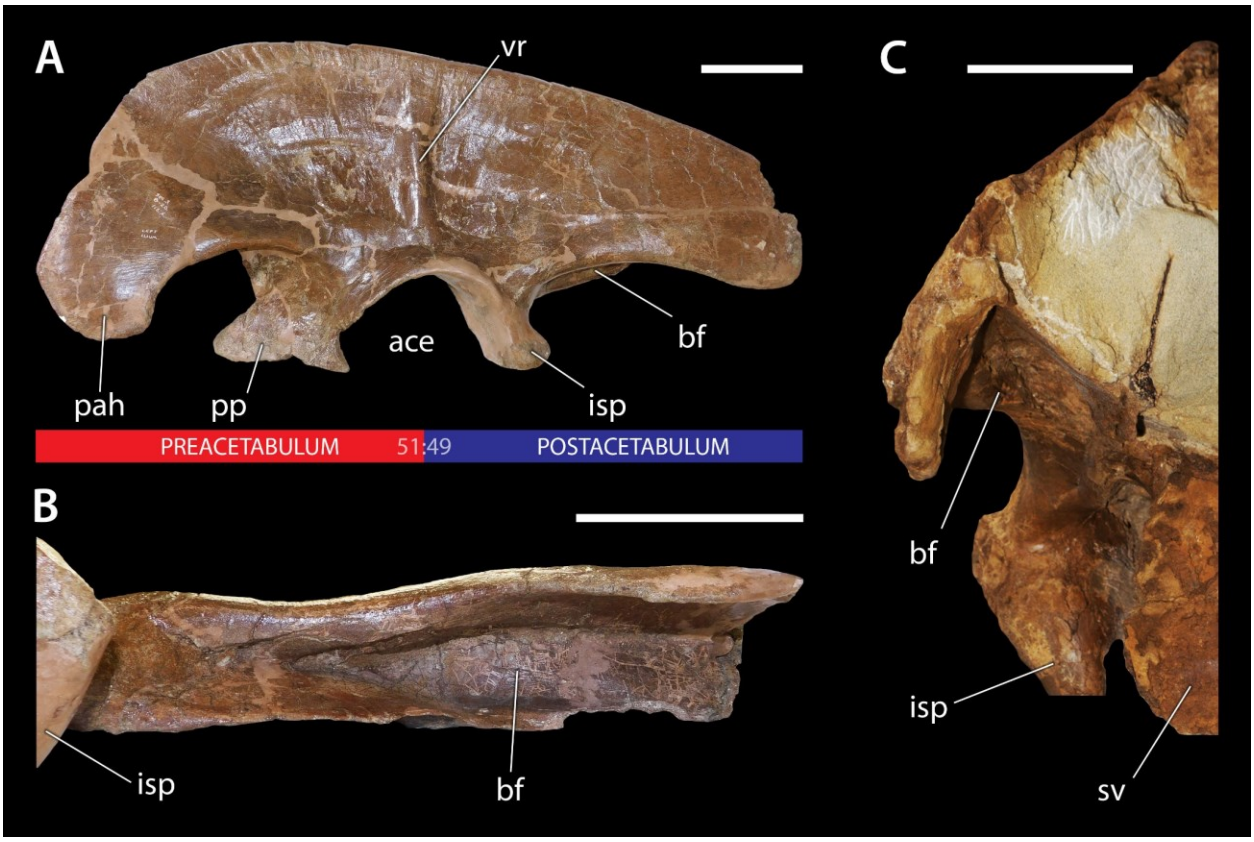

Figure 4.6. Iliac features and proportions of tyrannosaurids. Preacetabular:postacetabular proportions and relative brevis fossae size as proxies for major hind limb flexor and extensor muscle groups are highlighted. Left ilium of *Albertosaurus sarcophagus* (CMN 11315) in lateral view (A) and brevis fossa in ventral view (B); note dorsoventrally deep brevis fossa despite taphonomic distortion that resulted in some mediolateral compression. Left ilium of *Daspletosaurus torosus* (UALVP 52981) in posterior view (C). Scale bars are 10 cm. **Abbreviations: ace,** acetabulum; **bf,** brevis fossa; **isp,** ischiadic peduncle; **pah,** preacetabular hook; **pp,** pubic peduncle; **vr,** vertical ridge.

Figure 4.7. Iliac features and proportions of ornithomimids. Preacetabular:postacetabular proportions and relative brevis fossae size as proxies for major hind limb flexor and extensor

muscle groups are highlighted. Left ilium of indeterminate ornithomimid (CMN 8897) in lateral view (A) and brevis fossa in ventral (B) and posterior (C) views. Left ilium of *Dromiceiomimus brevitertius* (UALVP 16182) in lateral view (D) and right brevis fossa (reversed) in ventral view (E). Right ilium of indeterminate ornithomimid (TMP 1981.019.0299, reversed) in posterior view (F). Scale bars are 10 cm. **Abbreviations: bf,** brevis fossa; **isp,** ischiadic peduncle; **pah,** preacetabular hook; **pp,** pubic peduncle; **sac,** supraacetabular crest; **vs,** vertical sulcus.

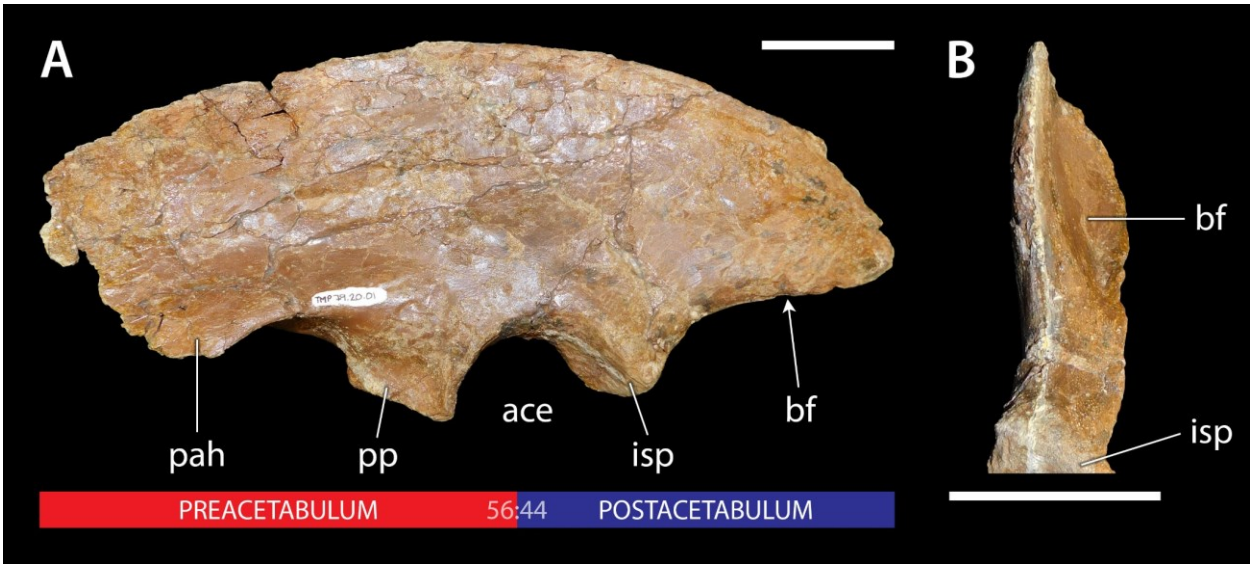

Figure 4.8. Iliac features and proportions of caenagnathids. Preacetabular:postacetabular proportions and relative brevis fossa size as proxies for major hind limb flexor and extensor muscle groups are highlighted. Left ilium of *Chirostenotes pergracilis* (TMP 1979.020.0001) in lateral view (A) and brevis fossa in ventral view (B). Scale bars are 5 cm. **Abbreviations: ace,** acetabulum; **bf,** brevis fossa; **isp,** ischiadic peduncle; **pah,** preacetabular hook; **pp,** pubic peduncle.

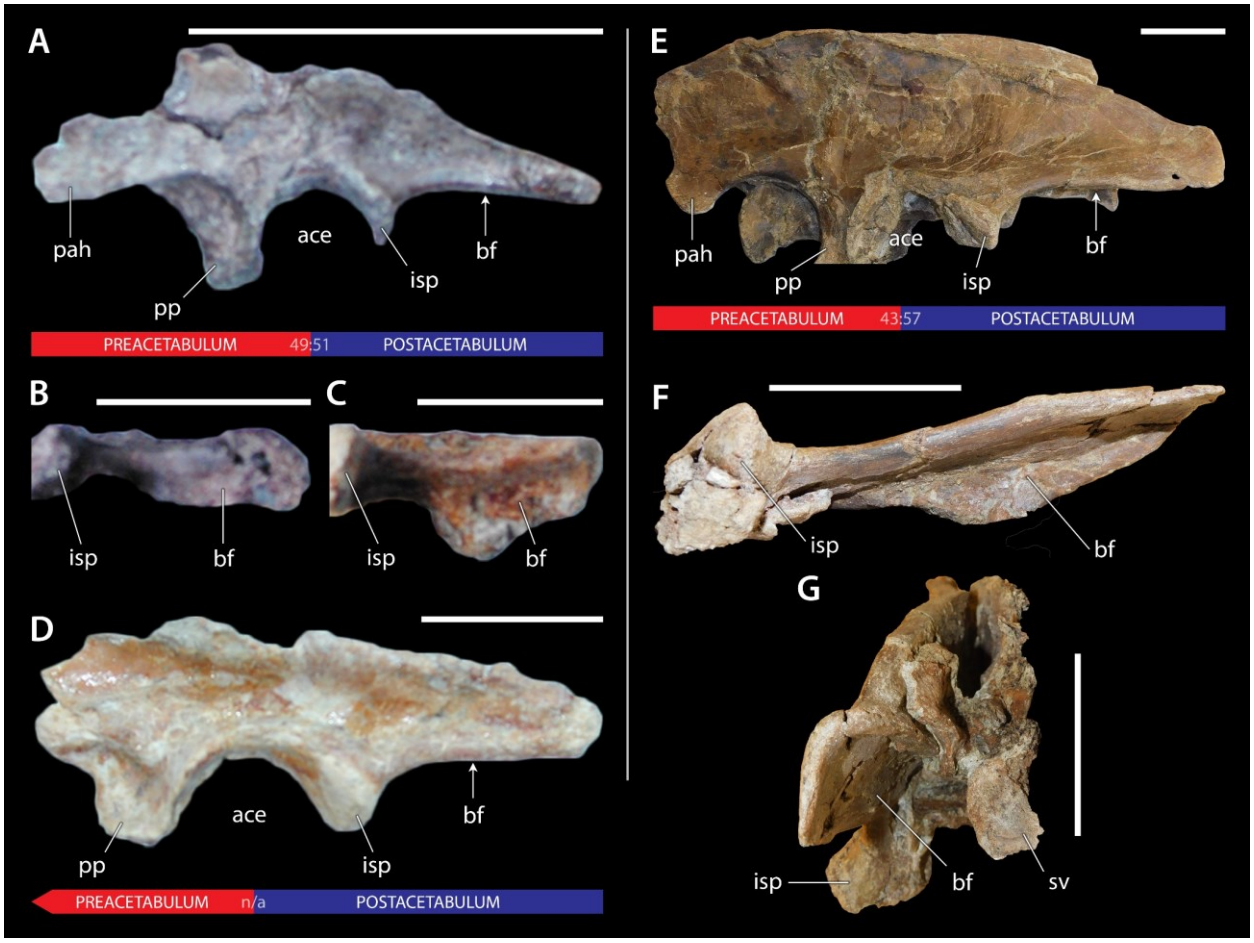

Figure 4.9. Iliac features and proportions of troodontids. Preacetabular:postacetabular proportions and relative brevis fossae size as proxies for major hind limb flexor and extensor muscle groups are highlighted. Right ilium of *Sinovenator changii* (IVPP V12615, reversed) in lateral view (A) and brevis fossa in ventral view (B). Left ilium of *Sinovenator changii* (IVPP V12583) showing brevis fossa in ventral view (C) and ilium in lateral view (D). Right ilium of *Latenivenatrix mcmasterae* (UALVP 52981, reversed) in lateral view (E) and brevis fossa in ventral (F) and posterior (G) views. Scale bars are 5 cm. **Abbreviations: ace,** acetabulum; **bf,** brevis fossa; **isp,** ischiadic peduncle; **pah,** preacetabular hook; **pp,** pubic peduncle.

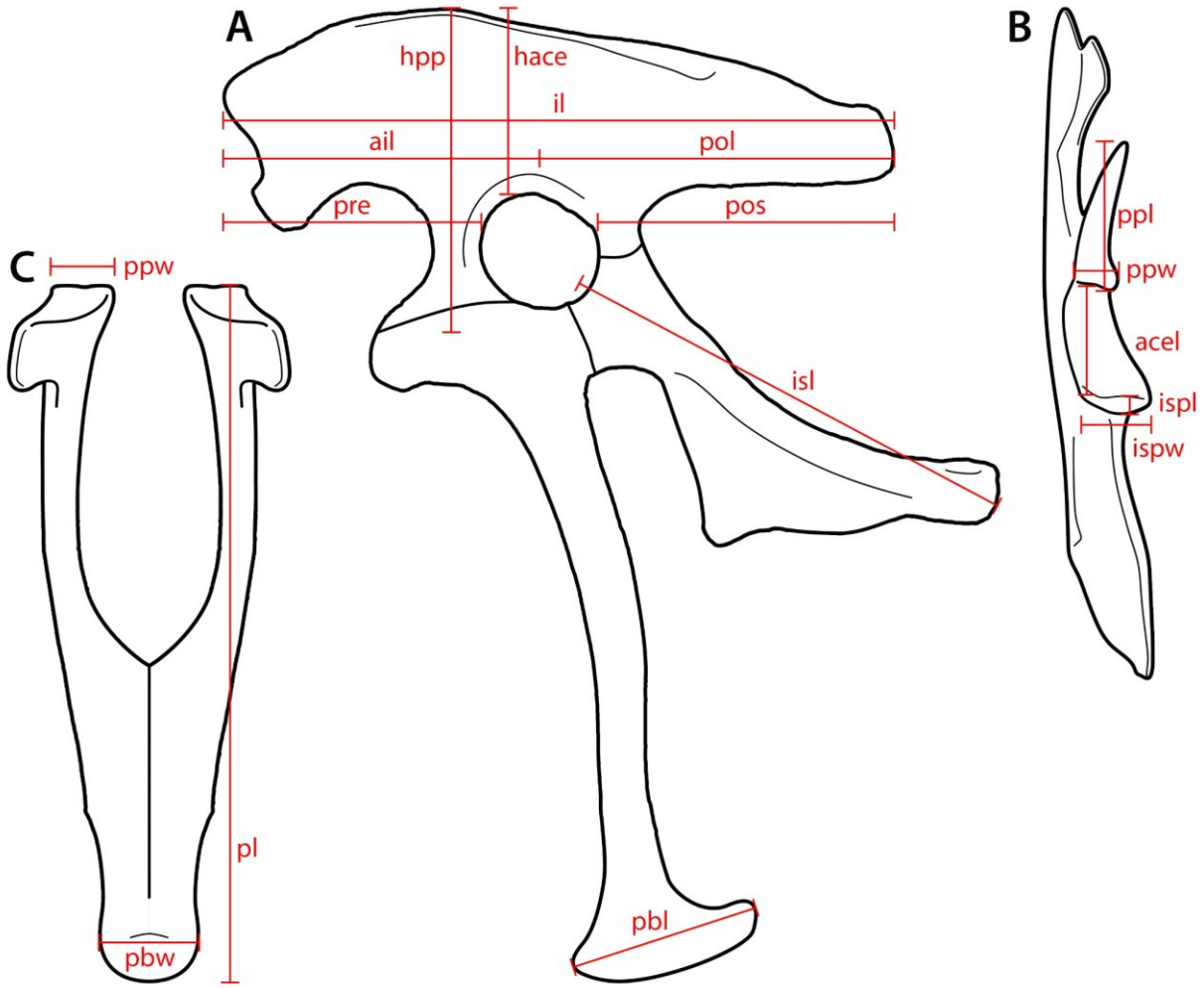

Figure 4.10. Measurement protocol. Reconstructed troodontid pelvis in left lateral view (A), ilium in ventral view (B, anterior to top), and pubes in anterior view (C). Ilium and pubis based on *Latenivenatrix mcmasterae* (UALVP 55804), pubic boot modeled after *Gobivenator mongoliensis* (Tsuihiji et al. 2014), and ischium based on *Saurornithoides mongoliensis* (AMNH FR 6516). **Abbreviations: acel,** acetabulum length; **ail,** antilium length; **hace,** height above acetabulum; **hpp,** height above pubic peduncle; **il,** ilium length; **isl,** ischium length; **ispl,** ischiadic peduncle length; **ispw,** ischiadic peduncle width; **pbl,** pubic boot length; **pbw,** pubic boot width; **pl,** pubis length; **pol,** postilium length; **pos,** postacetabulum length; **ppl,** pubic peduncle length; **ppw,** pubic peduncle width; **pre,** preacetabulum length.

Table 4.1. Pelvic material examined or referenced for muscle attachment sites. Note: AMNH, American Museum of Natural History; DLXH, Dalian Xinghai Museum; IVPP, Institute for Vertebrate Paleontology and Paleoanthropology; RM, Redpath Museum; ROM, Royal Ontario Museum; UALVP, University of Alberta Laboratory for Vertebrate Palaeontology; UAMZ, University of Alberta Museum of Zoology; UMNH VP, Utah Museum of Natural History.

Taxon	Specimen number	Status and element(s)
Troodontidae		
Jianianhualong tengi	DLXH 1218	Fossil; articulated skeleton with semi-articulated pelvis
Latenivenatrix mcmasterae	UALVP 55804	Fossil; ilia, both pubes missing distal ends
Saurornithoides mongoliensis	AMNH FR 6516	Fossil; associated skeleton with semi-articulated pelvis dissociated during preparation
Sinovenator changii	IVPP V12583, V12615	Fossil; articulated skeleton dissociated during preparation
Talos sampsoni	UMNH VP 19479	Fossil; ilium fragments, proximal ends of both pubes and ischia
Aves		
Apteryx haastii	RM 8369	Articulated skeleton mount
Corvus corax	UAMZ (uncatalogued)	Dissected
Dromaius novaehollandiae	ROM R6843, ROM R7654, UAMZ B-FIC2014.260	Disarticulated, associated skeletons (ROM); articulated skeleton mount (UAMZ)
Gallus gallus	RM 8355	Articulated skeleton mount
Rhea americana	RM 8499	Disarticulated, associated skeleton
Struthio camelus	ROM 1080, ROM 1162, ROM 1933, ROM 2136, ROM 2305, UAMZ 7159	Disarticulated, associated skeletons
Crocodylia		
Alligator mississippiensis	ROM R343	Postcranial skeleton
Alligator sp.	UAMZ HER-R654	Articulated skeleton mount
Caiman crocodilus	RM 5242; UAMZ	Disarticulated, associated

	(uncatalogued)	skeleton (RM), dissected (UAMZ)
Osteolaemus tetraspis	RM 5216	Articulated skeleton mount
Squamata		
Tupinambis teguixin	ROM R436	Semi-prepared skeleton
Varanus albigularis	RM 5220	Disarticulated, associated skeleton
Varanus exanthematicus	UAMZ (uncatalogued)	Dissected
Varanus jobiensis	RM 5219	Disarticulated, associated skeleton
Varanus komodoensis	ROM R7565	Disarticulated, associated skeleton
Varanus niloticus	RM 5221	Disarticulated, associated skeleton
Varanus rudicollis	ROM R7318	Articulated skeleton mount
Varanus salvator	RM 5222, RM 5223, RM 5224	Disarticulated, associated skeleton

Table 4.2. Pelvic muscle homologies in crocodylians and avians. Modified from Carrano and Hutchinson (2002) and Hutchinson et al. (2005).

Crocodylia	Aves
Triceps femoris	
M. iliotibialis 1 (IT1)	M. iliotibialis cranialis (IC)
M. iliotibialis 2, 3 (IT2, IT3)	M. iliotibialis lateralis (IL)
M. ambiens (AMB)	M. ambiens (AMB)
M. iliofibularis (ILFB)	M. iliofibularis (ILFB)
Deep dorsal group	
M. iliofemoralis (IF)	M. iliofemoralis externus (IFE) + M. iliotrochantericus caudalis (ITC)
M. puboischiofemoralis internus 1 (PIFI1)	M. iliofemoralis internus (IFI)
M. puboischiofemoralis internus 2 (PIFI2)	M. iliotrochantericus cranialis (ITCR) + M. iliotrochantericus medius (ITM)
Flexor cruris group	
M. puboischiotibialis (PIT)	(absent)
M. flexor tibialis internus 1 (FTI1)	(absent)
M. flexor tibialis internus 2 (FTI2)	(absent)
M. flexor tibialis internus 3 (FTI3)	M. flexor cruris medialis (FCM)
M. flexor tibialis internus 4 (FTI4)	(absent)
M. flexor tibialis externus (FTE)	M. flexor cruris lateralis pars pelvica (FCLP)
Mm. adductores femorum	
M. adductor femoris 1 (ADD1)	M. puboischiofemoralis pars medialis (PIFM)
M. adductor femoris 2 (ADD2)	M. puboischiofemoralis pars lateralis (PIFL)
Mm. puboischiofemorales externi	
M. puboischiofemoralis externus 1 (PIFE1)	M. obturatorius lateralis (OL)
M. puboischiofemoralis externus 2 (PIFE2)	M. obturatorius medialis (OM)
M. puboischiofemoralis externus 3 (PIFE3)	(absent)
M. ischiotrochantericus (ISTR)	M. ischiofemoralis (ISF)
Mm. caudofemorales	
M. caudofemoralis brevis (CFB)	M. caudofemoralis pars pelvica (CFP)
M. caudofemoralis longus (CFL)	M. caudofemoralis pars caudalis (CFC)

Table 4.3. Pelvic muscles inferred as present in Troodontidae. Muscles originating from the pelvis are listed by anatomical/functional group. Modified from Carrano and Hutchinson (2002) and using levels of inference based on Witmer (1995).

Muscle	Origin	Level of inference
Triceps femoris		
IT1	Lateral surface of anterodorsal margin of ilium	(I)
IT2	Dorsolateral surface of dorsal margin of ilium	(I)
IT3	Dorsolateral surface of postacetabular margin of ilium	(I)
AMB	Near preacetabular tubercle	(I)
M. iliofibularis		
ILFB	Lateral surface of postacetabular portion of ilium between IFE and FTE	(I')
Deep dorsal group		
IFE	Lateral surface of ilium between ITC and ILFB	(I)
ITC	Lateral surface of preacetabular portion of ilium	(I)
PIFI1	Shallow depression on anterolateral surface of pubic peduncle of ilium	(II)
PIFI2	Cuppedicus fossa of ilium including medial side of preacetabular hook	(II)
Flexor cruris group		
FTI1	Tubercle on dorsal edge of ischial shaft at distal end	(II')
FTI3	Proximodistally elongate tuberosity on proximal, dorsal edge of ischial shaft, distal to ISTR	(II)
FTE	Posterolateral corner of ilium, posterior to ILFB	(I)
Mm. adductores femorum		
ADD1	Anteroventral portion of lateral surface of obturator process	(I')
ADD2	Faint scar distal to FTI3 on dorsal edge of ischial shaft	(II)
Mm. puboischiofemorales externi		
PIFE1	Anterior surface of pubic apron	(II)
PIFE2	Posterior edges of pubic apron and shafts	(II)
PIFE3	Ischial apron and posterior portion of obturator process, distal to ADD1	(II)
M. ischiotrochantericus		
ISTR	Medial side of ischium at proximal end, near iliac contact	(II)
Mm. caudofemorales		
CFB	Brevis fossa of ilium	(II)

Table 4.4. Measurements of troodontid pelvic elements. All measurements in millimetres (mm) following system depicted in Fig. 4.10. Note: UALVP, University of Alberta Laboratory for Vertebrate Palaeontology; UMNH VP, Utah Museum of Natural History; ?, unknown/not measureable; *, incomplete measurement based on preserved fragment; n/a, not applicable; $^{L/R}$, paired elements; a-p, anteroposterior; d-v, dorsoventral; m-l, mediolateral; p-d, proximodistal.

Measurement	Axis	UALVP 55804	UMNH VP 19479
ILIUM			
Length (il)	a-p	$242^{*L}/303^{R}$	?
Antilium (ail)	a-p	$138^{L}/131^{*R}$	?
Postilium (pol)	a-p	$91^{*L}/163^{R}$	?
Preacetabulum (pre)	a-p	$110^{L}/98^{*R}$	?
Postacetabulum (pos)	a-p	$74^{*L}/124^{R}$	?
Acetabulum length (acel)	a-p	$57^{*L}/67^{R}$	19*
Height over pubic peduncle (hpp)	d-v	$128^{L}/145^{R}$	?
Height over acetabulum (hace)	d-v	$72^{L}/82^{R}$	?
Pubic peduncle length (ppl)	a-p	$?^{L}/70^{R}$	?
Pubic peduncle width (ppw)	m-l	$?^{L}/21^{R}$	?
Ischiadic peduncle length (ispl)	a-p	$4^{*L}/5^{R}$	?
Ischiadic peduncle width (ispw)	m-l	$19^{*L}/32^{R}$	?
PUBIS			
Length (pl)	p-d	$199^{*L}/196^{*R}$	$121^{*L}/95^{*R}$
Pubic boot length (pbl)	a-p	?	?
Pubic boot width (pbw)	m-l	?	?
ISCHIUM			
Length (isl)	p-d	n/a	$55^{*L}/75^{*R}$

Chapter 5. The microraptorine lateral pubic tubercle: homology, form, and function

5.1 Introduction

As the twentieth century drew to a close, the small dromaeosaurid *Sinornithosaurus millenii* (Xu et al. 1999b) was described based on an associated skeleton with traces of integument. Among other features, it was distinguished by a laterally oriented midshaft tubercle on the pubis. This gives the pubis a kinked appearance in lateral view with a posteriorly oriented and spatulate pubic boot. Over the following years, several more dromaeosaurids with prominent lateral pubic tubercles were discovered and united in the clade Microraptorinae (Senter et al. 2004, Turner et al. 2012), in part because of the presence of these tubercles. Descriptions of other paravian taxa (Novas et al. 2018, Rauhut et al. 2018) are limited to identifying the presence or absence of the lateral pubic tubercle in comparison to microraptorines. The questions that remain are three-fold: what is the homology of the lateral pubic tubercle, how does it vary, and what role did it serve?

The skeleton is a frame of hard tissue that anchors, and is moved by, various soft tissues. The pubis has attachment sites for pelvic, trunk, and tail soft tissues. However, muscles, tendons, ligaments, and membranes are rarely fossilized and can be challenging to reconstruct. Recognition of former attachment sites relies on comparison to the condition in the closest living relatives (Witmer 1995). Dissection and identification of a soft tissue feature and its associated bony landmark (osteological correlate) in living representatives allow inferences to be made on the presence or absence in an extinct taxon.

Archosaur pelvic soft tissue has been well studied (Hutchinson 2001a, 2002) and used to reconstruct locomotory musculature in various dinosaurs (Hutchinson et al. 2005, 2008, Grillo

and Azevedo 2011, Maidment and Barrett 2011, Bates et al. 2012, Maidment et al. 2014b). Similarly, archosaur trunk anatomy sheds light on respiratory adaptations in extinct and extant taxa alike (Carrier and Farmer 2000, Claessens 2004, O'Connor and Claessens 2005, Farmer 2015a, 2015b). These studies have revealed much about archosaur locomotion and respiration, but are inherently restricted in their focus on a particular aspect or module of an organism. Although focus on the pelvis or trunk compartmentalizes information to achieve specific research goals, it can leave gaps in knowledge between adjacent modules of the body.

Candidates for soft tissue that attached to the lateral pubic tubercle in microraptorines can be assessed by comparative and descriptive techniques. Positive identification of pubic soft tissues in the closest living relatives based on dissection and literature review of crocodylian and avian pelvic anatomy (Baumel et al. 1990, Proctor and Lynch 1993, Carrier and Farmer 2000, Claessens 2009, Fechner et al. 2013, Fechner and Schwarz-Wings 2013, Klinkhamer et al. 2017) allows the condition in fossil material to be inferred. Data incorporated from hard and soft tissues help determine the homology of the lateral pubic tubercle, which can then be described and investigated for function. In turn, this synthesis between pelvic and abdominal studies bridges a knowledge gap in theropod soft tissue, offers insight into functional implications related to respiration and locomotion, and encourages further research in proper biological and phylogenetic context.

5.2 Materials and Methods

The microraptorine *Hesperonychus elizabethae* (UALVP 48778) was directly observed for osteological correlates of pubic soft tissues. The conditions in other microraptorines relied on available descriptions and photographs. Other pelvic material across a range of avians,

crocodylians, and non-avian theropods were examined (Fig. 5.1) (Table 5.1). Lepidosaurs were used as an outgroup. The lateral pubic tubercle was assessed as a candidate for attachment of various pubic soft tissues with respect to parsimony and the condition observed in material of extant archosaurs (Table 5.2).

The underlying approach throughout this study is the Extant Phylogenetic Bracket (Bryant and Russell 1992, Witmer 1995). Using this method, identification of soft tissue attachment sites in an extinct taxon is inferred by comparison to the conditions observed in the closest living relatives, which are crocodylians and birds in the case of Microraptorinae. Comparative procedures follow previous studies that identify osteological correlates indicative of former soft tissue attachment in archosaurs (Hutchinson 2001a, Carrano and Hutchinson 2002, Hutchinson et al. 2005, 2008, Grillo and Azevedo 2011, Bates et al. 2012, Maidment et al. 2014b). To identify pelvic soft tissues in living representatives of the Extant Phylogenetic Bracket, a savannah monitor (*Varanus exanthematicus*), a spectacled caiman (*Caiman crocodilus*), and a common raven (*Corvus corax*) were dissected and compared to soft tissue descriptions in other studies (Romer 1923a, Baumel et al. 1990, Proctor and Lynch 1993, Carrier and Farmer 2000, Hutchinson 2001a, Gangl et al. 2004, Smith et al. 2006, 2007, Claessens 2009, Otero et al. 2010, Fechner et al. 2013, Fechner and Schwarz-Wings 2013, Klinkhamer et al. 2017). Directional terminology follows use of "anterior" and "posterior" instead of "rostral/cranial" and "caudal" to avoid confusion with relevant modules of the body. Anatomical terminology uses "lateral pubic tubercle" in reference to the structure on the lateral side of the midshaft of the pubis in microraptorines. One exception to this term is the "lateral pubic process" of *Hesperonychus elizabethae* (Fig. 5.2) (Longrich and Currie 2009), which is a hypertrophied form of the lateral pubic tubercle and is otherwise treated as the same structure throughout this

paper. The term “preacetabular tubercle” refers to the proximal structure that anchors the iliopubic and puboischiadic ligaments, hypaxial musculature, and sometimes M. ambiens (Hutchinson 2001a). The latter of these tissues may vary in site of origin (McKitrick 1991). This term is used instead of “pubic tubercle” and its synonyms (see Hutchinson 2001a and discussion therein) to avoid confusion with other pubic structures and the non-homologous pubic tubercle of lepidosaurs. Furthermore, the preacetabular tubercle in birds typically forms partially or entirely from the ilium, not solely from the pubis (Bellairs and Jenkin 1960). Although preacetabular tubercle is a term that is typically applied to avians (Baumel et al. 1993), it has been used in non-avian theropods (Bishop et al. 2018a) and is herein extended stemward to crocodylians for simplicity. Due to the morphological range of archosaur pelves, structures considered to be a homolog of the lateral pubic tubercle (HLPT) are abbreviated for clarity and consistency across distantly related taxa. This additionally avoids generating superfluous terminology or requiring positional or morphological qualifiers that are taxon-dependent. Inventing a new term for this structure based on inferred soft tissue attachment is only justifiable if (a) the osteological correlate for such tissue is only or primarily for the attachment of such soft tissue and (b) it can be inferred with high confidence (i.e. a Level I inference sensu Witmer 1995). Photographs were taken with a digital camera or Nikon SMZ1500 stereoscopic microscope using QImaging Retiga-4000R camera system and NIS-Elements BR image processing software. Illustrations were generated with Adobe Illustrator CS6 and Photoshop CS6 with a Wacom drawing tablet.

5.3 Results

The main research question is addressed in three parts. First, the homology of the microraptorine lateral pubic tubercle is evaluated to propose a hypothesis about its identity so

that it can be meaningfully compared to other taxa with the same feature. The holotype pelvis of the microraptorine *Hesperonychus elizabethae* (UALVP 48778) (Fig. 5.2) serves as the primary specimen upon which observations and inferences rely. Second, the various forms of the tubercle and its homologs (HLPTs) are described to outline how it appears among the taxa in which it is present. Third, with recognition of these aspects, the biological role and functional consequences of the tubercle in Microraptorinae can be inferred. Thereafter, pelvic anatomical terminology and relevant potential effects on palaeobiology can be discussed.

5.3.1 Homology

Assessing of the homology, or "equivalence", of anatomical structures follows Patterson (1982) with considerations from de Pinna (1991) and Rieppel (1994). In other words, homologous structures in different organisms are corresponding features developed through shared ancestry. A putatively homologous structure is supported as such if it passes the three tests of homology: similarity, conjunction, and congruence (Patterson 1982). However, congruence is ultimately the only true "test", whereas similarity is what primary homology statements are based upon and conjunction is indicative of non-homology (de Pinna 1991). Recognition of homology is nevertheless a hypothesis based on morphological similarity, which has capacity for phylogenetic information pending the test of congruence (Rieppel 1994). Congruence, or compatibility with other characters, is necessary to consider structures as homologous to one another. Homology in muscle reconstruction was outlined by Witmer (1995). The test of similarity is ideally passed if a 1:1 relationship exists between a given soft tissue and an osteological correlated (landmark on the skeleton). The test of conjunction ensures that multiple states of a given muscle or osteological correlate do not coexist in any one taxon, and

the test of congruence requires that these patterns are consistent with descendants of the common ancestor and thus are congruent with the Extant Phylogenetic Bracket (Witmer 1995). The scope of this study limits the results to a statement of primary homology sensu de Pinna (1991) as it undergoes the tests of similarity but, although it undertakes a test of conjunction, does not formally submit the data to a test of congruence.

The lateral pubic tubercle is not positioned to function or otherwise be involved in a direct bone-bone joint, ruling out its direct association with any hard tissues. The only adjacent bones to the pubis are the ilium, ischium, femur, and gastralia. However, the ilium and ischium are directly connected by sutures at the proximal end of the pubis, and are not positioned near the lateral pubic tubercle. The femur articulates with the pelvis via a ball-and-socket joint, which also involves the proximal end of the pubis and is located away from the tubercle. The gastralia are embedded in the M. rectus abdominis and indirectly attached to the anterior pubic cartilage by means of a ligamentous sheet in living crocodylians (Claessens 2004, Claessens and Vickaryous 2012). These dermal bones begin ossifying well after birth, beginning with the lateral elements of the most posterior row of gastralia, which are tethered to the pubes via paired ligaments (Vickaryous and Hall 2008). Although gastralia are absent in living avians, the M. rectus abdominis also inserts near the distal ends of the pubes in a similar fashion via aponeurosis. Membranes and other soft tissues anchor to the pubis in both crocodylians (Carrier and Farmer 2000, Claessens 2009, Fechner and Schwarz-Wings 2013) and avians (Shufeldt 1890, Baumel et al. 1990, Fechner et al. 2013). Therefore, pelvic soft tissues in extant archosaurs (Table 5.2) provides insight into potential candidates for structures associated with the microraptorine lateral pubic tubercle to determine its putative homology. For each muscle, its

attachment site (origin or insertion) nearest the pubis is considered in both extant crocodylians and avians as comparative taxa with observable soft tissue.

Trunk muscles that attach to the pubis in archosaurs include M. obliquus abdominis externus, M. obliquus abdominis internus, M. transversus abdominis, and M. rectus abdominis (Table 5.2). The osteological correlates for the first three of these muscles in crocodylians are the lateral gastralia. The M. rectus abdominis attaches to the most posterior row of gastralia, which anchors to the pubis by means of a ligamentous sheet along the midline (Claessens 2009, Fechner and Schwarz-Wings 2013). In birds, the first three of these muscles attach to the anteroventral margin of the ilium and pubis and either the iliopubic ligament (external and internal obliques) or the posterior vertebral ribs (transversus) (Baumel et al. 1990, Proctor and Lynch 1993, Fechner et al. 2013). The M. rectus abdominis is indirectly attached to the distal ends of the pubes by an aponeurosis. None of these muscles attach directly to the pubis in crocodylians. In avians, all of these muscles are sheet-like and are connected directly to the pubis by broad attachment sites. These correlates are present in microraptorines and none involve the lateral pubic tubercle, as is the case in other non-avian theropods. For these reasons, the lateral pubic tubercle is not inferred as an osteological correlate for any trunk muscles, which are thereby eliminated as candidates associated with this structure.

Pelvic muscles connected to the pubis in archosaurs are the M. ambiens, M. ischiopubis, M. ischiotruncus, and crocodylian Mm. puboischiofemorales externii 1 and 2 (avian Mm. obturatorius lateralis and medius, respectively) (Hutchinson 2001a, 2002, Carrano and Hutchinson 2002). The origin of the M. ambiens is at the proximal end of the pubis in crocodylians and similarly on the preacetabular tubercle in avians. The M. ischiopubis connects the two bones from which its name is derived by attachment to the epipubic cartilage. From the

ischium, the M. ischiotruncus passes ventral to the pubis and also inserts onto the epipubic cartilage along with hypaxial trunk musculature (Fechner and Schwarz-Wings 2013). In crocodylians, the origins of the Mm. puboischiofemorales externi 1 and 2 are, respectively, on the anterodorsal and posteroventral surfaces of the pubic apron. In birds, the origins of the homologous muscles (Mm. obturatorii lateralis and medialis) are, respectively, on the margin of the obturator foramen and the medial surface of the puboischiadic membrane. Concerning non-avian theropods, the osteological correlate of the M. ambiens is the preacetabular tubercle (Hutchinson 2001a), which is present at the proximal end of the pubis in microraptorines (Fig. 5.2). The M. ischiopubis may have been absent in theropods as it requires a kinetic pubis to function given its insertion point (Carrier and Farmer 2000, Claessens 2004, Macaluso and Tschopp 2018). If present, its common insertion site with the M. ischiotruncus means that both of these muscles passed ventral to the pubis and inserted at the distal end of this bone. Each non-avian theropod possesses a pubic apron and the Mm. puboischiofemorales externi 1 and 2 are inferred as present with origins in the same locations as in crocodylians. In *Hesperonychus elizabethae* (UALVP 48778), distomedial-proximolateral oriented striations clearly indicate the origin of the first head of this muscle on the anterior surface of the pubic apron, whereas a shallow depression formed by the posterior surface of the pubic apron marks the origin of the second head (Figs. 5.3–5.4). Osteological correlates for pelvic muscles in microraptorines are either clearly identified on the pubis lacking association with the lateral pubic tubercle, not located directly on the pubis, or presumably absent. All of these pelvic muscles are rejected as candidates associated with the lateral pubic tubercle as evidence indicates that their attachment sites are located elsewhere.

Tail muscles with attachment sites on the pubis in archosaurs include M. truncocaudalis in crocodylians and Mm. pubocaudales externus and internus in avians. In crocodylians, the M. truncocaudalis extends anteriorly from the tail and wraps around the ventral surface of the pelvis to insert on parts of the M. obliquus externus and M. rectus abdominis (Fechner and Schwarz-Wings 2013). In birds, the Mm. pubocaudales externus and internus attach to the pubis along its posterior margin at the distal end (Baumel et al. 1990). All of these muscles in extant archosaurs attach to the ventral or posterior surfaces of the distal ends of the pubes and are generally strap-shaped with somewhat broad attachment sites. The anterior curve of the lateral pubic process in *Hesperonychus elizabethae* (Longrich and Currie 2009) may also suggest that the associated soft tissue is attached to its anterior and/or lateral side, and is not involved in a function towards the rear. Given that the insertion of crocodylian tail musculature is distal to the pubis, that the attachment of avian tail muscles is on the posterior borders of the pubis, and that the attachment site formed by all of these muscles is somewhat broad and strap-shaped, none of these are inferred as likely candidates associated with the lateral pubic tubercle in microraptorines.

The pubis anchors other soft tissues such as ligaments, membranes, and cartilages. Both crocodylians and birds possess iliopubic ligaments, puboischiadic ligaments, and puboischiadic membranes. Crocodylians additionally have pubogastralial cartilages and ligaments (Romer 1923a) that are absent in birds. The non-avian theropod *Anchiornis* sp. preserves evidence of a cartilage cap on the distal end of the pubis (Wang et al. 2017) that may have been part of, or associated with, a pubogastralial cartilage. The iliopubic and puboischiadic ligaments affix to the preacetabular tubercle in crocodylians. The same condition exists for the iliopubic ligament in birds, but the puboischiadic ligament arises from the obturator tuberosity, which is distal to the preacetabular tubercle along the posterodorsal side of the pubic shaft. The correlate for the

puboischiadic membrane in crocodylians is the medial, posterior border of the pubis, and in birds is a ridge along the posterior margin of the pubic shaft (Hutchinson 2001a). A crocodylian possesses a pubogastralial cartilage bridging the gap between the epipubic cartilage on the anterior margin of the pubis and the most posterior row of gastralia on the midline (Claessens 2009). Small, paired, pubogastralial ligaments are also present and attach to the anterolateral corners of the pubes near the midshaft (Hutchinson 2001a). In all microraptorines, a ridge along the posterior edge of the pubic shafts and dorsal edge of the pubic boot are clearly visible as landmarks for the lateral and median parts of the puboischiadic membrane (Fig. 5.2). The preacetabular tubercle is comparable to those of more plesiomorphic non-avian theropods suggestive of a similar attachment of the iliopubic and puboischiadic ligaments to those of crocodylians. As the pubogastralial cartilage, if present, was a single, midline element at the anterior margin of the pubic boot, it is unlikely that it attached to the paired lateral pubic tubercles in microraptorines. However, the osteological correlate for the pubogastralial ligaments in crocodylians, the anterolateral corners of the pubes, are aligned in the same positions as the lateral pubic tubercles; the tubercles are similarly positioned on the anterolateral sides of the midshafts of the pubes. Additionally, the lateral pubic tubercles curves anteriorly, which makes sense if they provided attachment for ligaments connected to the most posterior row of gastralia. The pubogastralial ligaments and associated bony structures are absent in birds, but it is the only pubic soft tissue with reasonable morphology and an osteological correlate consistent with the structure of the lateral pubic tubercles.

Well preserved fossils provide further evidence that the lateral pubic tubercle anchored the pubogastralial ligament. Microraptorines preserved with articulated gastralia consistently show they are associated with the anterolateral side of the midshaft of the pubis. The association

can be seen in specimens of *Changyuraptor yangi* (Han et al. 2014), *Microraptor zhaoianus* (Xu et al. 2003b), *Wulong bohaiensis* (Poust 2014), and *Zhenyuanlong suni* (Lü and Brusatte 2015). The holotype specimen of the non-microraptorine dromaeosaurid *Linheraptor exquisitus* (Xu et al. 2010a) includes an articulated gastral basket with the most posterior few rows of gastralia preserved against the anterolateral surface of the pubis at midshaft. Although there is no lateral pubic tubercle, and soft tissues like cartilages or ligaments are not evident, a clear association remains between the gastralia and the middle of the pubic shaft. The same condition exists in a cast of a velociraptorine dromaeosaurid (Fig. 5.5), as well as in troodontids *Almas ukhaa* (Pei et al. 2017), *Gobivenator mongoliensis* (Tsuihiji et al. 2014), *Jianianhualong tengi* (Xu et al. 2017), and *Sinornithoides youngi* (Russell and Dong 1993), and in the paravian *Archaeopteryx* sp. (Rauhut et al. 2018). This phylogenetically widespread association between the gastralia and pubes in theropods supports the lateral pubic tubercles in microraptorines as homologous to the anterolateral corners of the pubes as an attachment site for the M. rectus abdominis via pubogastralial ligaments (Hutchinson 2001a). Although this association is widespread among theropods, the lateral pubic tubercle is mysteriously unique to microraptorines. The lateral pubic tubercle and its homologous counterparts must be described to reveal evolutionary patterns and potential functional implications.

5.3.2 Form

The form of the homologs of the lateral pubic tubercle (HLPTs) in archosaurs is described phylogenetically from crocodylians to avians. This is done to show macroevolutionary patterns among theropods (Hendrickx et al. 2015) across theropod evolution. Morphological differences on this scale make trends subtle between closely related taxa. Certain groups with

shared general features are described together for simplicity and to highlight major changes in morphology, although overall, they each represent points on a spectrum of morphological change.

Crocodylians have a HLPT described and figured in Hutchinson (2001) as the anterolateral corners of the pubes (Fig. 5.6). At the distal end of the pubis, the anterolateral corner of the bone is rugose along its lateral margin. A small prominence may be visible here in dorsal view as in ROM R343 of *Alligator mississippiensis* (Fig. 5.6C–F). However, smaller specimens of this species such as UAMZ HER-R654 and other taxa including *Caiman* sp. do not clearly express this feature despite the preservation of intact pubogastralial cartilages and/or ligaments in some skeletonized specimens (Fig. 5.6A–B, G). Whereas pubogastralial cartilage is broad and occurs across the midline along the anterior and anteromedial edges of both pubes, the pubogastralial ligaments are restricted to small attachment sites along the lateral edges of the anterolateral corners (Fig. 5.6H).

The HLPT in non-coelurosaurian theropods (Figs. 5.7–5.8) are broadly similar to those of crocodylians. The distal ends of the pubes, however, are not spatulate with thin anterior margins. Rather, they were fused together in life and boot-shaped in lateral view with modest anterior and prominent posterior expansions. Observed material of *Ceratosaurus* sp. includes a specimen with an intact pubic boot slightly damaged on the left side (Fig. 5.7A–C). The anterior margin is convex both in lateral and ventral views but has a surface texture evocative of that seen in crocodylians for the attachment of pubogastralial cartilage (Fig. 5.7C). In ventral view, a laterally projecting triangular eminence forms the lateral edge of the pubic boot with its apex roughly halfway along the anteroposterior axis of the boot. It is appropriately situated for a pubogastralial ligament and is probably homologous to the crocodilian anterolateral corner of the

pubis, and is therefore a HLPT. A similar condition exists in the megalosaurid *Torvosaurus tanneri* (Fig. 5.7D–E), although this laterally positioned eminence is closer to the anterior end of the pubic boot. The allosaurid *Allosaurus fragilis* has a pubic boot with a dorsoventrally compressed, dorsally concave anterior expansion (Fig. 5.8). This gives the boot a slightly anterodorsally pointed appearance in lateral view (Fig. 5.8F–G). The texture of the anterior margin is consistent with attachment for a pubogastralial cartilage, and the anterolateral corner of the pubis is rugose for attachment of a pubogastralial ligament. These are positioned in similar locations to those of megalosaurids, but are more anterior than those of ceratosaurids, possibly because of the more pronounced anterior expansion of the boot compared to those of more plesiomorphic taxa.

Non-paravian coelurosaurians have a HLPT with distinct anterolateral processes for pubogastralial ligaments (Figs. 5.9–5.11). Tyrannosaurids such as *Albertosaurus sarcophagus*, *Daspletosaurus torosus*, and *Gorgosaurus libratus* each have a pubic boot with a cleft at the anterior end along the midline, separating the right and left pubes into distinct, rounded, tab-like processes that project anterolaterally. One specimen of *Gorgosaurus* (CMN 2120) has a gastralium preserved in articulation with the pubis abutted against this process (Fig. 5.9E). In ventral view of the pubic boot, a midline sulcus is present in *Albertosaurus* (CMN 11315) (Mallon et al. 2019) continuous with the anterior cleft separating the anterior ends of the left and right pubes. This groove becomes confluent with the ventral surface of the boot posteriorly and the pubes taper in the same direction. This morphology is mirrored in ornithomimids such as cf. *Ornithomimus* sp. (CMN 12070) and *Ornithomimus edmontonicus* (CMN 8632), the latter of which is a remarkably well preserved, articulated partial skeleton. Not only are distinct, rounded tab-like processes present on the anterolateral corner of the pubis, they are also preserved clearly

in articulation with the most posterior row of gastralia of an articulated gastral basket (Fig. 5.10A–B) (Sternberg 1933) in the same manner observed in crocodylians. Therizinosaurians such as *Falcarius utahensis* (Zanno 2010a) and *Enigmosaurus mongoliensis* (Zanno 2010b) possess processes on the pubes similar to ornithomimids and tyrannosaurids, but the anterior expansion of the pubic boot is less pronounced (Fig. 5.11A–E). Although all observed material consists of separate, unfused pubes, reconstructed pelves suggest that each pair of processes on the anterolateral corners of the pubes are separated by a shallow notch equivalent to the cleft present in ornithomimids and tyrannosaurids. Caenagnathid material is limited but seems similar to therizinosaurian material (Fig. 5.11F–H). A small portion of intact cortex on the medial side of the left anterolateral process in a specimen consisting only of the pubic boot shows that, given better preservation, a small cleft was present between it and its right counterpart (Fig. 5.11F).

Non-avian paravians are varied in HLPT morphology (Figs. 5.12–5.13) but tend to share a lack of an anteriorly expanded pubic boot and a proximally displaced articulation with the gastral basket based on well preserved fossils. Microraptorines are characterized by a lateral pubic tubercle or process for the pubogastralial ligaments (Fig. 5.12A). The texture on the lateral edges of this correlate suggests soft tissue attachment, but there is no clear correlate for a pubogastralial cartilage or other median connection of the M. rectus abdominis to the pelvis. Within Unenlagiinae, the small anterior expansion of the pubic boot depicted for *Unenlagia paynemili* (Calvo et al. 2004) may be another bone fragment (Novas et al. 2018) and is inconsistent with the strongly reduced anterior projections of other members in this family. This reduced, albeit present, anterior projection is consistent with the attachment site for the pubogastralial cartilage, but HLPTs are unclear. In *Unenlagia* sp. (Novas and Puerta 1997, Calvo et al. 2004) and *Unquillosaurus ceibali* (Novas and Agnolin 2004), the pubes have a sinuous

lateral margin in anterior view that effectively gives the midshafts a slight lateral bulge, which may offer area for attachment of the pubogastralial ligaments. This morphology is similar in the dromaeosaurids *Linheraptor exquisitus* (Xu et al. 2010a), indeterminate velociraptorine cast (Fig. 5.12B–C), and *Saurornitholestes langstoni* (Fig. 5.12D), all with gastralia preserved in articulation and similar lateral bulges on the pubes as putative HLPTs. However, the pubis of *Buitreraptor gonzalezorum* (Novas et al. 2018) has a relatively straight lateral margin and lacks a clear bulge that could indicate an osteological correlate for these ligaments. Relatively basal troodontids preserved with gastralia like *Jianianhualong tengi* (Xu et al. 2017) show a relatively close association between the gastral basket and midshaft of the pubis (Fig. 5.13D), which also has a slight lateral bulge akin to those of *Linheraptor* or *Unenlagia*. Derived troodontids such as *Latenivenatrix mcmasterae* (van der Reest and Currie 2017) do not appear to have such a sinuous edge, but this taxon does have a small spiculate tubercle on the lateral side of the left pubis towards its distal end (Fig. 5.13A–C). This region is not preserved on the right side, so it is unknown whether it represents an anomaly or an actual feature. In a similar anatomical position, derived troodontid *Gobivenator mongoliensis* (Tsuihiji et al. 2014) has a few gastralia preserved near the distal end of the pubis, but it is currently unknown whether or not a similar tubercle is present. In other paravians, such as *Anchiornis huxleyi* (Hu et al. 2009), clear osteological correlates for neither pubogastralial cartilage nor ligaments are apparent. A new specimen of *Archaeopteryx* sp. (Rauhut et al. 2018) has gastralia articulated with the midshaft of the pubis, but a HLPT is notably absent and there is no anterior expansion of the pubic boot.

The overall pattern throughout Paraves is gradual proximal migration of the HLPT until gastralia are lost during the evolution of birds (Fig. 5.14). Non-paravian theropods generally maintain similar arrangements to those of crocodylians. An anterior expansion of the pubic boot

seems to be an osteological correlate for pubogastralial cartilage along the midline and is present in non-paravian theropods. As this bone surface for attachment along the midline was reduced, some taxa gained enlarged paired HLPTs in the form of lateral pubic tubercles or processes. Other paravians, however, had both surfaces reduced without any clear sites of attachment. The causal mechanisms or evolutionary drivers behind these changes remains uncertain. However, they may be related to improvement of costal ventilation in Maniraptora and resulting changes to the gastralia (and their points of attachment) as cuirassal ventilation became reduced and eventually replaced (Macaluso and Tschopp 2018). Based on the attachment sites and relationships among other soft tissues on the pubis, the lateral pubic tubercle would have interfered with the paths of certain muscles. How, then, did this impact other soft tissues, and what might explain why its presence is limited to Microraptorinae?

5.3.3 Function

The role of the lateral pubic tubercle may be determined by examining the arrangement of surrounding soft tissues. Many of these pubic tissues (Table 5.2) were external to, or did not pass directly over, the lateral pubic tubercle. Tissues closely associated with the tubercle are limited to the M. rectus abdominis via pubogastralial ligaments and cartilages, and pelvic muscles Mm. puboischiofemorales externi 1 and 2. The texture of the lateral edge of the lateral pubic tubercle is indicative of pubogastralial ligament attachment. The correlate for pubogastralial cartilage or the M. rectus abdominis is unclear but would have been medial to these tubercles on the anterior or ventral surfaces of the pubis. The origin of the M. puboischiofemoralis externus 2 on the posterior surface of the pubic apron is near, but not on the lateral pubic tubercle. Its insertion on the posterior surface of the femoral head (Hutchinson

2002) is common with that of the other heads of the Mm. puboischiofemorales externi. The origin of the M. puboischiofemoralis externus 1 on the anterior surface of the pubic apron requires the belly of the muscle to wrap around the lateral edge of the pubic shaft in crocodylians (Romer 1923a, Klinkhamer et al. 2017), and probably in non-avian theropods (Hutchinson et al. 2005, 2008). It is separated from the origin of the second head of this muscle by none other than the pubogastralial ligament. In microraptorines, the pubic apron is distal to the lateral pubic tubercles and pubogastralial ligaments, the latter of which gives these dromaeosaurids a characteristically kinked pubis with a posteriorly directed boot. This is visible in *Hesperonychus elizabethae* (Figs. 5.3–5.4, 5.12A) and is also revealed by a number of microraptorine descriptions (Xu et al. 2000, Hwang et al. 2002, Gong et al. 2012, Pei et al. 2014, Xu and Li 2016). This deflection results in the origin of the M. puboischiofemoralis externus 1 to be displaced ventral and posterior to the pubogastralial connection relative to the HLPT in other archosaurs. The path of this muscle around the pubic shaft is interrupted by the lateral pubic tubercle, which is hypertrophied into a wing-shaped, anteriorly convex pulley in *Hesperonychus elizabethae*. This causes the M. puboischiofemoralis externus 1 to wrap around the lateral edge of the pubic shaft and remain medial to the pubogastralial ligaments (Fig. 5.15). This muscle, much like the pubis on which it anchors, was likewise kinked by its relationship to the lateral pubic tubercle.

5.4 Discussion

5.4.1 General remarks

Some limitations of this study should be remarked on here. As previously mentioned, pubogastralial tissues within Archosauria are only observable in crocodylians. Modern birds,

representing the other side of this Extant Phylogenetic Bracket (Bryant and Russell 1992, Witmer 1995), lack gastralia and a direct connection of the M. rectus abdominis to the pubis (a decisive negative assessment). This limits the confidence of inferring pubogastralial soft tissues as present in non-avian theropods, which is somewhat speculative regardless. Osteological correlates consistent with pubogastralial cartilages or ligaments provides support for the presence of such soft tissues. Due to the presence of pubogastralial cartilages and ligaments in one extant sister taxon (crocodylians) and presence of osteological correlates for both of these tissues in non-paravian theropods, the former presence of pubogastralial cartilages and ligaments qualifies as a Level II inference (Witmer 1995). Aside from *Archaeopteryx*, despite clear preservation of gastralia in association with the pubis, paravians tend to have osteological correlates for either pubogastralial cartilages or ligaments and also meet the criteria of a Level II inference. The condition of *Archaeopteryx* is limited to a Level II' inference (Witmer 1995). Although admittedly more speculative than in other theropods, this still provides a fair degree of confidence for the presence of pubogastralial soft tissues given the fortunate good preservation of some specimens (Rauhut et al. 2018). The results here comprise a primary homology statement (sensu de Pinna 1991), which formulate a hypothesis of homology that would be complemented by subsequent submission to the test of congruence. This would allow better evaluation in a phylogenetic framework of the purported homology of the lateral pubic tubercle as an osteological correlate for the pubogastralial ligament.

Establishing the homology, form, and function of osteological correlates for pubogastralial soft tissues allows further study to investigate other effects on palaeobiology. A more concrete identification of the microraptorine lateral pubic tubercle allows deeper discussion beyond noting its presence or absence in newfound taxa (Rauhut et al. 2018, Novas et al. 2018).

It is useful for further study on the loss of gastralia in birds, which is curiously complicated by *Archaeopteryx* in which the lack of osteological correlates for pubogastralial tissues would indicate the absence of gastralia if not for the well preserved nature of some specimens. The condition of the microraptorine pubis with a mesopubic proximal portion and opisthopubic distal end offers an intriguing case study on the relationship between cuirassal ventilation and pubic retroversion that would benefit from further study. The presence of gastralia and their role as an accessory breathing structure, however, suggests that cuirassal ventilation still imparted more benefit than cost despite concomitant improvements to ventilatory efficiency (Macaluso and Tschopp 2018) and unidirectional airflow as a plesiomorphic condition among archosaurs, or even diapsids (Farmer 2015a, 2015b, 2015c). Although this study is not decisive on terminology for anatomical structures of the pubis within this phylogenetic context, it highlights potential issues with current vocabulary. Ironically, it also underpins the challenges of standardization. Perhaps a more comprehensive review of archosaur pelvic anatomy deserves revisiting to update current views on the homology and terminology of pelvic structures. This would additionally improve communication among researchers and within disciplines, hopefully also improving consistency.

5.4.2 Terminology and transformational homology

This study proposes that the microraptorine lateral pubic tubercle is homologous with other structures on the pubes of other archosaurs that anchor the pubogastralial ligaments. It is enlarged in microraptorines because of its position relative to the proximal end of the pubic apron. The wide phylogenetic context of this study highlights some challenges of describing broad evolutionary trends in the absence of standardized terminology such as those used for birds

(Baumel et al. 1993), humans (FCAT 1998), and mammals (ICVGAN 2017). A few approaches to this problem have been proposed, but there is a lack of consensus on how standardization should be implemented, if at all (Harris 2004, Wilson 2006). Furthermore, this study underscores the challenges of establishing consistent terminology that is suitable at large taxonomic scales. The variable topology and morphology of the HLPT across phylogenetically disparate taxa requires positional descriptors (e.g. anterolateral vs. lateral) and morphological qualifiers (e.g. tubercle vs. process) that depend on the state of the homolog rather than the homology itself. For example, the anterolateral corner of the pubis is appropriate for crocodylians and non-coelurosaurian theropods. However, this is not quite accurate for ornithomimids or tyrannosaurids with anteriorly projecting processes. It is even less suitable to describe the form in microraptorines with lateral pubic tubercles entirely separate from the pubic apron and distal ends of the pubes. Renaming the lateral pubic tubercle and HLPTs as a distal pubic tubercle akin to that of ischial processes present in some theropods (e.g. dorsal/proximal and ventral/distal ischial processes; see Hutchinson 2001) runs into similar issues. Possession of a distal tubercle implies the presence of a proximal tubercle. Although this is technically true when the preacetabular tubercle is present and may work for non-paravian theropods, it requires another modifier when the preacetabular tubercle is absent or reduced, causes confusion with non-homologous structures as explained in the Methods section, is not quite accurate for microraptorines with tubercles located at the midshaft instead of the distal end, and is not appropriate for taxa that lack a tubercle but possess gastralia and by extension had a pubogastralial ligament. Alternatively, the structure could be named after the soft tissue attached to it like some other bony processes (e.g. deltopectoral crest of the humerus). The eponymous soft tissue in this case is only evident in extant crocodylians and cannot currently be confirmed

by direct observation in any other archosaur. Hence, the criteria for naming osteological correlates based on associated soft tissues outlined previously (see Methods) is not currently met given this evidence and Level II inference. Nevertheless, one issue can be clarified here given this information. The pubogastralial ligament has been referred to as a tendon (Romer 1923a), muscle (Xu et al. 1999b), and ligament (Claessens 2004). As observed in dissections of extant crocodylians, the pubogastralial ligament does not consist of muscle tissue that moves bones relative to a joint (muscle) or collagen that connects bone to muscle (tendon). It is therefore correctly described as a ligament as it consists of connective tissue that connects bone to bone in order to stabilize a contact.

Whereas the presence and attachment of gastralia and the M. rectus abdominis are shared among archosaurs, the relative positions of the pubic apron and lateral pubic tubercle in Microraptorinae explains why the tubercle is only expressed in this subfamily. The distal position of the pubic apron and origin of the M. puboischiofemoralis externus 1 relative to the pubogastralial ligament attachment site requires modification of the latter to accommodate the former (Fig. 5.15). Otherwise, the path of this pelvic muscle would have been pinched or impeded by the most posterior row of gastralia. Therefore, the lateral pubic tubercle is absent in non-microraptorine archosaurs because the pubic attachment site of the pubogastralial ligament is distal to the proximal edge of the pubic apron. When this is not the case, the lateral pubic tubercle or process is present to allow the belly of the M. puboischiofemoralis externus 1 to pass between the pubis and pubogastralial ligament and insert onto the femur. This also explains why the lateral pubic tubercle is not present in other taxa (Novas et al. 2018, Rauhut et al. 2018) as they do not satisfy these conditions. Although some specimens may have been affected by post-mortem collapse of the abdominal air sacs that displaced the gastralia proximally, this is still

congruent with the proposed hypothesis as the gastralia would have attached near or distal to their preserved position. This falsifiable hypothesis regarding the relationship between the pubogastralial attachment site and pubic apron can be tested with archosaurs hitherto described and others yet to be discovered.

5.4.3 Osteological correlates in paravian theropods

This study supports that an anterior expansion of the pubic boot is an osteological correlate for the pubogastralial cartilage, but a lack of this correlate is not consistent with the loss of gastralia. Although an anterior expansion is absent in some dromaeosaurids, gastralia are still clearly preserved in plesiomorphic and derived species alike across this family. Lack of an anterior expansion may simply indicate that the pubogastralial cartilage was absent, but the M. rectus abdominis was still present as inferred by phylogenetic bracketing. Perhaps the midline connection was similar to that of extant birds in that the M. rectus abdominis inserted onto soft tissue in the area rather than onto cartilage or bone (Baumel et al. 1990). Alternatively, the pubic callosity on the distal end of the pubis reported in *Anchiornis* sp. (Wang et al. 2017) may be associated with pubogastralial cartilage. Non-avian theropods tend to have at least one clear correlate for pubogastralial tissues—an anterior expansion of the pubic boot or paired lateral tubercles—although *Archaeopteryx* is a notable exception. Specimens preserved with gastralia (Rauhut et al. 2018 and discussion therein) lack both anterior expansions of the pubic boots and lateral tubercles or other distinct HLPTs. Extant birds lack gastralia, and therefore lack both osteological correlates of pubogastralial tissues on the pubes. However, the exception of *Archaeopteryx* indicates that the lack of both osteological correlates on the pubis is not a universal indicator of the lack of gastralia. Although outside the scope of this study, it may be

that a more reliable osteological correlate exists for the attachment of the gastral basket for its anterior end on the sternum, assuming there is an ossified sternum. Currently, the condition present in *Archaeopteryx* remains a peculiar irregularity.

Early birds, particularly enantiornitheans, offer additional insight. Enantiornithean fossils are typically preserved two-dimensionally in slabs and gastralia are often only mentioned to document their presence and number (Zhang et al. 2001, 2004, Zhou et al. 2008, Wang and Zhou 2019). However, in both Enantiornithes and Ornithuromorpha, the number and robusticity of gastralia were independently reduced until the former went extinct at the end of the Cretaceous Period and the latter lost them entirely (Lambertz and Perry 2015). This parallelism was preceded by a gradual but progressive reduction in the number of gastralial pairs beginning well before the divergence of birds. Presumably, the gastral basket performed an accessory ventilatory function that either reinforced sternal movements in taxa with an ossified sternum, or fulfilled a compensatory role in taxa without (Zheng et al. 2014, Zhang et al. 2014, Lambertz and Perry 2015). Gastral aspiration may have also compensated for differences in physiology and sternal rib morphology in enantiornitheans compared to the more efficient breathing system in ornithuromorphs (Zhang et al. 2014). Nevertheless, there appears to be no clear relationship between size and gastralial number, nor between the number of gastralia and presence or absence of an ossified sternum (O'Connor et al. 2015). There may be some trend between posteriorly extensive sterna and reduced gastralial number, but it seems that gastralia were retained until the evolution of a keeled sternum. In fact, gastralia may have retained a vital functional role in the absence of a complex, carinate sternum (O'Connor et al. 2015). This could explain both the variability of, and prolonged stepwise reduction in, gastralial number throughout theropod evolution. During this grade of theropod evolution, some early birds developed incipient

structures such as the hypopubic cup, which is associated with suprapubic musculature that facilitates abdominal air sac ventilation via tail and pelvic movements in modern birds (Ruben et al. 1997, Geist and Feduccia 2000). Curiously, both *Archaeopteryx* and *Confuciousornis* possess a hypopubic cup and have the same number of gastralial pairs (Zheng et al. 2014, Lambertz and Perry 2015), but only the latter has an ossified sternum (Martin et al. 1998). The loss of gastralia was therefore clearly not tied to the presence or absence of an ossified sternum, and when present, probably supplemented ventilatory movements and/or allowed additional space for flight muscle attachment. However, the development of a keeled sternum may coincide with the rapid loss of gastralia in ornithuromorph birds (O'Connor et al. 2015). The sternum is more firmly connected to the rest of the skeleton than the gastralia and, with a keel, offers both more surface area and a sturdier origin site for attachment of muscles for powerful flight. A carinate sternum also facilitates breathing, so maximizing sternum and keel size may have accelerated the complete loss of the gastral basket as a redundant anatomical unit. This key innovation, combined with more efficient breathing, higher metabolic rate, and other inferred advantages of ornithuromorphs over enantiornitheans (Zhang et al. 2014) may have implications for the K-Pg extinction. Ornithuromorphs may have had an evolutionary edge over enantiornitheans, which shared similar, overlapping niches, during the extinction because of these advantages. This could explain the survival of the former and the extinction of the latter when competition and other ecological stresses skyrocketed. Early birds and extinction hypotheses aside, it seems that Cretaceous theropods exhibited variability in gastralial number and any selective pressures affecting this were too weak to cause complete loss until the evolution of a keeled sternum.

5.4.4 Implications for respiration and locomotory muscles

The presence of a lateral pubic tubercle has implications for respiration in microraptorines. Two leading hypotheses for the evolutionary driver behind the evolution of the opisthopubic pelvis in dinosaurs are herbivory and loss of cuirassal ventilation (Rasskin-Gutman and Buscalioni 2001, Macaluso and Tschopp 2018). Mode of ventilation was found to be generally more strongly correlated with pubic retroversion by Macaluso & Tschopp (2018). Cuirassal ventilation, using gastralia as an accessory breathing structure, seems to become progressively reduced in importance as more efficient ventilatory mechanisms evolved. This includes an inferred switch from the M. ischiotruncus to M. truncocaudalis as the primary muscle acting on the gastral basket (Carrier and Farmer 2000), or perhaps uncinate processes on the ribs facilitating costal ventilation (Codd et al. 2008, Macaluso and Tschopp 2018). It is curious to note that microraptorines such as *Hesperonychus elizabethae* have pubes that are more or less mesopubic proximally, but strongly retroverted distally. Whatever the evolutionary pressure driving pubic retroversion, at least in the distal end of the pubis, some evolutionary pressure maintained mesopuby in its proximal end. The presence of the lateral pubic tubercle/process as the attachment site of the gastralia at the midshaft of the pubis happens to also separate the proximal mesopubic portion from the distal retroverted end of the bone. Hence, cuirassal ventilation may be related to this phenomenon. As a connection to the pubis is required for cuirassal ventilation, but the presence of gastralia seems limited to a threshold including only propubic or mesopubic pelves (Rasskin-Gutman and Buscalioni 2001), the microraptorine pubis may in fact be kinked to accommodate gastralia and other pressure(s) causing retroversion. Microraptorines lack a hypopubic cup, which suggests that they also lacked incipient, avian-like suprapubic musculature for tail and pelvic manipulation to aid airflow (Ruben et al. 1997, Geist

and Feduccia 2000). Because of this, microraptorines may have required—or were subject to strong selection pressure to retain—a relatively large gastral basket to facilitate breathing despite also having a relatively large sternum among non-avian theropods. Causation aside, the presence of gastralia in microraptorines and other paravians inherently shows that cuirassal ventilation was retained as an accessory breathing mechanism in non-avian paravians, even those without clear correlates of pubogastralial tissues. Additionally, the morphology of *Hesperonychus elizabethae* underscores the functional importance of gastralia in Cretaceous theropods, and highlights the peculiar difference in pubic orientation between its proximal and distal ends.

Locomotory muscles were also affected by the lateral pubic tubercle. Although not as imperative as the bearing of the tubercle on ventilatory mode, the path of the M. puboischiofemoralis externus 1 was forced around its anterior surface. In *Hesperonychus elizabethae*, the anterior and dorsal surfaces of the lateral pubic process are convex and form a smooth, trochlea-like structure, which would have facilitated muscle function. Although the distal end of the pubis appears retroverted, the M. puboischiofemoralis externus 1 origin remains ventral to the acetabulum. However, the M. puboischiofemoralis externus 2 line of action is not interrupted in this way by the lateral pubic tubercle as its origin is slightly posterior to that of the first head. Both of these muscles protract the femur in crocodylians and have some degree of lateral rotation (origins anteroventral to acetabulum), but are limited to lateral femoral rotation in avians (origins posteroventral to acetabulum) (Hutchinson and Gatesy 2000). However, both of these muscles probably had a modest degree of femoral protraction with origins intermediate between these two extremes. Theropods with a more strongly retroverted pubis (e.g. *Velociraptor mongoliensis*) demonstrate decent protraction capability despite these muscle origins in either a similar or more posterior position relative to the acetabulum (Hutchinson et al.

2008). Hence, the Mm. puboischiofemoralis externi 1 and 2 are inferred as capable of performing roles both in femoral protraction and lateral rotation even with interference to the first head by the lateral pubic tubercle. Perhaps the pulley system created by this interference affected the leverage of the M. puboischiofemoralis externus 1, which may have been useful for manipulating the hindwing with an abducted femur during gliding flight (Longrich 2006), although this requires testing. Whatever the causal mechanism behind this muscular arrangement in Microraptorinae, it resulted in a complex path for the M. puboischiofemoralis externus 1 around both the anterior and lateral sides of the pubic shaft and required modification of the pelvis to achieve this task.

5.5 Summary of the microraptorine lateral pubic tubercle

The microraptorine lateral pubic tubercle is putatively considered homologous with the anterolateral corner of the pubis of crocodylians as an osteological correlate of the pubogastralial ligament. This landmark varies in morphology with attached, observable pubogastralial soft tissue in crocodylians as a small eminence on the anterolateral corner of the pubis. It is a lateral or anterolateral eminence on the pubic boot in non-coelurosaurian theropods, a distinct anterolateral process in non-paravian coelurosaurians, and varied in paravians as absent, a shallow lateral bulge, or a discrete lateral tubercle or wing-shaped process near the midshaft of the pubis. The role of the microraptorine lateral pubic tubercle was to both anchor pubogastralial ligaments connecting the cuirass to the pelvis, and to allow the M. puboischiofemoralis externus 1 to pass freely around the lateral edge of the pubis toward its insertion on the femoral head. This study also offers insight on adaptations for ventilation and locomotion due to the presence and structure of the lateral pubic tubercle.

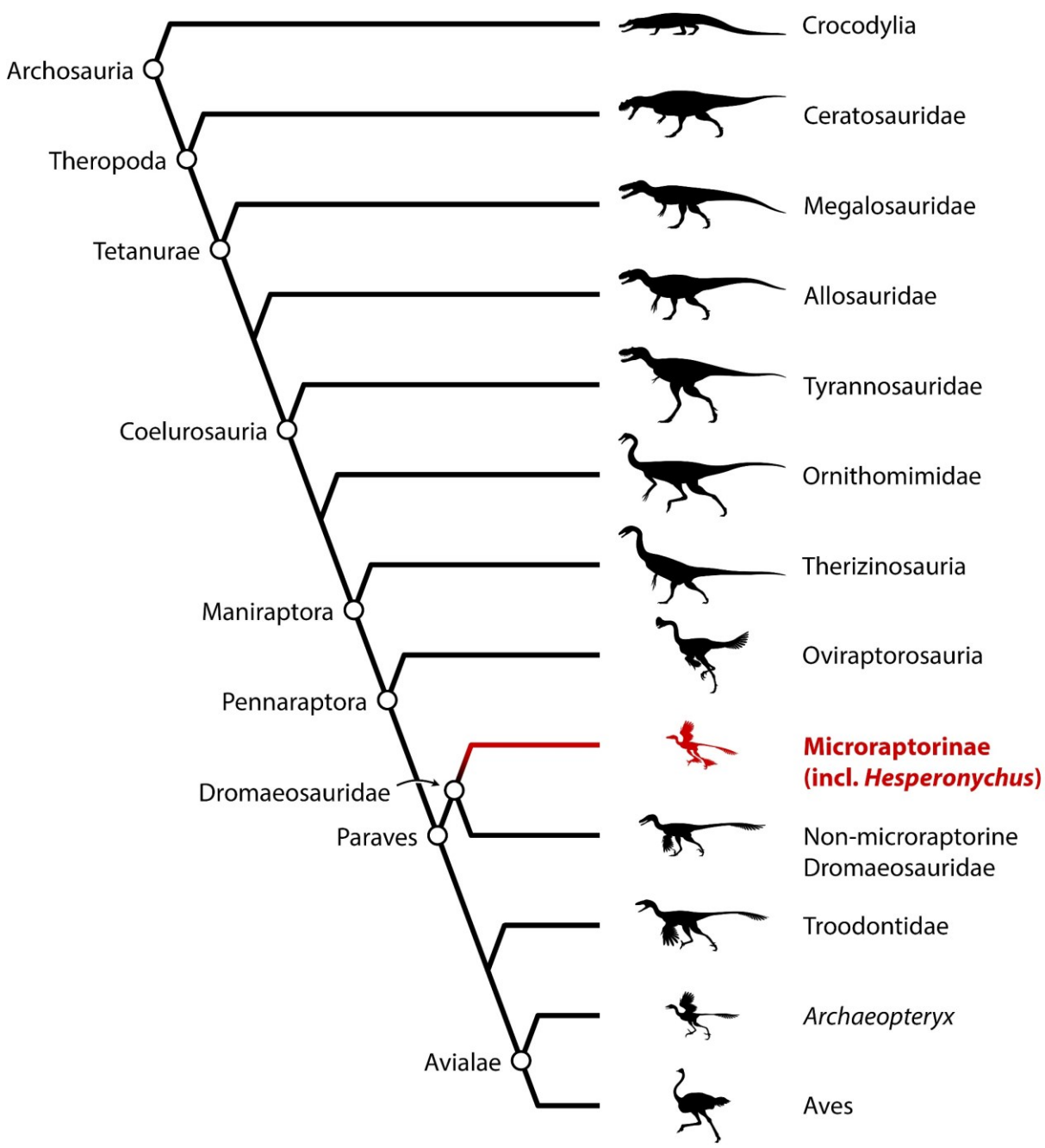

Figure 5.1. Simplified phylogeny of Microraptorinae among Archosauria. Phylogeny includes other theropod groups examined for correlates of pubogastralial tissues and representatives of its Extant Phylogenetic Bracket (Crocodylia and Aves).

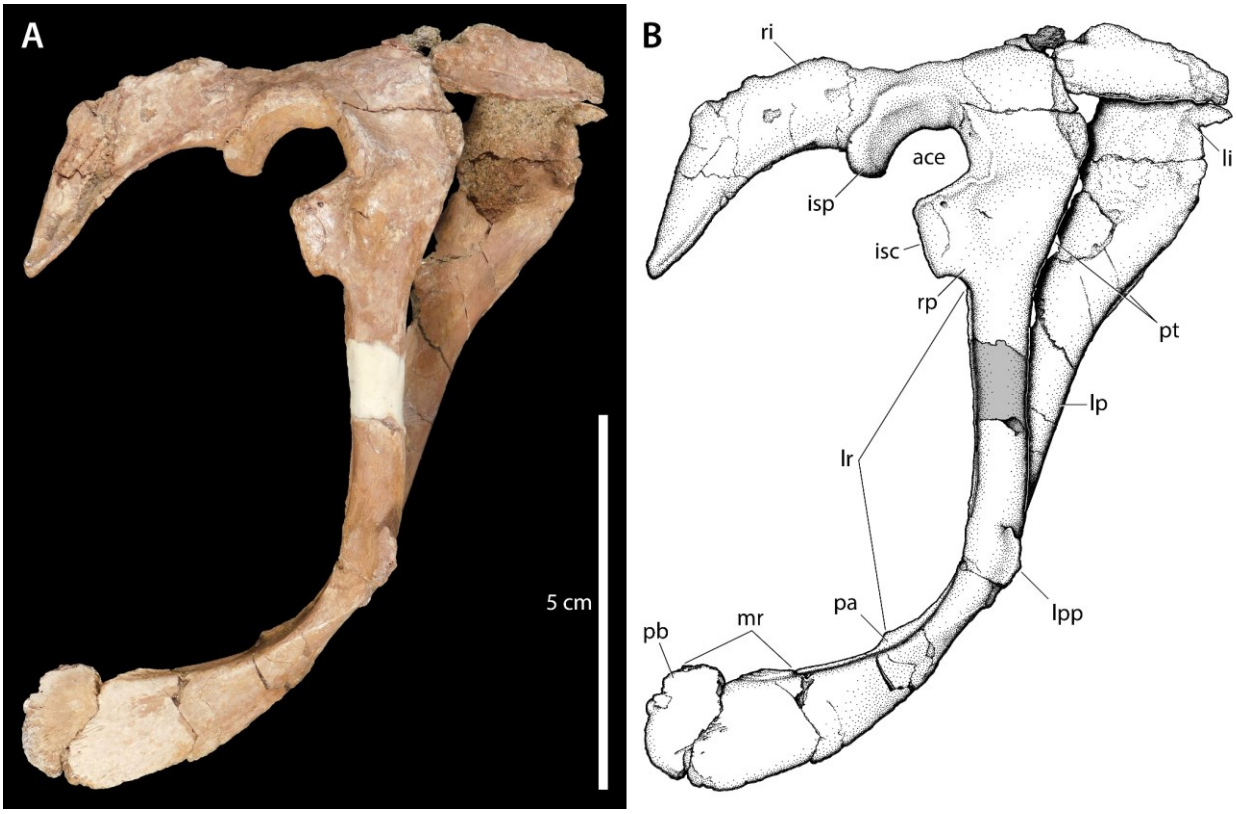

Figure 5.2. Holotype pelvis of *Hesperonychus elizabethae* (UALVP 48778). Photograph (A) and illustration (B) of the pelvis in right lateral view. Grey areas in illustration represent matrix obscured areas on dorsal end and reconstructed portion of right pubic shaft. Scale bar is 5 cm. **Abbreviations: ace,** acetabulum; **isc,** ischiadic contact; **isp,** ischiadic peduncle; **li,** left ilium; **lp,** left pubis; **lpp,** lateral pubic process; **lr,** lateral ridge of puboischiadic membrane; **mr,** median ridge of puboischiadic membrane; **pa,** pubic apron; **pb,** pubic boot; **pt,** preacetabular tubercle; **ri,** right ilium; **rp,** right pubis.

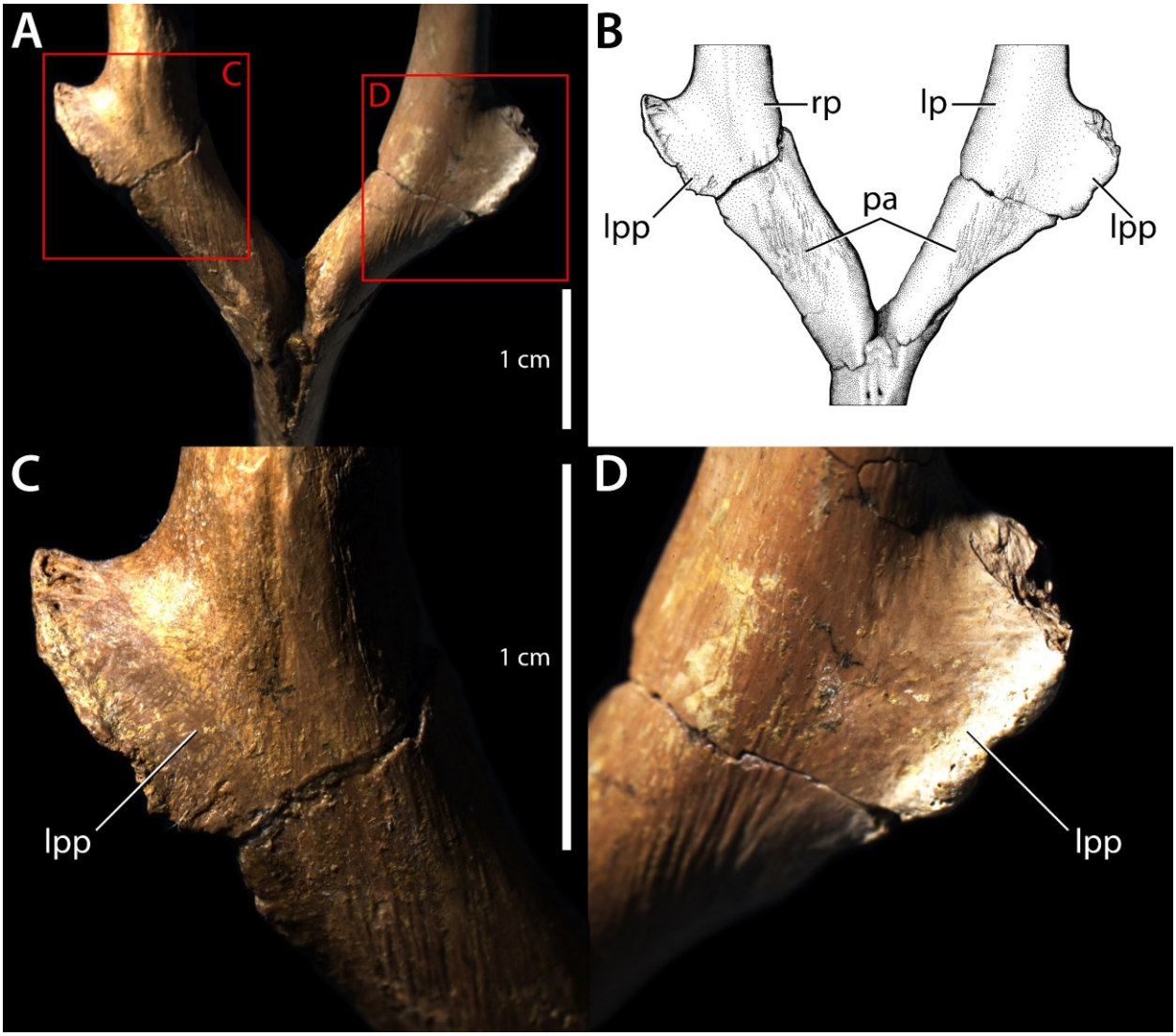

Figure 5.3. Anterior view of the lateral pubic processes in *Hesperonychus elizabethae* (UALVP 48778). Photographs and illustrations of the midshaft of the pubes (A–B) and right (C) and left (D) lateral pubic processes. Scale bars are 1 cm. **Abbreviations: lp,** left pubis; **lpp,** lateral pubic process; **pa,** pubic apron; **rp,** right pubis.

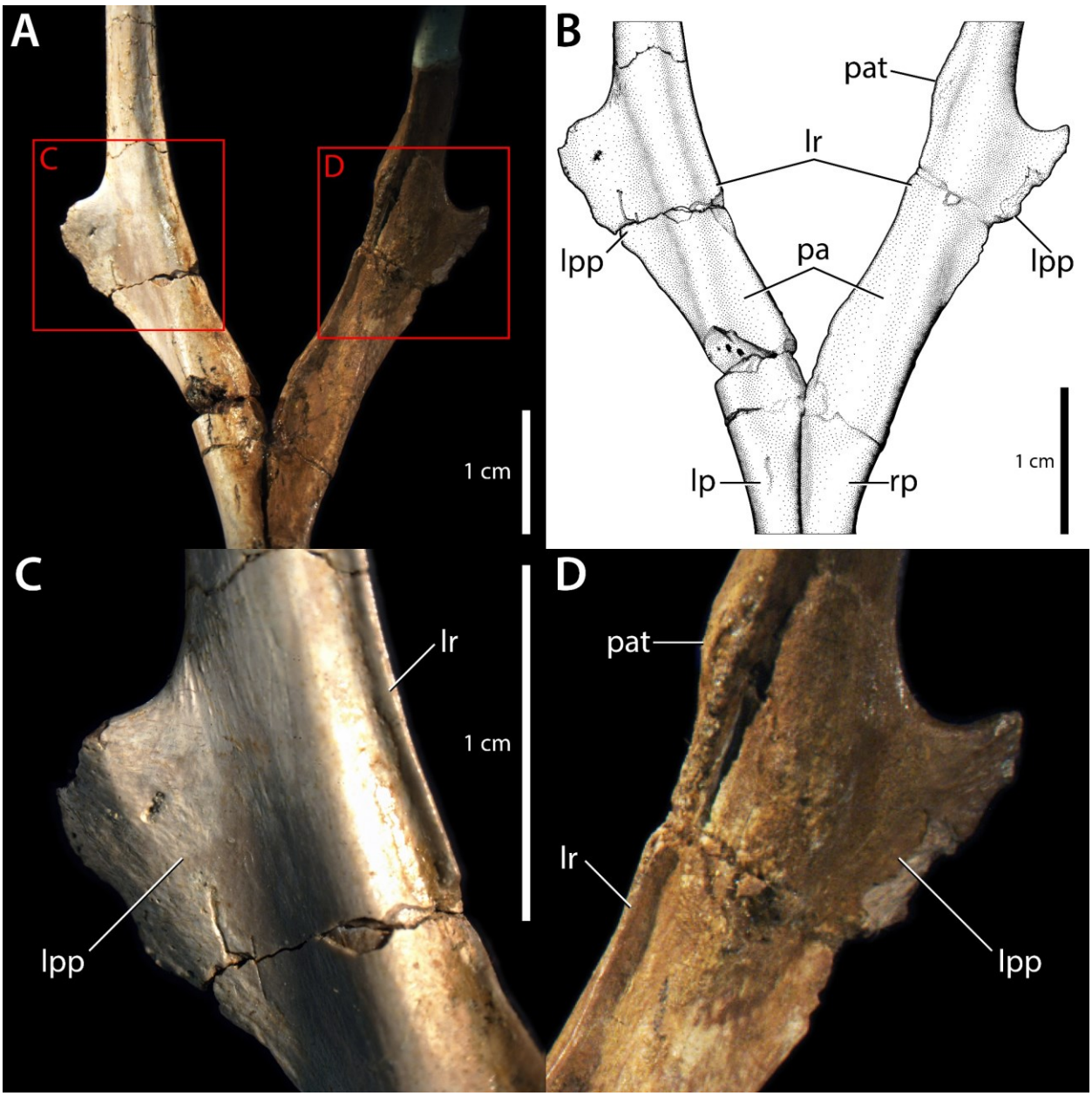

Figure 5.4. Posterior view of the lateral pubic processes in *Hesperonychus elizabethae* (UALVP 48778). Photographs and illustrations of the midshaft of the pubes (A–B) and left (C) and right (D) lateral pubic processes. Scale bars are 1 cm. **Abbreviations: lp,** left pubis; **lpp,** lateral pubic process; **lr,** lateral ridge of puboischiadic membrane; **pa,** pubic apron; **pat,** pathology; **rp,** right pubis.

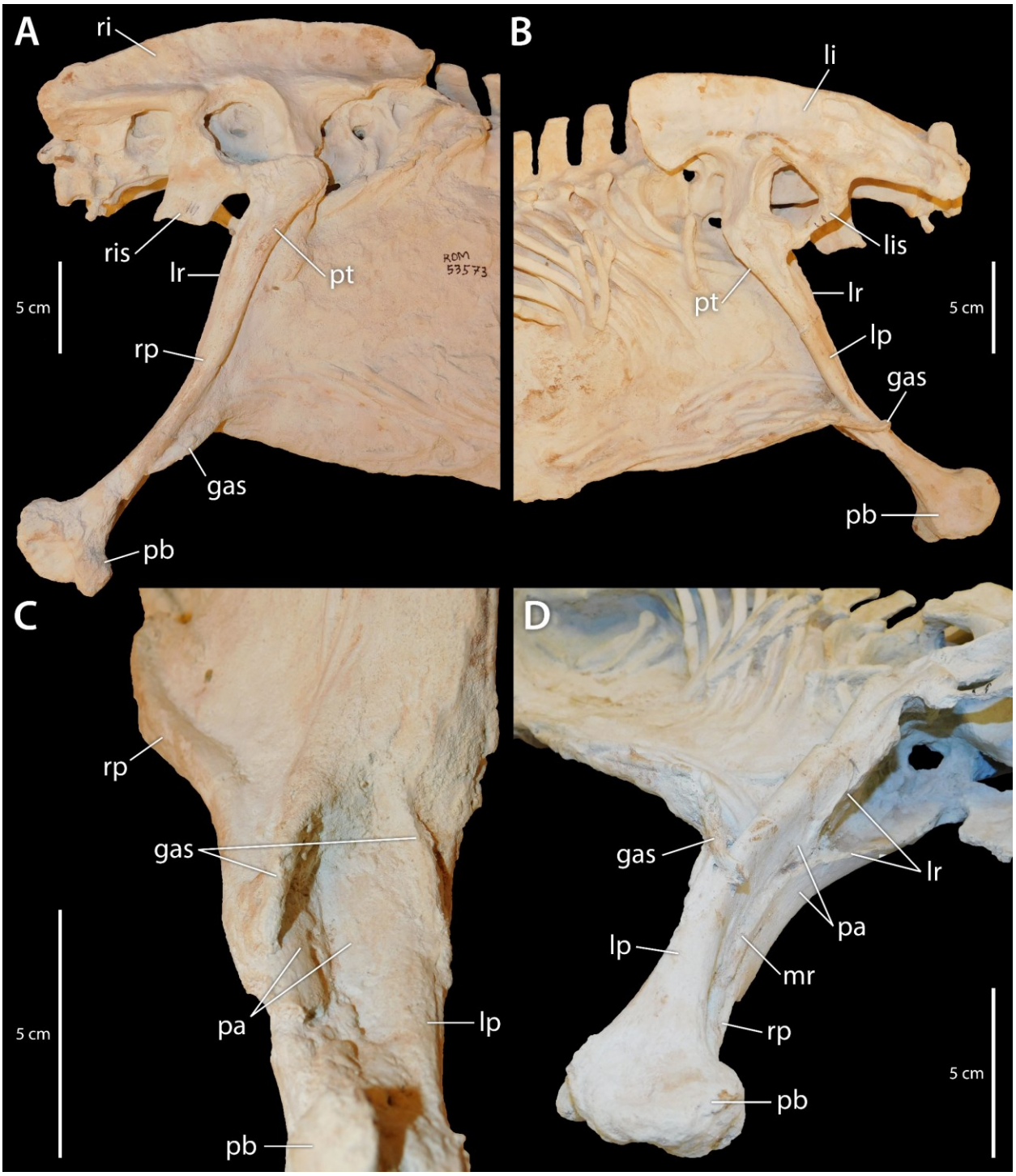

Figure 5.5. Articulated gastralia in a non-microraptorine dromaeosaurid. Photographs of a cast of a three-dimensionally preserved velociraptorine dromaeosaurid (ROM 53573). Pelvis and gastralia in right lateral (A) and left lateral (B) views; site of pubogastralial articulation in

anteroventral (C) and left posteroventrolateral (D) views. Scale bar is 5 cm. **Abbreviations: gas,** gastralia; **li,** left ilium; **lis,** left ischium; **lp,** left pubis; **lr,** lateral ridge of puboischiadic membrane; **mr,** median ridge of puboischiadic membrane; **pa,** pubic apron; **pb,** pubic boot; **pt,** preacetabular tubercle; **ri,** right ilium; **ris,** right ischium; **rp**, right pubis.

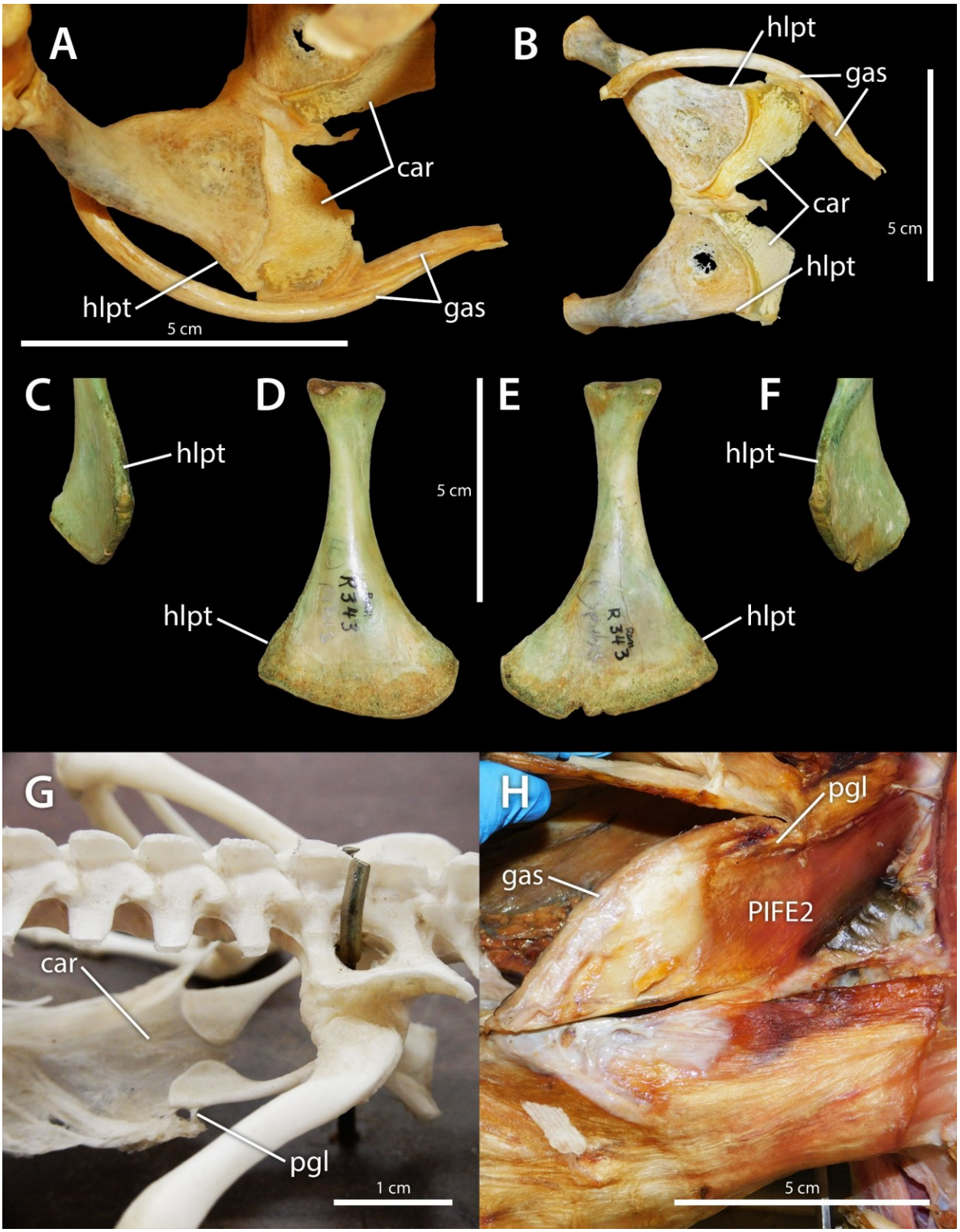
A
car
hlpt
gas
5 cm
B
hlpt
gas
car
hlpt
5 cm
C
hlpt
D
hlpt
5 cm
E
hlpt
F
hlpt
G
car
pgl
1 cm
H
pgl
gas
PIFE2
5 cm

Figure 5.6. Condition of the homolog of the lateral pubic tubercle in Crocodylia. Recent *Caiman* sp. (ROM no #) pubes with preserved anterior pubic cartilage in oblique anterolateral view (A, anterior to bottom-right) and ventral view (B, anterior to right). Recent *Alligator mississippiensis* (ROM R343) pubes in left lateral (C), left ventral (D), right ventral (E), and right lateral views. Recent *Alligator mississippiensis* (UAMZ HER-R654) skeleton with preserved anterior pubic cartilage and left pubogastralial ligament in left dorsolateral view (G, anterior to left). Dissection of *Caiman crocodilus* (UAMZ no #) showing pubes, right pubogastralial ligament, and most posterior gastralial row in ventral view (H, anterior to left). Scale bars are all 5 cm except for G, which is 1 cm. **Abbreviations: car,** cartilage; **gas,** gastralia; **hlpt,** homolog of the lateral pubic tubercle; **pgl,** pubogastralial ligament; **PIFE2,** M. puboischiofemoralis externus 2.

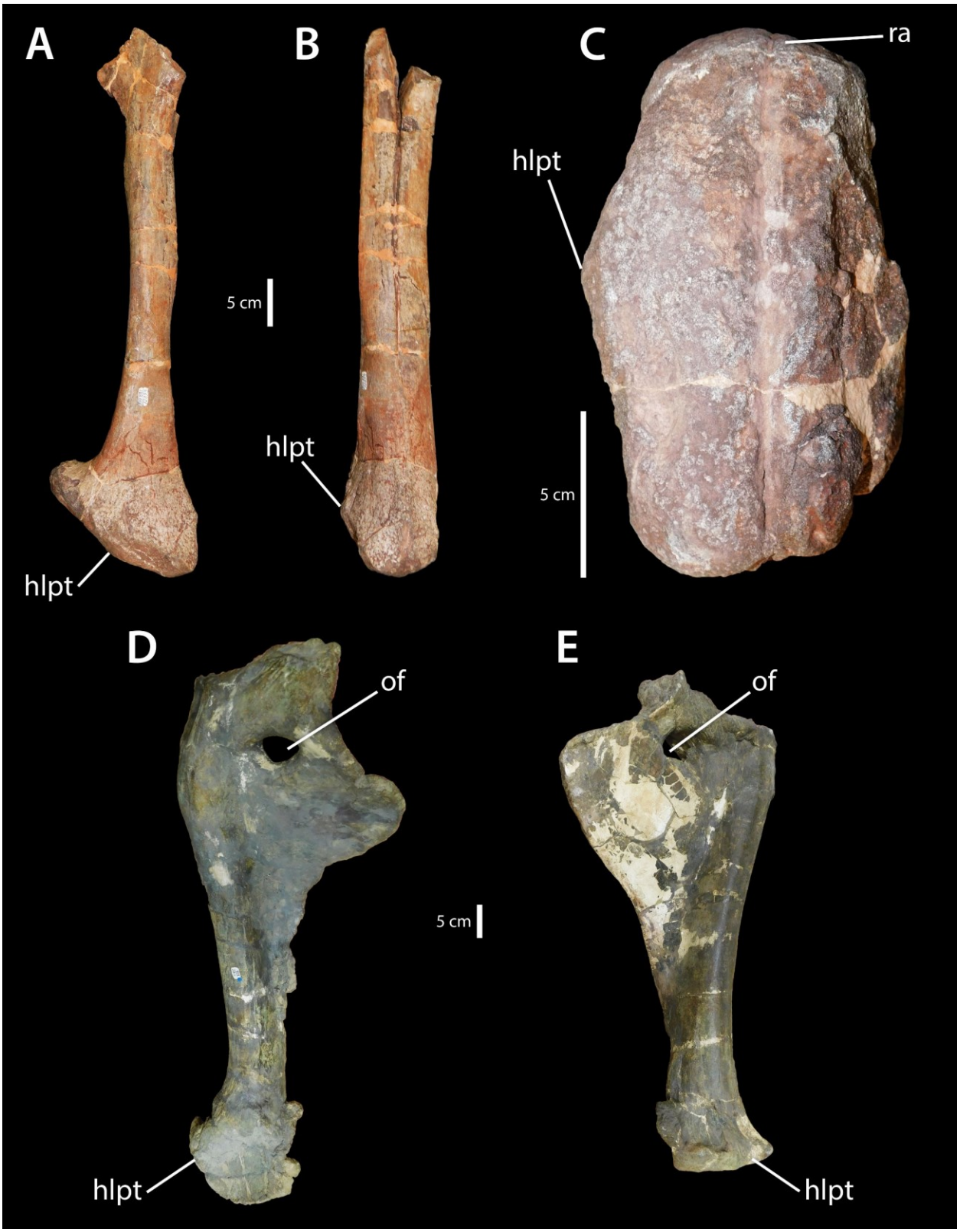
A
B
C
ra
hlpt
5 cm
hlpt
5 cm
hlpt
D
E
of
of
5 cm
hlpt
hlpt

Figure 5.7. Condition of the homolog of the lateral pubic tubercle in Ceratosauridae and Megalosauridae. Pubes of *Ceratosaurus* sp. (BYUVP 12893) in right lateral view (A, anterior to right) and anterior view (B), and pubic boot in ventral view (C, anterior to top). Pubes of *Torvosaurus tanneri* (BYUVP 2014) in left lateral view (D) and right lateral view (E). Scale bars are all 5 cm. **Abbreviations: hlpt,** homolog of the lateral pubic tubercle; **of,** obturator foramen; **ra,** osteological correlate of M. rectus abdominis.

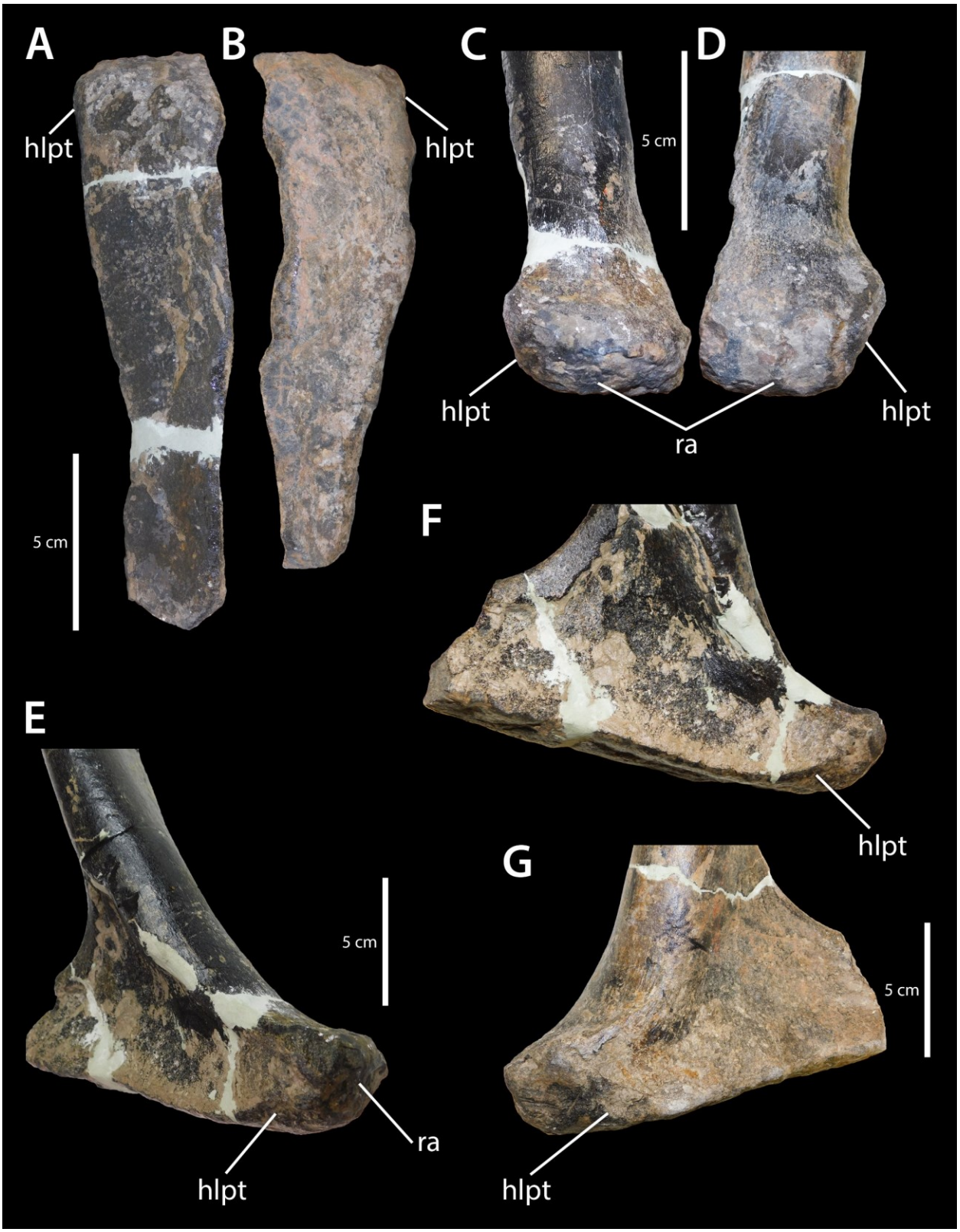
A
B
C
D
hlpt
hlpt
5 cm
hlpt
ra
hlpt
5 cm
F
hlpt
E
G
5 cm
5 cm
ra
hlpt
hlpt

Figure 5.8. Condition of the homolog of the lateral pubic tubercle in Allosauridae. Pubes of *Allosaurus fragilis* (CMN 38454). Left (A) and right (B) pubic boots in ventral view (anterior to top), right (C) and left (D) pubic boots in anterior view, right pubic boot in anterolateral (E) and right lateral (F) views, and left pubic boot in left lateral view (G). Scale bars are all 5 cm. **Abbreviations: hlpt,** homolog of the lateral pubic tubercle; **ra,** M. rectus abdominis (osteological correlate).

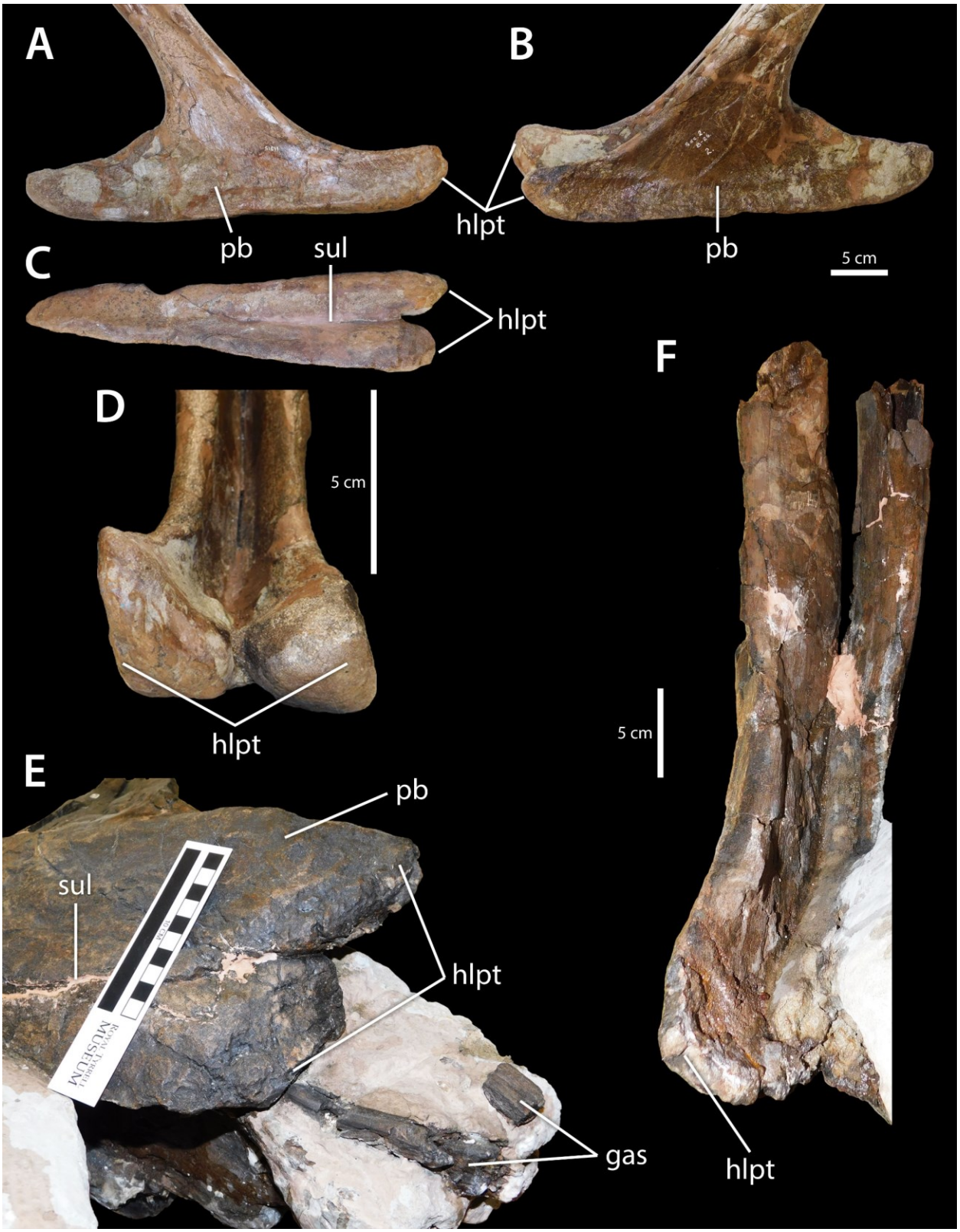
A
B
pb
hlpt
pb
5 cm
C
sul
hlpt
D
5 cm
hlpt
F
5 cm
E
pb
sul
hlpt
gas
hlpt

Figure 5.9. Condition of the homolog of the lateral pubic tubercle in Tyrannosauridae. Pubic boot of *Albertosaurus sarcophagus* (CMN 11315) in right lateral view (A), left lateral view (B), ventral view (C), and anterior view (D). Pubic boot of *Gorgosaurus libratus* (CMN 2120) with articulated gastralium in ventral oblique view (E) and anterior view (F). Scale bars are all 5 cm. **Abbreviations: gas,** gastralia; **hlpt,** homolog of the lateral pubic tubercle; **pb,** pubic boot; **sul,** midline sulcus.

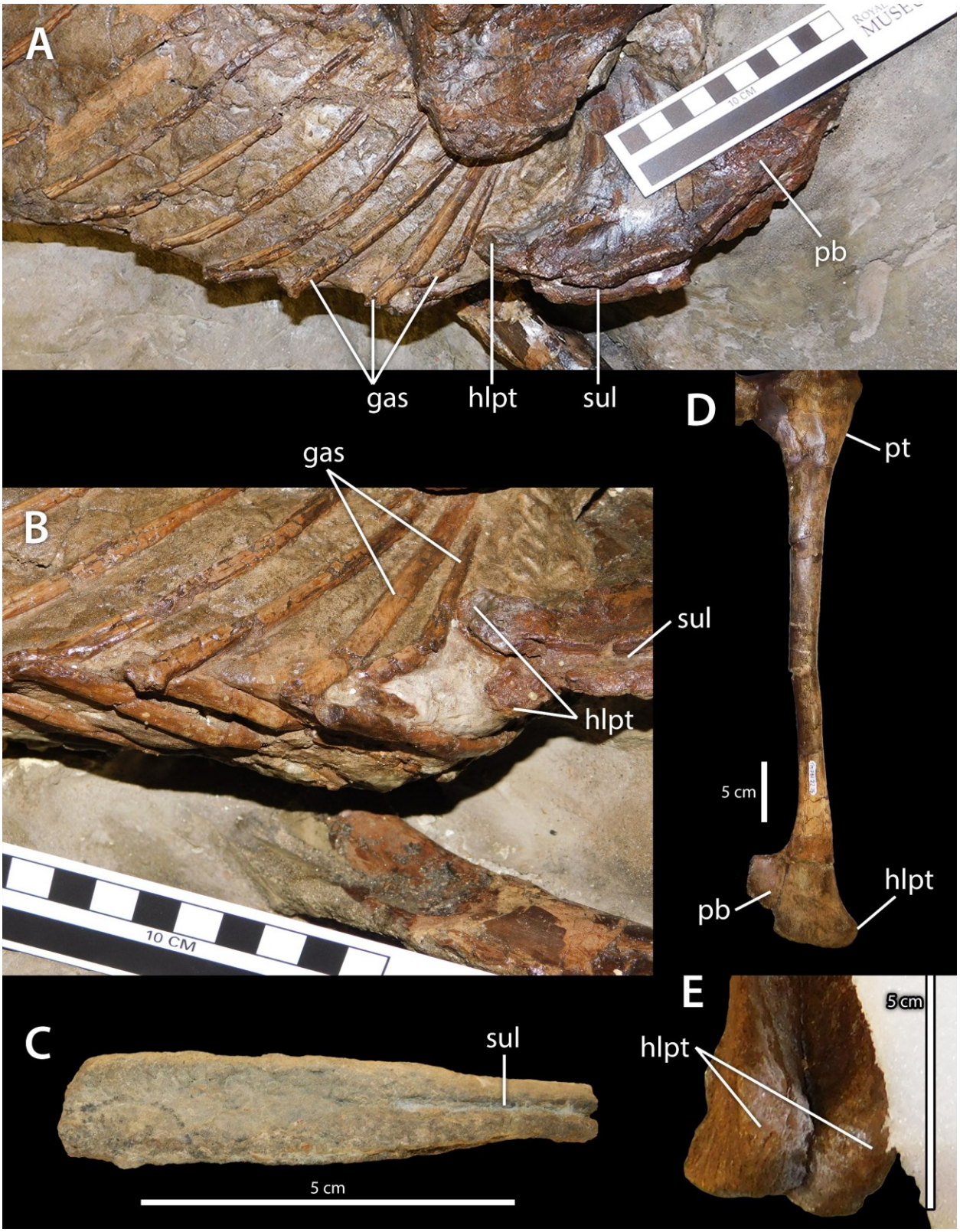
A
10 CM
pb
gas
hlpt
sul
B
gas
sul
hlpt
10 CM
C
sul
5 cm
D
pt
5 cm
hlpt
pb
E
5 cm
hlpt

Figure 5.10. Condition of the homolog of the lateral pubic tubercle in Ornithomimidae. Pubic boot of *Ornithomimus edmontonicus* (CMN 8632) with articulated cuirass in left lateral view (A) and ventral view (B, anterior to left). Pubic boot of cf. *Ornithomimus* sp. (CMN 12070) in ventral view (C, anterior to right). Pubes of Ornithomimidae indet. (TMP 1981.019.0299) in right lateral (D) and anterior (E) views. Scale bars are all 5 cm. **Abbreviations: gas,** gastralia; **hlpt,** homolog of the lateral pubic tubercle; **pb,** pubic boot; **pt,** preacetabular tubercle; **sul,** midline sulcus.

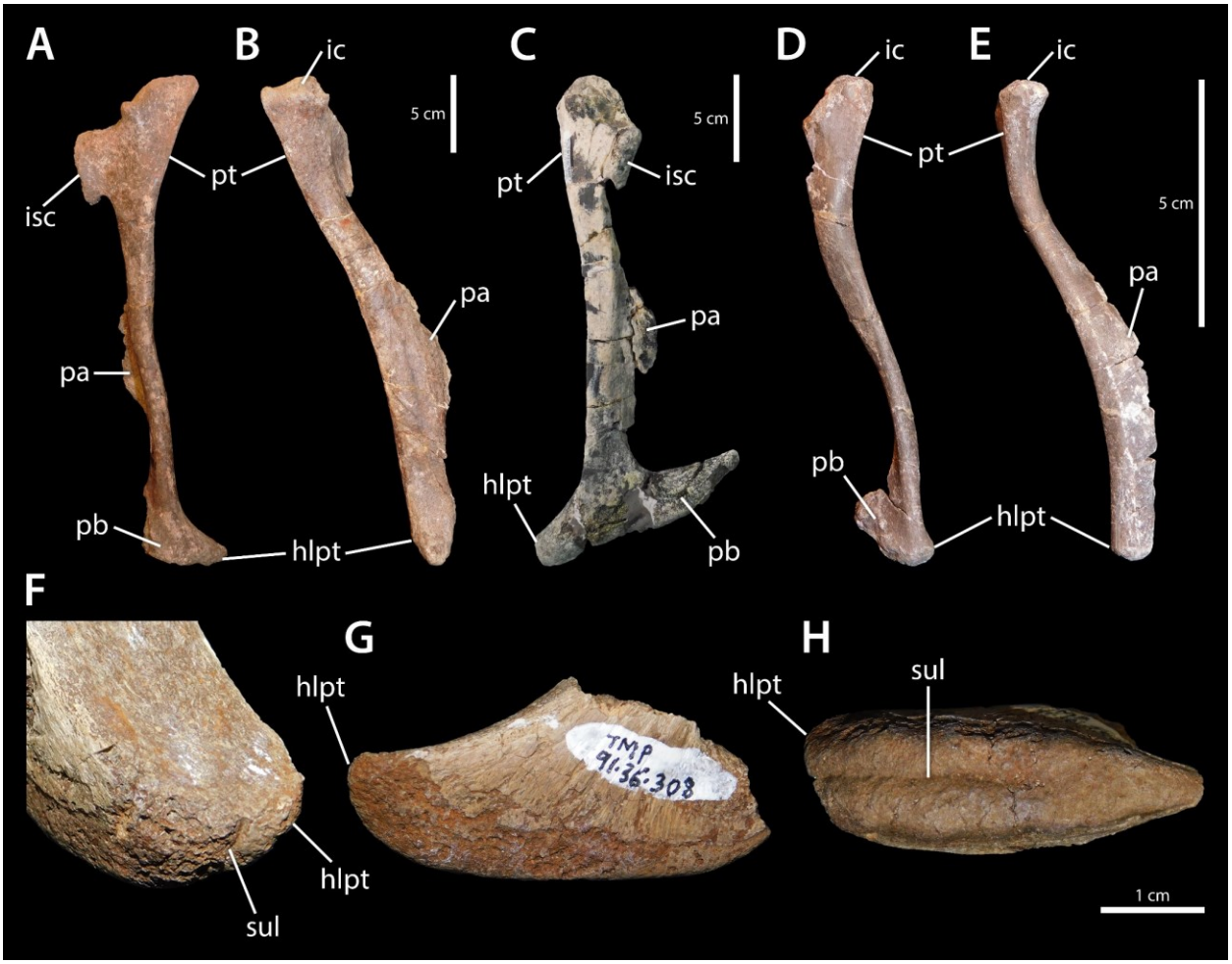

Figure 5.11. Condition of the homolog of the lateral pubic tubercle in Therizinosauria and Caenagnathidae. Right pubis of *Falcarius utahensis* (Courtesy of Natural History Museum of Utah, UMNH VP 14540) in right lateral view (A) and anterior view (B). Left pubis of *Falcarius* sp. (CEUM 77195) in left lateral view (C). Right pubis of *Falcarius utahensis* (Courtesy of Natural History Museum of Utah, UMNH VP no #) in right lateral view (D) and anterior view (E). Pubic boot of Caenagnathidae indet. (TMP 1991.036.0308) in oblique anterolateral view (F, anterior to bottom-right), left lateral view (G), and ventral view (H, anterior to left). Scale bars are 5 cm (A–E) or 1 cm (F–H). **Abbreviations: hlpt,** homolog of the lateral pubic tubercle; **ic,** iliac contact; **isc,** ischiadic contact; **pa,** pubic apron; **pb,** pubic boot; **pt,** preacetabular tubercle; **sul,** midline sulcus.

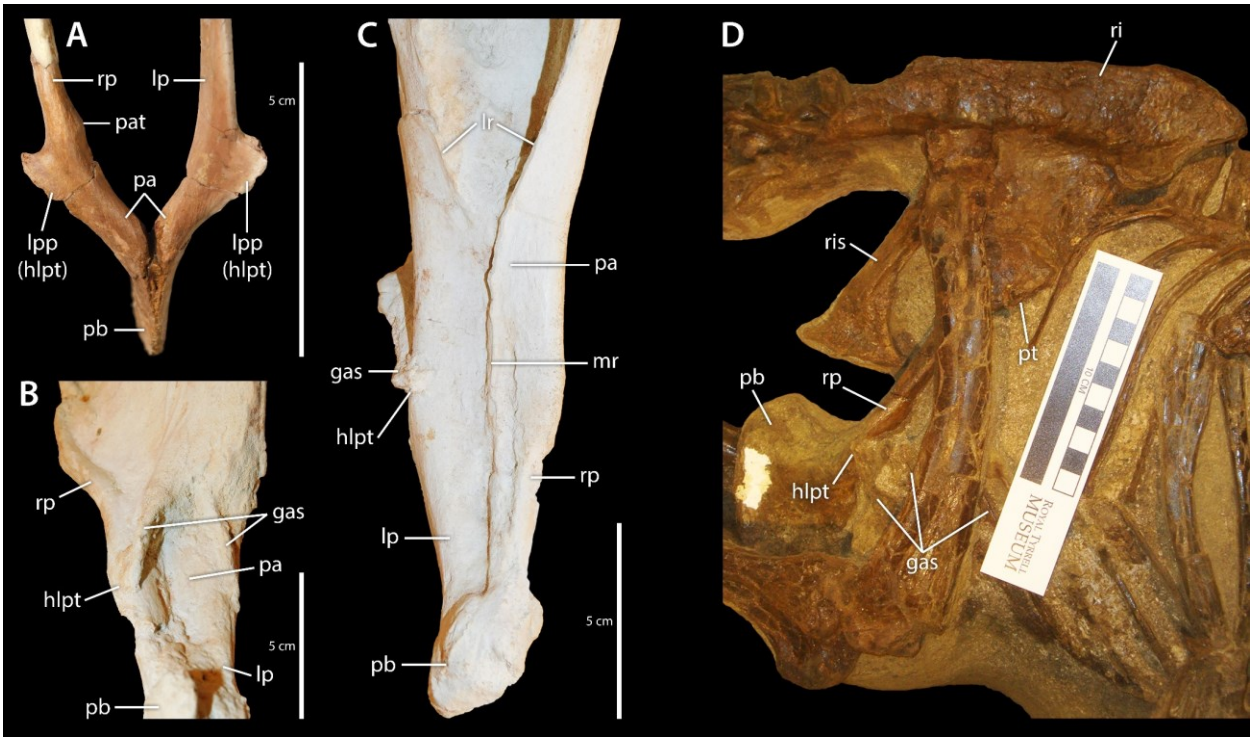

Figure 5.12. Condition of the homolog of the lateral pubic tubercle in Dromaeosauridae. Pubes of *Hesperonychus elizabethae* (UALVP 48778) in anterior view (A). Pubes of Velociraptorinae indet. (CMN 53573) in articulation with gastralia in anteroventral view (B) and posterior view (C). Pelvis of *Saurornitholestes langstoni* (UALVP 55700) in articulation with cuirass in right lateral view (D). Scale bars are all 5 cm. **Abbreviations: gas,** gastralia; **hlpt,** homolog of the lateral pubic tubercle; **lp,** left pubis; **lpp,** lateral pubic tubercle; **lr,** lateral ridge of puboischiadic membrane; **mr,** median ridge of puboischiadic membrane; **pa,** pubic apron; **pat,** pathology; **pb,** pubic boot; **pt,** preacetabular tubercle; **ri,** right ilium; **ris,** right ischium; **rp,** right pubis.

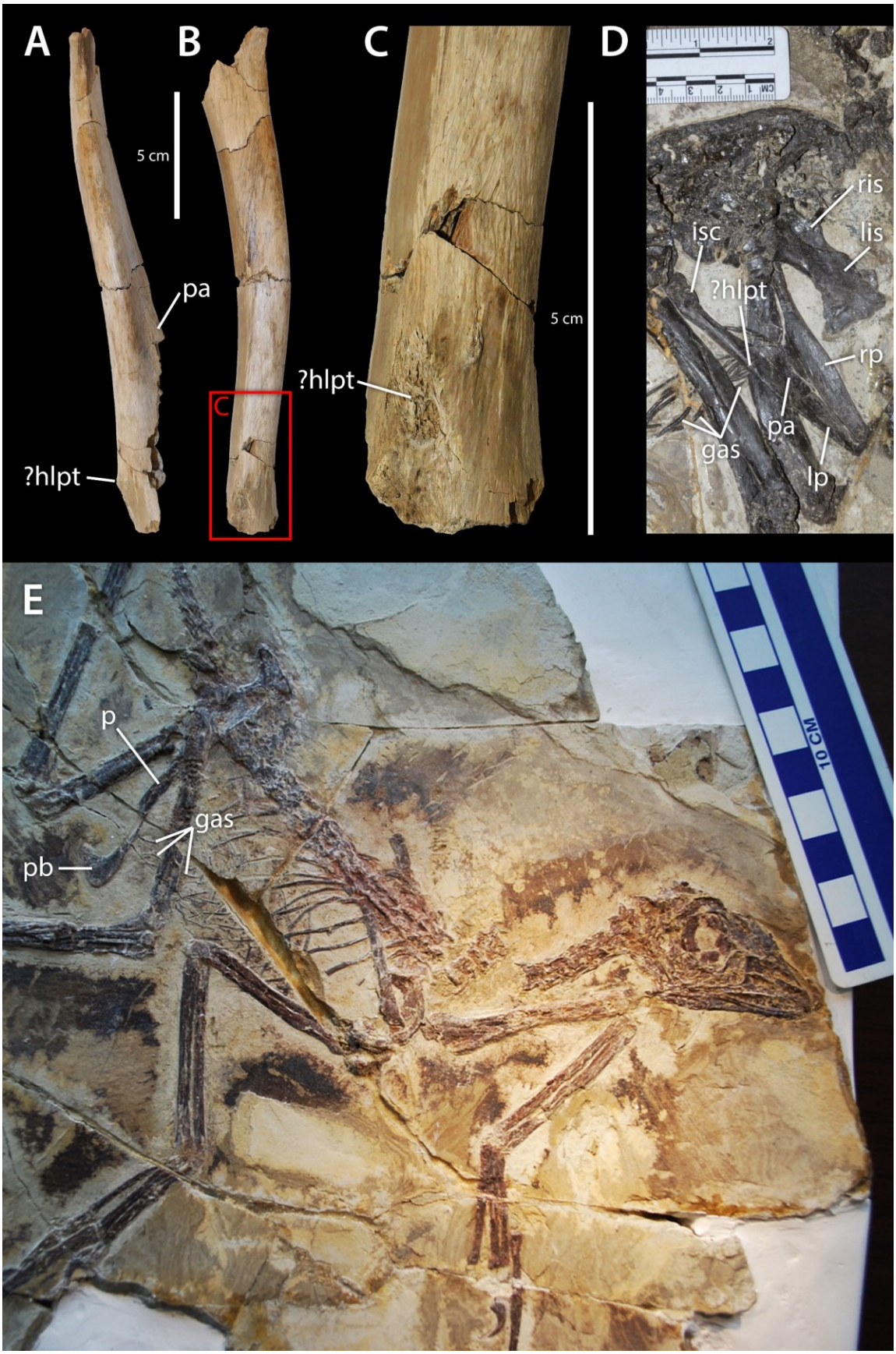
A
B
C
D
5 cm
pa
?hlpt
C
5 cm
?hlpt
ris
lis
isc
?hlpt
rp
gas
pa
lp
E
p
gas
pb
10 cm

Figure 5.13. Condition of the homolog of the lateral pubic tubercle in non-avian Paraves. Left pubis of *Latenivenatrix mcmasterae* (UALVP 55804) in posterior view (A) and left lateral view (B) with popout of spiculate tubercle (C). Pubes of *Jianianhualong tengi* (DLXH 1218) in articulation with gastralia in posterior view (D). Skeleton of *Anchiornis* sp. (IVPP V16055) with pelvis in articulation with cuirass in right lateral view (E). Scale bars are all 5 cm. **Abbreviations: gas,** gastralia; **hlpt,** homolog of the lateral pubic tubercle; **isc,** ischiadic contact; **lis,** left ischium; **lp,** left pubis; **p,** pubis; **pa,** pubic apron; **pb,** pubic boot; **ris,** right ischium; **rp,** right pubis.

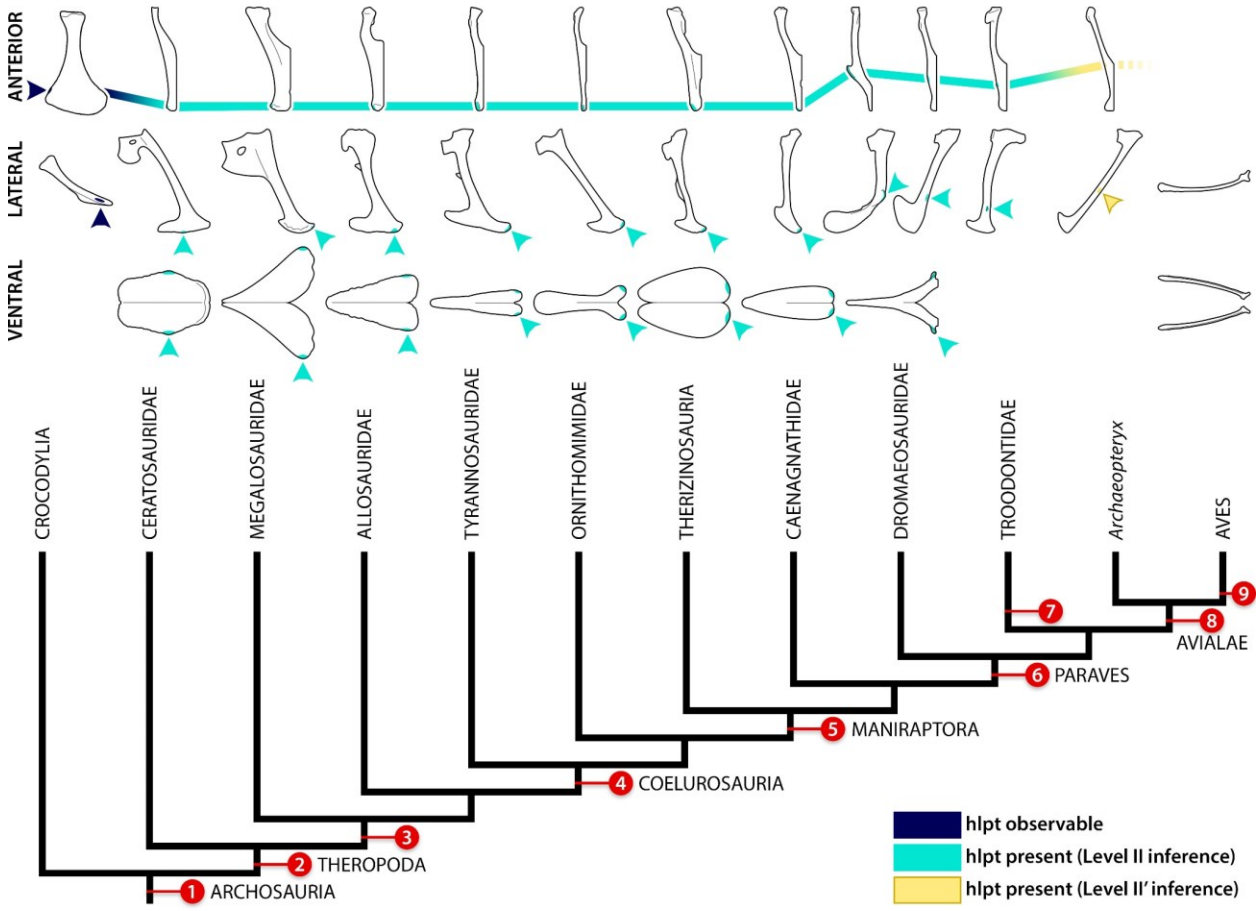

Figure 5.14. Distribution of the homolog for the lateral pubic tubercle (hlpt) across Archosauria. Described states mapped onto simplified phylogeny with topology based on Hendrickx et al. (2015). Diagrams show right pubis of relevant taxon in anterior (top) and lateral (middle) views, and pubic boot in ventral view (bottom, anterior to right). Although these representatives are points along a spectrum of morphological variation, major changes to capture general trends are indicated in numbered steps: presence of gastralia and pubogastralial tissues (1), expansion of distal end of pubis into boot (2), anterior migration of lateral eminence as a hlpt (3), development of distinct anterolateral processes as hlpt (4), reduced anterolateral processes (5), proximal migration of hlpt (6), hlpt may be present as spiculate tubercle (7), loss of clear hlpt despite retention of gastralia (8), and loss of gastralia and hlpt (9). Pubis based on *Alligator*

mississippiensis (ROM R343) for Crocodylia, *Ceratosaurus* sp. (BYUVP 12893) (Gilmore 1920) for Ceratosauridae, *Torvosaurus tanneri* (BYUVP 2014) (Galton and Jensen 1979) for Megalosauridae, *Allosaurus fragilis* (CMN 38454) (Gilmore 1920) for Allosauridae, *Albertosaurus sarcophagus* (CMN 11315) and *Daspletosaurus torosus* (UALVP 52981) for Tyrannosauridae, Ornithomimidae indet. (TMP 1981.019.0299) and *Ornithomimus edmontonicus* (CMN 8632) for Ornithomimidae, *Falcarius utahensis* (Courtesy of Natural History Museum of Utah, UMNH VP 14540) and reconstructed cast (CEUM no #) for Therizinosauria, Caenagnathidae indet. (TMP 1991.036.0308, 1994.012.0603, UALVP 55638) for Caenagnathidae, *Hesperonychus elizabethae* (UALVP 48778) for microraptorine dromaeosaurids in all views and *Saurornitholestes langstoni* (UALVP 55700) and Velociraptorinae indet. (ROM 53573) for non-microraptorine dromaeosaurids in anterior and lateral views, *Latenivenatrix mcmasterae* (UALVP 55804) for Troodontidae, *Archaeopteryx* sp. (Chatterjee 1997, Geist and Feduccia 2000) for *Archaeopteryx*, and *Dromaius novaehollandiae* (ROM R6843) for Aves.

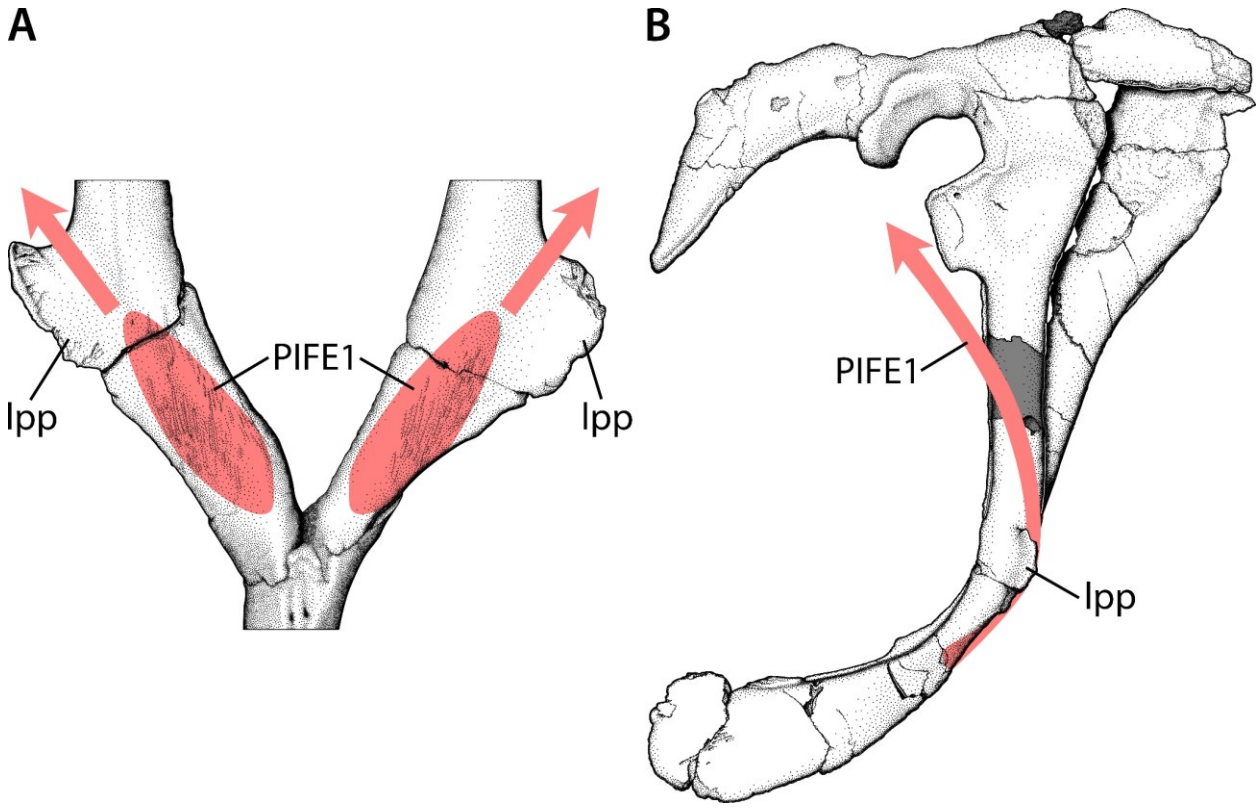

Figure 5.15. Muscle path of the M. puboischiofemoralis externus 1 with respect to the lateral pubic process in *Hesperonychus elizabethae* (UALVP 48778). Pubic apron in anterior view (A) depicts muscle origin and line of action (pink). Pelvis in right lateral view (B) shows muscle path around anterior surface of lateral pubic process and lateral to pubic shaft toward insertion on femur (arrowhead). **Abbreviations: lpp,** lateral pubic process; **PIFE1,** M. puboischiofemoralis externus 1.

Table 5.1. Archosaur and lepidosaur material examined for osteological correlates of soft tissues. Specimens are arranged by taxon and then alphabetically within each taxonomic group. Note: BYUVP, Brigham Young University Museum of Paleontology; CEUM, Utah State University Eastern Prehistoric Museum; CMN, Canadian Museum of Nature; RM, Redpath Museum; ROM, Royal Ontario Museum; TMP, Royal Tyrrell Museum of Palaeontology; UALVP, University of Alberta Laboratory for Vertebrate Palaeontology; UAMZ, University of Alberta Museum of Zoology; UMNH VP, Utah Museum of Natural History.

Taxon	Specimen number	Condition and element(s)
Non-coelurosaurian Theropoda		
Ceratosauridae		
Ceratosaurus sp.	BYUVP 12893	Fused pubes, ischia
Megalosauridae		
Torvosaurus tanneri	BYUVP 2014	Disarticulated pubes
Allosauridae		
Allosaurus fragilis	BYUVP 4891	Fused, partial pubes (apron and boot)
Allosaurus fragilis	BYUVP 5292	Disarticulated, intact pubes
Allosaurus fragilis	BYUVP 11430	Fused, intact pubes
Allosaurus fragilis	BYUVP 13625	Intact left pubis
Allosaurus fragilis	BYUVP 16774	Pubic boot
Allosaurus fragilis	BYUVP 17550	Fused, partial pubes (apron and boot)
Allosaurus fragilis	CMN 38454	Disarticulated, intact pubes
Non-paravian Coelurosauria		
Tyrannosauridae		
Albertosaurus sarcophagus	CMN 11315	Pubic boot
Daspletosaurus torosus	UALVP 52981	Fused, intact pubes (part of complete pelvis)
Gorgosaurus libratus	CMN 2120	Pubic boot in articulation with gastralium
Gorgosaurus libratus	UALVP 10	Fused, mostly intact pubes (part of complete pelvis)
Ornithomimidae		
Dromiceiomimus brevitertius	ROM 797	Fused, mostly intact pubes
Dromiceiomimus brevitertius	UALVP 16182	Fused, mostly intact pubes
Ornithomimus edmontonicus	CMN 8632	Pubic boot articulated with gastralia
Ornithomimus edmontonicus	ROM 851	Fused, mostly intact pubes
cf. *Ornithomimus* sp.	CMN 12070	Pubic boot
Ornithomimidae indet.	TMP 1981.019.0299	Fused, intact pubes (part of complete

		pelvis)
Therizinosauria		
Falcarius utahensis	UMNH VP 14540	Intact right pubis
Falcarius utahensis	UMNH VP (no #)	Intact right pubis (juvenile)
Falcarius sp.	CEUM 52424	Intact right pubis
Falcarius sp.	CEUM 77195	Intact left pubis
Falcarius sp.	CEUM 77233	Mostly intact right pubis
Falcarius sp.	CEUM 77290	Intact left pubis
Nothronychus graffami	UMNH VP 16420	Disarticulated, mostly intact pubes
Caenagnathidae		
Epichirostenotes curriei	ROM 43250	Fused, taphonomically damaged pubes
Caenagnathidae indet.	TMP 1991.036.0308	Pubic boot
Caenagnathidae indet.	UALVP 55638	Fused, mostly intact pubes
Non-avian Paraves		
Dromaeosauridae		
Hesperonychus elizabethae	UALVP 48778	Fused, intact pubes
Saurornitholestes langstoni	UALVP 55700	Fused, intact pubes (part of complete pelvis with articulated gastralia)
Velociraptorinae indet.	ROM 53573	Fused, intact pubes (cast of complete pelvis with articulated gastralia)
Troodontidae		
Latenivenatrix mcmasterae	UALVP 55804	Partial right and left pubes
Aves		
Apteryx haastii	RM 8369	Articulated pubes (part of complete pelvis)
Corvus corax	UAMZ (uncatalogued)	Dissected
Dromaius novaehollandiae	UAMZ B-FIC2014.260	Articulated pubes (part of complete pelvis)
Dromaius novaehollandiae	ROM R6843	Articulated pubes (part of complete pelvis)
Dromaius novaehollandiae	ROM R7945	Articulated pubes (part of complete pelvis)
Gallus gallus	RM 8355	Articulated pubes (part of complete pelvis)
Rhea americana	RM 8499	Disarticulated pubes (part of complete pelvis)
Rhea americana	ROM R7970	Articulated pubes (part of complete pelvis)
Struthio camelus	ROM R2136	Articulated pubes (part of complete pelvis)
Struthio camelus	ROM R7635	Disarticulated pubes (part of complete pelvis)

Struthio camelus	ROM R1933	Articulated pubes (part of complete pelvis)
Struthio camelus	ROM R2305	Disarticulated pubes (part of complete pelvis)
Struthio camelus	UAMZ 7159	Articulated pubes (part of complete pelvis)
Crocodylia		
Alligator mississippiensis	ROM R343	Disarticulated pubes (part of complete pelvis)
Alligator sp.	UAMZ HER-R654	Articulated pubes (part of complete pelvis with articulated gastralia and pubogastralial cartilage and ligaments)
Caiman crocodilus	RM 5242	Disarticulated pubes (part of complete pelvis)
Caiman crocodilus	UAMZ (uncatalogued)	Dissected
Caiman sp.	ROM (no #)	Articulated pubes (part of complete pelvis with articulated gastralia and pubogastralial cartilage)
Osteolaemus tetraspis	RM 5216	Articulated pubes (part of complete pelvis)
Lepidosauria		
Tupinambis teguixin	ROM R436	Articulated pubes (part of complete pelvis)
Varanus albigularis	RM 5220	Disarticulated pubes (part of complete pelvis)
Varanus exanthematicus	UAMZ (uncatalogued)	Dissected
Varanus jobiensis	RM 5219	Articulated pubes (part of complete pelvis)
Varanus komodoensis	ROM R7565	Disarticulated pubes (part of complete pelvis)
Varanus niloticus	RM 5221	Articulated pubes (part of complete pelvis)
Varanus rudicollis	ROM R7318	Articulated pubes (part of complete pelvis)
Varanus salvator	RM 5222	Articulated pubes (part of complete pelvis)
Varanus salvator	RM 5223	Articulated pubes (part of complete pelvis)
Varanus salvator	RM 5224	Articulated pubes (part of complete pelvis)

Table 5.2. Archosaur pubic soft tissue candidates for the lateral pubic tubercle. An asterisk (*) indicates that the osteological correlate is not located directly on the pubis. Some data from sources on avian and crocodylian anatomy (Romer 1923a, Baumel et al. 1990, Proctor and Lynch 1993, Carrier and Farmer 2000, Hutchinson 2001a, Claessens 2009, Fechner et al. 2013, Fechner and Schwarz-Wings 2013).

Soft tissue	Osteological correlate with respect to the pubis	
	Crocodylia	Aves
Trunk muscles		
M. obliquus abdominis externus	*Lateral gastralia	Anteroventral margin of ilium and pubis, iliopubic ligament
M. obliquus abdominis internus	*Lateral gastralia	Anteroventral margin of ilium and pubis, iliopubic ligament
M. transversus abdominis	*Lateral gastralia	Anteroventral margin of ilium and pubis, posterior vertebral ribs
M. rectus abdominis	*Posteriormost gastralial row	Distal end of pubis
Pelvic muscles		
M. ambiens	Proximal end of pubis (reduced preacetabular tubercle)	Preacetabular tubercle
M. ischiopubis	Anterior margin of epipubic cartilage	(absent)
M. ischiotruncus	M. rectus abdominis, M. obliquus externus, epipubic cartilage	(absent)
M. puboischiofemoralis externus 1 (= M. obturatorius lateralis)	Anterodorsal pubic apron	Obturator foramen, anterior margin
M. puboischiofemoralis externus 2 (= M. obturatorius medialis)	Posteroventral pubic apron	Puboischiadic membrane, medial surface
Tail muscles		
M. truncocaudalis	M. obliquus externus, M. rectus abdominis	(absent)
M. pubocaudalis externus	(absent)	Posterior margin of distal end of pubis, proximal and adjacent to M. pubocaudalis internus
M. pubocaudalis internus	(absent)	Posterior margin of distal end of pubis

Ligaments, membranes, and other		
Iliopubic ligament	Proximal pubis (reduced preacetabular tubercle)	Preacetabular tubercle
Puboischiadic ligament	Proximal pubis (reduced preacetabular tubercle)	Obturator tuberosity
Puboischiadic membrane	Medial, posterior margin of pubis	Ridge along posterior pubic shaft margin
Pubogastralial cartilage	Anterior margin of pubis (epipubic cartilage) via ligamentous sheet	(absent)
Pubogastralial ligament	Anterolateral surface of pubis, midshaft	(absent)

Chapter 6. Conclusion

Reconstruction of maniraptoran pelvic musculature reveals another perspective on the evolutionary patterns of locomotory adaptations in theropod dinosaurs. *Falcarius* has locomotory musculature largely expected and consistent with previous hypotheses that suggests a sharp reduction in caudofemoral musculature. Caenagnathids have hind limb extensor musculature seemingly less adapted for cursoriality than previously thought, increased reliance on hip flexion and knee control, and other morphological aspects that are reasonably consistent with adaptations of extant wading birds. In contrast, muscle reconstruction corroborates high cursoriality in troodontids, but the conditions in more basal members indicate that this adaptation was gained secondarily and primarily driven by intrinsic pelvic muscles. Muscle scars suggest that caenagnathids and troodontids both had a laterally displaced M. puboischiofemoralis externus 2, which does not fit in the current scheme of archosaur muscle evolution (Hutchinson 2002). The microraptorine lateral pubic tubercle is herein identified as an attachment site for the pubogastralial ligament and considered homologous with other osteological correlates of the same structure across Archosauria. The presence of the lateral pubic tubercle, hypertrophied into a wing-like process in *Hesperonychus*, is likely a functional consequence based on its relative proximodistal position to the M. puboischiofemoralis externus 1 on the anterior surface of the pubic apron. Returning to the main research question of this thesis, do signals from muscle reconstruction match inferences about locomotory adaptations based on skeletal data?

Congruence between skeletal and myological inferences are variable, which emphasizes the diversity and complexity of morphological experimentation in maniraptoran theropods. Locomotory musculature in *Falcarius* essentially gives the same signal as that from the skeleton. Adaptations in relative limb proportions (Zanno 2010a) and limited area for hind limb extensors

both indicate reduced running ability. This intermediate condition between "typical" maniraptorans and derived therizinosaurians is perhaps unsurprising. However, it is congruent with other evolutionary changes further developed in therizinosaurids including secondary enlargement of the first toe to become functionally tetradactyl, expansion of the preacetabular portion of the ilium concurrent with postacetabular reduction, and changes in leg proportions resulting in a femur longer than tibia and foreshortened metatarsus (Barsbold and Perle 1980, Xu et al. 1999a, Li et al. 2008a, Clark and Xu 2009, Zanno et al. 2009, Zanno 2010a, Pu et al. 2013, Yao et al. 2019). Reduction of the brevis fossa also signals reduction in caudofemoral musculature, which shows a sharp decrease compared to closely related, more plesiomorphic theropods. It additionally indicates partial caudal decoupling that is herein interpreted as a somewhat punctuated step preceding the evolution of birds. Although this does not radically change the current model of gradual, stepwise acquisition of avian features in theropods (Hutchinson and Allen 2009, Allen et al. 2013), it does suggest that this pattern was not a completely steady trend. It also offers some ideas for functional tail use, such as display, despite a probable lack of pennaceous feathers or a tail feather fan (Xu et al. 1999a, 2010b, Foth et al. 2014). Furthermore, reduction in cursoriality may provide circumstantial support for heightened sociality in *Falcarius* combined with a lengthened cochlea and preservation of paucispecific bonebeds (Kirkland et al. 2005, Walsh et al. 2009, Zanno 2010a, Smith et al. 2011, 2018). This trend may have also increased through evolutionary time in Therizinosauria.

In Caenagnathidae, locomotory inferences from pelvic muscle reconstruction conflict with those gained from skeletal data. Whereas limb proportions and metatarsus anatomy are indicative of a strong cursor (Holtz 1994, Carrano 1999, Snively et al. 2004), the reduced postacetabulum and accompanying reduction in leg extensors argues that cursoriality was

reduced. However, diminution of caudal musculature simultaneously corroborates the gradual decoupling of tail and hip muscles (Gatesy 1990, Gatesy and Dial 1996) as it indicates markedly less interaction between these two locomotor modules. In addition, the enlarged preacetabulum and associated increase in hip flexors and knee muscles may support the proposition that caenagnathids were adapted to a wading lifestyle. This interpretation is further supported by pedal morphology (Sternberg 1932, Currie and Russell 1988, Varricchio 2001). These points of confusion are understandable because of similarity in hind limb proportions to highly cursorial bipeds, and the effect on both femoral orientation and lifestyle in birds (Gatesy 1991, Barbosa and Moreno 1999a, 1999b, Zeffer et al. 2003). Aside from cursoriality and caudal decoupling, caenagnathids also have a unique origin for the M. puboischiofemoralis externus 2 among archosaurs. Caenagnathid pelvic myology corroborates some hypotheses regarding theropod locomotion, but contradicts others at the same time.

Inferences from troodontid pelvic musculature are also variable in agreement with skeletal data. Locomotory muscle reconstruction supports the interpretation of derived troodontids as highly cursorial, which is reflected in metatarsus anatomy (Holtz 1994, Snively et al. 2004) and limb proportions (Russell 1969, Wilson and Currie 1985, Carrano 1999, Persons and Currie 2016). However, this was gained secondarily within Troodontidae as more basal members lack the muscular setup typical of a strong cursor, including reduced tail muscles. Furthermore, extensor musculature enabling speedy movement in derived forms are dominated by those intrinsic to the pelvis, not the tail. Although caudal musculature seems to have been moderately enlarged, it is not to the same degree as in more basal, highly cursorial theropods. This not only harmonizes with the paradigm of caudal decoupling during theropod evolution (Gatesy 1990, Gatesy and Dial 1996), but also supports the growing body of evidence behind a

gradual transition from hip- to knee-driven locomotion and posture (Allen et al. 2013, Bishop et al. 2018a). One major twist revealed by troodontid pelvic myology is the origin of M. puboischiofemoralis externus 2. Similar to the condition in Caenagnathidae, the origin is laterally displaced and covers the posterior surfaces of the pubic shafts. But, unlike caenagnathids, the origin is also present on the posterior surface of the pubic apron. Although these two groups are superficially similar in a laterally shifted origin of M. puboischiofemoralis externus 2, the state in troodontids is also unique among archosaurs. Inferences from troodontid pelvic myology fall in line with many existing studies, but also demonstrate some inconsistency and new information.

Assessment of the microraptorine lateral pubic tubercle indicates that it is likely homologous with other archosaurian osteological correlates for pubogastralial ligaments. This study does not fit as cleanly in the framework of pelvic musculature evolution as the other studies but is inherently linked to muscles of the hip. The relative position of the pubic apron and path of the M. puboischiofemoralis externus 1 may indicate why the presence of lateral pubic tubercles is limited to Microraptorinae. This hypothesis can henceforth be tested in observation of described specimens and those yet to be discovered. In turn, it allows for a more fruitful discussion on the palaeobiological implications of the lateral pubic tubercle, ventilation, and function of gastralia in theropods. One odd example is *Archaeopteryx*, a taxon that curiously lacks an osteological correlate for the pubogastralial ligament, but is clearly preserved with a gastral basket in some specimens (Rauhut et al. 2018). Regardless, the M. puboischiofemoralis externus 1 would have wrapped laterally around the pubic shaft based on its condition in extant archosaurs and inferred evolutionary history (Hutchinson 2001a, 2002). In microraptorines, this may have required an anatomical modification, which is exaggerated in *Hesperonychus* into an anteriorly convex, wing-like pulley (Longrich and Currie 2009). The morphology of the homolog

for the lateral pubic tubercle is largely conserved across non-paravian theropods but appears variable in Paraves before being lost entirely in birds. Although this does not exactly match the previously reported gradual pattern of evolutionary changes, small stepwise changes do occur throughout Theropoda and culminate in rapid change near the dinosaur-bird transition. Cuirassal breathing remained an important biological function for theropods well into the evolution of early birds and may have only been lost with the evolution of a keeled sternum.

Non-maniraptoran theropods are relatively conservative in both skeletal and myological pelvic morphology, but non-avian maniraptorans show notable changes in both of these respects (Fig. 6.1). In a general sense, this falls in line with previous results showing an increased rate of morphological variation in maniraptorans (Allen et al. 2013). However, results from reconstruction of pelvic musculature in *Falcarius* may conservatively move this estimate back to the base of Maniraptora, rather than sometime within the clade. Despite this, general pelvic morphology and muscular arrangement remains grossly similar until the dinosaur-bird transition, which is accompanied by a surge in evolutionary changes (Fig. 6.1). This is also consistent with previous research that identified a burst in anatomical evolutionary rates around the dinosaur-bird transition and suggests that the evolution of the avian bauplan was a gradual, stepwise process (Hutchinson and Allen 2009, Dececchi and Larsson 2013, Brusatte et al. 2014). Although this pattern is exemplified by more basal members of each taxon, examination of pelvic musculature here underscores the acquisition of both divergent and convergent features after branching away from the stem. Pelvic muscle reconstruction provides another viewpoint on locomotory adaptations not possible by strictly relying on skeletal data (Fig. 6.2). Skeletal anatomy is not always congruent with myology, and thus cannot necessarily characterize the nature of a taxon on its own. In this way, soft tissue inferences provide a “check” on purely

skeletal data, which may support or refute interpretations based on the latter. Additionally, accounting for soft tissues may reveal unforeseen adaptations, conditions, or aspects of evolutionary histories. Locomotory muscles allow inference on the capacity for cursoriality, which itself is an adaptation evolved convergently in some maniraptorans. Similarly, caudal decoupling follows a relatively stable trajectory preceding the evolution of birds and is tracked by caudal musculature originating on the pelvis. However, troodontids appear to secondarily enlarge these muscles, but not to the same degree as their ancestors. The pelvis, as a junction between the abdomen, tail, and hind limb, also reveals information about adjacent modules of the body. In the case of microraptorine dromaeosaurids, the pelvis has clues about the evolution of pubogastralial tissues and its interplay with pelvic musculature. These results corroborate the extensive variability and homoplasy in the evolution of locomotory adaptations in dinosaurs (Carrano 2000), and accentuate the rich evolutionary history of maniraptoran theropods.

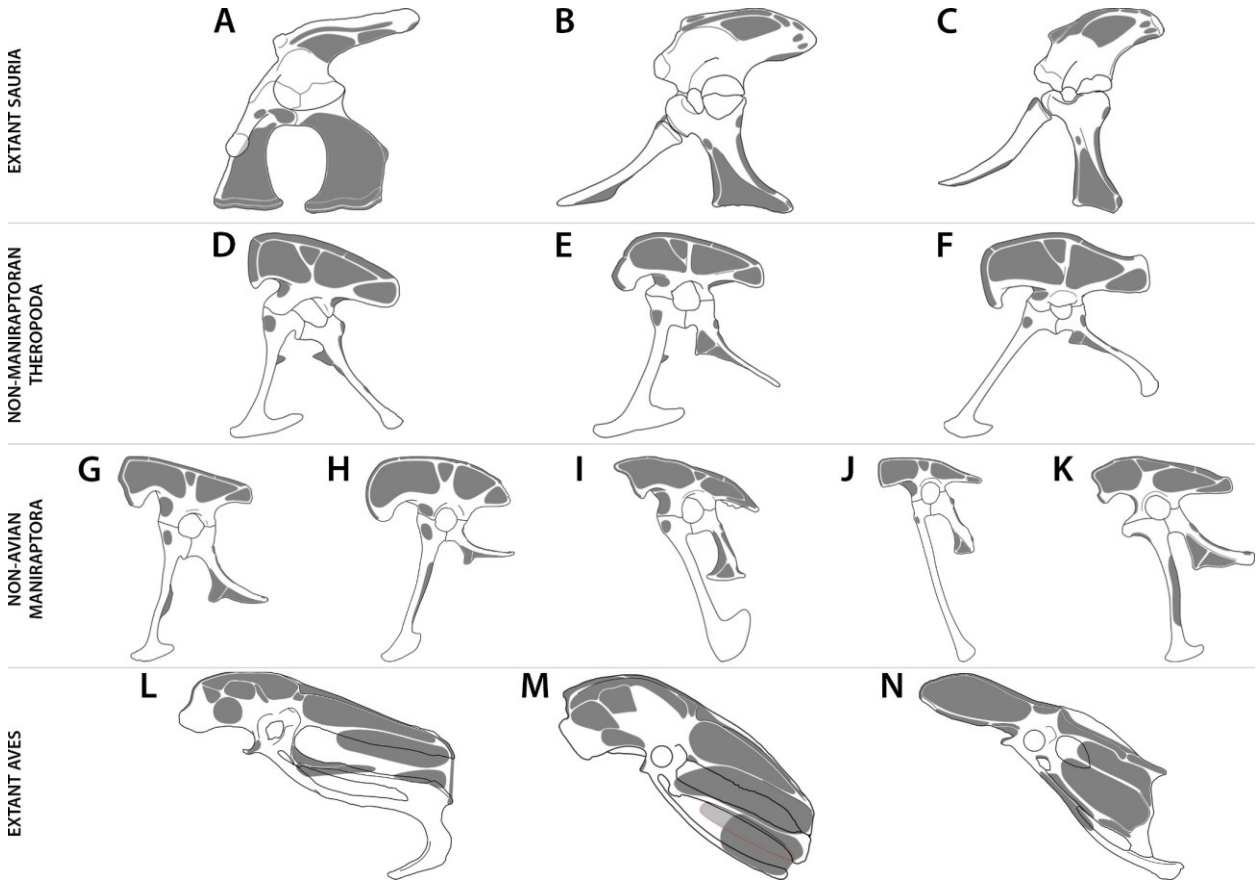

Figure 6.1. Saurian hips and musculature. Pelvis in left lateral view of *Varanus* (A; ROM R7565), *Alligator* (B; ROM R343), *Caiman* (C; RM 5242), Allosauridae (D; CMN 38454), Tyrannosauridae (E; CMN 11315, UALVP 52981), Ornithomimidae (F; CMN 8897, TMP 1981.019.0299), *Falcarius* (G; CEUM 74717, CEUM 77189, UMNH VP 14540), Caenagnathidae (H; TMP 1981.020.0001, UALVP 55638, UALVP 59791), Dromaeosauridae (I; BYUVP 20692, MOR 660, UALVP 55700), Early Cretaceous troodontid (J; DLXH 1218, IVPP V12583 IVPP V12615), Late Cretaceous troodontid (K; AMNH FR 6516, UALVP 55804, pubic boot modified from Tsuihiji et al. (2014)), *Struthio* (L; UAMZ 7159), *Dromaius* (M; UAMZ B-FIC2014.260), and *Gallus* (N; RM 8355).

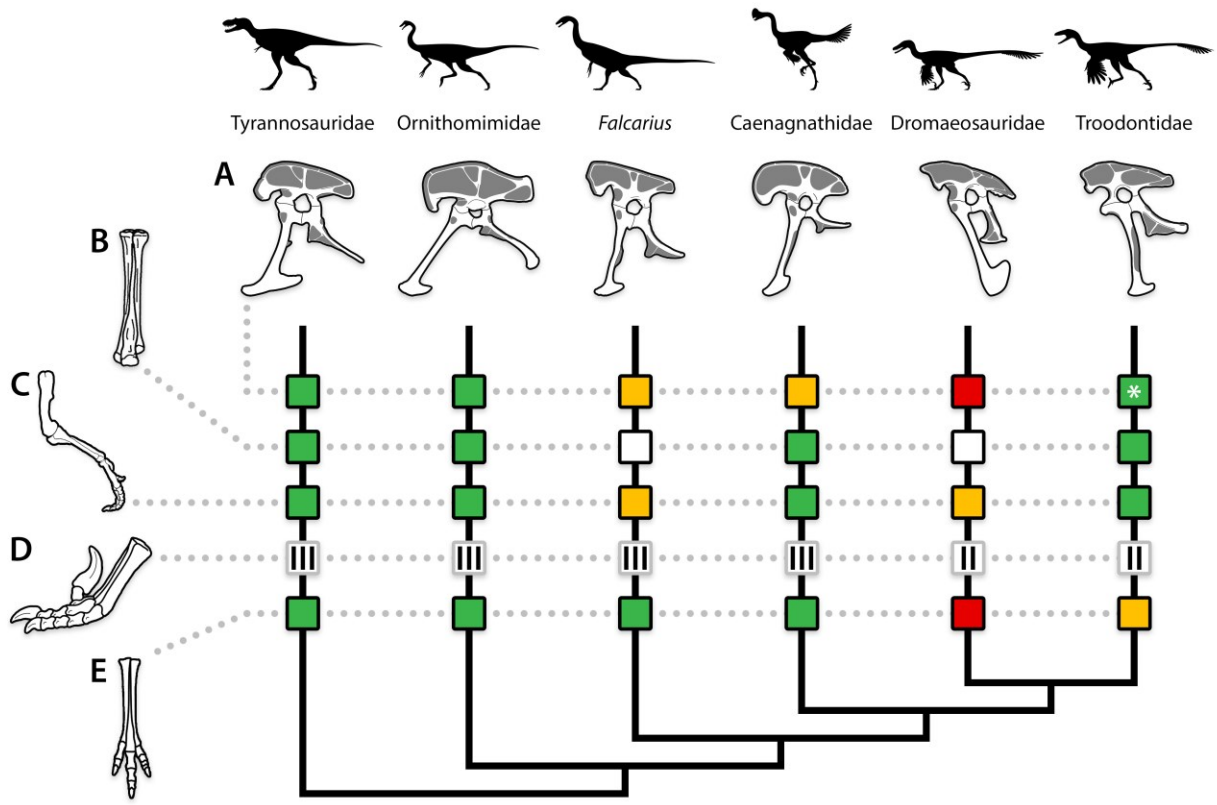

Figure 6.2. Morphological correlates of cursoriality. Non-avian coelurosaurian theropods and representative pelvic muscle reconstructions show comparison between myological data (A) and osteological data (B–E), which are not necessarily congruent with one another. Tyrannosauridae and Ornithomimidae are outgroups for Maniraptora. Features mapped onto simplified phylogeny with topology based on Hendrickx et al. (2015) include hind limb extensor musculature (A), arctometatarsus (B), hind limb element proportions (C), number of functional pedal digits (D, tallied in roman numerals), and foot symmetry (E). Green = strong/present, amber = moderate/partial, red = weak/poor, white = absent. Note that the asterisk (*) highlights Troodontidae as having convergently evolved high cursoriality primarily by means of intrinsic pelvic muscles rather than caudal muscles.

References

Alexander, D.E., Gong, E., Martin, L.D., Burnham, D.A., and Falk, A.R. 2010. Model tests of gliding with different hindwing configurations in the four-winged dromaeosaurid *Microraptor gui*. Proceedings of the National Academy of Sciences, **107**: 2972–2976. doi:10.1073/pnas.0911852107.

Alexander, R.M. 1985. The legs of ostriches (*Struthio*) and moas (*Pachyornis*). Acta Biotheoretica, **34**: 165–174.

Allen, V., Bates, K.T., Li, Z., and Hutchinson, J.R. 2013. Linking the evolution of body shape and locomotor biomechanics in bird-line archosaurs. Nature, **497**: 104–107. doi:10.1038/nature12059.

Allen, V., Molnar, J., Parker, W., Pollard, A., Nolan, G., and Hutchinson, J.R. 2015. Comparative architectural properties of limb muscles in Crocodylidae and Alligatoridae and their relevance to divergent use of asymmetrical gaits in extant Crocodylia. Journal of Anatomy, **225**: 569–582. doi:10.1111/joa.12245.

de Bakker, M.A.G., Fowler, D.A., Oude, K. den, Dondorp, E.M., Navas, M.C.G., Horbanczuk, J.O., Sire, J.-Y., Szczerbińska, D., and Richardson, M.K. 2013. Digit loss in archosaur evolution and the interplay between selection and constraints. Nature, **500**: 445–448. doi:10.1038/nature12336.

Bamman, M.M., Newcomer, B.R., Larson-Meyer, D.E., Weinsier, R.L., and Hunter, G.R. 2000. Evaluation of the strength-size relationship in vivo using various muscle size indices. Medicine & Science in Sports & Exercise, **32**: 1307–1313. doi:10.1097/00005768-200007000-00019.

Barbosa, A., and Moreno, E. 1999a. Hindlimb morphology and locomotor performance in waders: an evolutionary approach. Biological Journal of the Linnean Society, **67**: 313–330. doi:10.1111/j.1095-8312.1999.tb01936.x.

Barbosa, A., and Moreno, E. 1999b. Evolution of foraging strategies in shorebirds: an ecomorphological approach. The Auk, **116**: 712–725. doi:10.2307/4089332.

Barrett, P.M. 2005. The diet of ostrich dinosaurs (Theropoda: Ornithomimosauria). Palaeontology, **48**: 347–358. doi:10.1111/j.1475-4983.2005.00448.x.

Barrett, P.M., and Maidment, S.C.R. 2017. The evolution of ornithischian quadrupedality. Journal of Iberian Geology, **43**: 363–377. doi:10.1007/s41513-017-0036-0.

Barrett, P.M., and Rayfield, E.J. 2006. Ecological and evolutionary implications of dinosaur feeding behaviour. Trends in Ecology & Evolution, **21**: 217–224. doi:10.1016/j.tree.2006.01.002.

Barsbold, R. 1979. Opisthopubic pelvis in the carnivorous dinosaurs. Nature, **279**: 792–793.

Barsbold, R., Osmólska, H., Watabe, M., Currie, P.J., and Tsogtbaatar, K. 2000. A new oviraptorosaur (Dinosauria: Theropoda) from Mongolia: The first dinosaur with a pygostyle. Acta Palaeontologica Polonica, **45**: 97–106.

Barsbold, R., and Perle, A. 1980. Segnosauria, a new infraorder of carnivorous dinosaurs. Acta Palaeontologica Polonica, **25**: 187–195.

Bates, K.T., Benson, R.B.J., and Falkingham, P.L. 2012. A computational analysis of locomotor anatomy and body mass evolution in Allosauroidea (Dinosauria: Theropoda). Paleobiology, **38**: 486–507.

Bates, K.T., and Schachner, E.R. 2012. Disparity and convergence in bipedal archosaur locomotion. Journal of The Royal Society Interface, **9**: 1339–1353. doi:10.1098/rsif.2011.0687.

Baumel, J.J., King, A.S., Breazile, J.E., Evans, H.E., and Vanden Berge, J.C. (*Editors*). 1993. Handbook of Avian Anatomy: Nomina Anatomica Avium. *In* Publications of the Nuttall Ornithological Club, 2nd edition. Nuttall Ornithological Club, Cambridge.

Baumel, J.J., Wilson, J.A., and Bergren, D.R. 1990. The ventilatory movements of the avian pelvis and tail: function of the muscles of the tail region of the pigeon (*Columba livia*). Journal of Experimental Biology, **151**: 263–277.

Bellairs, A.D., and Jenkin, C.R. 1960. The skeleton of birds. *In* Biology and Comparative Physiology of Birds. Academic Press, New York, London. pp. 241–300. doi:10.1016/B978-1-4832-3142-6.50012-4.

Bishop, P.J., Hocknull, S.A., Clemente, C.J., Hutchinson, J.R., Farke, A.A., Barrett, R.S., and Lloyd, D.G. 2018a. Cancellous bone and theropod dinosaur locomotion. Part III—Inferring posture and locomotor biomechanics in extinct theropods, and its evolution on the line to birds. PeerJ, **6**: e5777. doi:10.7717/peerj.5777.

Bishop, P.J., Hocknull, S.A., Clemente, C.J., Hutchinson, J.R., Farke, A.A., Beck, B.R., Barrett, R.S., and Lloyd, D.G. 2018b. Cancellous bone and theropod dinosaur locomotion. Part I—an examination of cancellous bone architecture in the hindlimb bones of theropods. PeerJ, **6**: e5778. doi:10.7717/peerj.5778.

Botelho, J.F., Smith-Paredes, D., Soto-Acuña, S., Núñez-León, D., Palma, V., and Vargas, A.O. 2017. Greater growth of proximal metatarsals in bird embryos and the evolution of hallux

position in the grasping foot. Journal of Experimental Zoology Part B: Molecular and Developmental Evolution, **328B**: 106–118. doi:10.1002/jez.b.22697.

Brusatte, S.L. 2017. A Mesozoic aviary. Science, **355**: 792–794. doi:10.1126/science.aal2397.

Brusatte, S.L., Lloyd, G.T., Wang, S.C., and Norell, M.A. 2014. Gradual assembly of avian body plan culminated in rapid rates of evolution across the dinosaur-bird transition. Current Biology, **24**: 2386–2392. doi:10.1016/j.cub.2014.08.034.

Bryant, H.N., and Russell, A.P. 1992. The role of phylogenetic analysis in the inference of unpreserved attributes of extinct taxa. Philosophical Transactions of the Royal Society B: Biological Sciences, **337**: 405–418. doi:10.1098/rstb.1992.0117.

Bryant, H.N., and Seymour, K.L. 1990. Observations and comments on the reliability of muscle reconstruction in fossil vertebrates. Journal of Morphology, **206**: 109–117. doi:10.1002/jmor.1052060111.

Calvo, J.O., Porfiri, J.D., and Kellner, A.W.A. 2004. On a new maniraptoran dinosaur (Theropoda) from the Upper Cretaceous of Neuquén, Patagonia, Argentina. Arquivos do Museu Nacional, Rio de Janeiro, **62**: 549–566.

Carpenter, K. 1998. Evidence of predatory behaviour by carnivorous dinosaurs. Gaia, **15**: 135–144.

Carpenter, K., Miles, C., Ostrom, J.H., and Cloward, K. 2005. Redescription of the small maniraptoran theropods *Ornitholestes* and *Coelurus* from the Upper Jurassic Morrison Formation of Wyoming. *In* The Carnivorous Dinosaurs, 1st edition. *Edited by* K. Carpenter. Indiana University Press. pp. 49–71.

Carrano, M.T. 1998. Locomotion in non-avian dinosaurs: integrating data from hindlimb kinematics, in vivo strains, and bone morphology. Paleobiology, **24**: 450–469. doi:10.1017/S0094837300020108.

Carrano, M.T. 1999. What, if anything, is a cursor? Categories versus continua for determining locomotor habit in mammals and dinosaurs. Journal of Zoology, **247**: 29–42.

Carrano, M.T. 2000. Homoplasy and the evolution of dinosaur locomotion. Paleobiology, **26**: 489–512.

Carrano, M.T., and Biewener, A.A. 1999. Experimental alteration of limb posture in the chicken (*Gallus gallus*) and its bearing on the use of birds as analogs for dinosaur locomotion. Journal of Morphology, **240**: 237–249.

Carrano, M.T., and Hutchinson, J.R. 2002. Pelvic and hindlimb musculature of *Tyrannosaurus rex* (Dinosauria: Theropoda). Journal of Morphology, **253**: 207–228. doi:10.1002/jmor.10018.

Carrier, D.R., and Farmer, C.G. 2000. The evolution of pelvic aspiration in archosaurs. Paleobiology, **26**: 271–293. doi:10.1666/0094-8373(2000)026<0271:TEOPAI>2.0.CO;2.

Chadwick, K.P., Regnault, S., Allen, V., and Hutchinson, J.R. 2014. Three-dimensional anatomy of the ostrich (*Struthio camelus*) knee joint. PeerJ, **2**: e706. doi:10.7717/peerj.706.

Chatterjee, S. 1997. The Rise of Birds. Johns Hopkins Press, Maryland.

Chatterjee, S., and Templin, R.J. 2007. Biplane wing planform and flight performance of the feathered dinosaur *Microraptor gui*. Proceedings of the National Academy of Sciences, **104**: 1576–1580. doi:10.1073/pnas.0609975104.

Claessens, L.P.A.M. 2004. Dinosaur gastralia; origin, morphology, and function. Journal of Vertebrate Paleontology, **24**: 89–106. doi:10.1671/A1116-8.

Claessens, L.P.A.M. 2009. A cineradiographic study of lung ventilation in *Alligator mississippiensis*. Journal of Experimental Zoology Part A: Ecological Genetics and Physiology, **311A**: 563–585. doi:10.1002/jez.530.

Claessens, L.P.A.M., and Vickaryous, M.K. 2012. The evolution, development and skeletal identity of the crocodylian pelvis: revisiting a forgotten scientific debate. Journal of Morphology, **273**: 1185–1198. doi:10.1002/jmor.20059.

Clark, J.M., Norell, M.A., and Barsbold, R. 2001. Two new oviraptorids (Theropoda: Oviraptorosauria), Upper Cretaceous Djadokhta Formation, Ukhaa Tolgod, Mongolia. Journal of Vertebrate Paleontology, **21**: 209–213. doi:10.1671/0272-4634(2001)021[0209:TNOTOU]2.0.CO;2.

Clark, J.M., and Xu, X. 2009. Evolutionary transitions among dinosaurs: examples from the Jurassic of China. Evolution: Education and Outreach, **2**: 236–247. doi:10.1007/s12052-009-0137-0.

Codd, J.R., Manning, P.L., Norell, M.A., and Perry, S.F. 2008. Avian-like breathing mechanics in maniraptoran dinosaurs. Proceedings of the Royal Society B: Biological Sciences, **275**: 157–161. doi:10.1098/rspb.2007.1233.

Coombs, W.P. 1978. Theoretical aspects of cursorial adaptations in dinosaurs. The Quarterly Review of Biology, **53**: 393–418.

van Coppenolle, I., and Aerts, P. 2004. Terrestrial locomotion in the white stork (*Ciconia ciconia*): spatio-temporal gait characteristics. Animal Biology, **54**: 281–292. doi:10.1163/1570756042484683.

Currie, P., Funston, G., and Osmolska, H. 2015. New specimens of the crested theropod dinosaur *Elmisaurus rarus* from Mongolia. Acta Palaeontologica Polonica, **61**: 143–157. doi:10.4202/app.00130.2014.

Currie, P.J. 1998. Possible evidence of gregarious behaviour in tyrannosaurids. Gaia, **15**: 271–277.

Currie, P.J., and Dong, Z.-M. 2001. New information on Cretaceous troodontids (Dinosauria, Theropoda) from the People's Republic of China. Canadian Journal of Earth Sciences, **38**: 1753–1766. doi:10.1139/cjes-38-12-1753.

Currie, P.J., and Eberth, D.A. 2010. On gregarious behavior in *Albertosaurus*. Canadian Journal of Earth Sciences, **47**: 1277–1289. doi:10.1139/E10-072.

Currie, P.J., and Russell, D.A. 1988. Osteology and relationships of *Chirostenotes pergracilis* (Saurischia, Theropoda) from the Judith River (Oldman) Formation of Alberta, Canada. Canadian Journal of Earth Sciences, **25**: 972–986. doi:10.1139/e88-097.

Daley, M.A., Channon, A.J., Nolan, G.S., and Hall, J. 2016. Preferred gait and walk–run transition speeds in ostriches measured using GPS-IMU sensors. The Journal of Experimental Biology, **219**: 3301–3308. doi:10.1242/jeb.142588.

Dececchi, T.A., and Larsson, H.C.E. 2013. Body and limb size dissociation at the origin of birds: uncoupling allometric constraints across a macroevolutionary transition. Evolution, **67**: 2741–2752. doi:10.1111/evo.12150.

Degrange, F.J. 2017. Hind limb morphometry of terror birds (Aves, Cariamiformes, Phorusrhacidae): functional implications for substrate preferences and locomotor lifestyle. Earth and Environmental Science Transactions of the Royal Society of Edinburgh, **106**: 257–276. doi:10.1017/S1755691016000256.

DePalma, R.A., Burnham, D.A., Martin, L.D., Rothschild, B.M., and Larson, P.L. 2013. Physical evidence of predatory behavior in *Tyrannosaurus rex*. Proceedings of the National Academy of Sciences, **110**: 12560–12564. doi:10.1073/pnas.1216534110.

Dick, T.J.M., and Clemente, C.J. 2016. How to build your dragon: scaling of muscle architecture from the world's smallest to the world's largest monitor lizard. Frontiers in Zoology, **13**: 1–17. doi:10.1186/s12983-016-0141-5.

Erickson, G.M., and Olson, K.H. 1996. Bite marks attributable to *Tyrannosaurus rex*: preliminary description and implications. Journal of Vertebrate Paleontology, **16**: 175–178. doi:10.1080/02724634.1996.10011297.

Erickson, G.M., Van Kirk, S.D., Su, J., Levenston, M.E., Caler, W.E., and Carter, D.R. 1996. Bite-force estimation for *Tyrannosaurus rex* from tooth-marked bones. Nature, **382**: 706–708. doi:10.1038/382706a0.

Evangelista, D., Cam, S., Huynh, T., Kwong, A., Mehrabani, H., Tse, K., and Dudley, R. 2014a. Shifts in stability and control effectiveness during evolution of Paraves support aerial maneuvering hypotheses for flight origins. PeerJ, **2**: e632. doi:10.7717/peerj.632.

Evangelista, D., Cardona, G., Guenther-Gleason, E., Huynh, T., Kwong, A., Marks, D., Ray, N., Tisbe, A., Tse, K., and Koehl, M. 2014b. Aerodynamic characteristics of a feathered dinosaur measured using physical models. Effects of form on static stability and control effectiveness. PLOS ONE, **9**: e85203. doi:10.1371/journal.pone.0085203.

Farlow, J.O., Gatesy, S.M., Holtz, T.R., Hutchinson, J.R., and Robinson, J.M. 2000. Theropod locomotion. American Zoologist, **40**: 640–663. doi:10.1093/icb/40.4.640.

Farmer, C.G. 2015a. The evolution of unidirectional pulmonary airflow. Physiology, **30**: 260–272. doi:10.1152/physiol.00056.2014.

Farmer, C.G. 2015b. Similarity of crocodilian and avian lungs indicates unidirectional flow is ancestral for archosaurs. Integrative and Comparative Biology, **55**: 962–971. doi:10.1093/icb/icv078.

Farmer, C.G. 2015c. Unidirectional flow in lizard lungs: a paradigm shift in our understanding of lung evolution in Diapsida. Zoology, **118**: 299–301. doi:10.1016/j.zool.2015.06.001.

FCAT. 1998. Terminologia Anatomica: International Anatomical Terminology. Thieme, Stuttgart, New York.

Fechner, R., and Schwarz-Wings, D. 2013. The muscles of the infrapubic abdominal wall of a 6-month-old *Crocodylus niloticus* (Reptilia: Crocodylia). Anatomia, Histologia, Embryologia, **42**: 175–182. doi:10.1111/ahe.12000.

Fechner, R., Stratmann, M., Gößling, R., and Sverdlova, N. 2013. The functional role of the ischiopubic membrane for the mechanical loading of the pubis in the domestic fowl (*Gallus gallus*). Journal of Anatomy, **222**: 305–312. doi:10.1111/joa.12015.

Fiorillo, A.R., and Adams, T.L. 2012. A therizinosaur track from the Lower Cantwell Formation (Upper Cretaceous) of Denali National Park, Alaska. PALAIOS, **27**: 395–400. doi:10.2110/palo.2011.p11-083r.

Foth, C., Tischlinger, H., and Rauhut, O.W.M. 2014. New specimen of *Archaeopteryx* provides insights into the evolution of pennaceous feathers. Nature, **511**: 79–82. doi:10.1038/nature13467.

Fowler, D.W., Freedman, E.A., Scannella, J.B., and Kambic, R.E. 2011. The Predatory Ecology of Deinonychus and the Origin of Flapping in Birds. PLOS ONE, **6**: e28964. doi:10.1371/journal.pone.0028964.

Fowler, M.E. 1991. Comparative clinical anatomy of ratites. Journal of Zoo and Wildlife Medicine, **22**: 204–227.

Funston, G.F., and Currie, P.J. 2014. A previously undescribed caenagnathid mandible from the late Campanian of Alberta, and insights into the diet of *Chirostenotes pergracilis* (Dinosauria: Oviraptorosauria). Canadian Journal of Earth Sciences, **51**: 156–165. doi:10.1139/cjes-2013-0186.

Funston, G.F., and Currie, P.J. 2016. A new caenagnathid (Dinosauria: Oviraptorosauria) from the Horseshoe Canyon Formation of Alberta, Canada, and a reevaluation of the relationships of Caenagnathidae. Journal of Vertebrate Paleontology, **36**: e1160910. doi:10.1080/02724634.2016.1160910.

Funston, G.F., Currie, P.J., Eberth, D.A., Ryan, M.J., Chinzorig, T., Badamgarav, D., and Longrich, N.R. 2016. The first oviraptorosaur (Dinosauria: Theropoda) bonebed: evidence of gregarious behaviour in a maniraptoran theropod. Scientific Reports, **6**. doi:10.1038/srep35782.

Funston, G.F., Mendonca, S.E., Currie, P.J., and Barsbold, R. 2018. Oviraptorosaur anatomy, diversity and ecology in the Nemegt Basin. Palaeogeography, Palaeoclimatology, Palaeoecology, **494**: 101–120. doi:10.1016/j.palaeo.2017.10.023.

Funston, G.F., Persons, W.S., Bradley, G.J., and Currie, P.J. 2015. New material of the large-bodied caenagnathid *Caenagnathus collinsi* from the Dinosaur Park Formation of Alberta, Canada. Cretaceous Research, **54**: 179–187. doi:10.1016/j.cretres.2014.12.002.

Fuss, F.K. 1996. Tibiofibular junction of the South African ostrich (*Struthio camelus australis*). Journal of Morphology, **227**: 213–226. doi:10.1002/(SICI)1097-4687(199602)227:2<213::AID-JMOR7>3.0.CO;2-9.

Galton, P.M., and Jensen, J.A. 1979. A new large theropod dinosaur from the Upper Jurassic of Colorado. Brigham Young University Geology Studies, **26**: 1–12.

Gangl, D., Weissengruber, G.E., Egerbacher, M., and Forstenpointner, G. 2004. Anatomical description of the muscles of the pelvic limb in the ostrich (*Struthio camelus*). Anatomia, Histologia, Embryologia, **33**: 100–114. doi:10.1111/j.1439-0264.2003.00522.x.

Gatesy, S.M. 1990. Caudefemoral musculature and the evolution of theropod locomotion. Paleobiology, **16**: 170–186.

Gatesy, S.M. 1991. Hind limb scaling in birds and other theropods: implications for terrestrial locomotion. Journal of Morphology, **209**: 83–96. doi:10.1002/jmor.1052090107.

Gatesy, S.M. 1995. Functional evolution of the hindlimb and tail from basal theropods to birds. *In* Functional Morphology in Vertebrate Paleontology. *Edited by* J. Thomason. Cambridge University Press. pp. 219–234.

Gatesy, S.M., and Dial, K.P. 1996. Locomotor modules and the evolution of avian flight. Evolution, **50**: 331–340. doi:10.2307/2410804.

Gatesy, S.M., and Middleton, K.M. 1997. Bipedalism, flight, and the evolution of theropod locomotor diversity. Journal of Vertebrate Paleontology, **17**: 308–329. doi:10.1080/02724634.1997.10010977.

Geist, N.R., and Feduccia, A. 2000. Gravity-defying behaviors: identifying models for protoaves. American Zoologist, **40**: 664–675.

Gheţie, V. 1976. Atlas de Anatomie a Păsărilor Domestice. Editura Academiei Republicii Socialiste Romania, Bucharest.

Gierlinski, G., and Lockley, M. 2013. First report of probable therizinosaur (cf. *Macropodosaurus*) tracks from North America, with notes on the neglected vertebrate

ichnofauna of the Ferron Sandstone (Late Cretaceous) of central Utah. *In* At the Top of the Grand Staircase: The Late Cretaceous of Southern Utah. *Edited by* A.L. Titus and M.A. Loewen. Indiana University Press, Bloomington, Indianapolis. pp. 530–535.

Gilmore, C.W. 1920. Osteology of the carnivorous Dinosauria in the United States National Museum, with special reference to the genera *Antrodemus* (*Allosaurus*) and *Ceratosaurus*. Bulletin of the United States National Museum, **110**: 1–159.

Gong, E.-P., Martin, L.D., Burnham, D.A., Falk, A.R., and Hou, L.-H. 2012. A new species of *Microraptor* from the Jehol Biota of northeastern China. Palaeoworld, **21**: 81–91. doi:10.1016/j.palwor.2012.05.003.

Grillo, O.N., and Azevedo, S.A.K. 2011. Pelvic and hind limb musculature of *Staurikosaurus pricei* (Dinosauria: Saurischia). Anais da Academia Brasileira de Ciências, **83**: 73–98. doi:10.1590/S0001-37652011000100005.

Grossi, B., Iriarte-Díaz, J., Larach, O., Canals, M., and Vásquez, R.A. 2014. Walking like dinosaurs: chickens with artificial tails provide clues about non-avian theropod locomotion. PLOS ONE, **9**: e88458. doi:10.1371/journal.pone.0088458.

Halvorson, D.B. 1972. Differences in naming muscles of the pelvic limb of chicken. Poultry Science, **51**: 727–738. doi:10.3382/ps.0510727.

Han, G., Chiappe, L.M., Ji, S.-A., Habib, M., Turner, A.H., Chinsamy, A., Liu, X., and Han, L. 2014. A new raptorial dinosaur with exceptionally long feathering provides insights into dromaeosaurid flight performance. Nature Communications, **5**: 4382. doi:10.1038/ncomms5382.

Harris, J.D. 2004. Confusing dinosaurs with mammals: tetrapod phylogenetics and anatomical terminology in the world of homology. The Anatomical Record, **281A**: 1240–1246. doi:10.1002/ar.a.20078.

He, T., Wang, X.-L., and Zhou, Z. 2008. New genus and species of caudipterid dinosaur from the Lower Cretaceous Jiufotang Formation of western Liaoning, China. Vertebrata PalAsiatica, **46**: 178–189.

Henderson, D.M., and Snively, E. 2004. *Tyrannosaurus* en pointe: allometry minimized rotational inertia of large carnivorous dinosaurs. Proceedings of the Royal Society B: Biological Sciences, **271**: S57–S60. doi:10.1098/rsbl.2003.0097.

Hendrickx, C., Hartman, S.A., and Mateus, O. 2015. An overview of non-avian theropod discoveries and classification. PalArch's Journal of Vertebrate Palaeontology, **12**: 1–73.

Holtz, T.R. 1994. The arctometatarsalian pes, an unusual structure of the metatarsus of Cretaceous Theropoda (Dinosauria: Saurischia). Journal of Vertebrate Paleontology, **14**: 480–519. doi:10.1080/02724634.1995.10011574.

Hu, D., Hou, L., Zhang, L., and Xu, X. 2009. A pre-*Archaeopteryx* troodontid theropod from China with long feathers on the metatarsus. Nature, **461**: 640–643. doi:10.1038/nature08322.

Hudson, G.E., Lanzillotti, P.J., and Edwards, G.D. 1959. Muscles of the pelvic limb in galliform birds. American Midland Naturalist, **61**: 1–67. doi:10.2307/2422340.

Hutchinson, J.R. 2001a. The evolution of pelvic osteology and soft tissues on the line to extant birds (Neornithes). Zoological Journal of the Linnean Society, **131**: 123–168. doi:10.1006/zjls.2000.0254.

Hutchinson, J.R. 2001b. The evolution of femoral osteology and soft tissues on the line to extant birds (Neornithes). Zoological Journal of the Linnean Society, **131**: 169–197. doi:10.1111/j.1096-3642.2001.tb01314.x.

Hutchinson, J.R. 2002. The evolution of hindlimb tendons and muscles on the line to crown-group birds. Comparative Biochemistry and Physiology Part A, **133**: 1051–1086. doi:10.1016/S1095-6433(02)00158-7.

Hutchinson, J.R. 2004. Biomechanical modeling and sensitivity analysis of bipedal running ability. II. Extinct taxa. Journal of Morphology, **262**: 441–461. doi:10.1002/jmor.10240.

Hutchinson, J.R. 2006. The evolution of locomotion in archosaurs. Comptes Rendus Palevol, **5**: 519–530. doi:10.1016/j.crpv.2005.09.002.

Hutchinson, J.R., and Allen, V. 2009. The evolutionary continuum of limb function from early theropods to birds. Naturwissenschaften, **96**: 423–448. doi:10.1007/s00114-008-0488-3.

Hutchinson, J.R., Anderson, F.C., Blemker, S.S., and Delp, S.L. 2005. Analysis of hindlimb muscle moment arms in *Tyrannosaurus rex* using a three-dimensional musculoskeletal computer model: implications for stance, gait, and speed. Paleobiology, **31**: 676–701. doi:10.1666/04044.1.

Hutchinson, J.R., and Garcia, M. 2002. *Tyrannosaurus* was not a fast runner. Nature, **415**: 1018–1021.

Hutchinson, J.R., and Gatesy, S.M. 2000. Adductors, abductors, and the evolution of archosaur locomotion. Paleobiology, **26**: 734–751. doi:10.1666/0094-8373(2000)026<0734:AAATEO>2.0.CO;2.

Hutchinson, J.R., Miller, C., Fritsch, G., and Hildebrandt, T. 2008. The anatomical foundation for multidisciplinary studies of animal limb function: examples from dinosaur and

elephant limb imaging studies. *In* Anatomical Imaging. *Edited by* H. Endo and R. Frey. Springer Japan, Tokyo. pp. 23–38. doi:10.1007/978-4-431-76933-0_3.

Hutchinson, J.R., Rankin, J.W., Rubenson, J., Rosenbluth, K.H., Siston, R.A., and Delp, S.L. 2015. Musculoskeletal modelling of an ostrich (*Struthio camelus*) pelvic limb: influence of limb orientation on muscular capacity during locomotion. PeerJ, **3**: e1001. doi:10.7717/peerj.1001.

Hwang, S.H., Norell, M.A., Qiang, J., and Keqin, G. 2002. New specimens of *Microraptor zhaoianus* (Theropoda: Dromaeosauridae) from northeastern China. American Museum Novitates, **3381**: 1–44. doi:10.1206/0003-0082(2002)381<0001:NSOMZT>2.0.CO;2.

Ibáñez, B., and Tambussi, C.P. 2012. Foot-propelled aquatic birds: pelvic morphology and locomotor performance. Italian Journal of Zoology, **79**: 356–362. doi:10.1080/11250003.2011.650713.

ICVGAN. 2017. Nomina Anatomica Veterinaria. 6th edition. Editorial Committee, Hanover (Germany), Ghent (Belgium), Columbia, MO (USA), Rio de Janeiro (Brazil).

Jacobson, R.D., and Hollyday, M. 1982. A behavioral and electromyographic study of walking in the chick. Journal of Neurophysiology, **48**: 238–256. doi:10.1152/jn.1982.48.1.238.

Jindrich, D.L., Smith, N.C., Jespers, K., and Wilson, A.M. 2007. Mechanics of cutting maneuvers by ostriches (*Struthio camelus*). Journal of Experimental Biology, **210**: 1378–1390. doi:10.1242/jeb.001545.

Jones, E.J., Bishop, P.A., Woods, A.K., and Green, J.M. 2008. Cross-sectional area and muscular strength: a brief review. Sports Medicine, **38**: 987–994. doi:10.2165/00007256-200838120-00003.

Jones, T.D., Farlow, J.O., Ruben, J.A., Henderson, D.M., and Hillenius, W.J. 2000. Cursoriality in bipedal archosaurs. Nature, **406**: 716–718. doi:10.1038/35021041.

Kirkland, J.I., Zanno, L.E., Sampson, S.D., Clark, J.M., and DeBlieux, D.D. 2005. A primitive therizinosauroid dinosaur from the Early Cretaceous of Utah. Nature, **435**: 84–87. doi:10.1038/nature03468.

Klinkhamer, A.J., Wilhite, D.R., White, M.A., and Wroe, S. 2017. Digital dissection and three-dimensional interactive models of limb musculature in the Australian estuarine crocodile (*Crocodylus porosus*). PLOS ONE, **12**: e0175079. doi:10.1371/journal.pone.0175079.

Kobayashi, Y., Lu, J.-C., Dong, Z.-M., Barsbold, R., Azuma, Y., and Tomida, Y. 1999. Herbivorous diet in an ornithomimid dinosaur. Nature, **402**: 480–481. doi:10.1038/44997.

Lamanna, M.C., Sues, H.-D., Schachner, E.R., and Lyson, T.R. 2014. A new large-bodied oviraptorosaurian theropod dinosaur from the latest Cretaceous of Western North America. PLOS ONE, **9**: e92022. doi:10.1371/journal.pone.0092022.

Lamas, L.P., Main, R.P., and Hutchinson, J.R. 2014. Ontogenetic scaling patterns and functional anatomy of the pelvic limb musculature in emus (*Dromaius novaehollandiae*). PeerJ, **2**: e716. doi:10.7717/peerj.716.

Lambertz, M., and Perry, S.F. 2015. Remarks on the evolution of the avian sternum, dinosaur gastralia, and their functional significance for the respiratory apparatus. Zoologischer Anzeiger, **255**: 80–84. doi:10.1016/j.jcz.2015.02.008.

Langer, M.C. 2003. The pelvic and hind limb anatomy of the stem-sauropodomorph *Saturnalia tupiniquim* (Late Triassic, Brazil). PaleoBios, **23**: 1–30.

Lautenschlager, S. 2013. Cranial myology and bite force performance of *Erlikosaurus andrewsi*: a novel approach for digital muscle reconstructions. Journal of Anatomy, **222**: 260–272. doi:10.1111/joa.12000.

Lautenschlager, S. 2014. Morphological and functional diversity in therizinosaur claws and the implications for theropod claw evolution. Proceedings of the Royal Society B: Biological Sciences, **281**: 20140497. doi:10.1098/rspb.2014.0497.

Lautenschlager, S. 2017. Functional niche partitioning in Therizinosauria provides new insights into the evolution of theropod herbivory. Palaeontology, **60**: 375–387. doi:10.1111/pala.12289.

Li, D., You, H., and Zhang, J. 2008a. A new specimen of *Suzhousaurus megatherioides* (Dinosauria: Therizinosauroidea) from the Early Cretaceous of northwestern China. Canadian Journal of Earth Sciences, **45**: 769–779. doi:10.1139/E08-021.

Li, R., Lockley, M.G., Makovicky, P.J., Matsukawa, M., Norell, M.A., Harris, J.D., and Liu, M. 2008b. Behavioral and faunal implications of Early Cretaceous deinonychosaur trackways from China. Naturwissenschaften, **95**: 185–191. doi:10.1007/s00114-007-0310-7.

Lockley, M.G., and Matsukawa, M. 1999. Some observations on trackway evidence for gregarious behavior among small bipedal dinosaurs. Palaeogeography, Palaeoclimatology, Palaeoecology, **150**: 25–31. doi:10.1016/S0031-0182(99)00005-X.

Longrich, N. 2006. Structure and function of hindlimb feathers in *Archaeopteryx lithographica*. Paleobiology, **32**: 417–431. doi:10.1666/04014.1.

Longrich, N.R., Barnes, K., Clark, S., and Millar, L. 2013. Caenagnathidae from the Upper Campanian Aguja Formation of West Texas, and a Revision of the Caenagnathinae.

Bulletin of the Peabody Museum of Natural History, **54**: 23–49. doi:10.3374/014.054.0102.

Longrich, N.R., and Currie, P.J. 2009. A microraptorine (Dinosauria–Dromaeosauridae) from the Late Cretaceous of North America. Proceedings of the National Academy of Sciences, **106**: 5002–5007. doi:10.1073/pnas.0811664106.

Longrich, N.R., Currie, P.J., and Zhi-Ming, D. 2010. A new oviraptorid (Dinosauria: Theropoda) from the Upper Cretaceous of Bayan Mandahu, Inner Mongolia. Palaeontology, **53**: 945–960. doi:10.1111/j.1475-4983.2010.00968.x.

Lovegrove, B.G., and Mowoe, M.O. 2014. The evolution of micro-cursoriality in mammals. Journal of Experimental Biology, **217**: 1316–1325. doi:10.1242/jeb.095737.

Lü, J. 2002. A new oviraptorosaurid (Theropoda: Oviraptorosauria) from the Late Cretaceous of southern China. Journal of Vertebrate Paleontology, **22**: 871–875. doi:10.1671/0272-4634(2002)022[0871:ANOTOF]2.0.CO;2.

Lü, J., and Brusatte, S.L. 2015. A large, short-armed, winged dromaeosaurid (Dinosauria: Theropoda) from the Early Cretaceous of China and its implications for feather evolution. Scientific Reports, **5**: 1–11. doi:10.1038/srep11775.

Lü, J., Li, G., Kundrát, M., Lee, Y.-N., Sun, Z., Kobayashi, Y., Shen, C., Teng, F., and Liu, H. 2017. High diversity of the Ganzhou Oviraptorid Fauna increased by a new "cassowary-like" crested species. Scientific Reports, **7**: 6393. doi:10.1038/s41598-017-05016-6.

Lü, J., Tomida, Y., Azuma, Y., Dong, Z.-M., and Lee, Y.-N. 2004. New Oviraptorid Dinosaur (Dinosauria: Oviraptorosauria) from the Nemegt Formation of Southwestern Mongolia. Bulletin of the National Science Museum, Tokyo, Series C, **30**: 95–130.

Lü, J., Yi, L., Zhong, H., and Wei, X. 2013. A New Oviraptorosaur (Dinosauria: Oviraptorosauria) from the Late Cretaceous of Southern China and Its Paleoecological Implications. PLOS ONE, **8**: e80557. doi:10.1371/journal.pone.0080557.

Lull, R.S. 1904. Adaptations to aquatic, arboreal, fossorial and cursorial habits in mammals. The American Naturalist, **38**: 1–11. doi:10.1086/278375.

Macaluso, L., and Tschopp, E. 2018. Evolutionary changes in pubic orientation in dinosaurs are more strongly correlated with the ventilation system than with herbivory. Palaeontology, **61**: 703–719. doi:10.1111/pala.12362.

Maidment, S.C.R., and Barrett, P.M. 2011. The locomotor musculature of basal ornithischian dinosaurs. Journal of Vertebrate Paleontology, **31**: 1265–1291. doi:10.1080/02724634.2011.606857.

Maidment, S.C.R., and Barrett, P.M. 2012. Does morphological convergence imply functional similarity? A test using the evolution of quadrupedalism in ornithischian dinosaurs. Proceedings of the Royal Society B: Biological Sciences, **279**: 3765–3771. doi:10.1098/rspb.2012.1040.

Maidment, S.C.R., Bates, K.T., and Barrett, P.M. 2014a. Three-dimensional computational modelling of pelvic locomotor muscle moment arms in *Edmontosaurus* (Dinosauria, Hadrosauridae) and comparisons with other archosaurs. *In* Hadrosaurs. *Edited by* D.A. Eberth and D.C. Evans. Indiana University Press, Bloomington. pp. 433–448.

Maidment, S.C.R., Bates, K.T., Falkingham, P.L., VanBuren, C., Arbour, V., and Barrett, P.M. 2014b. Locomotion in ornithischian dinosaurs: an assessment using three-dimensional computational modelling. Biological Reviews, **89**: 588–617. doi:10.1111/brv.12071.

Maleev, E.A. 1954. A new turtle-like reptile from Mongolia. Priroda, **3**: 106–108.

Mallon, J.C., Bura, J.R., Schumann, D., and Currie, P.J. 2019. A problematic tyrannosaurid (Dinosauria: Theropoda) skeleton and its implications for tyrannosaurid diversity in the Horseshoe Canyon Formation (Upper Cretaceous) of Alberta. The Anatomical Record,: 1–18. doi:10.1002/ar.24199.

Martin, L.D., Zhou, Z., Hou, L., and Feduccia, A. 1998. *Confuciusornis sanctus* compared to *Archaeopteryx lithographica*. Naturwissenschaften, **85**: 286–289. doi:10.1007/s001140050501.

McGowan, C. 1979. The hind limb musculature of the brown kiwi, *Apteryx australis mantelli*. Journal of Morphology, **160**: 33–73. doi:10.1002/jmor.1051600105.

McKitrick, M.C. 1991. Phylogenetic analysis of avian hindlimb musculature. Miscellaneous Publications of the Museum of Zoology, University of Michigan, **179**: 1–85.

Mellett, F.D. 1994. A note on the musculature of the proximal part of the pelvic limb of the ostrich (*Struthio camelus*). Journal of the South African Veterinary Association, **65**: 5–9.

Nicholls, E.L., and Russell, A.P. 1985. Structure and function of the pectoral girdle and forelimb of *Struthiomimus altus* (Theropoda: Ornithomimidae). Palaeontology, **28**: 643–677.

Norell, M.A., Makovicky, P.J., Bever, G.S., Balanoff, A.M., Clark, J.M., Barsbold, R., and Rowe, T. 2009. A review of the Mongolian Cretaceous dinosaur *Saurornithoides* (Troodontidae: Theropoda). American Museum Novitates, **3654**: 1–63. doi:10.1206/648.1.

Norell, M.A., Makovicky, P.J., and Currie, P.J. 2001. The beaks of ostrich dinosaurs. Nature, **412**: 873–874. doi:10.1038/35091136.

Novas, F.E., and Agnolin, F.L. 2004. *Unquillosaurus ceibali* Powell, a giant maniraptoran (Dinosauria, Theropoda) from the Late Cretaceous of Argentina. Revista del Museo Argentino de Ciencias Naturales, **6**: 61–66.

Novas, F.E., Egli, F.B., Agnolin, F.L., Gianechini, F.A., and Cerda, I. 2018. Postcranial osteology of a new specimen of *Buitreraptor gonzalezorum* (Theropoda, Unenlagiidae). Cretaceous Research, **83**: 127–167. doi:10.1016/j.cretres.2017.06.003.

Novas, F.E., and Puerta, P.F. 1997. New evidence concerning avian origins from the Late Cretaceous of Patagonia. Nature, **387**: 390–392.

O'Connor, J.K., Xiao-Ting, Z., Xiao-Li, W., Xiao-Mei, Z., and Zhong-He, Z. 2015. The gastral basket in basal birds and their close relatives: size and possible function. Vertebrata PalAsiatica, **53**: 133–152.

O'Connor, P.M., and Claessens, L.P.A.M. 2005. Basic avian pulmonary design and flow-through ventilation in non-avian theropod dinosaurs. Nature, **436**: 253–256. doi:10.1038/nature03716.

Osborn, H.F. 1903. *Ornitholestes hermanni*, a new comsognathid dinosaur from the Upper Jurassic. Bulletin of the American Museum of Natural History, **19**: 459–464.

Osmólska, H. 1976. New light on the skull anatomy and systematic position of *Oviraptor*. Nature, **262**: 683–684.

Osmólska, H., Currie, P.J., and Barsbold, R. 2004. Oviraptorosauria. *In* The Dinosauria. *Edited by* D. Weishampel. University of California Press. pp. 165–183. doi:10.1525/california/9780520242098.003.0010.

Otero, A., Gallina, P.A., and Herrera, Y. 2010. Pelvic musculature and function of *Caiman latirostris*. Herpetological Journal, **20**: 173–184.

Palmer, C. 2014. The aerodynamics of gliding flight and its application to the arboreal flight of the Chinese feathered dinosaur *Microraptor*. Biological Journal of the Linnean Society, **113**: 828–835. doi:10.1111/bij.12328.

Patak, A.E., and Baldwin, J. 1998. Pelvic limb musculature in the emu *Dromaius novaehollandiae* (Aves: Struthioniformes: Dromaiidae): adaptations to high-speed running. Journal of Morphology, **238**: 23–37. doi:10.1002/(SICI)1097-4687(199810)238:1<23::AID-JMOR2>3.0.CO;2-O.

Patterson, C. 1982. Morphological characters and homology. *In* Problems of Phylogenetic Reconstruction, Systematics Association Special Volume 21. *Edited by* K.A. Joysey and A.E. Friday. Academic Press, London. pp. 21–74.

Paul, G.S. 1984. The segnosaurian dinosaurs: relics of the prosauropod–ornithischian transition? Journal of Vertebrate Paleontology, **4**: 507–515. doi:10.1080/02724634.1984.10012026.

Paul, G.S. 1998. Limb design, function and running performance in ostrich-mimics and tyrannosaurs. Gaia, **15**: 257–270.

Paxton, H., Anthony, N.B., Corr, S.A., and Hutchinson, J.R. 2010. The effects of selective breeding on the architectural properties of the pelvic limb in broiler chickens: a comparative study across modern and ancestral populations. Journal of Anatomy, **217**: 153–166. doi:10.1111/j.1469-7580.2010.01251.x.

Pei, R., Li, Q., Meng, Q., Gao, K.-Q., and Norell, M.A. 2014. A new specimen of *Microraptor* (Theropoda: Dromaeosauridae) from the Lower Cretaceous of Western Liaoning, China. American Museum Novitates, **3821**: 1–28. doi:10.1206/3821.1.

Pei, R., Norell, M.A., Barta, D.E., Bever, G.S., Pittman, M., and Xu, X. 2017. Osteology of a new Late Cretaceous troodontid specimen from Ukhaa Tolgod, Ömnögovi Aimag, Mongolia. American Museum Novitates, **3889**: 1–47. doi:10.1206/3889.1.

Perle, A. 1985. Comparative myology of the pelvic-femoral region in bipedal dinosaurs. Paleontological Journal, **19**: 105–109.

Persons, W.S., and Currie, P.J. 2011. The tail of *Tyrannosaurus*: reassessing the size and locomotive importance of the *M. caudofemoralis* in non-avian theropods. The Anatomical Record, **294**: 119–131. doi:10.1002/ar.21290.

Persons, W.S., and Currie, P.J. 2012. Dragon tails: convergent caudal morphology in winged archosaurs. Acta Geologica Sinica, **86**: 1402–1412.

Persons, W.S., and Currie, P.J. 2014. Duckbills on the run: the cursorial abilities of hadrosaurs and implications for tyrannosaur-avoidance strategies. *In* Hadrosaurs. *Edited by* D.A. Eberth and D.C. Evans. Indiana University Press, Bloomington. pp. 449–458.

Persons, W.S., and Currie, P.J. 2016. An approach to scoring cursorial limb proportions in carnivorous dinosaurs and an attempt to account for allometry. Scientific Reports, **6**: 19828. doi:10.1038/srep19828.

Persons, W.S., and Currie, P.J. 2017. The functional origin of dinosaur bipedalism: cumulative evidence from bipedally inclined reptiles and disinclined mammals. Journal of Theoretical Biology, **420**: 1–7. doi:10.1016/j.jtbi.2017.02.032.

Persons, W.S., and Currie, P.J. 2019. Feather evolution exemplifies sexually selected bridges across the adaptive landscape. Evolution, **73**: 1686–1694. doi:10.1111/evo.13795.

Persons, W.S., Currie, P.J., and Erickson, G.M. 2019. An older and exceptionally large adult specimen of *Tyrannosaurus rex*. The Anatomical Record, **(in press)**. doi:10.1002/ar.24118.

Persons, W.S., Currie, P.J., and Norell, M.A. 2014. Oviraptorosaur tail forms and functions. Acta Palaeontologica Polonica, **59**: 553–567. doi:10.4202/app.2012.0093.

Picasso, M.B.J. 2010. The hindlimb muscles of *Rhea americana* (Aves, Palaeognathae, Rheidae). Anatomia, Histologia, Embryologia, **39**: 462–472. doi:10.1111/j.1439-0264.2010.01017.x.

de Pinna, M.C.C. 1991. Concepts and tests of homology in the cladistic paradigm. Cladistics, **7**: 367–394. doi:10.1111/j.1096-0031.1991.tb00045.x.

Pittman, M., Gatesy, S.M., Upchurch, P., Goswami, A., and Hutchinson, J.R. 2013. Shake a Tail Feather: The Evolution of the Theropod Tail into a Stiff Aerodynamic Surface. PLOS ONE, **8**: e63115. doi:10.1371/journal.pone.0063115.

Poust, A.W. 2014, May. Description and ontogenetic assessment of a new Jehol microraptorine. M.Sc. Thesis, Montana State University, Bozeman, Montana.

Proctor, N.S., and Lynch, P.J. 1993. The musculature. *In* Manual of Ornithology: Avian Structure & Function. Yale University Press, New Haven. pp. 148–173.

Pu, H., Kobayashi, Y., Lü, J., Xu, L., Wu, Y., Chang, H., Zhang, J., and Jia, S. 2013. An unusual basal therizinosaur dinosaur with an ornithischian dental arrangement from northeastern China. PLOS ONE, **8**: e63423. doi:10.1371/journal.pone.0063423.

Qiang, J., Currie, P.J., Norell, M.A., and Shu-An, J. 1998. Two feathered dinosaurs from northeastern China. Nature, **393**: 753–761. doi:10.1038/31635.

Rankin, J.W., Rubenson, J., and Hutchinson, J.R. 2016. Inferring muscle functional roles of the ostrich pelvic limb during walking and running using computer optimization. Journal of The Royal Society Interface, **13**: 20160035. doi:10.1098/rsif.2016.0035.

Rasskin-Gutman, D., and Buscalioni, A.D. 2001. Theoretical morphology of the archosaur (Reptilia: Diapsida) pelvic girdle. Paleobiology, **27**: 59–78. doi:10.1666/0094-8373(2001)027<0059:TMOTAR>2.0.CO;2.

Rauhut, O.W.M., Foth, C., and Tischlinger, H. 2018. The oldest *Archaeopteryx* (Theropoda: Avialiae): a new specimen from the Kimmeridgian/Tithonian boundary of Schamhaupten, Bavaria. PeerJ, **6**: e4191. doi:10.7717/peerj.4191.

van der Reest, A.J., and Currie, P.J. 2017. Troodontids (Theropoda) from the Dinosaur Park Formation, Alberta, with a description of a unique new taxon: implications for deinonychosaur diversity in North America. Canadian Journal of Earth Sciences, **54**: 919–935. doi:10.1139/cjes-2017-0031.

Rieppel, O. 1994. Homology, topology, and typology: the history of modern debates. *In* Homology: The Hierarchical Basis of Comparative Biology. *Edited by* B.K. Hall. Academic Press, San Diego. pp. 63–100.

Roach, B.T., and Brinkman, D.L. 2007. A reevaluation of cooperative pack hunting and gregariousness in *Deinonychus antirrhopus* and other nonavian theropod dinosaurs. Bulletin of the Peabody Museum of Natural History, **48**: 103–138. doi:10.3374/0079-032X(2007)48[103:AROCPH]2.0.CO;2.

Romer, A.S. 1923a. Crocodilian pelvic muscles and their avian and reptilian homologues. Bulletin of the American Museum of Natural History, **48**: 533–552.

Romer, A.S. 1923b. The pelvic musculature of saurischian dinosaurs. Bulletin of the American Museum of Natural History, **48**: 605–617.

Romer, A.S. 1923c. The ilium in dinosaurs and birds. Bulletin of the American Museum of Natural History, **48**: 141–145.

Romer, A.S. 1927. The pelvic musculature of ornithischian dinosaurs. Acta Zoologica, **8**: 225–275. doi:10.1111/j.1463-6395.1927.tb00653.x.

Romer, A.S. 1962. Muscular System. *In* The Vertebrate Body, 3rd edition. W. B. Saunders & Co., Philadelphia, London. pp. 249–287.

Rothschild, B.M., Wilhite, D.R., McLeod, D.S., and Ting, H. 2015. Evidence from surface microscopy for recognition of fleshy and tendinous muscle insertion in extant vertebrate femora: implications for muscle reconstruction in fossils. Historical Biology, **28**: 842–848. doi:10.1080/08912963.2015.1049163.

Rowe, T. 1986. Homology and evolution of the deep dorsal thigh musculature in birds and other Reptilia. Journal of Morphology, **189**: 327–346. doi:10.1002/jmor.1051890310.

Ruben, J.A., Jones, T.D., Geist, N.R., and Hillenius, W.J. 1997. Lung structure and ventilation in theropod dinosaurs and early birds. Science, **278**: 1267–1270. doi:10.1126/science.278.5341.1267.

Rubenson, J., Lloyd, D.G., Heliams, D.B., Besier, T.F., and Fournier, P.A. 2011. Adaptations for economical bipedal running: the effect of limb structure on three-dimensional joint mechanics. Journal of The Royal Society Interface, **8**: 740–755. doi:10.1098/rsif.2010.0466.

Russell, A.P., and Bauer, A.M. 2008. The appendicular locomotor apparatus of *Sphenodon* and normal-limbed squamates. *In* Morphology I. The skull and appendicular locomotor

apparatus of Lepidosauria, 21. *Edited by* C. Gans, A.S. Gaunt, and K. Adler. Society for the Study of Amphibians and Reptiles, Ithaca, New York. pp. 1–784.

Russell, D.A. 1969. A new specimen of *Stenonychosaurus* from the Oldman Formation (Cretaceous) of Alberta. Canadian Journal of Earth Sciences, **6**: 595–612. doi:10.1139/e69-059.

Russell, D.A. 1972. Ostrich dinosaurs from the Late Cretaceous of western Canada. Canadian Journal of Earth Sciences, **9**: 375–402. doi:10.1139/e72-031.

Russell, D.A., and Dong, Z.-M. 1993. A nearly complete skeleton of a new troodontid dinosaur from the Early Cretaceous of the Ordos Basin, Inner Mongolia, People's Republic of China. Canadian Journal of Earth Sciences, **30**: 2163–2173. doi:10.1139/e93-187.

Ryan, M.J., Currie, P.J., Gardner, J.D., Vickaryous, M.K., and Lavigne, J.M. 1998. Baby hadrosaurid material associated with an unusually high abundance of *Troodon* teeth from the Horseshoe Canyon Formation, Upper Cretaceous, Alberta, Canada. Gaia, **15**: 123–133. doi:10.7939/R32B8VS51.

Schaller, N.U., Herkner, B., Villa, R., and Aerts, P. 2009. The intertarsal joint of the ostrich (*Struthio camelus*): anatomical examination and function of passive structures in locomotion. Journal of Anatomy, **214**: 830–847. doi:10.1111/j.1469-7580.2009.01083.x.

Segre, P.S., and Banet, A.I. 2018. The origin of avian flight: finding common ground. Biological Journal of the Linnean Society, **125**: 452–454. doi:10.1093/biolinnean/bly116.

Senter, P., Barsbold, R., Britt, B.B., and Burnham, D.A. 2004. Systematics and evolution of Dromaeosauridae (Dinosauria, Theropoda). Bulletin of Gunma Museum of Natural History, **8**: 1–20.

Shufeldt, R.W. 1890. The myology of the raven (*Corvus corax sinuatus*): a guide to the study of the muscular system in birds. Macmillan and Company, London.

Simões, T.R., Caldwell, M.W., Palci, A., and Nydam, R.L. 2017. Giant taxon-character matrices: quality of character constructions remains critical regardless of size. Cladistics, **33**: 198–219. doi:10.1111/cla.12163.

Smith, D.K., Sanders, R.K., and Wolfe, D.G. 2018. A re-evaluation of the basicranial soft tissues and pneumaticity of the therizinosaurian *Nothronychus mckinleyi* (Theropoda; Maniraptora). PLOS ONE, **13**: e0198155. doi:10.1371/journal.pone.0198155.

Smith, D.K., Zanno, L.E., Sanders, R.K., Deblieux, D.D., and Kirkland, J.I. 2011. New information on the braincase of the North American therizinosaurian (Theropoda, Maniraptora) *Falcarius utahensis*. Journal of Vertebrate Paleontology, **31**: 387–404. doi:10.1080/02724634.2011.549442.

Smith, N.C., Payne, R.C., Jespers, K.J., and Wilson, A.M. 2007. Muscle moment arms of pelvic limb muscles of the ostrich (*Struthio camelus*). Journal of Anatomy, **211**: 313–324. doi:10.1111/j.1469-7580.2007.00762.x.

Smith, N.C., Wilson, A.M., Jespers, K.J., and Payne, R.C. 2006. Muscle architecture and functional anatomy of the pelvic limb of the ostrich (*Struthio camelus*). Journal of Anatomy, **209**: 765–779. doi:10.1111/j.1469-7580.2006.00658.x.

Snively, E., and Russell, A. 2001. The tyrannosaurid metatarsus: bone strain and inferred ligament function. Senckenbergiana lethaea, **81**: 73–80. doi:10.1007/BF03043771.

Snively, E., and Russell, A.P. 2003. Kinematic model of tyrannosaurid (Dinosauria: Theropoda) arctometatarsus function. Journal of Morphology, **255**: 215–227. doi:10.1002/jmor.10059.

Snively, E., Russell, A.P., and Powell, G.L. 2004. Evolutionary morphology of the coelurosaurian arctometatarsus: descriptive, morphometric and phylogenetic approaches. Zoological Journal of the Linnean Society, **142**: 525–553. doi:10.1111/j.1096-3642.2004.00137.x.

Sternberg, C.M. 1932. Two new theropod dinosaurs from the Belly River Formation of Alberta. The Canadian Field Naturalist, **46**: 99–105.

Sternberg, C.M. 1933. A new *Ornithomimus* with complete abdominal cuirass. The Canadian Field Naturalist, **47**: 79–83.

Stoessel, A., Kilbourne, B.M., and Fischer, M.S. 2013. Morphological integration versus ecological plasticity in the avian pelvic limb skeleton. Journal of Morphology, **274**: 483–495. doi:10.1002/jmor.20109.

Sues, H.-D. 1997. On *Chirostenotes*, a Late Cretaceous oviraptorosaur (Dinosauria: Theropoda) from western North America. Journal of Vertebrate Paleontology, **17**: 698–716. doi:10.1080/02724634.1997.10011018.

Sullivan, C., Xu, X., and O'Connor, J.K. 2017. Complexities and novelties in the early evolution of avian flight, as seen in the Mesozoic Yanliao and Jehol Biotas of Northeast China. Palaeoworld, **26**: 212–229. doi:10.1016/j.palwor.2016.12.001.

Sullivan, R.M., Jasinski, S.E., and van Tomme, M.P.A. 2011. A new caenagnathid *Ojoraptorsaurus boerei*, n. gen., n. sp. (Dinosauria, Oviraptorosauria), from the Upper Cretaceous Ojo Alamo Formation (Naashoibito Member), San Juan Basin, New Mexico. Fossil Record 3, **New Mexico Museum of Natural History and Science Bulletin 53**: 418–428.

Tarsitano, S. 1983. Stance and gait in theropod dinosaurs. Acta Palaeontologica Polonica, **28**: 251–264.

Torices, A., Wilkinson, R., Arbour, V.M., Ruiz-Omeñaca, J.I., and Currie, P.J. 2018. Puncture-and-pull biomechanics in the teeth of predatory coelurosaurian dinosaurs. Current Biology, **28**: 1467–1474. doi:10.1016/j.cub.2018.03.042.

Tsai, H.P., Middleton, K.M., Hutchinson, J.R., and Holliday, C.M. 2018. Hip joint articular soft tissues of non-dinosaurian Dinosauromorpha and early Dinosauria: evolutionary and biomechanical implications for Saurischia. Journal of Vertebrate Paleontology, **38**: e1427593. doi:10.1080/02724634.2017.1427593.

Tsuihiji, T., Barsbold, R., Watabe, M., Tsogtbaatar, K., Chinzorig, T., Fujiyama, Y., and Suzuki, S. 2014. An exquisitely preserved troodontid theropod with new information on the palatal structure from the Upper Cretaceous of Mongolia. Naturwissenschaften, **101**: 131–142. doi:10.1007/s00114-014-1143-9.

Turner, A.H., Makovicky, P.J., and Norell, M.A. 2012. A review of dromaeosaurid systematics and paravian phylogeny. Bulletin of the American Museum of Natural History, **371**: 1–206. doi:10.1206/748.1.

Varricchio, D.J. 2001. Late Cretaceous oviraptorosaur (Theropoda) dinosaurs from Montana. *In* Mesozoic Vertebrate Life. *Edited by* D.H. Tanke, K. Carpenter, and M.W. Skrepnick. Indiana University Press. pp. 42–57.

Verstappen, M., Aerts, P., and De Vree, F. 1998. Functional morphology of the hindlimb musculature of the black-billed magpie, *Pica pica* (Aves, Corvidae). Zoomorphology, **118**: 207–223. doi:10.1007/s004350050070.

Vickaryous, M.K., and Hall, B.K. 2008. Development of the dermal skeleton in *Alligator mississippiensis* (Archosauria, Crocodylia) with comments on the homology of osteoderms. Journal of Morphology, **269**: 398–422. doi:10.1002/jmor.10575.

Walker, A.D. 1977. Evolution of the pelvis in birds and dinosaurs. *In* Problems in Vertebrate Evolution, 4. *Edited by* S.M. Andrews, R.S. Miles, and A.D. Walker. Academic Press, New York. pp. 319–358.

Walsh, S.A., Barrett, P.M., Milner, A.C., Manley, G., and Witmer, L.M. 2009. Inner ear anatomy is a proxy for deducing auditory capability and behaviour in reptiles and birds. Proceedings of the Royal Society B: Biological Sciences, **276**: 1355–1360. doi:10.1098/rspb.2008.1390.

Wang, M., and Zhou, Z. 2019. A new enantiornithine (Aves: Ornithothoraces) with completely fused premaxillae from the Early Cretaceous of China. Journal of Systematic Palaeontology, **17**: 1079–1092. doi:10.1080/14772019.2018.1527403.

Wang, X., Pittman, M., Zheng, X., Kaye, T.G., Falk, A.R., Hartman, S.A., and Xu, X. 2017. Basal paravian functional anatomy illuminated by high-detail body outline. Nature Communications, **8**: 14576. doi:10.1038/ncomms14576.

White, M.A. 2009. The subarctometatarsus: intermediate metatarsus architecture demonstrating the evolution of the arctometatarsus and advanced agility in theropod dinosaurs. Alcheringa, **33**: 1–21. doi:10.1080/03115510802618193.

Wilson, J.A. 2006. Anatomical nomenclature of fossil vertebrates: standardized terms or 'lingua franca'? Journal of Vertebrate Paleontology, **26**: 511–518. doi:10.1671/0272-4634(2006)26[511:ANOFVS]2.0.CO;2.

Wilson, M.C., and Currie, P.J. 1985. *Stenonychosaurus inequalis* (Saurischia: Theropoda) from the Judith River (Oldman) Formation of Alberta: new findings on metatarsal structure. Canadian Journal of Earth Sciences, **22**: 1813–1817. doi:10.1139/e85-192.

Witmer, L.M. 1995. The Extant Phylogenetic Bracket and the importance of reconstructing soft tissues in fossils. *In* Functional Morphology in Vertebrate Paleontology. Cambridge University Press, Cambridge, New York, Melbourne. pp. 19–33.

Xu, X., Cheng, Y., Wang, X., and Chang, C. 2003a. Pygostyle-like structure from *Beipiaosaurus* (Theropoda, Therizinosauroidea) from the Lower Cretaceous Yixian Formation of Liaoning, China. Acta Geologica Sinica, **77**: 294–298. doi:10.1111/j.1755-6724.2003.tb00744.x.

Xu, X., Choiniere, J.N., Pittman, M., Tan, Q., Xiao, D., Li, Z., Tan, L., Clark, J.M., Norell, M.A., Hone, D.W.E., and Sullivan, C. 2010a. A new dromaeosaurid (Dinosauria: Theropoda) from the Upper Cretaceous Wulansuhai Formation of Inner Mongolia, China. Zootaxa, **2403**: 1–9.

Xu, X., Currie, P.J., Pittman, M., Xing, L., Meng, Q., Lü, J., Hu, D., and Yu, C. 2017. Mosaic evolution in an asymmetrically feathered troodontid dinosaur with transitional features. Nature Communications, **8**: 14972. doi:10.1038/ncomms14972.

Xu, X., and Li, F. 2016. A new microraptorine specimen (Theropoda: Dromaeosauridae) with a brief comment on the evolution of compound bones in theropods. Vertebrata PalAsiatica, **54**: 269–285.

Xu, X., Norell, M.A., Wang, X., Makovicky, P.J., and Wu, X. 2002. A basal troodontid from the Early Cretaceous of China. Nature, **415**: 780–784. doi:10.1038/415780a.

Xu, X., Tan, Q., Wang, J., Zhao, X., and Tan, L. 2007. A gigantic bird-like dinosaur from the Late Cretaceous of China. Nature, **447**: 844–847. doi:10.1038/nature05849.

Xu, X., Tan, Q.-W., Wang, S., Sullivan, C., Hone, D.W.E., Han, F.-L., Ma, Q.-Y., Tan, L., and Xiao, D. 2013. A new oviraptorid from the Upper Cretaceous of Nei Mongol, China, and its stratigraphic implications. Vertebrata PalAsiatica, **51**: 85–101.

Xu, X., Tang, Z., and Wang, X. 1999a. A therizinosauroid dinosaur with integumentary structures from China. Nature, **399**: 350–354. doi:10.1038/20670.

Xu, X., Wang, X.-L., and Wu, X.-C. 1999b. A dromaeosaurid dinosaur with a filamentous integument from the Yixian Formation of China. Nature, **401**: 262–266.

Xu, X., Zheng, X., and You, H. 2009. A new feather type in a nonavian theropod and the early evolution of feathers. Proceedings of the National Academy of Sciences, **106**: 832–834. doi:10.1073/pnas.0810055106.

Xu, X., Zheng, X., and You, H. 2010b. Exceptional dinosaur fossils show ontogenetic development of early feathers. Nature, **464**: 1338–1341. doi:10.1038/nature08965.

Xu, X., Zhou, Z., Dudley, R., Mackem, S., Chuong, C.-M., Erickson, G.M., and Varricchio, D.J. 2014. An integrative approach to understanding bird origins. Science, **346**: 1253293. doi:10.1126/science.1253293.

Xu, X., Zhou, Z., and Wang, X. 2000. The smallest known non-avian theropod dinosaur. Nature, **408**: 705–708. doi:10.1038/35047056.

Xu, X., Zhou, Z., Wang, X., Kuang, X., Zhang, F., and Du, X. 2003b. Four-winged dinosaurs from China. Nature, **421**: 335–340. doi:10.1038/nature01342.

Yao, X., Liao, C.-C., Sullivan, C., and Xu, X. 2019. A new transitional therizinosaurian theropod from the Early Cretaceous Jehol Biota of China. Scientific Reports, **9**: 1–12. doi:10.1038/s41598-019-41560-z.

Zanno, L.E. 2006. The pectoral girdle and forelimb of the primitive therizinosauroid *Falcarius utahensis* (Theropoda, Maniraptora): analyzing evolutionary trends within Therizinosauroidea. Journal of Vertebrate Paleontology, **26**: 636–650. doi:10.1671/0272-4634(2006)26[636:TPGAFO]2.0.CO;2.

Zanno, L.E. 2010a. Osteology of *Falcarius utahensis* (Dinosauria: Theropoda): characterizing the anatomy of basal therizinosaurs. Zoological Journal of the Linnean Society, **158**: 196–230. doi:10.1111/j.1096-3642.2009.00464.x.

Zanno, L.E. 2010b. A taxonomic and phylogenetic re-evaluation of Therizinosauria (Dinosauria: Maniraptora). Journal of Systematic Palaeontology, **8**: 503–543. doi:10.1080/14772019.2010.488045.

Zanno, L.E., Gillette, D.D., Albright, L.B., and Titus, A.L. 2009. A new North American therizinosaurid and the role of herbivory in "predatory" dinosaur evolution. Proceedings of the Royal Society B: Biological Sciences, **276**: 3505–3511. doi:10.1098/rspb.2009.1029.

Zanno, L.E., and Makovicky, P.J. 2011. Herbivorous ecomorphology and specialization patterns in theropod dinosaur evolution. Proceedings of the National Academy of Sciences, **108**: 232–237. doi:10.1073/pnas.1011924108.

Zanno, L.E., Varricchio, D.J., O'Connor, P.M., Titus, A.L., and Knell, M.J. 2011. A new troodontid theropod, *Talos sampsoni* gen. et sp. nov., from the Upper Cretaceous Western

Interior Basin of North America. PLOS ONE, **6**: e24487. doi:10.1371/journal.pone.0024487.

Zeffer, A., Johansson, L.C., and Marmebro, Å. 2003. Functional correlation between habitat use and leg morphology in birds (Aves). Biological Journal of the Linnean Society, **79**: 461–484. doi:10.1046/j.1095-8312.2003.00200.x.

Zhang, F., Ericson, P.G.P., and Zhou, Z. 2004. Description of a new enantiornithine bird from the Early Cretaceous of Hebei, northern China. Canadian Journal of Earth Sciences, **41**: 1097–1107. doi:10.1139/e04-055.

Zhang, F., Zhou, Z., Hou, L., and Gu, G. 2001. Early diversification of birds: evidence from a new opposite bird. Chinese Science Bulletin, **46**: 945–949. doi:10.1007/BF02900473.

Zhang, Z., Chen, D., Zhang, H., and Hou, L. 2014. A large enantiornithine bird from the Lower Cretaceous of China and its implication for lung ventilation. Biological Journal of the Linnean Society, **113**: 820–827. doi:10.1111/bij.12330.

Zheng, X., O'Connor, J., Wang, X., Wang, M., Zhang, X., and Zhou, Z. 2014. On the absence of sternal elements in *Anchiornis* (Paraves) and *Sapeornis* (Aves) and the complex early evolution of the avian sternum. Proceedings of the National Academy of Sciences, **111**: 13900–13905. doi:10.1073/pnas.1411070111.

Zhou, Z., Clarke, J., and Zhang, F. 2008. Insight into diversity, body size and morphological evolution from the largest Early Cretaceous enantiornithine bird. Journal of Anatomy, **212**: 565–577. doi:10.1111/j.1469-7580.2008.00880.x.